TR3

The ETR-SAF-ST-SRMZ-PRT Trip*

The 11th Annual Spring Spectacular All-Department Geology Field Trip

January 27->29, 1994

—— brought to you by ——

Dunne/Collins and Co.

and

The Geology Club

* Eastern Transverse Ranges-San Andreas Fault-Salton Trough-Santa Rosa Mylonite Zone-Peninsular Ranges Terrain

GEOLOGIC OVERVIEW

Welcome to one of the most complex pieces of geological real estate in the world—southern California! Our trip will lead directly to or within sight of a number of rock units and structures that typify this complexity. Our trip will focus on the Transverse Ranges geologic province and the major fault structure—the San Andreas transform fault zone—that has played a key role in creating the unique geologic attributes of this province. We will also traverse parts of three other geologic/geomorphic provinces—the Mojave Desert, the Salton Trough, and the Peninsular Ranges—that flank the Transverse Ranges.

The name "Transverse Ranges" reflects the unusual west-northwest trend of these mountains, which contrasts with —is transverse to—the ~N. 30° W. trend of the other elongate geologic provinces in California. These ranges are genetically linked to the San Andreas fault, a broad right-lateral strike-slip fault zone with total slip of approximately 315 km in southern California, and especially to a peculiar geometric aspect of the fault zone, namely a major bend in the trend of the fault that impedes lateral motion of the fault zone. As a result, the rock masses on opposite sides of this "bent" portion of the fault not only slide sideways past each other along several different faults that compose the San Andreas fault system, but also expend a substantial portion of their energy squeezing against each other in a roughly north-south direction. These ~north-south-directed, inward-squeezing forces have been large enough to pervasively shorten and thicken the adjacent rock masses via thrust faults and folds. These structures, together with the continued application of north-south forces, have caused considerable topographic uplift of the Transverse Ranges, especially during the past ~2 million years. Such uplift, accompanied by periodic earthquakes, continues today.

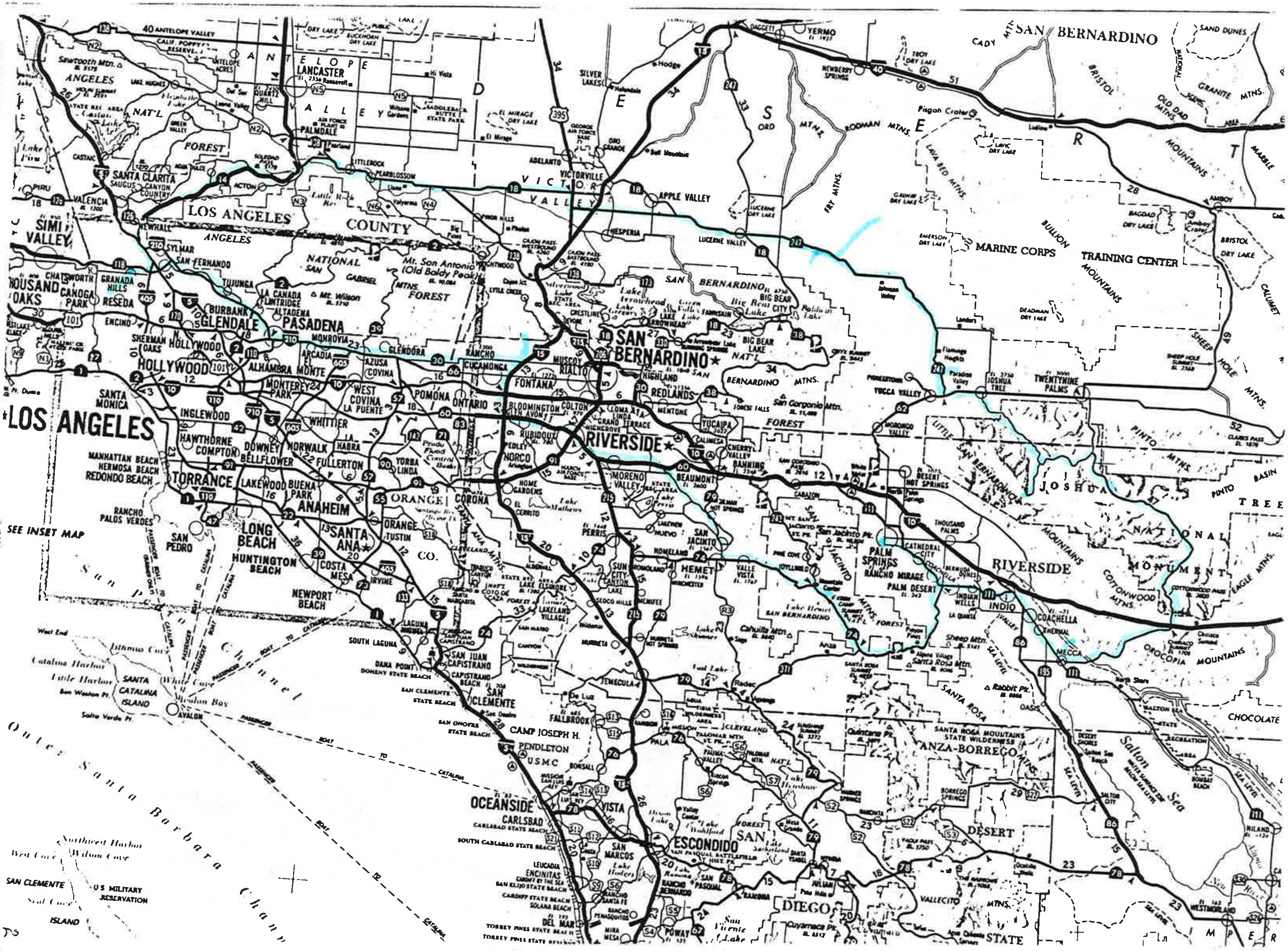
ANTELOPE VALLEY
LANCASTER
PALMDALE
SANTA CLARITA
LOS ANGELES COUNTY
ANGELES NATIONAL FOREST
SAN GABRIEL MTNS.
SIMI VALLEY
THOUSAND OAKS
CANOGA PARK
RESEDA
BURBANK
GLENDALE
PASADENA
HOLLYWOOD
SANTA MONICA
LOS ANGELES
INGLEWOOD
TORRANCE
LONG BEACH
ANAHEIM
SANTA ANA
ORANGE CO.
HUNTINGTON BEACH
NEWPORT BEACH
SAN CLEMENTE
OCEANSIDE
ESCONDIDO
SAN DIEGO
VICTORVILLE
APPLE VALLEY
HESPERIA
SAN BERNARDINO
RIVERSIDE
REDLANDS
ONTARIO
POMONA
FONTANA
CORONA
HEMET
PALM SPRINGS
INDIO
COACHELLA
YUCCA VALLEY
TWENTYNINE PALMS
MARINE CORPS TRAINING CENTER
JOSHUA TREE NATIONAL MONUMENT
SALTON SEA
ANZA-BORREGO DESERT STATE
SANTA CATALINA ISLAND
SAN CLEMENTE
SEE INSET MAP
Outer Santa Barbara Chann
San Pedro Channel


Monterey
Carmel
Pt. Sur
Salinas
Salinas Valley
Fresno
Coalinga
Kettleman Hills
L. Tulare (dry)
Bakersfield
422
Reef Ridge
Temblor Ra.
Carrizo Plain
La Panza Ra.
S.L.O.
San Luis Ra.
Pt. Sal
Pt. Concepcion
Santa Ynez Mts.
San Rafael Mts.
Topatopa Mts.
Mt. Pinos
8826
Santa Barbara
Vent
Santa Monica Mts.
Santa Cruz I.
Santa Rosa I.
Anacapa Is.
San Nicolas I.
Santa Catalina I.
San Clemente I.
Los Angeles
La Jolla
San Diego
Pt. Loma
Portal Ridge
Antelope Vol.
Aqueduct
Mojave Desert
San Gabriel
Cajon Pass
San Bernardino Mts.
San Jacinto Mt.
Santa Rosa Mts.
Laguna Mts.
Vallecito Mts.
Coachella
Salton Sea
Imperial Valley
Chocolate Mts.
Eagle Mt.
Bullion Mts.
Barstow
Soda L.
Silver L.
Devils Playground
Providence Mts.
Old Woman Mts.
Turtle Mts.
Dead Mts.
Panamint Ra.
Panamint Val.
Slate Mts.
Argus Mts.
Searles L.
China L.
Coso Ra.
Owens
Kern

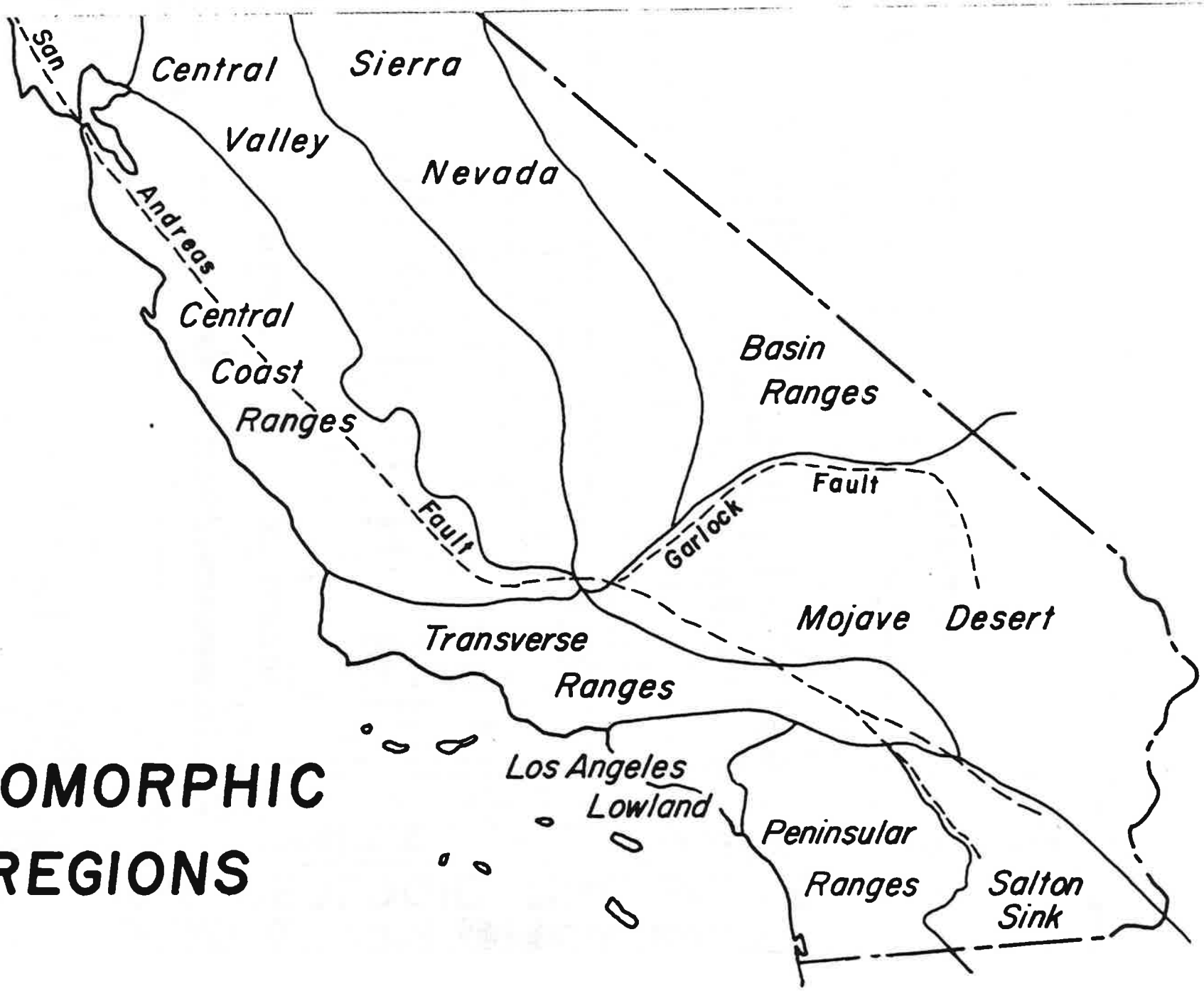

GEOMORPHIC REGIONS

DECADE OF NORTH AMERICAN GEOLOGY
1983 GEOLOGIC TIME SCALE

DNAG

GEOLOGICAL SOCIETY OF AMERICA

CENOZOIC

AGE (Ma)	PERIOD	EPOCH	AGE	PICKS (Ma)
	QUATERNARY	HOLOCENE		0.01
		PLEISTOCENE	CALABRIAN	1.6
	NEOGENE	PLIOCENE L	PIACENZIAN	3.4
		PLIOCENE E	ZANCLEAN	5.3
		MIOCENE L	MESSINIAN	6.5
			TORTONIAN	11.2
		MIOCENE M	SERRAVALLIAN	15.1
			LANGHIAN	16.6
		MIOCENE E	BURDIGALIAN	21.8
			AQUITANIAN	23.7
	PALEOGENE	OLIGOCENE L	CHATTIAN	30.0
		OLIGOCENE E	RUPELIAN	36.6
		EOCENE L	PRIABONIAN	40.0
			BARTONIAN	43.6
		EOCENE M	LUTETIAN	52.0
		EOCENE E	YPRESIAN	57.8
		PALEOCENE L	SELANDIAN: THANETIAN	60.6
			SELANDIAN: UNNAMED	63.6
		PALEOCENE E	DANIAN	66.4

MESOZOIC

AGE (Ma)	PERIOD	EPOCH	AGE	PICKS (Ma)	UNCERT (m.y.)
	CRETACEOUS	LATE	MAASTRICHTIAN	66.4	
			CAMPANIAN	74.5	4
			SANTONIAN	84.0	4.5
			CONIACIAN	87.5	
			TURONIAN	88.5	2.5
			CENOMANIAN	91	
		EARLY	ALBIAN	97.5	2.5
			APTIAN	113	4
		NEOCOMIAN	BARREMIAN	119	9
			HAUTERIVIAN	124	9
			VALANGINIAN	131	6
			BERRIASIAN	138	5
	JURASSIC	LATE	TITHONIAN	144	5
			KIMMERIDGIAN	152	12
			OXFORDIAN	156	6
		MIDDLE	CALLOVIAN	163	15
			BATHONIAN	169	15
			BAJOCIAN	176	34
			AALENIAN	183	34
		EARLY	TOARCIAN	187	34
			PLIENSBACHIAN	193	28
			SINEMURIAN	198	32
			HETTANGIAN	204	18
	TRIASSIC	LATE	NORIAN	208	18
			CARNIAN	225	8
		MIDDLE	LADINIAN	230	22
			ANISIAN	235	10
		EARLY	SCYTHIAN	240	22
				245	20

RAPID POLARITY CHANGES

PALEOZOIC

AGE (Ma)	PERIOD	EPOCH	AGE	PICKS (Ma)	UNCERT (m.y.)
	PERMIAN	LATE	TATARIAN	245	20
			KAZANIAN	253	20
			UFIMIAN	258	24
		EARLY	KUNGURIAN	263	22
			ARTINSKIAN	268	12
			SAKMARIAN		
			ASSELIAN	286	12
	CARBONIFEROUS: PENNSYLVANIAN	LATE	GZELIAN / KASIMOVIAN (S.)	296	10
			MOSCOVIAN (W.)		
			BASHKIRIAN (W.)	315	20
			SERPUKHOVIAN (N.)	320	
	CARBONIFEROUS: MISSISSIPPIAN	EARLY	VISEAN	333	22
			TOURNAISIAN	352	8
	DEVONIAN	LATE	FAMMENIAN	360	10
			FRASNIAN	367	12
		MIDDLE	GIVETIAN	374	18
			EIFELIAN	380	18
		EARLY	EMSIAN	387	28
			SIEGENIAN	394	22
			GEDINNIAN	401	18
	SILURIAN	LATE	PRIDOLIAN	408	12
			LUDLOVIAN	414	12
		EARLY	WENLOCKIAN	421	12
			LLANDOVERIAN	428	8
	ORDOVICIAN	LATE	ASHGILLIAN	438	12
			CARADOCIAN	448	12
		MIDDLE	LLANDEILAN	458	16
			LLANVIRNIAN	468	16
		EARLY	ARENIGIAN	478	16
			TREMADOCIAN	488	20
	CAMBRIAN	LATE	TREMPEALEAUAN / FRANCONIAN / DRESBACHIAN	505	32
		MIDDLE		523	36
		EARLY		540	28
				570	

PRECAMBRIAN

AGE (Ma)	EON	ERA	BDY. AGES (Ma)
	PROTEROZOIC	LATE	570
750			900
		MIDDLE	
1000			
1250			1600
1500		EARLY	
1750			
2000			
2250			2500
2500	ARCHEAN	LATE	
2750			
3000			3000
		MIDDLE	
3250			
3400			3400
3500		EARLY	
3750			3800?

Early Geologic Studies of the Transverse Ranges, California

GEOLOGY AND MINERAL WEALTH OF THE CALIFORNIA TRANSVERSE RANGES

Bruce Carter, Pasadena City College, Pasadena, CA 91106

The Transverse Ranges of southern California constitute a geomorphic and geologic province which is strikingly different from the other provinces of California, both in its obvious difference in geomorphic trend and in its geology. Rocks and structure in this province clearly contrast with those of the Coast Ranges, Great Valley and Sierra Nevada to the north and the Peninsular Ranges and Colorado Desert to the south. In recent years especially, understanding the nature of the Transverse Ranges has been important to achieving a full understanding of the ways in which plate tectonics has affected this part of California. The purpose of this volume is to provide an up-to-date collection of papers on the geology and mineral resources of the Transverse Ranges. The purpose of this paper, however, is to look at some of the earliest geologic studies of the Transverse Ranges in order to see how this unique and remarkable province was recognized and perceived by the first geologists in the area.

Geology is fundamentally an historical study: deducing the geologic history of an area based on what is seen in the rocks today. Along the same lines, it can sometimes be very interesting and instructive to look at the history of developments of a geologic idea (the concept of plate tectonics, Marvin, 1973), study of a geologic feature (the San Andreas Fault, Hill, 1981), or study of a specific area, such as the Transverse Ranges. Such historical accounts can provide background for understanding present concepts and problems relating to the subject, in this case the Transverse Ranges.

In addition, just as our enjoyment of a vacation trip is enhanced by a knowledge of the human history of the area, sometimes our enjoyment and appreciation of the geology of an area can similarly be enhanced by a knowledge of the history of geologic studies, ideas and concepts regarding that area. It is the intent of this paper to present a brief introduction to the geologic studies of the Transverse Ranges prior to 1930, and mostly prior to 1900, in order to document the early development of ideas regarding this unique geologic province and to serve as an introduction to the present extensive body of geologic knowledge of the Transverse Ranges, much of which is presented in the following papers. The selection of accounts presented below clearly reflect my own personal interests, and are by no means inclusive of all the information available. The reader who is interested in a more complete history of early geologic studies of the area should refer to Vogdes (1896) "A bibliography relating to the geology, paleontology, and mineral resources of California."

The strikingly anomalous east-west trend of the California coastline between Santa Monica bay and Point Conception may have been observed by Juan Rodriguez Cabrillo in his 1592 voyage, but was not noted in his account of the voyage. However Sebastian Rodriguez Cermeno, returning from the Philippines, passed this part of the coast on December 13-14, 1595 and described the east-west trending, bold coast which was bare and broken and provided no port for his launch (Wagner, 1929, p. 162). For the following 180 years, California served as little more than a convenient landfall and route back to Mexico for ships returning from the Orient.

In the 1770's several expeditions from Mexico, both by land and by sea, resulted in finding and settling Monterey Bay, the founding of several missions, and the claiming of "New California" as part of Mexico. On one of these expeditions, led by Gaspar de Portola in 1769, Pedro Fages, soldier of Spain, described their journey between the Santa Ana River (Rio de los Temblores) and the present site of Ventura, and goes on to say (Priestly, 1972, p. 18):

> "It is to be noted that, because terrifying earthquakes, which frequently recurred, had been experienced throughout a great part of this stretch of the journey, it was suspected that there might be some volcanoes in the mountains of the vicinage. Truly the indications did not belie this suspicion, for, at the foot of the range which runs toward the west, on the road lying between the Rio de la Porciuncula and the Ojo del Agua de los Alisos, the scouts found pools of bitumen bubbling out of the ground."

Although several of the explorers remarked on the earthquakes of 1769, there were few other mentions of the geology of the area until gold was found in Placerita Canyon in the early 1840s. An account of this discovery is given in Warner, Hayes, and Widney (1876, p. 19):

> "Sometime in the latter part of 1840, or the early part of 1841, a Mexican mineralogist, Don Andrea Castillero, traveling from Los Angeles to Monterey, while passing along the road over the Las Virgenes Rancho, saw and gathered up some small, waterworn mineralogical pebbles known by Mexican placer miners as tepostete*—a variety of pyrites—which he exhibited at the residence of Don Jose Antonio do la Guerra y Noriega, in Santa Barbara, where he was a guest, and stated, that wherever these pebbles were found in place, it was a good indication of placer gold fields. A Mr. Francisco Lopez, also known by the name of Cuso, a farmer and herdsman, living at the time upon the Piru Rancho, was present, and heard the statement and saw the pebbles. Not long after this incident, Mr. Lopez, in company with a fellow-herdsman, was one day searching for strayed animals until their riding horses were jaded. At a suitable place they dismounted, and picketing their horses that they might rest and feed, Lopez busied himself in gathering a parcel of wild onions, a bed of which was near at hand, to carry home for a mess of greens. In pulling the onions from the ground he noticed a pebble, similar to the one he had seen in the hands of Mr. Castillero, and remembering what was then said about its being a sign of gold, he scopped up a handful of the earth, which he had loosened by gathering the onions, and rubbing it in his hand, found a grain of gold."
>
> "The news of this discovery soon spread among the inhabitants, from Santa Barbara to Los Angeles, and in a few weeks hundreds of people were engaged in washing and winnowing the sands and earth of these gold fields."

An account of the gold in this area is given by Mofras (1844), who goes on to describe nearby silver ores, and further observes that the Indians often bring in from the mountains, grains of copper, fragments of opal, and pieces of galena.

*Tepostetes (Sonora, Mex): Bowlders of specular iron ore found in gold placers" (Fay, 1920). These were evidently pieces of ilmenite washed out of the anorthosite-syenite body of the nearby western San Gabriel Mountains.

Trask (1855), the first state geologist of California, reported on his investigations of the Coast Mountains in 1853 and 1854 in which he states (p. 12-13):

"Beyond the junction of the coast mountains, the San Bernardino Chain makes its inception, and forms the coast-line for a considerable distance to the south . . . The position and course of the San Bernardino chain, with its extent and altitude forms a striking feature in the geography of the State, and the climatical features incident to the effects produced by position and altitude, are really distinctive; the products arising from these pecularities, are equally marked in all their forms, while its zoology partakes of the general mutation which supervenes to as great an extent as is manifest in the pecularities of the climate; not less characterized are the native inhabitants, their pursuits and interests; there seems but little to unite them with other parts of the State, as each and every natural product, methods of living, and political feelings, are as distinct as the almost impassable mountain barrier that separates them from the northern portions of the State."

He goes on to say (p. 20-21):

"These mountains are made up for the most part of the primitive rocks, and consist chiefly of the granitic series; they form by far the most of all the higher ridges and more elevated peaks belonging to the chain . . . On both sides of this chain we find the miocene deposits, evidently of the same period, occupying different levels, and the same beds presenting different lines of dip; in one case a great degree of horizontality prevailing while in another the beds will be highly inclined."

Trask also postulated that the islands forming the west (south) coast of the Santa Barbara channel were originally united and formed a mountain range which was part of the mainland (p. 23). He also observed that the sedimentary rocks formed a basin-shaped structure under the Los Angeles plains and suggested the possibility of obtaining water through artesian borings (p. 23). Trask remarked on the terraced structure of the coastal parts of the range and the interior valleys (p. 24), and also noted that (p. 40):

"The transverse chain of the Pacific coast (San Bernardino chain) appear thus to act as a barrier, and to have cut off almost completely the rich mineral deposits found in the mountains of the more northern sections."

He did go on, however, to remark on the abundance of bitumen, its adaptability to manufacture of gas for illumination, and the likelihood that in the future it will be used to considerable extent in this country (p. 40).

One of the most extensive and interesting early reports on the geology of the Transverse Ranges is that by William P. Blake, who was the geologist on the 1853-1854 Williamson exploration and survey to ascertain the most practical and economical route for a railroad from the Mississippi River to the Pacific Ocean. Blake's report, published in volume 5 of the report in 1857, is a treasure house of interesting observations (mostly made in 1853) on the geology of the Transverse Ranges. In the beginning of Chapter IX he states (p. 133):

"That portion of the continent within the limits of the State of California presents a greater variety in the relief of its surface, and in its climate and vegetable productions, than any other portion of equal area. The lofty chains of mountains, towering into the regions of perpetual snow, are perhaps not more striking and peculiar than the broad, plainlike valleys which lie at their base, and separate the principal ranges."

"The prominent orographic features are developed on a grand scale, and with such simple relations that a conception of them is readily formed. The chief range—the Sierra Nevada—rises like a great wall of separation between the State and the elevated semi-desert region of the Great Basin, and extends from the northern boundary as far south as the parallel of 35°. Parallel with this, and extending over a similar distance, we find the Coast Mountains; the two systems of ranges being separated by the broad plains of the Sacramento, San Joaquin, and the Tulares, but uniting in latitude 35 degrees; thus terminating the extended, interior valleys on the south."

"South of this point of junction of the Sierra Nevada with the Coast Mountains, there is but one prominent range of mountains separating the coast-slope from the Great Basin and desert plains of the interior. Its direction is also different from either the Sierra Nevada or Coast Mountains, being nearly transverse to them, extending a few degrees south of east for more than 100 miles to the peak of San Bernardino. This is described in the notes as the *transverse chain*, the *Bernardino Mountains*, or *Bernardino Sierra.*"

He went on to say (p. 136-137):

"The mountains having this transverse direction do not, however, end abruptly at the end of the Sierra Nevada, but preserve their direction beyond it, towards Point Conception on the coast, thus crossing the southern ends of the Coast Mountains also. The chain is rendered distinct from the Coast Mountains, not only by its direction, but by its geological structure, it being granitic and metamorphic, while the ranges of the Coast Mountains are chiefly of more modern and sedimentary strata. The limits of the Bernardino Sierra, on the west, may thus be considered to be at the termination of the high granitic ridges north of Santa Barbara, although, topographically, it is believed to be prolonged nearly to the Point Conception . . . The whole length of the chain from San Bernardino to its eastern end is between 170 and 200 miles, it being about 200 from Point Conception to the mountain . . . Subordinate parts of the Bernardino Sierra are known under local names, as, for example: Qui-quai-mungo range, San Gabriel range, San Fernando range, and Santa Inez range. The whole chain, or a portion of it, was formerly called *Sierra Madre* by the Padres—probably from the fact that the Sierra Nevada, the Coast Mountains, and other ranges seem to spring from it. The name, however, appears to have been applied in the most general manner, and has not passed into use; . . . The name *Bernardino Sierra* is therefore proposed."

In October of 1853, the party explored the area between the Canada de las Uvas (Tejon Pass) and Williamson's Pass (Soledad Pass) and crossed both San Francisquito and Williamson's Passes. In that area, Blake made an interesting observation (p. 62):

"Before passing, however, to a notice of the phenomena observed there, a retrospective glance should be given to the peculiar and fertile character of the strip of country at the base of the north side of the main chain of the Bernardino Sierra. This fertile strip consists of the chain of longitudinal valleys connecting by their ends, formed by outlying low ridges, either of granite or sedimentary hills, at a short distance from the main ridges of the Sierra. Nearly all these valleys, extending

over a distance of more than forty miles, or from the center of the Canada de las Uvas to Williamson's Pass, are adapted to cultivation. Grass grows luxuriantly in most of them, and the soil is deep and rich. There is no lack of water, which, though not found in running streams of any size, is abundantly furnished by springs and ponds."

The above clearly shows that Blake observed the ground water effects of the San Andreas fault in that area, even though he did not recognize the fault itself. The first description of the Pelona Schist was given by Blake (p. 59-60) who described an outcrop of "Talcose and auriferous slates" about nine miles south of the summit of San Francisquito Pass. On October 24, 1853, they crossed Williamson's pass and started down the Santa Clara River toward San Francisquito rancho. Along this route Blake described several interesting rocks (p. 69-71):

"*White Granite.* The mountains on the left of this part of the pass are high rugged peaks, composed of light-colored granite, in which hornblende is seldom present. The decomposition of this granite appears to be rapid, and its surface becomes as white as chalk; so that whenever it is visible between the thick growth of dwarf oaks it looks like patches of snow. When a high wind blows over these hills it raises a cloud of white dust, formed by the disintegrating feldspar. The granite seems to be almost wholly formed of white feldspar or albite; and both quartz and mica are in small proportion, and are also very white."

Describing a creek containing large boulders coming in from the south side of the pass, he says (p. 70):

"The rocks thus transported along this creek were mostly granitic and metamorphic, much white granite being found. I picked up several masses, which had a delicate purple or lilac tint, produced by the feldspar. This, however, was a syenite, no mica being visible, but an abundance of hornblende of an olive-green color. The crystals were so disposed throughout the rock that the surface looked as if it had been written upon. The rock in fact is a beautiful *graphic syenite.*"

He includes a sketch of this graphic syenite, and goes on to describe the large masses of ore in the same creek. It is clear from the above that Blake was describing rocks of the San Gabriel anorthosite-syenite body exposed to the south of the pass. His "white granite" perfectly matches the lithologic and outcrop characteristics of the anorthosite, his "graphic syenite" corresponds to the ophitic leucogabbro, and the ore masses refer to the ilmenite boulders eroded from the same body.

In 1861 J. D. Whitney, State geologist of California, examined the eastern part of the Santa Monica Mountains where he discovered that the core of this part of the range was composed of "dark siliceous slate" intruded and metamorphosed by granite and that an anticline existed in this old slate in the vicinity of Santa Monica Canyon (p. 171):

"So that we have here one of the best possible examples of a truly anticlinal range of mountains, with a central core of granite, having all the appearance of an intrusive rock which has burst asunder and elevated the slaty strata, producing a highly metamorphic condition of the sedimentary beds along the lines of contact of the granitic mass."

In the 1876 report of the George M. Wheeler geographical surveys west of the one hundredth meridian, J. Marcou reported on the geology of the area between Los Angeles and Fort Tejon. He described a number of fossils in the Tertiary rocks of this area, and the relationship of these rocks to the crystalline rocks of the Santa Monica Mountains and the San Gabriel Mountains near Pacoima Canyon (see sections on p. 159-160). He noted that the crystalline rocks are the same throughout the Sierra Madre chain, from Cajon pass to Pacoima Canyon, and discussed the great lithological resemblance between the Tertiary rocks of California and those of Switzerland. He went on the summarize some of his observations (p. 171-172):

" . . . the Tertiary strata were pressed back against the obstacle of the Sierra Madre and were in some places folded back (*repliees*) upon themselves, becoming contorted, and their beds being turned in an opposite direction, perpendicular to that of these granitic and crystalline mountain chains. I have not seen any indications which prove that the Sierra Madre was ever subjected to the uplifts of the Tertiary epochs. But, then, at the close of the Quaternary epoch, and perhaps even in the Modern epoch, there are proofs of uplifts and dislocations, which are particularly perceptible on the eastern side of the chains of the Sierra Madre throughout the whole length of the California Desert."

"*En resume*, the Sierra Madre is altogether the most ancient and the most modern mountain chain of this region of Southern California; that is to say, that the granite, pegmatite, gneiss, dioritic,and metamoprhic rocks which form its principal mass date from times anterior to the Paleozoic epochs, *ou tout au plus paleozoiques memes*; and that the counterforts of sand, sandstone, and conglomerate which form the summit of Canjon Pass and of other portions of the eastern region of this chain, date from the Post Pliocene or Quaternary epoch."

"In consequence of their directions being from west to east, this system of mountains enters the Pacific Ocean on one side and the Sierra Madre on the other, and interesects and completely isolates Southern California from the central and northern portions of the State . . . In reality, Southern California is more disconnected and isolated from California proper than is the latter from the States of Nevada and Oregon."

Schuyler (1896) in a paper concerning irrigation reservoirs, described a fault (the San Andreas) running through Alpine (Palmdale) reservoir on the north side of the Sierra Madre Mountains (p. 711-712):

"This reservoir has special interest, not only as the first one of any magnitude completed on the . . . Antelope Valley side of the Sierra Madre in Southern California, but because it lies directly in the line of what is known as the great earthquake crack . . . This remarkable line of fracture can be traced for nearly 200 miles through San Bernardino, Los Angeles, Kern and San Luis Obispo counties . . . there appears to have been a distinct "fault" along the line, the portion lying south of the line having sunken, and that to the north of it being raised in a well defined ridge."

LATE CRETACEOUS INTRA-ARC THRUSTING IN SOUTHERN CALIFORNIA

Daniel J. May[1]

Department of Geological Sciences, University of California, Santa Barbara

Abstract. Thick zones of mylonitic rock are exposed in or between a number of the suspect crystalline terranes in the Transverse Ranges and eastern Peninsular Ranges of southern California. After palinspastic reconstruction of strike-slip displacements along Neogene faults in the region the mylonite zones appear in a semicontinuous belt several hundred kilometers long. Mylonitic deformation in these areas is of a similar style and age. Lineation trends in the mylonitic rocks are closely aligned when palinspastic reconstruction takes into account the block rotations in the region, and the sense of shear is consistently west directed. The mylonite zones appear to have formed concurrently in a major midcrustal thrust system that juxtaposed the basement terranes during the Late Cretaceous. A kinematic model is proposed in which a west directed ductile thrust zone along the eastern side of the Peninsular Ranges is offset by a sinistral tear fault or lateral thrust ramp along the southern margin of the San Gabriel Mountains from a ductile thrust underlying crystalline basement terranes to the north. This model requires the suspect basement rocks of the Peninsular and Transverse Ranges to be linked tectonically by the latest Cretaceous. This Late Cretaceous thrust system also appears to continue directly into autochthonous basement rocks in the San Bernardino Mountains. The Late Cretaceous westward displacement of basement rocks in the Transverse Ranges relative to the northern end of the Peninsular Ranges batholith is mirrored by similar tectonic movement around the southern end of the Sierra Nevada batholith. It is argued here that a formerly continuous batholithic belt was breached by ductile west directed thrusting during the Late Cretaceous between the two still recognizable batholiths. The Salinia terrane represents the westernmost portion of this westward escaping arc segment and would have been established as a crustal salient by the latest Cretaceous. This model implies that the basement terranes involved in this thrusting episode are parautochthonous fragments of a Cretaceous continental arc and refutes suggestions that they have been accreted in the Cenozoic.

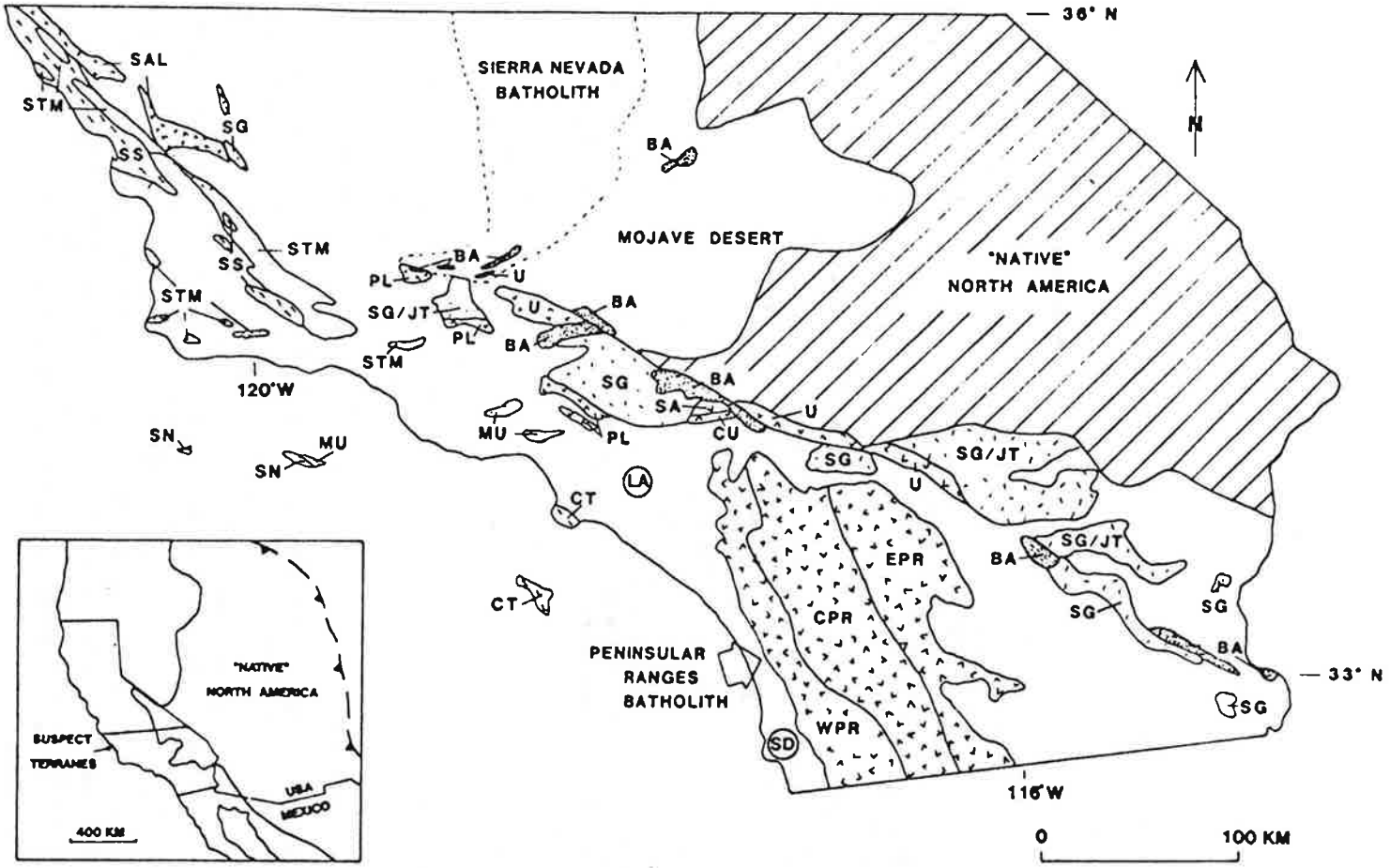

Fig. 2. Suspect terranes of southern California. Modified from Blake et al. [1982] to show only those terranes presumed to have been accreted during the Cretaceous or Cenozoic. Therefore suspect terranes appearing in the western Mojave Desert or as pendants in the Sierra Nevada batholith are not shown. Terrane designations are largely those of Blake et al. [1982], however, the composite Tujunga terrane has been subdivided into its amalgamated components [Powell, 1981, 1982, 1986b; Dibblee, 1982; Frizzell and Powell, 1982; May and Walker, 1989]. Sub- division of the Peninsular Ranges batholith is based on the observations of pendant composition in batholithic rocks by Gastil [1985] rather than terrane designations of Blake et al. BA, Baldy terrane; CPR, pendants of the central Peninsular Ranges; CT, Catalina terrane; CU, Cucamonga terrane; EPR, pendants of the eastern Peninsular Ranges; MU, Malibu terrane; PL, Placerita terrane; SA, San Antonio terrane; SAL, Salinia terrane; SG, San Gabriel terrane; SG/JT, amalgamated San Gabriel and Joshua Tree terranes juxtaposed along the Mesozoic(?) Red Cloud thrust [Powell, 1981]; SN, San Nicolas terrane; SS, San Simeon terrane; STM, Stanley Mountain terrane; U, undesignated; WPR, pendants of the western Peninsular Ranges. Terrane patterns: "v" symbol, Cretaceous batholithic rocks with varied types of pendants (SAL, PL, U, SA, CU, WPR, CPR, EPR); dashed, Precambrian continental crust with Mesozoic intrusives (SG, SG/JT); light stipple, Mesozoic ophiolite fragments and/or overlying strata (STM, SN, MU); tilde symbol, Mesozoic accretionary greywacke (SS, CT); dark stipple, metamorphosed oceanic affinity rocks (BA). Unlabeled areas surrounding suspect terranes consist largely of late Mesozoic and Cenozoic sedimentary rocks. Inset map shows region underlain by suspect terranes (stippled) in the western part of the Cordillera [after Coney et al., 1980]. Barbed line is eastern limit of Cordilleran Mesozoic-Cenozoic deformation.

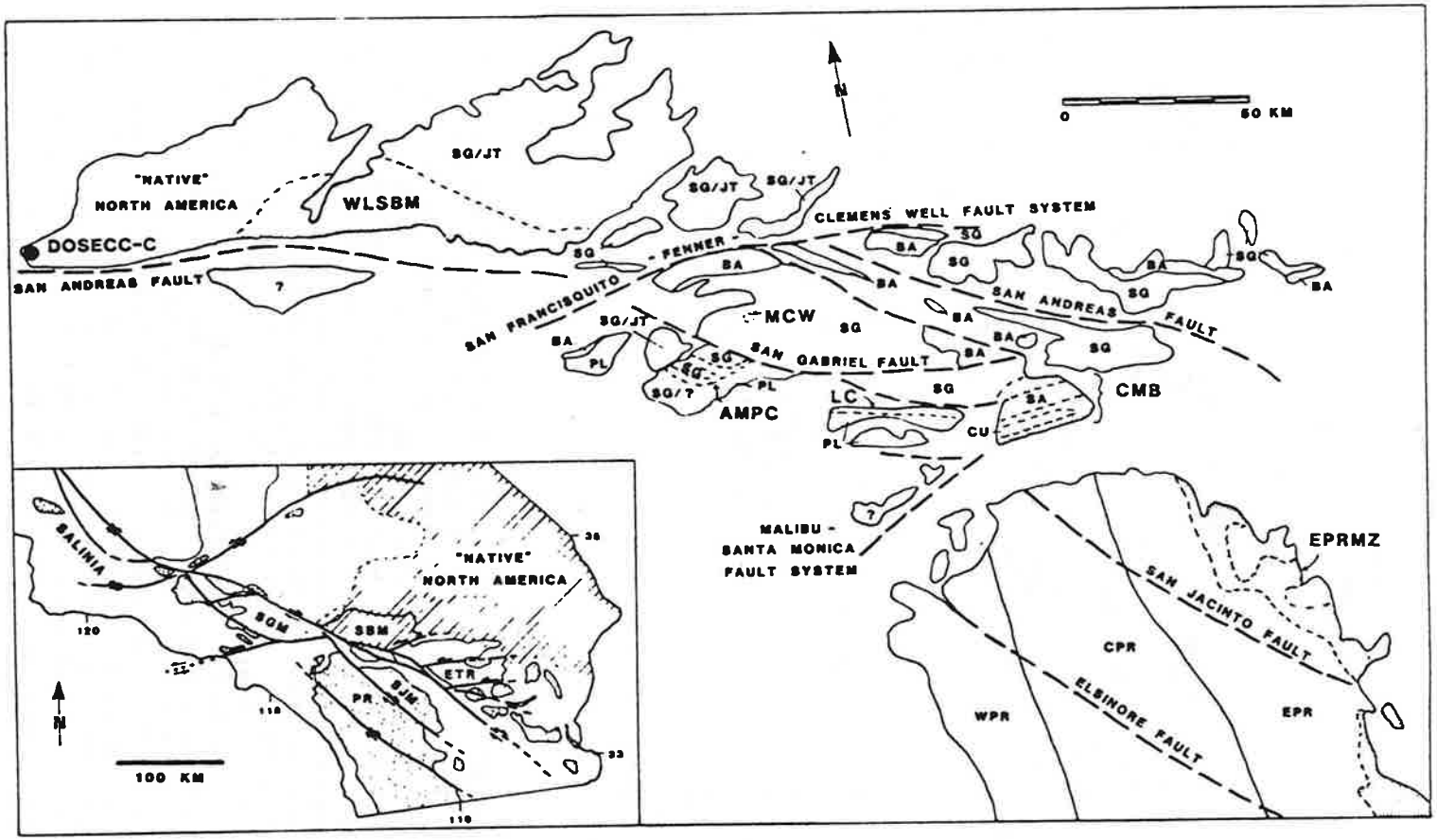

Fig. 3. Distribution of basement terranes in southern California after palinspastic reconstruction of the San Andreas and older fault systems. Note that this reconstruction accounts only for displacements along strike-slip fault traces and that tectonic block rotations in the Transverse Ranges Province [Luyendyk et al., 1980, 1985; Hornafius et al., 1986] are not completely accounted for when restoring translations along the present-day curved fault traces. Reconstruction of terranes in San Gabriel Mountains is from May and Walker [1989]. Terrane abbreviations as in Figure 2. Queried basement blocks are of uncertain affinity. Stippled areas represent Late Cretaceous age mylonite zones: AMPC, Alamo Mountain and Piru Creek shear zones; CMB, mylonite belts of the Cucamonga region; DOSECC-C, strongly deformed granitic and gneissic rocks encountered in Cajon Pass deep drillhole; EPRMZ, eastern Peninsular Ranges mylonite zone; LC, Limerock Complex; MCW, Mill Canyon window; WLSBM, mylonitic and cataclastic rocks of western Little San Bernardino Mountains. Note that mylonitic rocks structurally overlying the Baldy terrane (i.e., associated with the latest Cretaceous or early Tertiary Vincent - Chocolate Mountains thrust system) are not shown. Inset map is a simplified version of Figures 1 and 2 showing present-day outcrop of suspect crystalline terranes and main Cenozoic faults used in reconstruction. ETR, eastern Transverse Ranges; PR, Peninsular Ranges; SBM, San Bernardino Mountains; SGM, San Gabriel Mountains (part of the western Transverse Range province); SJM, San Jacinto Mountains in the northeastern Peninsular Ranges.

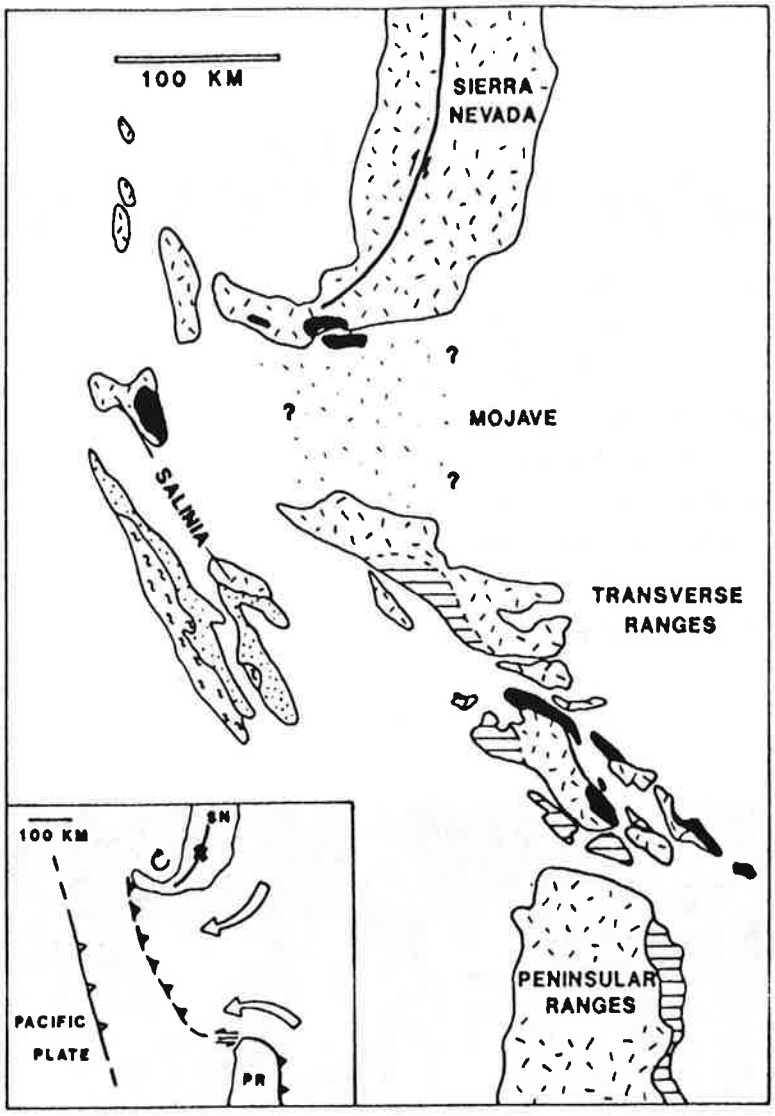

Fig. 5. Distribution of selected Late Cretaceous features and rock types on a palinspastic base for southern California with effects of Neogene and Quaternary faulting removed [after Burchfiel and Davis, 1981]. No attempt has been made to compensate for Neogene rotations in Transverse Ranges and western Mojave or effects of low-angle normal faulting in the Mojave region. Rock symbols are short dashes, Cretaceous and older Mesozoic plutonic rocks, metasedimentary pendants, and Precambrian crystalline rocks (distribution poorly known in Mojave desert); horizontal lines, Late Cretaceous age mylonitic rocks associated with the proposed synplutonic thrust system; solid, subducted oceanic affinity rocks (Baldy terrane); dots, ophiolite basement and overlying forearc basin strata (Stanley Mountain terrane and correlatives); tilde symbols, accreted greywacke or subduction complex rocks (i.e., Franciscan Formation in San Simeon terrane). Inset shows model for westward breaching of a continuous batholithic belt between the southern Sierra Nevada batholith (SN) and the Peninsular Ranges batholith (PR). Hypothetical position of subduction zone margin with the Pacific plate (i.e., Farallon or Kula plate at this time) is also shown.

DAY ONE
CSUN TO JOSHUA TREE NATIONAL MONUMENT

Leg 1	CSUN to Victorville area
Stop 1	Gas/Potty/Geoview near Victorville
Leg 2	Victorville Area to Blackhawk area
Stop 2	Blackhawk Landslide
Leg 3	Blackhawk area to Landers 'quake scarps
Stop 3	Landers earthquake scarps
Leg 4	Landers to Joshua Tree area
Stop 4	Triassic megaporphyry
Leg 5	Joshua Tree area to Keys View

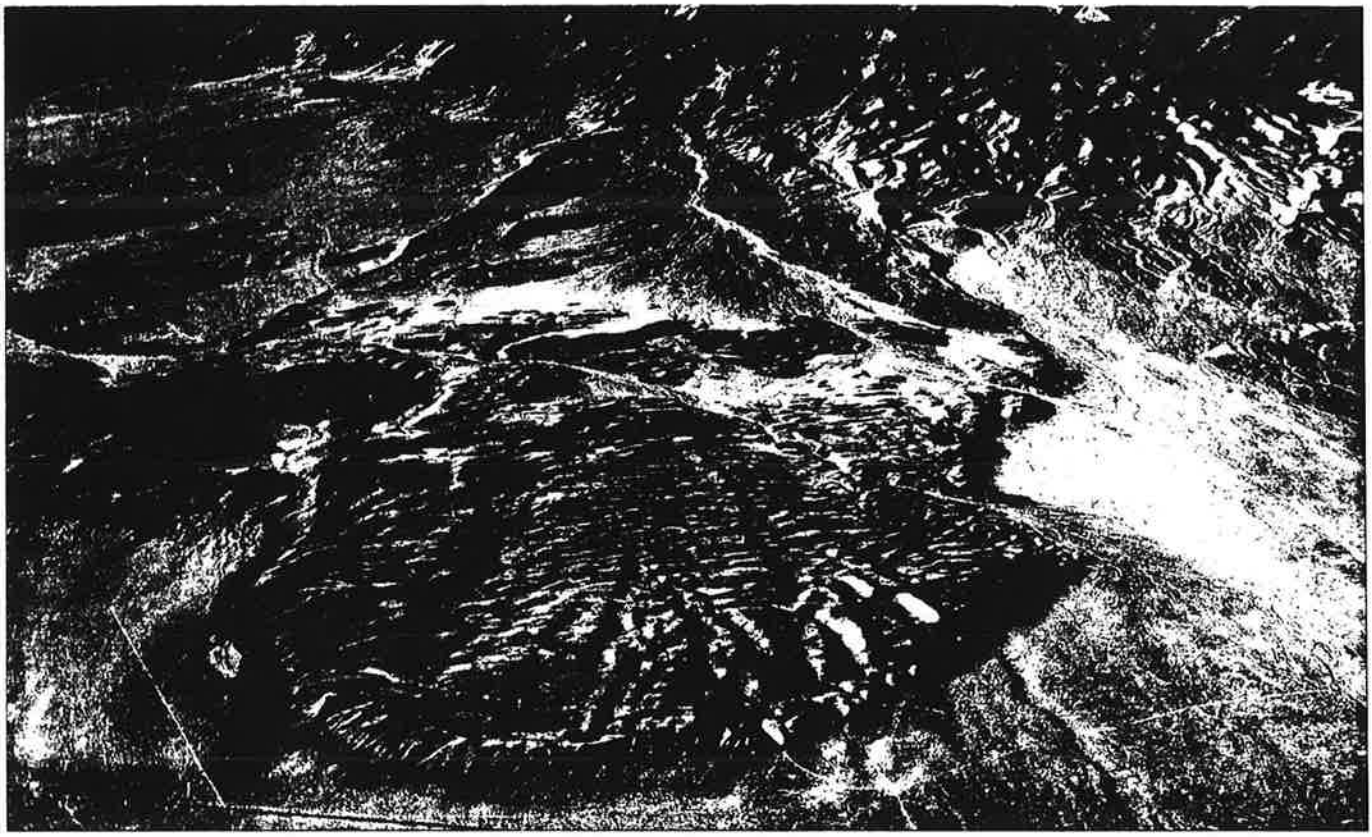

Overview of the San Andreas fault system (and its left-lateral conjugates) in southern California

San Jacinto fault. Path. The San Jacinto fault zone transects the northeastern Peninsular Ranges between Borrego Valley in the Salton trough and the San Bernardino Valley, north of which it splays as it enters the southeastern San Gabriel Mountains. (For a history of study of the San Jacinto fault zone, see Sharp, 1967). Although some investigators have concluded that the San Jacinto fault merges northward with the San Andreas fault between the San Gabriel and San Bernardino Mountains (Noble, 1954a, b; Ehlig, 1975a, 1981; R. J. Weldon, 1989, written communication), others have demonstrated that the recognized strands of the San Jacinto fault in the southeastern San Gabriel Mountains do not join the San Andreas fault at the surface (Dibblee, 1968a; Morton, 1975a, b; Morton and Matti, this volume).

Previous estimates of displacement. Measurements of right-lateral displacement of Mesozoic crystalline rocks along the San Jacinto fault zone in the Peninsular Ranges province range between about 24 and 30 km (Sharp, 1967; Baird and others, 1970; Bartholomew, 1970; R. I. Hill, 1981). Eckis (1930) postulated that the distribution of Miocene and Pliocene strata along the San Jacinto fault in the vicinity of Borrego Valley indicates a dextral displacement of 29 to 32 km. Fluvial and lacustrine units near the base of the Pliocene and Pleistocene San Timoteo badlands section, initially estimated to be offset 18 to 19 km (English, 1953; Dutcher and Garrett, 1963, p. 38; see also Sharp, 1967; Bartholomew, 1970) along the San Jacinto fault, have more recently been demonstrated to be offset 23 to 26 km (Matti and Morton, 1975). The Pleistocene Bautista Beds of Frick (1921) are distributed along the San Jacinto fault and evidently accumulated during movement (Sharp, 1967, 1981). Restoration of 18 to 24 km of dextral slip aligns the Cucamonga and Banning faults, and some investigators have inferred that these faults are in part an old feature that was disrupted by the San Jacinto fault (Allen, 1957; Sharp, 1967; Dibblee, 1968a; Baird and others, 1971; Jahns, 1973), although recent reverse movement on the Cucamonga and Banning faults is coeval with movement on the San Jacinto fault (Woodford, 1960; Jahns, 1973; Matti and others, 1985). At its northern end where it enters the San Gabriel Mountains, however, the main splays of the San Jacinto fault offset contacts in the crystalline rocks only about 11 to 13 km (Arnett, 1949; Dibblee, 1968a; Morton, 1975a, b), although subordinate fault splays account for another 2 or 3 km (Morton, 1975a, b).

Reckoning of displacement. In the reconstruction shown in Figure 11 and Plate II, a displacement of about 28 km is restored along the San Jacinto fault. Of the overall dextral displacement on the San Jacinto fault, 13 km has been documented to enter the southeastern San Gabriel Mountains, where it is absorbed by left-lateral faulting on the San Antonio Canyon and Stoddard Canyon faults (see Reconciliation and Synthesis section). The disposition of the remaining 15 km is not resolved but seems too large to be absorbed in compression associated with uplift of the San Gabriel Mountains. In Figures 8 through 11 and in Plate II, the remaining 15 km is passed onto the San Andreas fault east of the splays recognized in the southeastern San Gabriel Mountains by means of a stepping transfer mechanism (Matti and others, 1985; Morton and Matti, this volume), perhaps in combination with movement on a connecting fault buried beneath the San Bernardino basin.

Timing of movement. Movement on the San Jacinto fault zone began no earlier than about 5 or 6 Ma and probably no later than about 1.5 Ma (Fig. 13), although Morton and Matti (this volume) argue that movement on the fault began at about 1 Ma. The strata near the base of the San Timoteo badlands section contain the late Hemphillian Mount Eden mammalian fauna (Frick, 1921; May and Repenning, 1982) that is about 5 m.y. old on the basis of magnetostratigraphic correlation of these vertebrate faunal assemblages in fossil occurrences in Texas and Kansas (Lindsay and others, 1975). The estimate of 23 to 26 km of displacement of the strata containing the Mount Eden fauna is either slightly less than or the same as the overall displacement of older units. If this difference is real, then movement on the San Jacinto fault had begun by about 5 Ma; otherwise, it began later. The Bautista Beds of Frick (1921; see also Sharp, 1967), which accumulated during movement on the fault, include the 0.7-Ma Bishop ash bed (Merriam and Bischoff, 1975; Sarna-Wojcicki and others, 1984) and locally contain an Irvingtonian mammalian fauna (Hibbard and others, 1965) that is less than 2 m.y. old on the basis of magnetostratigraphic correlation of these vertebrate faunal assemblages in fossil occurrences in Texas and Kansas (Lindsay and others, 1975; Lundelius and others, 1987).

There is abundant geologic and seismic evidence that the San Jacinto fault is currently active (see, for example, U.S. Geological Survey, 1972; Sharp, 1981; Sanders and Kanamori, 1984; Hill and others, 1990; Wesnousky and others, 1991).

Elsinore fault. Path. The Elsinore fault transects the Peninsular Ranges from about the United States–Mexico border on the west side of the Salton trough to about Corona at the north end of the Peninsular Ranges (for discussions of nomenclature and histories of study of the fault zone, see Kennedy, 1977; Weber, 1977; Lamar and Rockwell, 1986). Just south of Corona, the Elsinore fault zone bifurcates northward into the Whittier and Chino faults.

Previous estimates of displacement. Measurements of right-lateral displacement of crystalline rocks along the Elsinore fault zone range from less than 1 (Mann, 1955; Gray, 1961) to about 40 km (Lamar, 1961; Sage, 1973a, b; Campbell and Yerkes,

1976). The most convincing measurements of displacement, however, lie in the range from about 5 to 11 km (Woodford, 1960; Sharp, 1966; Baird and others, 1970; Woodford and others, 1971; Kennedy, 1977; Weber, 1977; Johnson and others, 1983). Crystalline rocks interpreted by some investigators to limit strike-slip displacement along the southern part of the Elsinore fault to about 2 km (Todd, 1978; Todd and Hoggatt, 1979; Lowman, 1980) have been interpreted by others to comprise a landslide that partially covers the fault (Pinault, 1984; Rockwell and others, 1986).

Reckoning of displacement. In the reconstruction shown in Figure 11 and Plate II, a displacement of about 5 km is restored along the Elsinore fault.

Timing of movement. Movement on the Elsinore fault zone apparently began no earlier than about 5 or 6 and no later than about 1.5 to 2 Ma (Fig. 13). An abrupt facies boundary in an unnamed Pleistocene formation of sandstone and conglomerate is offset more than 5 km along one strand of the Elsinore fault (Kennedy, 1977). The unit contains cobbles of basalt derived from flows that were extruded at about 7 Ma (Morton and Morton, 1979) and an intrastratified ash that is correlated with the 0.7-Ma Bishop ash bed (Merriam and Bischoff, 1975; Sarna-Wojcicki and others, 1984). The unnamed unit has been correlated in part with the Temecula Arkose of Mann (1955) (see also Kennedy, 1977), which contains a late Blancan mammalian fauna (Golz and others, 1977) that is about 2 to 3 m.y. old on the basis of magnetostratigraphic correlation of a similar fauna found in fossil occurrences in Texas and Kansas (Lindsay and others, 1975; Lundelius and others, 1987). If the offset of the unnamed unit is the full displacement on the Elsinore fault, then movement began after 2 or 3 Ma.

There is abundant geologic and seismic evidence that the Elsinore fault is currently active (see, for example, Kennedy, 1977; Weber, 1977; Rockwell and Lamar, 1986; Hill and others, 1990).

Kinematic role of Peninsular Ranges faults in the evolving San Andreas fault system. Along with the San Andreas fault zone, the San Jacinto and Elsinore faults were associated with the opening of the Salton trough at the north end of the Gulf of California (Hamilton, 1961; Biehler and others, 1964; Hamilton and Myers, 1966; Lomnitz and others, 1970; Elders and others, 1972; Fuis and others, 1982; Fuis and Kohler, 1984; Sharp, 1982). Evidently, the San Jacinto fault and presumably the Elsinore fault as well evolved in conjunction with the left-lateral faults in the eastern Transverse Ranges and southern San Gabriel Mountains and with the growth of the deflection in the San Andreas fault through San Gorgonio Pass (Allen, 1957; Garfunkel, 1974; Crowell, 1981; Matti and others, 1985; Meisling and Weldon, 1989). The kinematic model incorporated into the reconstruction in Plate II is one in which sinistral faulting along the southern margin of the San Gabriel Mountains and along the Pinto Mountain fault and dextral faulting along the San Andreas fault mutually deflected one another. Coeval dextral faulting developed along the San Jacinto and Elsinore faults in the Peninsular Ranges block south of the sinistral fault zone in the San Gabriel Mountains. Displacement on the sinistral fault system kinematically absorbed the complementary right-lateral displacement on the Elsinore fault and about the first half of that on the San Jacinto fault. Ultimately, the San Andreas fault, as it was deflected, intersected the San Jacinto and the second half of displacement on the San Jacinto fault was transferred northward onto the San Andreas. As discussed above in the section on relative rotations of crustal blocks, it seems likely from the reconstruction that the domain of dextral faulting in the Peninsular Ranges remained fixed in orientation. If the current angle of intersection of about 25° between the San Jacinto and San Andreas faults has also remained constant since they were linked, then, from equation (1), displacement on the San Andreas fault increases by an amount equal to (14 km)cos 25°, or by 13 km, north of the intersection (see Fig. 15). The timing of movement on the various faults permits this scenario to have evolved in as little as the last 1.5 m.y. or as much as the last 5 m.y.

From their alignment, one might be tempted to infer a link between the Elsinore fault and the Vasquez Creek fault of the San Gabriel system, but such an inference is inconsistent with what is known about the timing of movement on the two faults.

Mojave Desert

Paths. The Mojave Desert crustal block has been sliced by numerous northwest- to north-northwest–trending, steeply dipping faults arrayed en echelon in a belt that reaches from near the Garlock fault in the northwest at least to the eastern end of the Pinto Mountains (Dibblee, 1961a; Garfunkel, 1974; Powell, 1981; Dokka, 1983) and probably from there through the southeastern Mojave Desert (Hope, 1966; Pelka, 1973; Rotstein and others, 1976; Powell, 1981; Stone and Pelka, 1989) and possibly across the Colorado River into Arizona (Miller and McKee, 1971; Sumner and Thompson, 1974; Powell, 1981). In the north-central Mojave Desert, these faults comprise zones of aligned faults, including the Helendale, Lockhart-Lenwood, Harper–Harper Lake–Camp Rock–Emerson, Blackwater–Calico–Mesquite Lake, and Pisgah-Bullion faults. Smaller faults, including the Old Woman Springs, Johnson Valley, Homestead Valley, and Galway Lake faults, splay off these major zones. The Ludlow and Bristol Mountains faults are two additional north-northwest–trending faults located in the east-central Mojave Desert. Identified and inferred northwest-trending faults in the southeastern Mojave Desert include the Sheep Hole fault and several unnamed faults within and bounding the Coxcomb, Palen, McCoy, Little Maria, and Maria Mountains. In southwestern Arizona, unnamed northwest-trending faults have been identified in the Plomosa Mountains and the area southeast of Yuma.

Previous estimates of displacement. Right-lateral displacement has occurred along the north-northwest–trending faults in the northwestern Mojave Desert (Dibblee, 1961a, 1967a, 1980; Hawkins, 1975; Miller and Morton, 1980; Miller, 1980; Powell, 1981, p. 334–336; Dokka and Glazner, 1982a; Dokka, 1983;

Dokka and Travis, 1990a), southeastern Mojave Desert (Hope, 1966, p. 102–104; Silver and others, 1977; Pelka, 1973; Powell, 1981, p. 336–338; Miller and others, 1982), and in southwestern Arizona (Miller, 1970; Miller and McKee, 1971; Sumner and Thompson, 1974). Most of the individual faults have accumulated displacements of less than 5 km, although a few have displacements of as much as 10 km. Garfunkel (1974) liberally estimated a cumulative dextral displacement in the range of 65 to 105 km on the faults in the northwestern Mojave Desert, whereas subsequent investigators have provided more conservative estimates of about 14 km (Miller, 1980, not including estimates for the Helendale and Bristol Mountains faults), 25 to 65 km (Powell, 1981, not including an estimate for the Bristol Mountains fault), and 26.7 to 38.4 km (Dokka, 1983). Dokka and Travis (1990a) tabulated observed displacements on dextral faults in the central Mojave Desert that summed to 28 to 40 km, and predicted an additional 39 km on the Bristol Mountains and Granite Mountains faults of the northeastern Mojave Desert based on their tectonic model, for total of about 65 km. These latter two faults lie east of the reconstruction in Plate II. Estimated dextral separation on the north-northwest–trending faults of the southeastern Mojave Desert sum to something in the range of 25 to 35 km (Powell, 1981), and cumulative right separation on the faults in southwesternmost Arizona includes 5 to 10 km on faults in the Plomosa Mountains (Miller and McKee, 1971) and 16 to 23 km on faults southeast of Yuma (Sumner and Thompson, 1974).

LEFT-LATERAL FAULTS

Transverse Ranges east of the San Andreas fault

Paths. R. T. Hill (1928, p. 144–146, Plate I/II) first depicted the easterly physiographic and structural trend in the eastern Transverse Ranges province, recognizing three prominent fault-controlled physiographic lineaments. Subsequent investigators have shown that the east-west physiographic grain of the province is controlled by several east-trending left-lateral strike-slip faults, the largest of which are 60 to 85 km long (Hope, 1969; Merifield and Lamar, 1975; Silver and others, 1977, Figs. 4-4, 4-5; Powell, 1981, p. 315–333, Plate I, 1982a).

From north to south, the principal throughgoing left-lateral faults in the eastern Transverse Ranges include the three recognized by Hill, now known as the Pinto Mountain, Blue Cut, and Chiriaco faults, and the Salton Creek fault (Plate I). The Pinto Mountain fault (Hill, 1928, p. 146; Allen, 1957; Bacheller, 1978) extends eastward from the Mission Creek fault of the San Andreas zone, through the southernmost San Bernardino Mountains, then along the northern margin of the Little San Bernardino and Pinto Mountains. The trace of the Pinto Mountain fault is marked by abundant evidence for the breakage of surficial deposits between its intersection with the Mission Creek fault and its junction with the Mesquite fault just east of Twentynine Palms (Allen, 1957; Dibblee, 1967e, f, 1968b; Bacheller, 1978). The lack of such evidence east of that junction led Dibblee (1975a, 1980, Fig. 8, 1982d) to conclude that the Pinto Mountain fault terminates at the Mesquite fault and Hatheway and West (1975) to conclude that it is deflected into the Pinto Mountains east of the junction. However, the continued linear escarpment along the northern front of the Pinto Mountains is seemingly controlled by a major fault, probably the buried eastward extension of the Pinto Mountain fault (Bassett and Kupfer, 1964, p. 40; Bacheller, 1978, p. 127–128; Powell, 1981, p. 317), and the relatively small displacement of crystalline rock patterns across east-trending faults within the range indicate that they are at most only splays of the Pinto Mountain fault.

The trace of the Blue Cut fault (Pruss and others, 1959; Hope, 1966, 1969) extends eastward from the central Little San Bernardino Mountains through the Hexie Mountains and Pinto Basin. The fault, exposed only in the vicinity of the Blue Cut in the Little San Bernardino Mountains, forms the central break in an array of faults responsible for Hill's (1928, p. 147) Eagle Mountain lineament.

The Chiriaco fault (Powell, 1975, 1981, 1982a) extends eastward from the northern Mecca Hills through Chiriaco Summit, Hayfield Lake, and Desert Center. The fault underlies alluvium in Shavers and Chuckwalla Valleys (Brown, 1923, p. 53, 238; Miller, 1944, p. 72), but may be responsible for linear shoreline segments of Hayfield Lake. The fault has also been referred to as the Orocopia lineament (Hill, 1928, p. 147–148; Merifield and Lamar, 1975) and the Hayfield fault (Dibblee, 1982h).

The Salton Creek fault (Crowell, 1962, Fig. 3; Crowe and others, 1979; Crowell and Ramirez, 1979; Powell, 1981, 1982a) extends eastward from the southern Mecca Hills up Salt Creek (Salton Wash) between the Orocopia and Chocolate Mountain, then transects the Chuckwalla Mountains along an unnamed wash between the wide northern part of the range and the narrow southern part. The fault is exposed along the north flank of the Chocolate Mountains along Salt Creek.

Shorter, less prominent faults are present between the major faults, some as splays. The Corn Springs Wash fault splays southeastward from the Chiriaco fault between the Orocopia and Chuckwalla Mountains and transects the latter range along Corn Springs Wash; similarly, the Niggerhead fault probably splays southeastward from the Pinto Mountain fault before curving eastward through the eastern Pinto Mountains.

Other subordinate faults do not connect with the throughgoing major faults. The Porcupine Wash and Substation faults and the Smoke Tree Wash and Victory Pass faults occur as two aligned pairs separated by about 3 to 5 km between the Blue Cut and Chiriaco faults, the Ship Creek fault occurs between the Corn

Springs Wash and Salton Creek faults, and the Graham Pass fault is located south of the Salton Creek fault. Although the Porcupine Wash and Substation faults and the Victory Pass and Smoke Tree Wash faults are aligned and their displacements are nearly equal, the two faults that make up each pair are separated by gaps of 12 to 13 km across which geologic units and contacts are not broken. The Porcupine Wash fault extends from the lip of the Little San Bernardino escarpment through the Hexie Mountains to the Pinto Basin Road, where it disappears within the alluviated granodiorite of the southernmost Pinto Basin; along strike, the Substation fault transects the east-central Eagle Mountains before disappearing beneath alluvium in Chuckwalla Valley. The Smoke Tree Wash fault, which underlies the east-west reaches of Smoke Tree Wash and Pinkham Canyon, dies out westward as it nears the Little San Bernardino Mountains and disappears eastward beneath alluvium; along strike, the Victory Pass fault transects the southeastern Eagle Mountains, where it controls much of the course of Big Wash before passing eastward beneath the alluvium of Chuckwalla Valley. The Ship Creek fault transects the Chuckwalla Mountains along Ship Creek, dying out in the western part of the range and passing east beneath alluvium in Chuckwalla Valley.

Small left-lateral displacements also have been proposed to accompany or follow reverse displacement on the Santa Ana and Cleghorn faults in the San Bernardino Mountains (Meisling and Weldon, 1982; Powell and others, 1983b). Oblique displacement with components of left and reverse slip makes the style of these faults more akin to coeval east- to northeast-trending faults in the Transverse Ranges west of the San Andreas fault than to the other left-slip faults east of the fault.

Displacements. Overall displacements on the left-lateral faults are well constrained by disrupted paleogeologic patterns in the Proterozoic and Mesozoic crystalline rocks of the eastern Transverse Ranges (Fig. 8, Plate II). Disrupted bedrock patterns in the eastern Transverse Ranges include northwest-trending belts of Proterozoic plutonic and metamorphic units of the Eagle and Hexie Mountains assemblages, Mesozoic plutonic units of the central and eastern plutonic belts, and northwest- and northeast-trending dike swarms, and the Orocopia Schist. For the major sinistral faults, reassembly of these features into their pre–late Cenozoic paleogeologic pattern indicate displacements of 16 km on the Pinto Mountain fault (within the range of 16 to 20 km measured by Dibblee, 1967b, 1975a, 1980, 1982d; Bacheller, 1978), 5 km on the Blue Cut fault (Hope, 1966, 1969; Powell, 1981, 1982a), 11 km on the Chiriaco fault (Powell, 1975, 1981, 1982a), 8 km on the Chuckwalla Mountains segment of the Salton Creek fault (Powell, 1982a), and as much as 14 km on the Salt Creek segment of the Salton Creek fault (Powell, 1991).

For the major faults, incremental displacement has been established only on the Pinto Mountain fault. By matching clasts of Jurassic porphyritic monzogranite in lower Quaternary fanglomerate in the Twentynine Palms area north of the Pinto Mountain fault to the nearest exposures of such monzogranite that could have been a source for the clasts in the Pinto Mountains south of the fault, Bacheller (1978) measured about 9 km of displacement on the Pinto Mountain fault since the deposition of the fanglomerate. About 7 km of displacement occurred prior to deposition of the fanglomerate.

For the subordinate sinistral faults, reassembly of the crystalline terrane into its pre–late Cenozoic paleogeologic pattern indicates overall displacements of about 2 km on the Niggerhead fault (Hope, 1966, 1969), 3 km on the Porcupine Wash and Substation faults (Hope, 1966; Powell, 1981, 1982a), 1 to 1.5 km on the Smoke Tree Wash and Victory Pass faults (Hope, 1966; Powell, 1981, 1982a), 2.5 to 3 km on the Corn Springs Wash fault (Powell, 1981, 1982a), and about 2 km on the Ship Creek fault (Powell, 1981, 1982a). In the San Bernardino Mountains, the Santa Ana fault shows 2.4 km of left separation of Early Proterozoic gneiss, upper Proterozoic quartzite, and Mesozoic quartz diorite (Powell and others, 1983b), and the Cleghorn fault exhibits 3 to 4 km of displacement, both of an antiformal axis in a crystalline terrane of foliated Mesozoic plutonic rocks and marble pendants and of a steeply dipping contact between the crystalline rocks and the lower and middle Miocene Punchbowl Formation of Cajon Pass (Meisling and Weldon, 1982, 1989; Weldon, 1986; Weldon and Springer, 1988).

In addition to the left-lateral displacement of crystalline bedrock patterns across the Blue Cut and Chiriaco fault zones, vertical displacement of late Cenozoic basalt flows and broad alluviated valleys provide evidence for young graben-like faulting associated with the strike-slip faults (Hope, 1966, p. 61, 67, 91, 92; Powell, 1981, Plate I) and for extension contemporaneous with shear in the province. Similarly, the Morongo Valley fault, branching south from the Pinto Mountain fault near its west end, appears to be a normal fault with the north side down. The Cleghorn fault, which formed as a reverse fault in the late Miocene, also may have experienced normal displacement in association with left slip in the Quaternary (Weldon and others, 1981; Weldon and Springer, 1988; Meisling and Weldon, 1989). This association of extension with sinistral shear in the eastern Transverse Ranges contrasts with a combination of compression and sinistral shear indicated by oblique reverse and left-lateral slip on coeval east-trending faults in the Transverse Ranges west of the San Andreas fault.

Timing and rates of movement. Although the magnitude of overall displacement on the left-lateral faults is well constrained by matching crystalline rock patterns, much of the evidence for the timing of that movement is less clear. The time of inception of faulting is especially difficult to ascertain. Because the Chiriaco and Salton Creek faults appear to truncate the Eocene Maniobra and the upper Oligocene and lower Miocene Diligencia Formations in the Orocopia Mountains and unnamed upper Oligocene and lower Miocene volcanic rocks in the Chuckwalla Mountains, movement on the left-lateral faults in the province is probably no older than middle Miocene in age. Although the Salton Creek fault has been inferred to have been a locus of intrusion for 30-Ma volcanic domes and to have been overlapped by 17-Ma basalt.

Relation to right-lateral faults of the San Andreas system. The evidence for timing of movement on the left-lateral faults of the eastern Transverse Ranges requires that their displacement accumulated coevally with that on the San Andreas fault. In accord with this interpretation, there is no evidence for a crosscutting relation between right-lateral strands of the San Andreas fault zone and any of the left-lateral faults in the eastern Transverse Ranges. In particular, at the intersection of the Pinto Mountain and Mission Creek faults, the two faults mutually deflect one another (Allen, 1957; Matti and others, 1985), indicating that they are coeval and interact with one another. Moreover, restoration of crystalline rock patterns does not permit those models in which the left-lateral faults in the eastern and western Transverse Ranges are displaced along the San Andreas fault (see, for example, Hope, 1966, p. 140–143; Jahns, 1973).

Rather than behave as a rigid block along the northeast wall of the San Andreas fault, the eastern Transverse Ranges block has deformed internally by rotation of subblocks along the left-lateral faults, and in changing shape, the block has been extended along the San Andreas fault (Fig. 16). Rotation of the sinistral fault blocks must be accompanied by lateral displacement along either the San Andreas fault or the boundary with the Mojave Desert,

The San Andreas fault serves as the west boundary against which the fault blocks of the eastern Transverse Ranges are rotated. If one requires that the northwest corner of the rotated domain remain in contact with the unrotated San Bernardino Mountains, then the rotation of the eastern Transverse Ranges fault blocks has contributed southeastwardly increasing right-lateral displacement to the San Andreas fault. The overall increase in displacement along the segment of the San Andreas fault that intersects the left-lateral faults is equal to the amount by

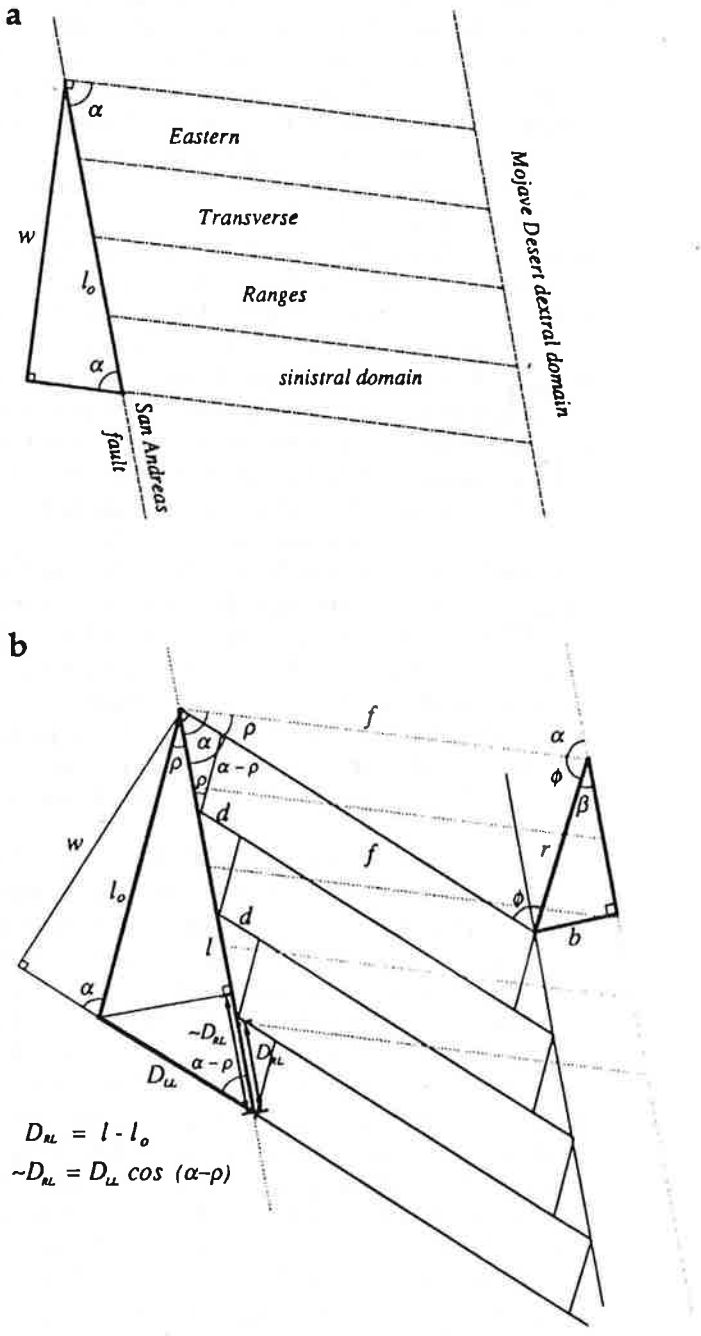

Figure 16. Fault-block rotation model for domain of clockwise rotation and sinistral faults of the eastern Transverse Ranges. For San Andreas system, this figure represents the interaction between the sinistral faults of the eastern Transverse Ranges and the San Andreas fault to the west and the Mojave Desert domain of dextral shear to the east. a, Initial orientation of faults. Symbols: α = initial angle of intersection between sinistral faults and left boundary of domain of clockwise rotation; w = width of domain of sinistral faulting; l_o = initial length of domain of clockwise rotation along its left boundary. b, Orientation of faults after clockwise rotation, superimposed on initial orientation. Symbols: ρ = angle of clockwise rotation; $\alpha - \rho$ = angle of intersection between sinistral faults and left boundary of domain of clockwise rotation after rotation; l = length of domain of clockwise rotation along its left boundary after rotation; D_{LL} = overall displacement on sinistral faults; D_{RL} = dextral displacement along left boundary of rotated domain, where upper left corner of rotated domain is held fixed; $-D_{RL}$ = approximation of D_{RL}; b = amount by which the eastern Transverse Ranges block has decreased in width as a consequence of clockwise fault block rotation. D_{RL} corresponds to additional displacement that occurs along the San Andreas fault as a consequence of clockwise rotation and sinistral faulting in the eastern Transverse Ranges; b corresponds with the magnitude of the bend in the San Andreas fault at the north end of the sinistral domain. See text for discussion.

Evolving San Andreas fault system

The palinspastic reconstruction in Plate II specifies the sequence of faulting and the interactions among various faults of the San Andreas system. The development of faulting required by the reconstruction provides new insight into the evolution of the San Andreas fault system as an intracontinental transform system.

Dextral shear accompanied by right-oblique extension probably occurred in southern California prior to movement on any throughgoing strike-slip fault (Powell, 1986; see also Weldon and others, this volume). The Pelona and Orocopia Schists have been uplifted in a train of right-stepping en echelon antiforms that prefigure part of the later course of the Clemens Well–Fenner–San Francisquito fault (Powell, 1981, p. 365, 369–372, Plates VI, VII). The antiforms, which developed along a tectonic belt that is delineated by en echelon(?) sedimentary and volcanic basins of Oligocene and early Miocene age, began growing in the late Oligocene or early Miocene, but also were active in the middle, and, perhaps, late Miocene. This tectonic belt shows evidence for dextral oroclinal bending of crystalline rocks units (Plate IIC) that occurred prior to movement on the Clemens Well–Fenner–San Francisquito fault and for pre–12 Ma clockwise rotation of late Oligocene and early Miocene volcanic rocks (Luyendyk and others, 1985; Terres and Luyendyk, 1985) that occurred prior to and/or during movement on the Clemens Well–Fenner–San Francisquito fault. The basins—including those in which the Simmler, Plush Ranch, Vasquez, Tick Canyon, and Diligencia Formations and the volcanic rocks of southeasternmost California accumulated—were bounded by normal faults and characterized by syntectonic deposition of coarse sedimentary breccia in terrestrial sections. The Tick Canyon and Diligencia Formations have yielded late Arikareean vertebrate fossils. Most of the volcanic rocks have yielded K-Ar ages that range from 26 or 25 to 23 or 22 Ma, although some ages from southeasternmost California fall in the range of 32 to 26 Ma and some in the range of 22 to 18 or 17 Ma. Thus, early dextral shear accompanied by extensional tectonism was distributed in a northwest-trending belt in southern California between 26 and 22 Ma and probably also between 32 and 26 Ma. This belt of dextral shear included the future path of the throughgoing, right-lateral Clemens Well–Fenner–San Francisquito fault.

The interval between 22 and 17 Ma was transitional between the early stage of distributed dextral shear and later stages characterized by the discrete, throughgoing strike-slip faults of the San Andreas system. The Clemens Well–Fenner–San Francisquito fault formed either during or at the end of this interval.

The Clemens Well–Fenner–San Francisquito fault, as a throughgoing strike-slip fault was the earliest manifestation of the San Andreas fault system in southern California. Prior to the formation of the San Gabriel fault, the Clemens Well–Fenner–San Francisquito–San Andreas fault accumulated a displacement of 100 or 110 km during some or all of the interval between about 22 and 13 Ma (Plate IIC to IIB). Either the Clemens Well–Fenner–San Francisquito fault formed at 22 Ma and moved at a relatively slow rate (~10 to 15 mm/yr) until 13 Ma, or it formed at 17 or 18 Ma and moved at a relatively fast rate (~20 to 30 mm/yr). The latter interpretation is favored by the evidence that the Diligencia Formation, which contains an Arikareean (-Hemingfordian?) vertebrate fauna and volcanic rocks as young as about 20 Ma, is fully displaced along the Clemens Well–Fenner–San Francisquito, San Gabriel, and San Andreas faults, and by Stanley's (1987) evidence that Saucesian strata in the Coast Ranges are offset by the full displacement of the San Andreas fault.

The Clemens Well–Fenner–San Francisquito fault was the active strand of the San Andreas fault system in southern California during the late early and early middle Miocene, and it formed a continuous structure with the early San Andreas fault zone northwest of Tejon Pass. This fault probably connected to the northward-migrating Mendocino triple junction at the north end of the San Andreas transform system. The Clemens Well–Fenner–San Francisquito fault is crosscut by the San Andreas fault proper in the Transverse Ranges, and diverges southeastward from that fault east of the Salton trough. The available evidence indicates that, unlike displacement on the younger San Andreas fault proper in southern California, displacement on the Clemens Well–Fenner–San Francisquito fault was not associated with the right-stepping system of transforms and spreading axes that, beginning around 4 or 5 Ma, accompanied the rifting of the Salton trough and the Gulf of California. The timing of movement on the Clemens Well–Fenner–San Francisquito fault is older than that of the seafloor spreading and most of the extensional tectonics in the gulf, and the southwestern end of the strike-slip fault does not merge into either the Salton trough or the gulf. Extensional faulting that occurred after 15 and before 13 Ma on Isla Tiburon (Neuhaus and others, 1988) and perhaps elsewhere in the southern part of the gulf (Henry, 1989) may have been coeval with movement on the Clemens Well–Fenner–San Francisquito fault, but no structural connection has been established.

Displacement on the Clemens Well–Fenner–San Francisquito fault is inferred to have stepped westward to the continental margin, where a dextral fault is postulated to have connected with the southward-migrating triple junction at the south end of the San Andreas transform system (cf. Campbell and Yerkes, 1976). The East Santa Cruz basin fault, which is inferred to have accumulated a right-lateral displacement of 180 km in the southern California continental borderland during the interval between 20 and 13 Ma (Howell and others, 1974; Howell, 1976), may be that fault. Movement on the Clemens Well–Fenner–San Francisquito fault probably accompanied both extension in southeasternmost California and southwesternmost Arizona, and sinistral kinking and faulting along the southern margin of the Transverse Ranges margin (Fig. 12c).

Although extensional tectonics began in the late Oligocene or early Miocene, prior to movement on the Clemens Well–Fenner–San Francisquito–San Andreas fault, as indicated both by syndepositional normal faulting and by widespread volcanism, detachment faulting continued through the early Miocene in both southeasternmost California and southwestern Arizona. Detachment led to truncation of the lower Miocene formations and eventually to exhumation of the Pelona and Orocopia Schists in the middle Miocene. The detachment faults are overlapped by middle Miocene units such as the Caliente and Mint Canyon

Formations in the Transverse Ranges and the fanglomerate of Bear Canyon of Dillon (1976) in the Chocolate Mountains. This timing is coeval with slip on the Clemens Well–Fenner–San Francisquito fault, and, hence, consistent with the suggestion that the detachment and strike-slip faulting are somehow related.

Between 22 to 20 and 18 or 17 Ma, a zone of sinistral deformation began to develop along the southern boundary of the incipient Transverse Ranges province and in southeasternmost California. During the interval from 17 to 13 Ma, left-lateral kinking and faulting were accompanied by extension and widespread volcanism in the western Transverse Ranges and vicinity (Yeats, 1968; Weigand, 1982) and in southeasternmost California and southwesternmost Arizona (Crowe and others, 1979; Shafiqullah and others, 1980; Frost and others, 1982; Murray, 1982; Tosdal and Sherrod, 1985; Sherrod and Tosdal, 1991). During the middle Miocene, this zone of deformation accumulated 50 to 80 km of sinistral displacement west of the present-day Los Angeles River and about 40 km east of the river. As much as about 40 km of this displacement may have been accommodated by kinking between 22 to 20 and 13 Ma and the rest by later faulting. This zone of sinistral deformation is postulated here to have formed between the southeastern terminus of the Clemens Well–Fenner–San Francisquito–San Andreas fault and the northwestern terminus of the dextral East Santa Cruz basin fault offshore in the continental borderland. Evidence for timing of deformation permits one to infer either that the left- and right-lateral faults and the zone of sinistral deformation developed synchronously or that the right-lateral faults developed slightly earlier.

In the Transverse Ranges, the San Gabriel fault system, including from oldest to youngest, the Canton, San Gabriel, and Vasquez Creek faults began to develop as a splay off the Clemens Well–Fenner–San Francisquito–San Andreas fault perhaps as early as 13 Ma (Plate IIB to IIA). The San Gabriel fault system has accumulated a displacement of 42 to 45 km since then, moving at an overall average rate of about 5 mm/yr and deforming the older fault in the process. Between about 13 and 10 Ma, a displacement of as much as 15 km accumulated on the Canton fault and its now-buried extension southward between the Santa Monica and Verdugo Mountains. Subsequently, between 10 and 5 Ma, the San Gabriel fault propagated southeastward through the southern San Gabriel Mountains, accumulating a displacement of 22 to 23 km, followed by 5 km on the Vasquez Creek fault. The San Gabriel fault system merged northwestward with the early San Andreas segment of the Clemens Well–Fenner–San Francisquito–early San Andreas fault, while movement ceased to the southeast on the Clemens Well–Fenner–San Francisquito segment of the fault.

To the south, at least about half of the displacement on the faults of the San Gabriel system is hypothesized to have been absorbed by clockwise fault block rotation in the sinistral domain of the Transverse Ranges west of the San Gabriel system and by left-oblique extension along the zone of sinistral deformation between the Transverse and Peninsular Ranges. The magnitude of the left-lateral faulting component of the middle Miocene deformation is difficult to assess, but if the hypothesized 40 km of kinking is real, then a displacement of only 10 to 40 km is required during the middle Miocene on the hypothetical ancestral Malibu Coast–Santa Monica sinistral fault, and no displacement is required on any eastward projection of that fault. The remaining 10 to 40 km of displacement (35 km in Plate II) inferred for the middle Miocene Malibu Coast–Santa Monica fault is a reasonable magnitude to be associated with a clockwise rotation of 50° in the sinistral domain of the western Transverse Ranges west of the San Gabriel system. This displacement, together with left-oblique extension associated with opening of the Ventura and Los Angeles basin, is enough to absorb a displacement of 20 km on the Canton and Vasquez Creek faults of the San Gabriel system. Presumably, right slip on the San Gabriel fault system stepped west via the domain of sinistral deformation to a dextral fault on the continental margin that connected to the southward-migrating triple junction at the south end of the San Andreas transform system.

The displacement of 22 to 23 km that follows the San Gabriel–Icehouse Canyon–Miller–Banning fault path of the San Gabriel system can be disposed of in two ways. Either it is transformed by left-oblique extension along the zone of sinistral deformation between the Transverse and Peninsular Ranges (Fig. 14b, Plate II), or it is linked with early rifting indicated by the deposition of upper Miocene marine strata at the north end of the "proto-Gulf" in the Salton trough–Gulf of California region (Fig. 14c). In the latter case, the San Gabriel–Icehouse Canyon–Miller–Banning fault is the first strike-slip fault to link the Mendocino triple junction with extension in the Gulf of California region that began as early as 15 to 13 Ma (Neuhaus and others, 1988; Henry, 1989), but most of which has occurred since about 12 or 13 Ma (Lonsdale, 1989; Stock and Hodges, 1989; Humphreys and Weldon, 1991).

In the Salinian block, the San Gregorio–Hosgri and Rinconada-Reliz faults developed coevally with the San Gabriel fault and also merged northwestward with the early San Andreas fault (=Clemens Well–Fenner–San Francisquito fault) (Plate IIB to IIA), but unlike the San Gabriel fault have continued to accumulate displacement since the end of the Miocene. To the southeast, displacement on the Salinian block faults terminates against the western Transverse Ranges and presumably are absorbed by sinitral deformation there. South of their junction, the San Gregorio-Hosgri and Rinconada-Reliz faults have displacements of 105 and 45 km, respectively. The combined displacement on the San Gregorio-Hosgri and Rinconada-Reliz faults north of Monterey Bay is about 150 km (Clark and others, 1984; Ross, 1984), which increases the overall displacement on the San Andreas fault proper to nearly 450 km between San Francisco and Point Arena. The San Gregorio-Hosgri and Rinconada-Reliz faults are largely responsible for extending the Salinian block along the San Andreas fault (Johnson and Normark, 1974).

The modern San Andreas fault developed at about 5 Ma (Plate IIA to Plate I). In southern California, the modern San

Andreas fault diverged eastward from the San Gabriel fault and crosscut the Clemens Well–Fenner–San Francisquito fault to merge southeastward with the Salton trough at the north end of the Gulf of California. The Punchbowl fault primarily served as an early fault strand in the anastomosing San Andreas fault zone along its Mojave Desert segment (Plate IIA to Plate I) (Dibblee, 1967a, 1968a, 1975b; Morton, 1975a, b; Barrows and others, 1985; Morton and Matti, this volume). In conjunction with the system of spreading axes and transform faults in the Gulf of California, the modern San Andreas fault provided a new transform link between the Mendocino triple junction to the north and the southern triple junction that had migrated south of the mouth of the gulf.

Despite its role as a transform fault, the long-term average slip rate on the post–5-Ma San Andreas fault proper is only about 20 to 35 mm/yr (Sieh and Jahns, 1984; Weldon and Sieh, 1985; Harden and Matti, 1989; Perkins and others, 1989; Prentice, 1989; Prentice and others, 1991; Weldon and others, this volume), which is roughly ½ to ¾ of the rate of plate motion between Baja California and the North American plate, most recently calculated at about 48 mm/yr (DeMets and others, 1987, 1990; Kroger and others, 1987; Ward, 1990). The deficit in slip rate and the resulting shortfall in overall displacement on the San Andreas fault are compensated by the growth of an auxiliary system of right- and left-lateral strike-slip faults since the inception of the modern San Andreas (see also Bird and Rosenstock, 1984; Weldon and Humphreys, 1986).

In southern California, faults that developed coevally with the San Andreas include the right-lateral San Jacinto and Elsinore faults west of the San Andreas fault in the Peninsular Ranges, right-lateral faults east of the San Andreas in the Mojave Desert and the Death Valley area, left-lateral faults in the Transverse Ranges both east and west of the San Andreas, and the left-lateral Garlock fault (Plate IIA to Plate I). The existence of these faults indicates that crustal blocks adjoining the San Andreas fault have not behaved rigidly, and the faults serve both to increase the magnitude of displacement measured along the San Andreas fault and to provide paths for displacement in addition to that measured on the San Andreas. The left-lateral faults east of the San Andreas fault have interacted both with conjugate right-lateral faults in the Mojave Desert and Death Valley area and with the San Andreas fault. Clockwise fault block rotation that accompanied left-lateral faulting in the eastern Transverse Ranges has contributed a component of displacement to the San Andreas fault and opened triangular holes along the San Andreas that have filled with Pliocene and Pleistocene strata, including those in the Mecca and Indio Hills. Interaction between the San Andreas and both the Pinto Mountain and Garlock faults has resulted in sinistral deflections in the trend of the San Andreas near San Gorgonio and Tejon Passes, respectively, where these deflections have been accompanied by contractional deformation. The San Jacinto and Elsinore faults interacted with the zone of sinistral deformation along the southern boundary of the Transverse Ranges; the San Jacinto fault also has interacted with the San Andreas. All of the displacement on the Elsinore fault and about the first half of that on the San Jacinto fault were absorbed by compensating left slip or left-oblique slip of as much as 10 km along the zone of sinistral deformation during the Pliocene and Quaternary. The remaining half of the displacement on the San Jacinto fault has been transferred to the San Andreas fault and contractional deformation in the southeastern San Gabriel Mountains. Since about 1.5 to 3 Ma, about 10 km left-oblique contraction has occurred along the southern flank of the San Gabriel Mountains and as much as a few tens of kilometers of contraction has occurred in the Transverse Ranges west of the San Gabriel fault.

COMMENTARY, FIRST DAY

The east-west-trending San Fernando Valley and the bounding ranges (Santa Susana and San Gabriel Mountains to the north, and the Santa Monica Mountains to the south) have come into existence within the past few million years as a result of generally north-south compression caused by movement of the San Andreas fault around its "big bend". As the San Fernando earthquake of 1971 reminded us, these mountains and valleys are still being formed. We live in an active mountain-forming tectonic setting.

Moving north along the 405 freeway, we encounter roadcuts through the Mission Hills that expose steeply inclined and faulted exposures of late Miocene marine shale and Pliocene marine and non-marine sandstone and shale. This region lay beneath marine waters until Late Pliocene time, about 3 million years ago.

About 3 miles north of the Mission Hills we enter the Santa Susana-San Gabriel Mountains. Steeply inclined and strongly deformed strata of the Saugus and Pico Formations which range in age from Pliocene to Early Pleistocene. A few miles along Highway 14, we pass the Placerita oilfield. Before reaching the next road summit we cross the hidden trace of the San Gabriel fault which is interpreted to be a major ancestral strand of the San Andreas fault system.

In another few miles we drop down into the Soledad basin in which is exposed the terrestrial Mint Canyon Formation. At and a few miles beyond Sand Canyon Road, note the striking angular unconformities between tilted Miocene strata and subhorizontal Pleistocene gravels that are exposed in the freeway roadcuts. At Aqua Dulce Road, the coarse conglomerates lie near the base of the Mint Canyon Formation. To the north this conglomerate horizon is progressively replaced by sandstone and shale, whereas to the south this conglomerate becomes even coarser. This distribution of rock types suggests a southern source for this part of the Mint Canyon Formation. This interpretation is supported by the observation that the clasts are of distinctive metamorphic and igneous rock types (especially anorthosite) that are only exposed in the San Gabriel Mountains to the south.

Just beyond Aqua Dulce turnoff, we enter exposures of the Vasques Formation that is composed of terrestrial sedimentary and volcanic rock.

Approximately 0.5 mi beyond Soledad Canyon exit we pass through exposures of the Lowe granodiorite, a 230 million year old intrusive widely exposed in the San Gabriel Mountains.

Late Cenozoic tectonics of the northwestern San Bernardino Mountains, southern California

KRISTIAN E. MEISLING *ARCO Oil and Gas Company, 2300 West Plano Parkway, Plano, Texas 75075*
RAY J. WELDON *Department of Geological Sciences, University of Oregon, Eugene, Oregon 97403*

ABSTRACT

The late Cenozoic structural and stratigraphic history of the northwestern San Bernardino Mountains supports two distinct episodes of uplift, in late Miocene to earliest Pliocene and Quaternary time, that we hypothesize are related to movements on low-angle structures beneath the range. In this paper, we document the nature, distribution, and timing of late Cenozoic deformation and deposition in the northwestern San Bernardino Mountains, and we illustrate the neotectonic evolution of the area in a series of interpretive paleotectonic block diagrams.

In the first episode of deformation, late Miocene to earliest Pliocene motion on the south-southwest–directed Squaw Peak thrust system disrupted drainage in pre-existing Miocene nonmarine basins and uplifted the western third of the present range to form the ancestral San Bernardino Mountains. Crystalline rocks of the San Bernardino Mountains were thrust southward across the present site of the San Andreas fault between 9.5 and 4.1 Ma, at a time when the San Gabriel fault was the active strand of the San Andreas transform system. We speculate that the Liebre Mountain crystalline block at the northern margin of the Ridge Basin may be the missing upper plate of the Squaw Peak thrust, now offset along the San Andreas fault.

The second episode of deformation began with uplift of the northern plateau of the modern San Bernardino Mountains on north-directed, range-front thrusts in early Pleistocene time, between 2.0 and 1.5 Ma. Synchronous uplift of the northern plateau, recorded in early Pleistocene fanglomerates on the northwestern margin of the range, is interpreted to be the result of movement of a relatively coherent crustal block northward up a south-dipping detachment ramp beneath the central range. In middle Pleistocene time, activity on the northern range front began to wane, and the locus of uplift shifted to a narrow zone of arching and northward tilting adjacent to the San Andreas fault, which subsequently migrated rapidly northwestward along the San Andreas fault from the western San Bernardino Mountains into the northeastern San Gabriel Mountains. We attribute this pattern of deformation to the passage of a bulge or strike-slip ramp attached to the southwest side of the San Andreas fault at depth.

The San Bernardino Mountains are the principal topographic expression of the Transverse Ranges province east of the San Andreas fault (Fig. 1). The northern San Bernardino Mountains are capped by a broad plateau of mature geomorphic landforms that stands 2 km above sea level, and 1 km above the floor of the Mojave Desert to the north. A narrow western extension of the range links the San Bernardino Mountains with the San Gabriel Mountains across the trace of the San Andreas fault. The southern San Bernardino Mountains are underlain by the San Gorgonio massif, which includes some of the highest peaks in southern California that stand more than a kilometer above the northern plateau and 2 km above San Gorgonio Pass to the south. All along the margins of the central and western range, steep canyons contrast sharply with the reduced mature landforms of the flat range crest, underscoring both the recency of uplift and the vigorous activity of structures marginal to the range. Existing tectonic models do not satisfactorily address the manner in which convergence along the San Andreas fault is translated into uplift in the central Transverse Ranges, nor do they adequately address the timing of this uplift as reflected in the rock record.

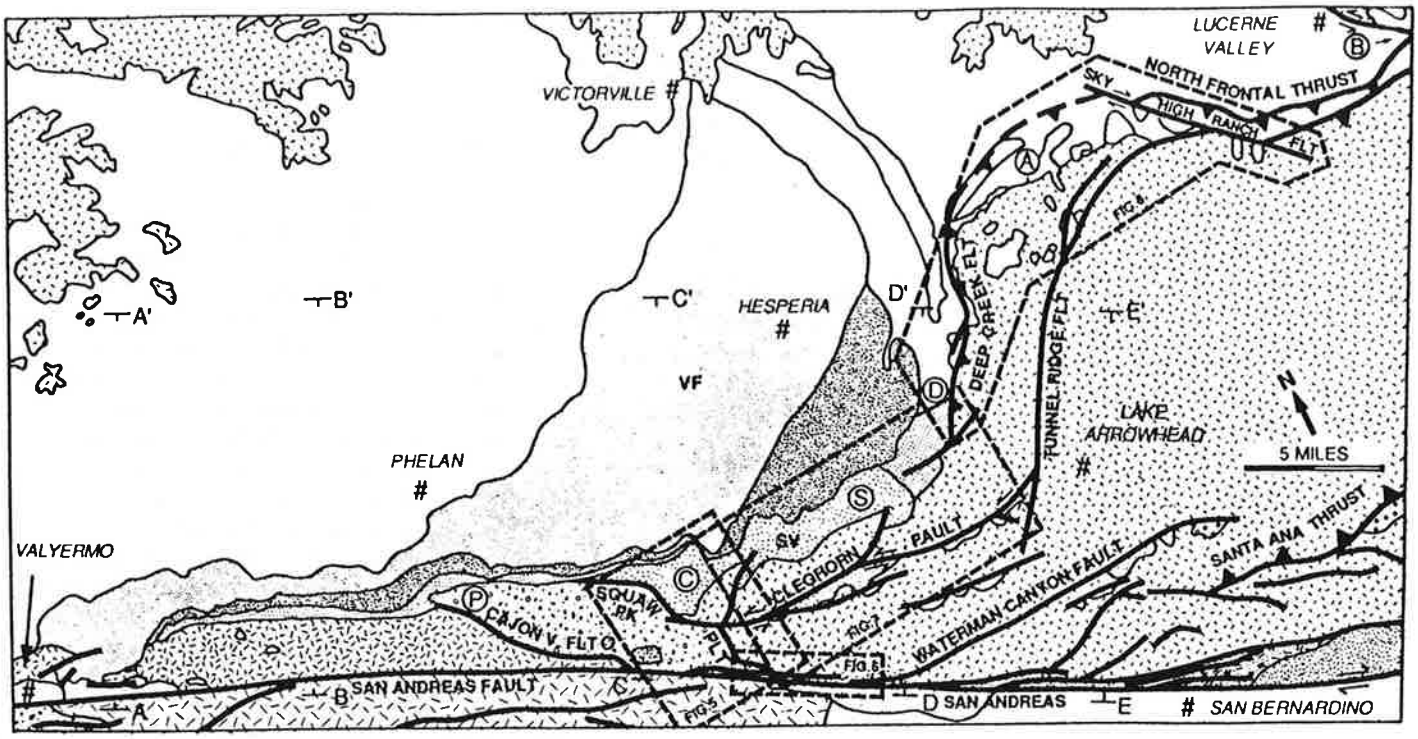

Figure 2. Simplified geologic map of the study area showing locations of regional cross sections of Figure 3, stratigraphic columns of Figure 4, and detailed geologic maps of Figures 5 through 8. See Figure 4 for key to geologic unit symbols. P: Phelan Peak column; C: Crowder Canyon column; S: Silverwood Lake column; D: Deep Creek column; A: Arrastre Canyon column; B: Blackhawk Canyon column (see Fig. 1); VF: Victorville fan; SV: Summit Valley.

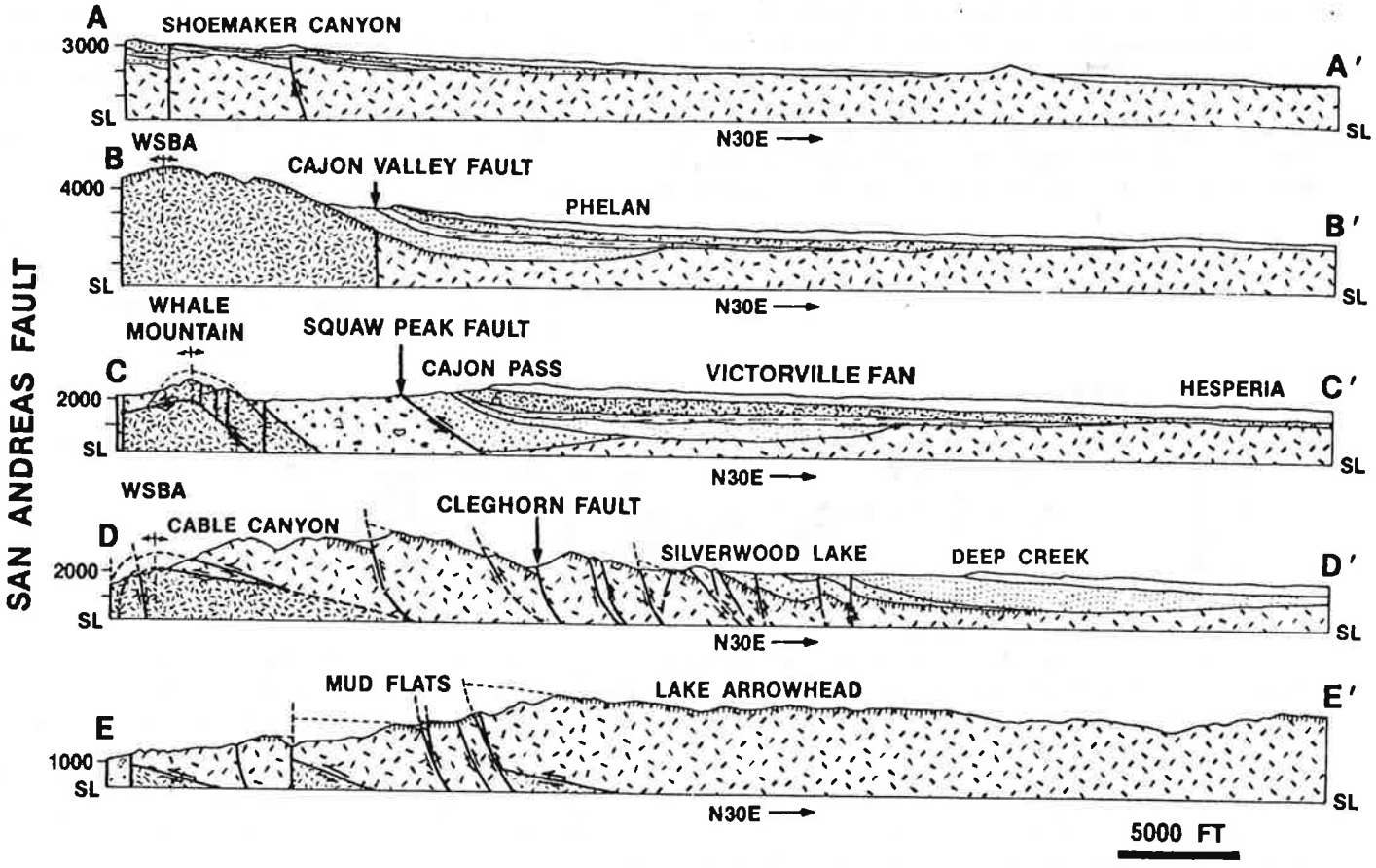

Figure 3. Regional cross sections trending northeast from San Andreas fault between Lake Arrowhead and Valyermo. See Figure 2 for location of lines of cross section, and Figure 8 for geologic unit symbols. San Andreas fault is at left edge of each section. Cedar Springs and Cleghorn faults are interpreted to flatten out into Squaw Peak thrust or deeper low-angle structures beneath the western San Bernardino Mountains. The Western San Bernardino arch (WSBA) deforms basement, late Cenozoic cover, and Squaw Peak thrust plane just northeast of the San Andreas fault. The northwestward migration of uplift associated with the WSBA is recorded in the Victorville fan, which was shed northeastward from the San Gabriel Mountains on the southwest side of the San Andreas fault.

Quaternary Structures

Quaternary structures in the northwestern San Bernardino Mountains can be grouped into two distinct deformational systems according to vergence, style, timing, and distribution. In early to middle Pleistocene time, uplift of the broad north-central plateau was associated with deformation on the North Frontal thrust system along the northern margin of the range. Starting in middle Pleistocene time, uplift shifted to the southern and western margin of the range. Middle to late Pleistocene uplift of the westernmost San Bernardino Mountains is expressed in a northwestwardly migrating locus of arching and tilting along the San Andreas fault called the "Western San Bernardino arch."

Early Quaternary Structures. Early to middle Pleistocene structures in the northwestern San Bernardino Mountains exhibit predominantly northward vergence. They are grouped together in this section to emphasize their collective role in the rapid early to middle Pleistocene uplift of the north-central plateau of the modern San Bernardino Mountains. This uplift is interpreted to have occurred on a deep-seated, north-directed thrust ramp and associated structures, herein named the "North Frontal thrust system." The North Frontal thrust system is made up of the North Frontal thrust zone, the Deep Creek fault zone, the Tunnel Ridge fault, and the Cleghorn fault (Fig. 8).

A system of Pleistocene thrust faults extends along the northern margin of the San Bernardino Mountains from Summit Valley to Old Woman Springs (Fig. 8; Santa Fe and Voorheis thrusts of Woodford and Harriss, 1928; Grapevine thrust of Shreve, 1968; White Mountain thrust of Sadler, 1981, and Meisling, 1984). Displacement on these thrusts appears to decrease away from the central range front on the basis of a systematic decrease in range-front relief westward from Lucerne Valley. Total shortening on the range-front thrust system is probably not more than a few kilometers (2–3 km, Baird and others, 1974; 4,000+ ft, Shreve, 1968, Pl. 1). Where exposed, thrust planes dip gently both south and north (Sadler 1981).

Thrusting on the northern range front began in early Pleistocene time (Vaughan, 1922, Woodford and Harriss, 1928; Shreve, 1968; Sadler 1981, 1982b), recorded by the dramatic change in provenance, texture and sorting from the Plio-Pleistocene fluvial-lacustrine Old Woman Sandstone to early Pleistocene marble fanglomerates of the Cushenbury Springs Formation (Shreve, 1968), both of which are overridden by the range front thrusts (Richmond, 1960; Sadler, 1981). A maximum age for the onset of thrusting at the range front is provided by the maximum possible age of the uppermost beds of the Old Woman Sandstone beneath the Cushenbury Springs Formation (Fig. 4), dated at 3.2–2.0 Ma (May and Repenning, 1982) based on mammalian fauna.

Monoclinal warps are associated with range-front thrusting. Southeast of Lucerne Valley, thrusts are deformed into a northeast-block–down northwest-trending monocline, with dips reaching 85° northeast in the Old Woman Sandstone (Shreve, 1968). Although thrusts generally dip south along the range front (Shreve, 1968, Pl. 1), surfaces are commonly observed to roll over and dip northward (Sadler, 1981; Meisling, 1984). Large landslides are common where thrusts have been warped and are dipping parallel to range-front slope (Shreve, 1959, 1968). Monoclinal warps are also commonly expressed in the early Miocene weathering surface along the range front (Meisling, 1984). The size of these range front warps suggests folding of foliated basement rocks above deep-seated structures.

Microseismicity data provide some insight into the possible nature of structures beneath the San Bernardino Mountains. The San Bernardino Mountains are characterized by a diffuse zone of microseismicity which roughly coincides with the area of the physiographic range (Corbett, 1984). The lower limit of this seismicity beneath the range defines a south-dipping plane descending from about 5 km beneath the Mojave Desert to about 12 km beneath the San Gorgonio massif, a distance of about 40 km (Fig. 9; Corbett, 1984). The seismicity "floor" suggests a 10° south-dipping zone of decoupling or contrast in mechanical behavior of the crust beneath the San Bernardino Mountains. The scale of this structure is such that 6 km of northward motion on it would result in 1 km of uplift across the entire northern plateau of the San Bernardino Mountains. We use this seismicity floor as a basis for locating our proposed deep crustal detachment in the discussion of tectonostratigraphic evolution that follows.

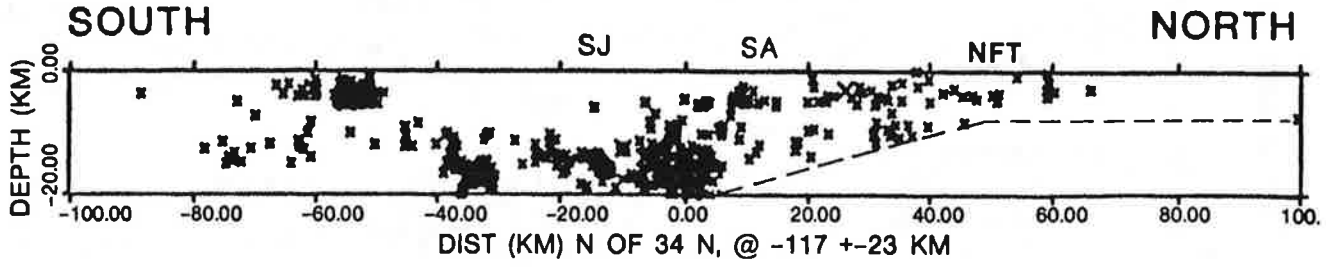

Figure 9. Microseismicity beneath the central San Bernardino Mountains. Cross section shows depth of seismic events of quality A from October 1981 to August 1983 projected to longitude 117° (the center line of the northern-central plateau; see Fig. 1) from the region between 116°45′ and 117°15′. SA and SJ indicate the location of the San Andreas and San Jacinto faults, respectively. NFT indicates the location of the North Frontal thrust system. Seismic events do not occur below a "floor" (dashed line) which rises from about 12 km beneath San Gorgonio Pass to less than 5 km beneath the Mojave Desert. Our proposed early Pleistocene detachment ramp coincides with the seismicity "floor," which is interpreted to reflect a contrast in mechanical behavior or decoupling in the upper crust. The seismicity ramp would project to the surface 20 to 30 km north of the north frontal thrusts; we postulate that it actually flattens and merges with a horizontal detachment plane at about 5 km beneath the Mojave block (figure adapted from Corbett, 1984).

The ~1,000-m-high escarpment in Lucerne Valley has developed since the end of deposition of the Old Woman Sandstone less than 2 m.y. ago, which requires an uplift rate of at least 0.5 mm/yr (1,000 m in a total of 2 m.y.). Scarps in alluvial surfaces that are tentatively considered ~0.5 m.y. in age, based on correlation with the older alluvium surface of the Victorville fan (Meisling, 1984), are generally less than 25 m in height. Taking the 25 m displacement of these ~0.5-m.y.-old alluvial surfaces into account, early to middle Pleistocene range-front uplift rates would be greater than 0.65 mm/yr (975 m in ~1.5 m.y.) in contrast with late Pleistocene rates of 0.05 mm/yr (25 m in ~0.5 m.y.). These admittedly crude estimates suggest a late Pleistocene decrease in rates of at least an order of magnitude, leading us to the conclusion that a pulse of uplift in early to middle Pleistocene time was followed by waning deformation on the northern range front.

Pleistocene uplift rates on the west flank of the Ord Mountains, crudely estimated from scarp heights in alluvial fans and the distribution of early Quaternary deposits, also suggest a dramatic decrease in deformation in late Pleistocene time. The 400-m-high western escarpment of the Ord Mountains largely developed since deposition of the Ord River deposits, which contains few clasts of Ord Mountain affinity, at about 1.5 Ma. This suggests an uplift rate of nearly 0.3 mm/yr (400 m in 1.5 m.y.). Scarps averaging about 50 m in height displace fans graded to the level of the older alluvium and estimated to be ~0.7 m.y. in age, yielding a late Pleistocene uplift rate of 0.07 mm/yr (50 m in 0.7 m.y.). If 50 m of uplift since 0.7 Ma is removed, middle Pleistocene uplift rates on the Ord Mountains range front exceed 0.4 mm/yr (350 m in 0.8 m.y.). Thus a change in style and decrease in rate of activity on the North Frontal thrust system accompanied the middle to late Pleistocene shift in the locus of uplift to structures nearer the San Andreas fault.

Implications for Uplift in the Central Transverse Ranges

Sadler and Reeder (1983; Sadler, 1981, 1982b) proposed that convergence in the San Bernardino Mountains is the surface expression of a basement-involved flower structure, drawing on analogous upwardly diverging fault geometries observed in both experimental and naturally occurring strike-slip systems (Wilcox and others, 1973; Bartlett and others, 1981). They cite (1) en echelon depositional trends of the Santa Ana Sandstone and Old Woman Sandstone, (2) symmetry of opposing frontal thrusts north and south of the range, and (3) the oblique orientation of the long axis of uplift relative to the trend of the San Andreas fault, as evidence consistent with the relationship predicted for compressional structures along a major wrench zone (Wilcox and others, 1973). If basins and structures developed in en echelon systems during growth of a flower structure, however, they should be roughly contemporaneous (Harland, 1971; Lowell, 1972; Wilcox and others, 1973). The wide range in age of depositional units and structural elements in the San Bernardino Mountains seems inconsistent with the symmetrical evolution of a simple flower structure. Furthermore, if south-directed thrusting on the Santa Ana thrust were a late Miocene or early Pliocene event contemporaneous with motion on the Squaw Peak fault system, it may be unrelated to the Quaternary uplift of the mountains.

Several authors have proposed deep-seated, low-angle faults beneath the Mojave Desert and San Bernardino Mountains to explain observed patterns of deformation in the eastern Transverse Ranges (Yeats, 1980, 1981; Powell, 1981; Silver, 1982). Hadley and Kanamori (1977) advanced a hypothesis in which the plate boundary in the upper mantle lies east of the crustal trace of the San Andreas fault in the region of the east-central Transverse Ranges and western Mojave Desert. Seismic first-motion studies (Webb and Kanamori, 1985) appear to confirm the presence of detachment-style earthquake events over a broad area, including the San Bernardino Mountains. If such detachment zones exist, it seems reasonable to assume that they might have interacted with the San Andreas fault during the uplift of the San Bernardino Mountains.

The migrating Quaternary pattern of deformation documented on the Western San Bernardino arch suggests that steps, ramps, or bulges in the San Andreas fault at depth may be as effective as surface restraining-bends in producing secondary compression. The observed pattern of migratory uplift implies that the causative bulge at depth is located near the north end of the San Jacinto fault, at its junction with the San Andreas fault. When the uplift of the San Bernardino Mountains began at 2 Ma, the north end of the San Jacinto fault was just southwest of the major restraining bend in the San Andreas fault in San Gorgonio Pass (see Fig. 1; assuming 50 km of offset on the San Andreas fault at 2.5 cm/yr). It has been suggested that the bend developed in response to left-lateral motion on the Pinto Mountain fault (Matti and others, 1985). It appears that the onset of rapid slip on the San Jacinto fault and the deflection of the smooth trace of the San Andreas fault by the Pinto Mountains fault are related. In our models, uplift of the north-central plateau was the first response to rapid convergence across the bend in the San Andreas fault, taking advantage of pre-existing low-angle structures within the San Bernardino Mountains and the Mojave Desert blocks. As the topographic load of the plateau became an impediment to further uplift, a shift in the locus of deformation to the southern margin of the range was favored. In time, the San Jacinto fault, which lies south of the San Andreas fault, and the Pinto Mountain fault, which lies north, became separated by motion on the San Andreas fault, localizing uplift in San Gorgonio Pass and the western wing at the northern terminus of the San Jacinto fault.

Thus, the hypothesized northeastward bulge of the lower San Andreas fault near the San Jacinto–Cucamonga–San Andreas junction may be the present-day subsurface expression of the left step that originated in San Gorgonio Pass due to motion on the Pinto Mountain fault. The Banning thrust would be the surface expression of the step, and the deep step is northwest of the San Jacinto termination. If one imagines rocks underlying the Mojave Desert moving southeast along the San Andreas fault, they would first be lifted up as they slid past the deep manifestation of the step under the western wing, then slide undeformed until they were uplifted again at the surface manifestation of the step near San Gorgonio Pass.

Implications for Offset on the Modern San Andreas Fault

Matti and others (1985) and Frizzell and others (1986) have noted the similarity between rocks in the Liebre Mountain area (Fig. 1) and the south-central San Bernardino Mountains. They proposed that the two masses have been offset by the San Andreas fault about 160 km. The strong similarity of the arcuate style and east-west trend of fault patterns in the Liebre Mountains crystalline block with those in the western San Bernardino Mountains also support the correlation. The Liebre Mountain thrust system, which bounds the Liebre Mountain crystalline block to the south, could be the offset portion of the Squaw Peak thrust. Movement on the Squaw Peak thrust system is constrained to have occurred between 9.5 and 4 Ma. The timing of movement on the Liebre Movement thrust system between 8 and 4 Ma (Ensley and Verosub, 1982) is consistent with motion on the Squaw Peak system. Although published cross sections of the Ridge Basin show the Liebre thrusts steepening with depth (for example, Crowell and Link, 1982), we speculate that this low-angle structure may project all the way to the San Andreas fault, and that the crystalline rocks of Liebre Mountain may be an allochthonous sheet from the San Bernardino Mountains.

Our hypothesis not only explains the origin of Mio-Pliocene relief in the ancestral San Bernardino Mountains, but also places this relief northeast of the Ridge Basin. This provides a ready source for Ridge Basin sediments which contain clast types attributed to sources in the San Bernardino Mountains and are inferred to have come from highlands to the northeast across the site of the San Andreas fault (Crowell, 1982). Ramirez (1983) has proposed that the late Miocene to Pliocene Hungry Valley Formation of the Ridge Basin was derived from the eastern San Bernardino Mountains. We suggest that a more likely source for the sediment in the Hungry Valley Formation is the western San Bernardino Mountains and Cajon Pass area, because the eastern part of the range was not uplifted until the Quaternary time. Uplift of the ancestral San Bernardino Mountains in late Miocene to Pliocene time provides the needed source, supplying debris derived from both the Miocene basins and underlying basement southward into the Ridge Basin.

Correlation of the Liebre Mountain fault with the Squaw Peak thrust, which supports the proposed match of basement rocks and total offset of 160 km on the modern San Andreas fault (Matti and others, 1985), opens up new possibilities for reconstruction of the San Andreas fault which incorporates significant horizontal displacements on low-angle structures. The difference between the observed offset of 160 km on the modern San Andreas fault and the widely cited offset of up to 270 km for the entire San Andreas system (Crowell, 1982, p. 30) requires that about 100 km of right slip be taken up on earlier structures (Powell, 1981). If any of these structures passed through the region of Squaw Peak thrusting, they may have been displaced and obscured by low-angle deformation.

PROVENANCE AND STRUCTURE OF LATE CENOZOIC SEDIMENTS IN THE NORTHEAST SAN BERNARDINO MOUNTAINS

Peter M. Sadler
Department of Earth Sciences
University of California
Riverside, California 92521

INTRODUCTION

The upland plateaus of the San Bernardino Mountains north of the San Gorgonio massif are dominated by outcrops of monzonitic and dioritic plutons. In this respect they resemble the ranges of the southernmost Mojave Desert. The main distinguishing feature is the extensive survival of roof pendants and septa, especially in the north central San Bernardino Mountains. Pendants comprising marbles, quartzites, and mafic gneiss and schist are largely confined to a wide, SE-trending belt from Ord Mountain through Onyx Peak. Such pendant materials extend only a short distance east of the Helendale fault system. In the lower, block-faulted parts of the range east of this fault zone, monzonites intrude gneiss and schist and are associated with leucocratic orthogneisses.

Pendants comprising marble and quartzite appear rarely and are rather small in the southern Mojave Desert. Their best development is seen north of Victorville. There they are associated with volcanic and metavolcanic units. The San Bernardino Mountains include almost none of the variety of volcanic rocks present in the southern Mojave Desert. There are only the small outcrops of a porphyry dyke system in Holcombe Valley (Richmond, 1960) and the late Miocene basalts (Neville and Chambers, this volume).

The differences in roof pendant and post plutonic rock types conveniently serve to distinguish the north central San Bernardino Mountains provenance from Mojave Desert sediment sources. It is also convenient and not coincidental, that the topographically lower areas peripheral to the high ground with marble and quartzite pendants include the best record of late Cenozoic sediments (Fig. 1). It is in these sediments that the provenance changes associated with the uplift of the San Bernardino Mountains will be recorded.

The relatively mildly dissected plateaus of the northern San Bernardino Mountains are evidently the product of young orogenesis (Vaughn, 1922; Dibblee, 1975). Therefore, when looking for the provenance changes indicative of this young uplift, we should expect the newly established source areas to have approximately their present relief. It will be important to consider both the compositional and the textural characteristics of sediments deliverable from the central San Bernardino Mountains. The modern stream sediments indicate the prevalence of granitoid debris, especially in the sand and granule fractions. Marble, quartzite or gneiss cobbles and boulders characterize most of the gravel fractions. These cobbles and boulders are typically poorly rounded. The quartzite clasts in particular remain sub-angular even after extensive, first-cycle transport by modern streams. Transport down Rattlesnake Creek to Old Woman Springs, or from Sugarloaf Mountain and down the Santa Ana River, provides good examples.

The following section catalogues the structural setting and sedimentological character of the crucial late Cenozoic stratigraphic sections around the area of uplifted quartzite- and marble-bearing roof pendants. Preliminary examination of them was made during a 1:24,000 quadrangle mapping project sponsored in part by the Regional Mapping Program of the California Divison of Mines and Geology (Sadler, 1981). A pattern emerges from this description, which includes frequent facies changes but striking similarities in structural setting. These aspects are discussed in the concluding sections.

LOCAL SYNOROGENIC SEQUENCES

Poorly consolidated, dominantly arkosic, sands and gravels of Miocene and Pliocene age associated with late Miocene basalts include the record of pre- and synorogenic provenance. Younger, surficial deposits, which are structurally less disturbed, relate more obviously to late or postorogenic drainage patterns. Structural differences between these two groups of late Cenozoic sediments serve to identify the mechanism of orogeny. Figure 2 summarizes the crucial local sequences of sedimentary and structural relationships. They are discussed below, beginning with the northern range front where the sequence is best exposed and was first appreciated. The discussion then moves south to consider evidence exposed along an east-west tract from the Santa Ana River to Pioneertown. Finally attention is drawn to the rather sporadic but critical occurrences recently discovered between those two tracts.

Northern Range Front

Over 50 years ago Woodford and Harriss (1928) described the unparalleled window into range-front structure provided by the incision of Blackhawk Canyon. They described thrust faults which have carried the marbles and gneisses of the San Bernardino Mountains basement over Tertiary sandstones later termed Old Woman Sandstone (Richmond, 1960; Shreve, 1968).

Old Woman Sandstone

The numerous, structurally dislocated outcrops of the Old Woman Sandstone are the key to mapping Cenozoic structures along the range front. Unfortunately, the unit is easily obscured beneath more resistant colluvium from the overriding basement rocks. It must be mapped carefully. Its outcrop pattern as confirmed by shallow excavation is more extensive than most maps suggest (Sadler, 1981). Around the area of its initial description at Blackhawk Canyon, the Old Woman Sandstone is predominantly a buff-colored, frequently cross-bedded, pebbly arkose with clasts of gneissic and

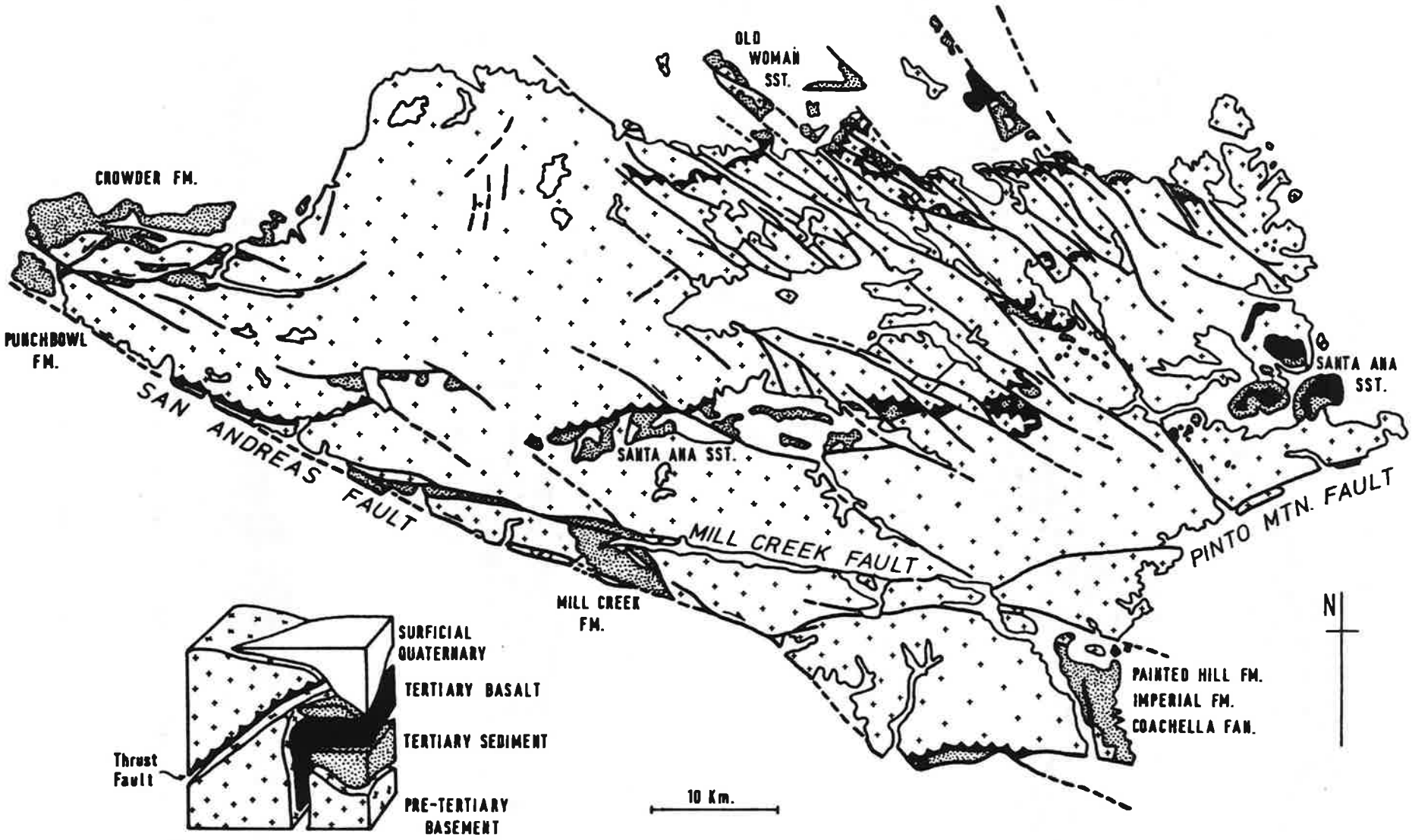

Figure 2. Tertiary sediments and volcanic rocks of the San Bernardino Mountains. After: Allen, 1957; Rogers, 1967; Gibson, 1971; Woodburne and Golz, 1972; Morton and Miller, 1975; Foster, 1980; Sadler, 1981; Weldon and others, 1981; Strathouse, this volume.

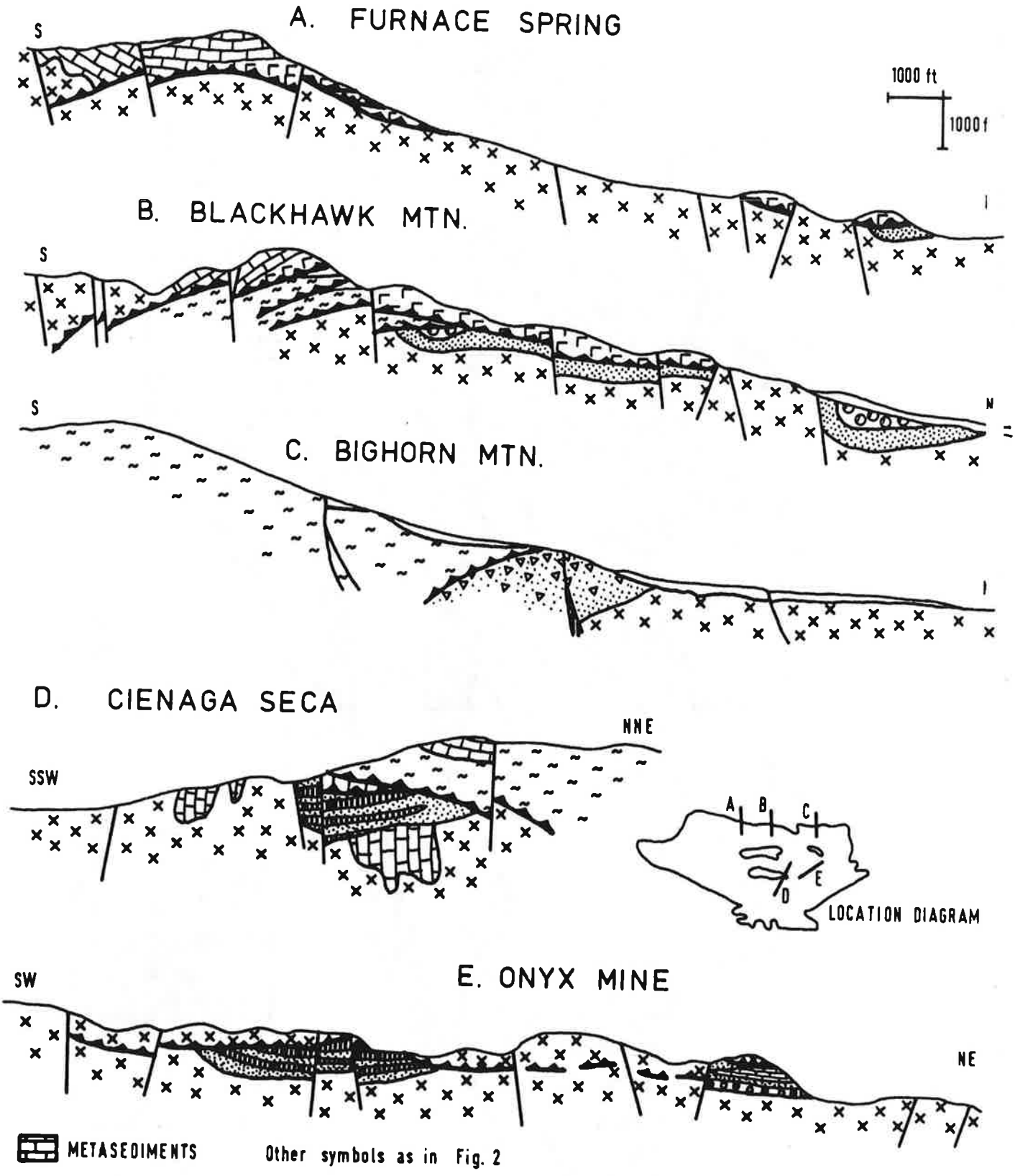

Figure 3. Structure sections through the thrust faults.

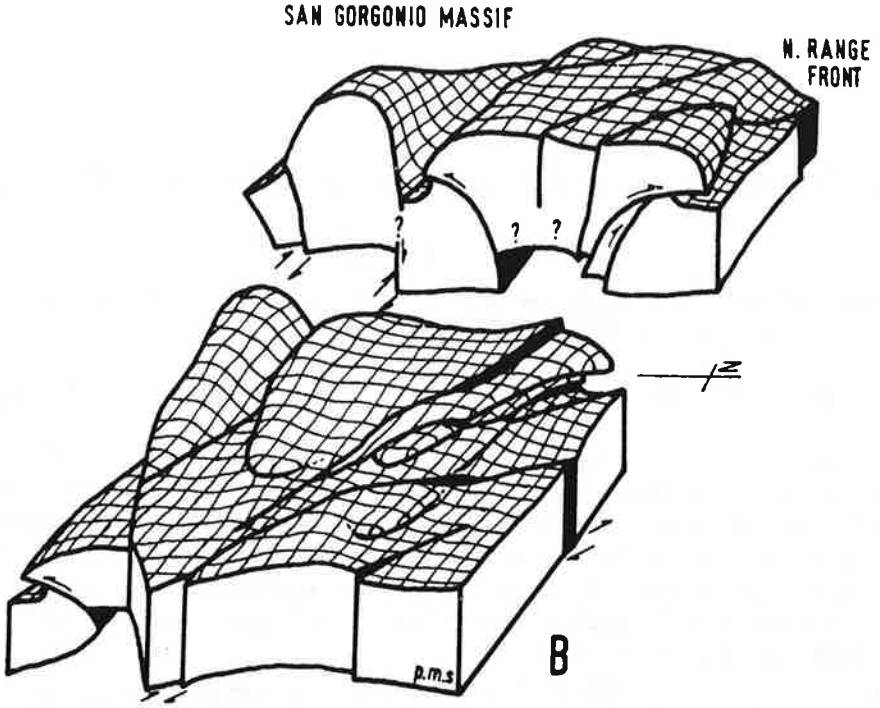

B: Schematic diagram of the thrust geometry in the San Bernardino Mountains.

plutonic basement rocks and abundant basalt cobbles and boulders. Since the nearest basalt outcrops are off to the west, and because basalt clasts are quite rare in the surficial deposits, the Old Woman Sandstone can be traced best by digging through colluvium wherever it contains basalt fragments.

Following Dibblee (1964, 1967) the Old Woman Sandstone can be extended east and west from the type outcrops described by Shreve (in Richmond, 1960). In both directions there are major facies changes, so the type area is termed the central facies (Fig. 2b). The typical central facies is dominated by up to 800 ft of pebbly, basalt-bearing, buff-red arkoses. Silty beds appear toward the northwest and include vertebrate fossils, but the most significant lithological changes are found at the top and bottom of the formation.

The central facies of the formation often begins with a brown arkosic wacke which is probably residual. The lowest arkosic arenites include a relatively high proportion of large gneissic clasts as well as a few quartzites and coarse, white marble clasts. These two metasedimentary clast types are conspicuously absent through the bulk of the formation. The oldest part of the central facies records the erosion of minor metasediment pendants from a monzonite, migmatite and gneiss terrain. The metasediment sources seem to have been rapidly exhausted. In the higher parts of this facies clasts of two types of basalt appear. Both can be derived from the east and southeast. The source area must have had the character of the present southernmost Mojave Desert, or the low northeast ramp of the San Bernardino Mountains, which is not very different. The central San Bernardino Mountains cannot have occupied their present proximal position during deposition of this part of the central facies.

The arrival of a nearby, San Bernardino Mountains source is strikingly recorded at the top of the formation by abrupt conformable influxes of coarse, almost monolithologic, marble-cobble conglomerates. These conglomerates include the fuller range of marble types available in the mountains now immediately to the south, and are texturally comparable with younger range-front fan deposits in the same area. Shreve (1968) included these conglomerates with the younger fanglomerates and slide deposits of his Cushenbury Springs Formation. But the conglomerates interfinger with type Old Woman Sandstone arkoses, include basalt clasts, and are structurally quite distinct from the fanglomerates that cover them unconformably. The conglomerates should be separated from younger fans, and are here regarded as an upper member of the Old Woman Sandstone.

PATTERNS OF PROVENANCE

The late Cenozoic local stratigraphies found in the lower ground peripheral to the north central San Bernardino Mountains repeat a simple history of provenance. The locally-derived clast suites, with compositions and textures appropriate to a post orogenic source are almost entirely restricted to the young surficial deposits.

The earlier arkoses have a provenance comparable to the southernmost Mojave Desert and the low eastern ramp of the mountains. They include locally-derived basalt clasts and arkosic grus, with an admixture of quartzite and porphyry clasts attibutable to the southern Mojave Desert. Presumably there was an eastern drainage route from the Victorville area, subordinate to that which fed the Punchbowl and Crowder deposits to the west. The route must have been established before the late Miocene basalt eruptions. Apart from these anomalous clasts the preorogenic sediments are a patchwork of variable facies and thickness indicative of small local basins and, probably, modest intervening ranges. The sediments certainly lack the full clast suites and textures attributable to the currently proximal mountains.

Blackhawk landslide, southwestern San Bernardino County, California

Ronald L. Shreve, Department of Earth and Space Sciences and Institute of Geophysics and Planetary Physics, University of California, Los Angeles, California 90024

LOCATION AND ACCESSIBILITY

The Blackhawk landslide is located in southeastern Lucerne Valley at the southern edge of the Mojave Desert 85 mi (135 km) east of the Los Angeles, California, civic center. It lies across the eastern half of the line separating the Cougar Buttes and Big Bear City, California, U.S. Geological Survey 7½-minute Topographic Quadrangles. Its distal (lower) end is readily apparent on both the map and the ground near 34°25′N, 116°47′W.

The easiest way to reach the landslide is to take I-15 to Victorville, then California 18 east through Apple Valley, approximately 25 mi (40 km) to the center of the town of Lucerne Valley, and finally County Highway 247 (CH247, Fig. 1) east 8.7 mi (13.9 km) to its intersection with Santa Fe Road (SFR, Fig. 1). The steep, gray, 50-ft (15-m) scarp approximately 2,000 ft (600 m) to the southeast is the distal edge of the landslide. It can most conveniently be visited on foot either from the prospectors' road (moderate clearance or four-wheel drive advisable) that enters the highway at Santa Fe Road or from the highway itself about 0.6 mi (1.0 km) farther east. Features along the west side of the landslide can be reached along Blackhawk Canyon Road (BCR, Fig. 1; moderate clearance or four-wheel drive advisable), which crosses the highway 1.05 mi (1.7 km) west of the Santa Fe Road intersection. Features within the landslide lobe can be reached by taking Blackhawk Canyon Road south from the highway 1.05 mi (1.7 km) to the remains of a jeep trail that goes eastward, following it (four-wheel drive strongly advisable) to the dry wash nearest the landslide, and driving up the wash. Alternatively, these features can be visited on foot by hiking from the roads to the west and south. Features of the proximal (upper) part of the landslide can best be reached by taking County Highway 247 east from the Santa Fe Road intersection 3.25 mi (5.2 km) to a well-graded mine road marked by a large white marble boulder, then taking the mine road (low hill on right 4.4 mi (7.1 km) from highway is eastern lateral ridge of Silver Reef landslide) southwest 5.3 mi (8.5 km) to a prospectors' road (intersection about 1,400 ft (425 m) northeast of Round Mountain), next taking the prospectors' road (moderate clearance or four-wheel drive advisable) west approximately 0.25 mi (0.4 km) to where it crosses another similar road, and finally taking the other road northwest 1.6 mi (2.6 km) to the mouth of Blackhawk Canyon (BCM, Fig. 2). Features in the vicinity can be visited either on foot or, in most cases if road conditions permit, by vehicle (moderate to high clearance and low gear or four-wheel drive advisable). Good views of the landslide lobe on the alluvial slope and of its source area on Blackhawk Mountain can be obtained from the mine road (high clearance and low gear or four-wheel drive strongly advisable) that climbs the ridge just east of Blackhawk Canyon (VP, Fig. 2).

An ample supply of fuel and water should always be carrie in the area, regardless of season. Only County Highway 247 an Santa Fe Road are regularly maintained. All other roads and trails are unpatrolled and are only sporadically maintained by tl local ranchers, miners, and prospectors, so they can, and often d change drastically in condition or even location.

SIGNIFICANCE OF SITE

The Blackhawk is among the largest landslides known Earth, although it is small compared to some on Mars. It is th type example for a class of relatively rare large landslides that Shreve (1966, p. 1642; 1968a, p. 37–38) proposed slid on a lay of trapped, compressed air, in order to explain not only their hi speed, low friction, and long runout but also their special peculiarities of form and structure, which are nearly all outstanding exemplified at this site. The mechanism is still controversial, anc variety of alternatives to air-layer lubrication have been proposed: simple unlubricated sliding (McSaveney, 1978, p. 232; Cruden. 1980, p. 299); sliding lubricated not by air but by water-saturat mud (Buss and Heim, 1881, p. 145; Voight and Pariseau, 197 , p. 31; Johnson, 1978, p. 502–503), by frictionally melted ice, snow, or rock (Lucchitta, 1978, p. 1607; Erismann, 1979, p. 3 by frictionally vaporized ice, snow, or ground water (Hab 1975, p. 194; Goguel, 1977, p. 697–698), or by carbon dioxide from disassociated carbonate rock (Erismann, 1979, p. 34); a "thixotropic" fluidization of the debris by interstitial water, air, dust (Heim, 1932; Kent, 1966, p. 82; Hsü, 1975, p. 135; Lucchitta, 1979, p. 8111), by intergranular impacts (mechanical fluidization, or inertial grain flow; Heim, 1882, p. 83; Hsü, 19 1975, p. 134; Davies, 1982, p. 14), or even by intense sou waves (acoustic fluidization; Melosh, 1983, 1979, p. 7513). The Blackhawk-type landslides and many of these mechanisms ha also been invoked, in most cases equally controversially, in c nection with large volcanic debris avalanches (Siebert, 1984, p. 180), pyroclastic flows (Sparks, 1976, p. 175), underwa debris flows (Foley and others, 1978, p. 115), Tertiary megabr cias (Brady, 1984, p. 145, 152; Kerr, 1984, p. 239), the cryptc Heart Mountain structure in northeastern Wyoming (Hsü, 1969, p. 945; Kehle, 1970, p. 1649), the Tsiolkovsky Crater ejecta l on the Moon (Guest, 1971, p. 99; Guest and Murray, 19 , p. 133), and the huge landslides (as much as 60 mi (100 km) of runout) and rampart craters of Mars (Lucchitta, 1978, 19 ; Schultz and Gault, 1979, p. 7681).

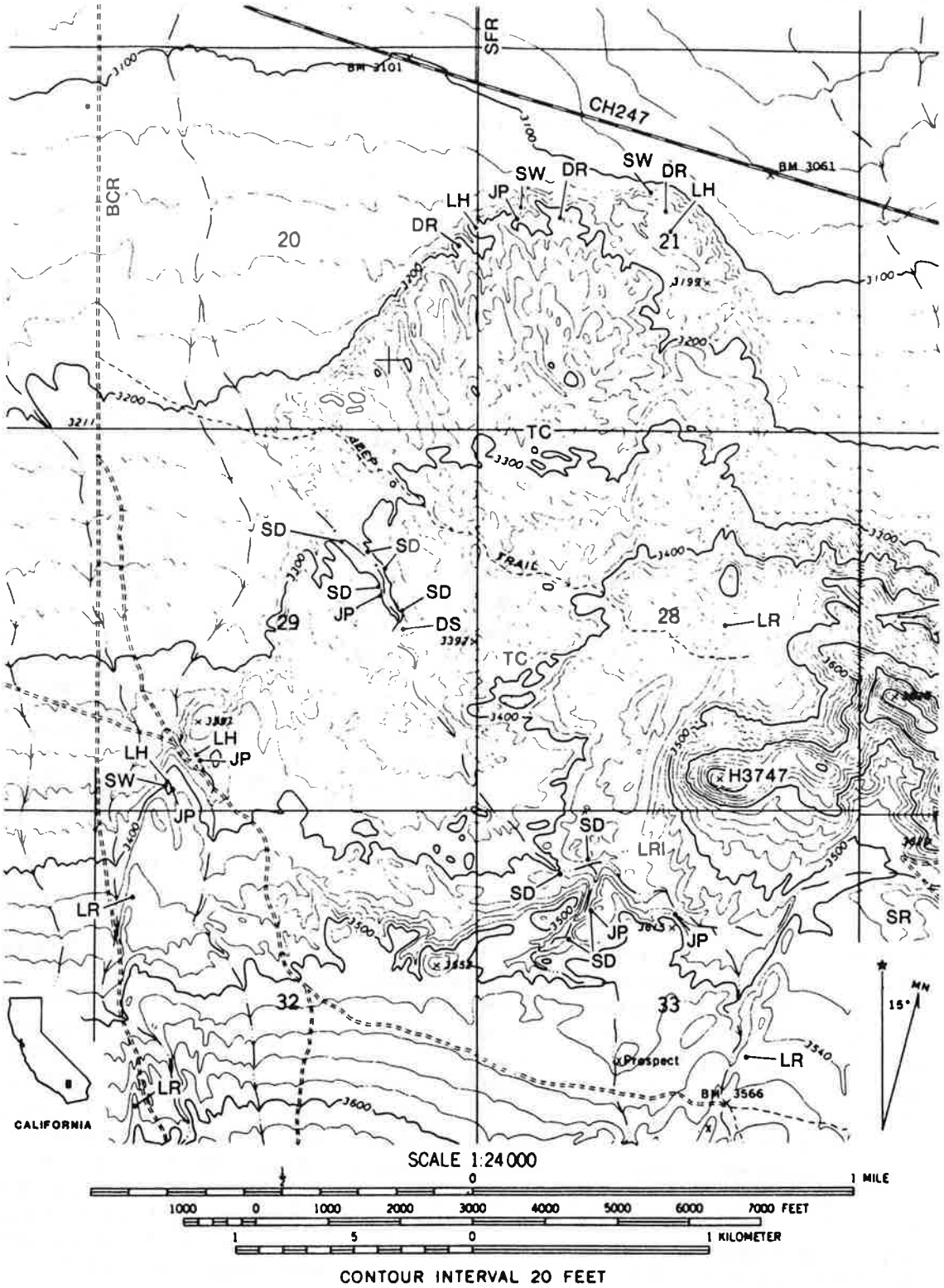

Figure 1. Distal part of Blackhawk landslide. DR, distal rim; DS, dated shells; JP, three-dimensional jigsaw-puzzle structure; LH, local homogeneity of debris; LR, lateral ridge; LRI, interior lateral ridge; SD, crushed-sandstone dike; SW, crushed-sandstone wedge; TC, transverse corrugations. JP, LH, LR, and TC are also present at many unlabelled localities. BCR, Blackhawk Canyon Road; CH247, County Highway 247; H3747, Hill 3747; SFR, Santa Fe Road; SR, Silver Reef landslide. Base map from U.S. Geological Survey Cougar Buttes, California, 7½-minute Topographic Quadrangle, 1971. Contour interval 20 ft (6.1 m).

SITE INFORMATION

The Blackhawk landslide was first recognized by Woodford and Harriss (1928), who described many of its peculiarities of form and structure and suggested that it was a debris outrush like the landslide of 1881 at Elm, Switzerland (Buss and Heim, 1881; Heim, 1882). It was studied in detail by Shreve (1968a), who likened it not only to the Elm landslide but also to the landslide of 1903 from Turtle Mountain at Frank, Alberta, Canada (McConnell and Brock, 1904; Daly and others, 1912), to the landslide of 1964 on the Sherman Glacier near Cordova, Alaska (Shreve, 1966; McSaveney, 1978), and to an adjacent older landslide, the Silver Reef (SR, Figs. 1 and 2; Shreve, 1968a, p. 16, 30, and Plate 2, facing p. 28). It was briefly restudied by Johnson (1978), who confirmed the previous observations and discovered sandstone dikes intruded upward into the distal parts of the landslide lobe, and by Stout (1977, p. 102–103), who obtained a radiocarbon age of 17,400 ±550 yr from fresh-water gastropod and pelecypod shells found in calcareous-mudstone pond deposits on the landslide surface (DS, Fig. 1).

The landslide originated as a huge rockfall from the summit of Blackhawk Mountain, which consists of resistant marble thrust northward over uncemented sandstone and weathered gneiss. It fell 2,000 ft (600 m) vertically and 7,000 ft (2,000 m) northward to the mouth of Blackhawk Canyon (BCM, Fig. 2), where it debouched onto the alluvial slope to form a narrow, symmetrical lobe of nearly monolithologic marble breccia 30 to 100 ft (10 to 30 m) thick (estimated), 1 to 2 mi (2 to 3 km) wide, and 5 mi (8 km) long. Its volume is 1×10^{10} ft^3 (3×10^8 m^3).

The edges of the proximal 3 mi (5 km) of the lobe (that is, the part nearest the source) are bounded by straight, narrow lateral ridges (LR, Figs. 1 and 2), like levees, that rise 50 to 100 ft (15 to 30 m) above the surrounding terrain. In places, the major ridge is accompanied, usually on its interior side, by parallel subsidiary lateral ridges (LRS, Fig. 2). The edge of the distal 2 mi (3 km) of the lobe is bounded by a somewhat sinuous scarp about 50 ft (15 m) high, whose crest generally rises a few feet (2–3 m) above the nearby landslide surface to form a definite distal rim (DR, Fig. 1). The surface of the lobe, where it is not buried by later alluvial fan gravels, is covered with low rounded hills and small closed basins with about 10 to 30 ft (3 to 10 m) of local relief. In the distal 2 mi (3 km) of the lobe these hills and valleys are elongate and form a strong pattern of transverse corrugations (TC, Fig. 1). The higher hills on the landslide lobe probably reflect underlying gneiss knobs that projected above the former alluvial surface. The most prominent of these is Hill 3747 (H3747, Fig. 1) near the eastern edge of the lobe about 2 mi (3 km) from its distal end, which blocked the progress of the landslide across a zone 1,500 ft (500 m) wide. The subparallel ridges on the western and southwestern slopes of the hill doubtless are interior lateral ridges (LRI, Fig. 1) that were successively formed and abandoned as the unimpeded middle region of the landslide adjusted to the arrested motion of the debris ascending the hill.

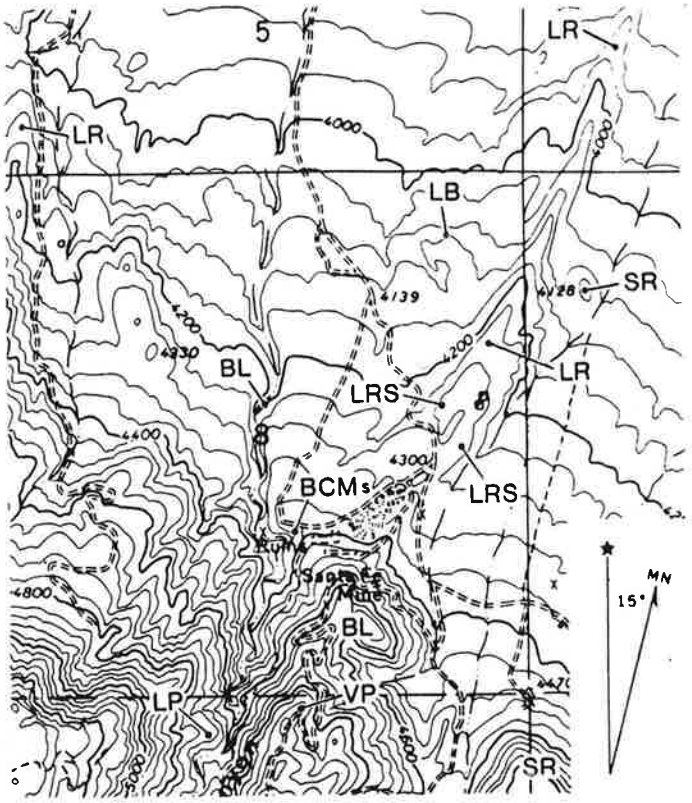

Figure 2. Proximal part of Blackhawk landslide. BL, base of landslide debris; LB, largest block on landslide; LP, launch point; LR, lateral ridge LRS, subsidiary lateral ridge. BCM, mouth of Blackhawk Canyon; SR, Silver Reef landslide; VP, view point. Base map from U.S. Geological Survey Big Bear City, California, 7½-minute Topographic Quadrangle 1971, photorevised 1979. Map scale same as in Figure 1; contour interval 40 ft (12.2 m).

The landslide lobe consists almost exclusively of crushed marble. The individual fragments are roughly equant, and range in size from powder to about 10 in (250 mm), the most common (that is, the modal) diameter being approximately 1 in (25 mm). A few exceptionally large blocks of a well-cemented older breccia range up to 35 ft (11 m) in maximum dimension (LB, Fig. 2). Neither the size distribution nor the lithologic characteristics of the fragments varies systematically with position on the landslide lobe. Locally, however, the debris tends to consist predominantly of a certain size of fragment or variety of rock; that is, it displays local homogeneity (LH, Fig. 1). In many places the fragments in roughly lenticular zones up to 20 ft (6 m) across are all pieces of a single source block that are loosely fitted together, giving a distinctive three-dimensional jigsaw-puzzle structure (JP, Fig. 1), in which color bands, for example, continue from fragment to fragment without significant offset.

Along the distal end and western edge of the landslide, the marble debris is nearly everywhere underlain by a wedge of crushed sandstone (SW, Fig. 1) and minor gneiss that was transported more than 4 mi (7 km) down the alluvial slope. The contact between the two generally dips toward the interior of the

landslide, normally is marked by up to 6 in (150 mm) of clayey green gouge, and is quite sharp, although in places scattered angular fragments of marble are mixed with the crushed sandstone within about 1 to 2 ft (0.5 m) of the contact. At the distal end of the lobe, several mildly contorted layers of marble debris as much as several feet (a few meters) thick, alternating with thinner layers of crushed sandstone and gneiss in sheared contact, overlie the sandstone wedge and extend at least 150 ft (50 m) toward the interior of the landslide lobe. Crushed-sandstone dikes (SD, Fig. 1) intrude the marble debris in arroyo walls at several localities 1 to 2 mi (2 to 3 km) from the edges of the lobe (Johnson, 1978, p. 492–493), which suggests that the whole landslide may be underlain by a layer of crushed sandstone. Unfortunately, the base of the landslide debris is exposed in very few places (BL, Fig. 2).

No remnants of crushed sandstone are present anywhere on the upper surface of the landslide, however. This implies that, barring a remarkable coincidence, the landslide cannot have crossed the alluvial slope simply as an unusually large debris flow. In debris flows, material at the forward edge necessarily arrives there by way of the upper surface, because the surface material in any relatively wide flow moves faster than the forward edge, eventually overtakes it, and is rolled under. Thus, the presence of crushed sandstone at the distal edge of the Blackhawk landslide unaccompanied by similar material anywhere on its upper surface means that it could not have been a flow in the normal sense. Instead, it must have had essentially a sliding mode of movement.

The landslide overtopped Hill 3747 (H3747, Fig. 1), which would require a minimum speed of 75 mph (35 m/s or 120 km/hr) if accomplished solely by conversion of kinetic energy to potential energy. The actual minimum would of course differ to the extent that the debris ascending the hill was pushed from behind by that descending the alluvial slope (Johnson, 1978, p. 497), which is a process that cannot be treated quantitatively in general terms. Support for the approximate correctness of the conservation-of-energy estimate, however, comes from the Elm and Frank landslides, which are the two historical cases that most closely resemble the Blackhawk. Conservation of energy gives minimum speeds of 65 mph (30 m/s or 105 km/hr) and 110 mph (50 m/s or 175 km/hr) for the two, in reasonable agreement with the average speeds of 110 mph (50 m/s or 175 km/hr) and 90 mph (40 m/s or 145 km/hr) estimated from eyewitness accounts (Heim, 1932, p. 93; McConnell and Brock, 1904, p. 8). The same witnesses also reported that both landslides decelerated from high speeds to a complete halt with remarkable abruptness. Thus, the Blackhawk probably also traveled at a high speed and stopped abruptly.

The assemblage of characteristics just described defines a remarkable genre of landslides that Shreve (1966, p. 1639) termed Blackhawk type. These landslides are exemplified not only by the Blackhawk but also by the Silver Reef, Elm, Frank, and Sherman landslides, and doubtless others. Indeed, had the Elm not been entirely obliterated (Shreve, 1968a, p. 33) by subsequent agricultural rehabilitation, it would have been an even better type example, because it not only had all the same characteristics but also was seen in action; and, as Voight and Pariseau (1978, p. 28) noted, it has precedence.

Not all large, high-speed, long-runout landslides are Blackhawk type; a notable exception is the Huascarán, Peru, landslide of 1970 (Plafker and Ericksen, 1978). Nor does Blackhawk type imply air-layer lubrication, as Voight and Pariseau (1978, p. 32) mistakenly assumed. Rather, it implies an assemblage of characteristics that the air-layer lubrication hypothesis was put forward to explain.

Other landslides of the Blackhawk type have additional characteristics either originally lacking or subsequently lost in the Blackhawk. In the Silver Reef, the Elm, and possibly the Sherman, but not the Blackhawk or Frank, for example, the preserved sequence of lithologic and other characteristics demonstrates that the lower part of the source block became the distal part of the landslide lobe (Heim, 1882, p. 102–103; Shreve, 1966, p. 1641, 1968a, p. 30, 36) and gives further support to the inference that the mode of movement was more akin to sliding than to flowing. A different mode of failure of the source block could explain the lack of this characteristic in the Blackhawk and Frank. The surfaces of the Elm, Frank, and Sherman were also dotted by scattered debris cones, which would long since have disappeared if originally present on the Blackhawk and Silver Reef. These cones consist of finer debris usually piled at the angle of repose atop single large blocks (Heim, 1882, p. 101, 104; McConnell and Brock, 1904, p. 9; Shreve, 1966, p. 1642). About a third of the cones on the Sherman are xenolithologic debris cones, in which both the cone and its underlying block have identical peculiarities not present in the surrounding surface debris, such as an uncommon rock type or distinctive quartz veining (Shreve, 1966, p. 1642).

A striking feature of the Sherman landslide, which sets it apart from the Blackhawk, Silver Reef, Elm, and Frank landslides, is the pattern of hundreds of parallel shallow V-shaped longitudinal grooves that covers almost its entire surface (Shreve, 1966, p. 1641). Although some of the more prominent grooves were formed by shear between substreams of the debris, the vast majority were not, and are probably the result of lateral spreading. Similar longitudinal grooves are present on many contemporaneous landslides in the vicinity, as well as on the Martian landslides (Lucchitta, 1978, p. 1602–1603; 1979, p. 8098), on the ejecta blankets of certain Martian rampart craters (Mouginis-Mark, 1979, p. 8013), and on the ejecta lobe associated with Tsiolkovsky Crater on the Moon (Guest, 1971, p. 99). All these grooved features seem to have formed in the presence of strong ground shaking. The cause was a magnitude-8.5 earthquake in the case of the Sherman and its contemporaries; possibly earthquake or impact in the Martian landslides, as indicated by widespread synchroneity (Lucchitta, 1979, p. 8106); and almost certainly impact in the case of the crater ejecta.

According to the hypothesis of air-layer lubrication proposed by Shreve (1966, p. 1642, 1968a, p. 37–38), landslides of the Blackhawk type start as huge rockfalls which acquire so much

momentum in their fall that at a projecting rib of rock or abrupt steepening of slope they leave the ground, overriding and trapping a cushion of compressed air, upon which they slide with little friction. The Elm and Frank definitely left the ground and overrode substantial volumes of air (Buss and Heim, 1881, p. 145; McConnell and Brock, 1904, p. 8), as hypothesized; and the Blackhawk and Sherman (Shreve, 1966, p. 1642) almost certainly did so, the launch point for the Blackhawk being a projecting spur ridge about 2,000 ft (600 m) upstream of the mouth of Blackhawk Canyon (LP, Fig. 2; see Johnson, 1978, p. 501, for photograph taken from the source area).

The high speed, the long runout, the local homogeneity of the debris, the distal wedge of crushed sandstone bulldozed from sources near the proximal end of the landslide, and, where present, the preserved sequence of lithologic and other characteristics result because the air layer is so easily sheared. The dikes (also present in the Sherman landslide; Shreve, 1966, p. 1641) originate from a relatively thin basal layer of lower permeability crushed sandstone (or, in the other cases, mud or snow) that necessarily had to be present in order for the pressure drop in the leaking air to be sufficient to counterbalance the weight of the loose fragments at the underside of the debris sheet (Shreve, 1968b, p. 655–656). The lateral ridges form where leakage allows the sides of the sliding sheet to fall and stop, forming levees that stand higher than the thinner debris that arrives later. The subsidiary lateral ridges form where air escapes along the interior side of an existing lateral ridge or ridges; and the interior lateral ridges form where it escapes at shear zones between sublobes of debris. The original ridge in some cases may not be the main one, because it can be smaller than a later one, and hence be subsidiary (Fig. 2). The debris cones form where large blocks, carrying on their tops finer debris from within the landslide, emerge from the moving debris as it spreads and thins, so that its surface settles around them (Heim, 1882, p. 101). They are xenolithologic where the debris at depth is lithologically homogeneous and differs from that at the surface.

The abrupt stop occurs and the distal rim and scarp form when the air layer becomes spread so thin that the leading edge of the sheet of debris hits the ground, slows rapidly, and causes the debris behind to pile up. The pattern of transverse corrugations reflects an imbricate internal structure that forms as the zone of impact propagates rearward up the landslide lobe, in the process destroying any lontigudinal grooves present. However, when the initial impact occurs toward the proximal end of the sheet of debris, the zone of impact propagates forward down the landslide lobe, in which case the stop, though still quick, is somewhat less abrupt, no distal rim or transverse corrugations form (unless the zone of impact meets a second one propagating rearward), and longitudinal grooves are preserved. The three-dimensional jigsaw-puzzle structure forms where the impact shatters large blocks into fragments that remain loosely fitted together because of the near lack of further movement.

The hypotheses advanced as alternatives to air-layer lubrication are motivated by doubts, predominantly intuitive, as to

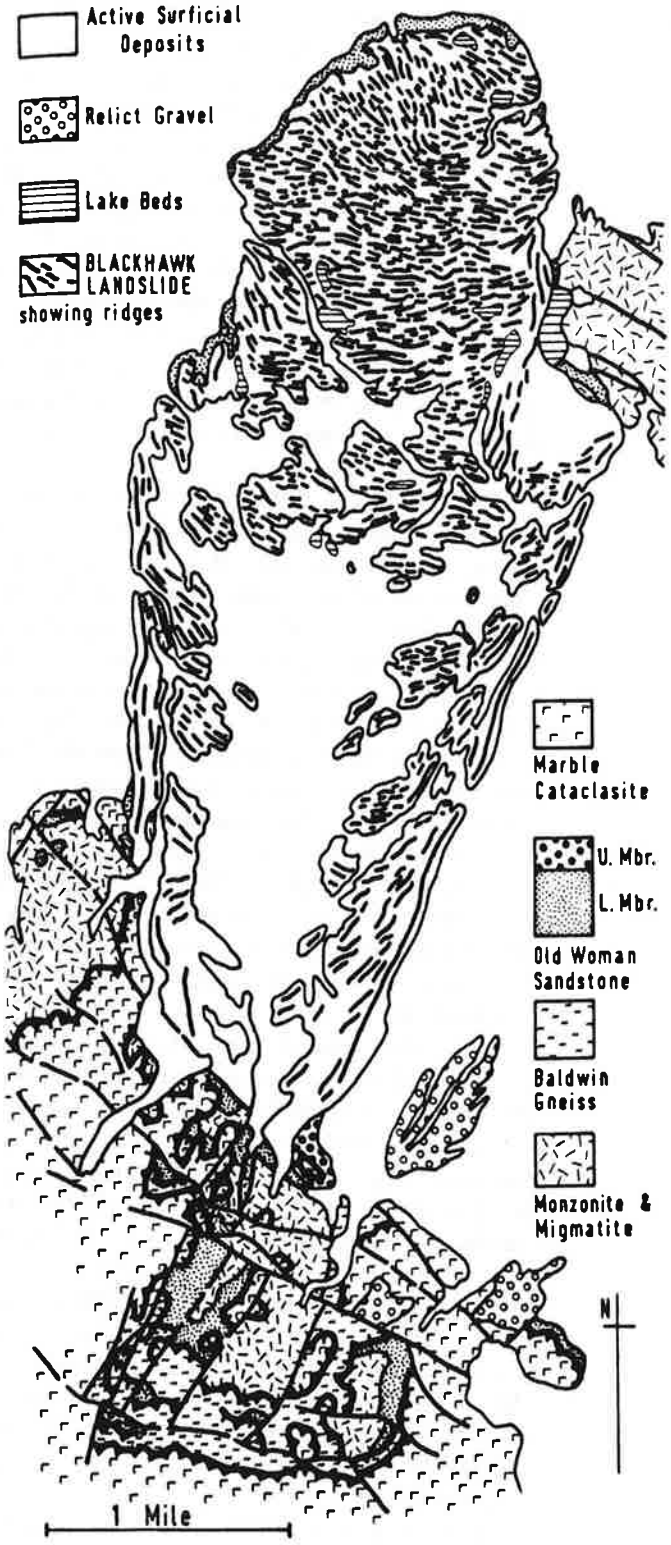

Figure 4. Map of the Blackhawk Landslide.

Surface Faulting Associated with the June 1992 Landers Earthquake, California

EARL W. HART, WILLIAM A. BRYANT, AND JEROME A. TREIMAN, Geologists
Division of Mines and Geology

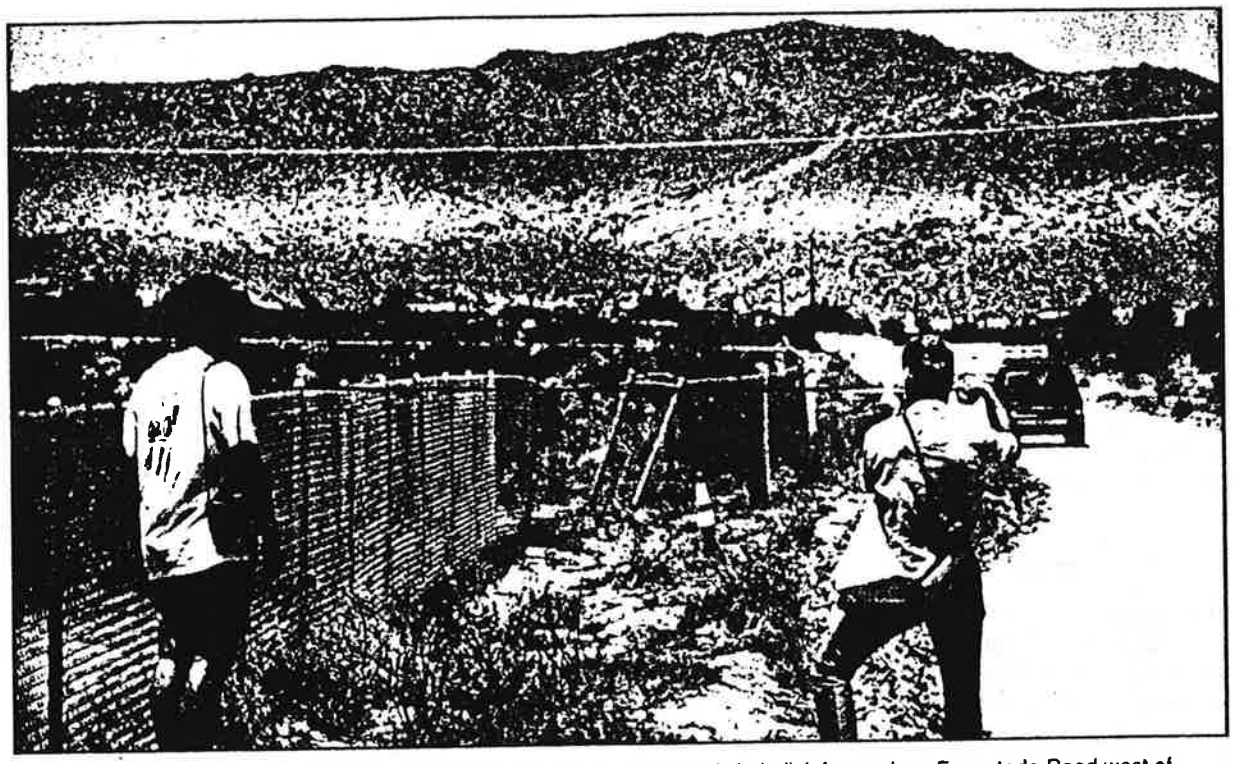

Photo 1. Geologists measuring 9.5 feet (2.9 m) of right-lateral offset of chain-link fence along Encantado Road west of Landers. *Photo courtesy of Geomatrix Consultants.*

INTRODUCTION

Surface fault rupture associated with the June 28, 1992 Landers earthquake occurred in San Bernardino County, from the vicinity of Yucca Valley to the Rodman Mountains, a distance of 53 miles (85 km). This was the largest fault-rupture event in California since the 1906 earthquake on the San Andreas Fault which had as much as 250 miles (400 km) of rupture and 15 to 20 feet (4.6 to 6.1 m) of right-lateral slip. Ruptured during the Landers event were the Johnson Valley, Homestead Valley, Emerson, and Camp Rock faults, all of which were active and previously mapped (Photo 1 and Figure 1). Also, several previously unknown faults ruptured, including the Eureka Peak and Burnt Mountain faults in Yucca Valley and the Kickapoo Fault* in Homestead Valley.

These ruptures came as a big surprise to the earth scientists who had studied these faults because: 1) faults previously considered to be separate structures were found to connect (Figure 1); 2) the amount of surface displacement was two or three times as large as generally anticipated; 3) the magnitude** of the earthquake was much larger than envisioned by seismologists for individual faults; and 4) seismicity was continuous across the active Pinto Mountain Fault.

RESPONSE

The Landers earthquake was felt by many in southern California, including author Jerome Treiman. He and other earth scientists checked for fault rupture as soon as the epicenter was located. Other geologists from the Division of Mines and Geology (DMG), the U.S. Geological Survey (USGS), the California Institute of Technology (CIT), universities, consulting firms, and other organizations arrived during the next few days.

Initially, the extent, magnitude, and sense of rupture were determined. Much of this information was channeled through DMG's clearinghouse (see Toppozada and others, this issue). By July 1 or 2, most of the main ruptures had been identified and, to some extent, measured, but the desert terrain and its limited features did not permit most rupture traces to be plotted accurately on topographic base maps.

Aerial photographs (scale of 1:6,000, or 1 inch = 500 feet), taken by I.K. Curtis for USGS on June 30 and available July 3, greatly facilitated the mapping of

* Also referred to as the Landers Fault.

** See page 16 for explanation of magnitude.

fault ruptures. Although many of the faults could be seen on the air photos, it was necessary to examine them in the field to measure magnitude of slip and to provide continuity. Because of the large number of ruptures and because fractures degrade rapidly in soft alluvium, DMG joined the USGS and others to map the many strands of faults. The results presented in this article are preliminary and generalized. More detailed and complete results will be published jointly with the USGS. Other preliminary reports on the Landers earthquake have been prepared by Earthquake Engineering Research Institute (1992) and Geomatrix Consultants (1992).

The authors would like to acknowledge the dozens of geologists from DMG, the USGS, and other organizations for making their preliminary data available for this report.

TECTONIC SETTING

The Landers earthquake occurred along part of a group of right-lateral, northwest-trending late Quaternary faults in the central Mojave Desert (Figure 1). Near its southern end, the rupture zone is traversed by the east-west-trending Pinto Mountain Fault. The region is bounded on the southwest by the San Andreas Fault Zone and on the north by the Garlock Fault.

The principal faults and general structure of the Mojave Desert region have been summarized and discussed by Dibblee (1980). According to Dokka (1983), the principal northwest-trending faults of the south-central Mojave Desert have had 0.9 to 9.0 miles (1.5 to 14.5 km) of right-lateral displacement in late Cenozoic time. Recently-active traces of these faults have been mapped by Bull (1978), Morton and others (1980), and Hart and others (1988) using tectonic geomorphology. Geodetic measurements between 1934 and 1982 suggest cumulative right-lateral slip (strain) of 0.26 ± 0.05 inch (6.6 ± 1.3 mm) per year along the northwest-trending faults of this region (Sauber and others, 1986). Based on the development of tectonic geomorphic features and offset late Quaternary geologic units, the Pisgah-Bullion, Calico, and related faults to the west each appears to have a late Quaternary slip rate approaching 0.04 inch (1 mm) per

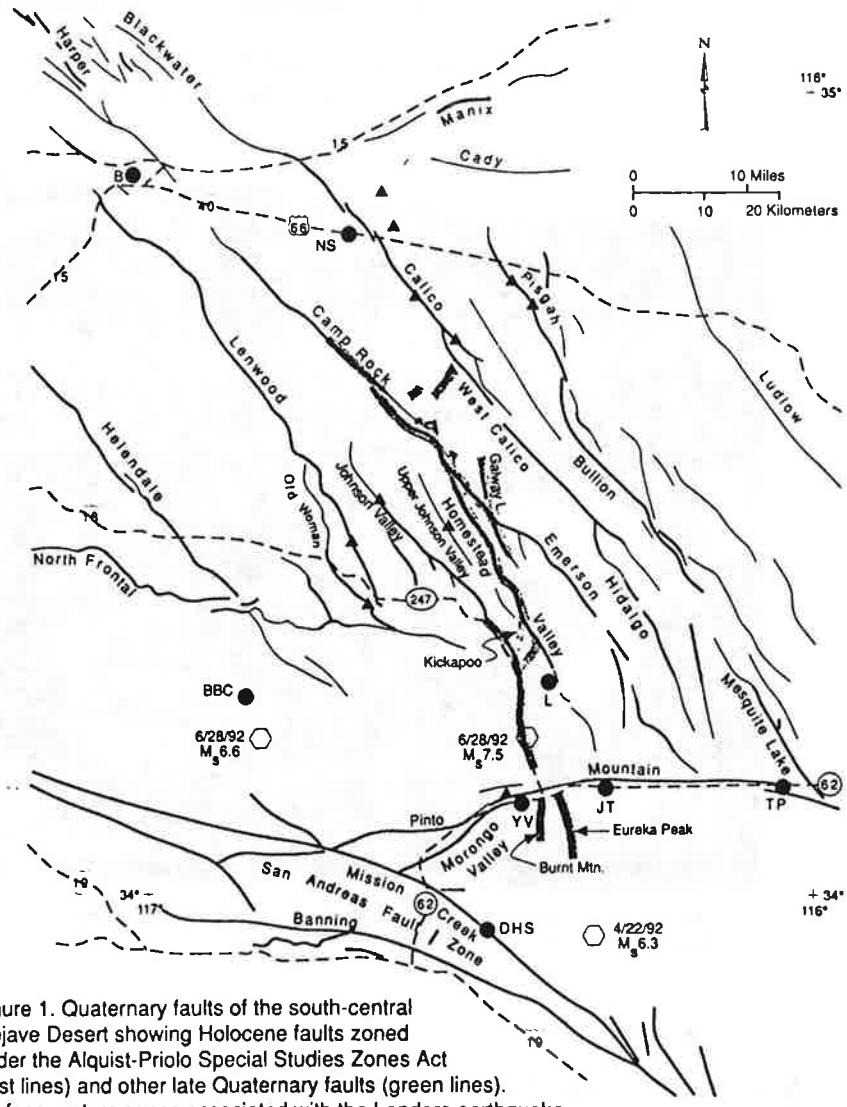

Figure 1. Quaternary faults of the south-central Mojave Desert showing Holocene faults zoned under the Alquist-Priolo Special Studies Zones Act (rust lines) and other late Quaternary faults (green lines). Surface rupture zones associated with the Landers earthquake are identified by gray lines; triggered slip on other faults is shown by triangles. Hexagons mark epicenters. Letters identify cities: B = Barstow; BBC = Big Bear City; DHS = Desert Hot Springs; JT = Joshua Tree; L = Landers; NS = Newberry Springs; TP = Twentynine Palms; YV = Yucca Valley.

year (Hart and others, 1988). Surface rupture in the central Mojave Desert prior to the Landers event was minor—it occurred on the Manix Fault in 1947 (Richter, 1958), the Galway Lake Fault in 1975 (Hill and Beeby, 1977), and the Homestead Valley and Johnson Valley faults in 1979 (Hill and others, 1980).

DESCRIPTION OF SURFACE RUPTURES

The epicenter was located south of Landers on the Johnson Valley Fault and ruptured mainly northward to the Homestead Valley, Emerson, and Camp Rock faults (Figure 2). Rupture along the Johnson Valley Fault died out southward just north of Yucca Valley, but rupture appeared again to the south of the Pinto Mountain Fault. The zone of aftershocks is continuous and shows the Johnson Valley Fault to connect in the subsurface with the Burnt Mountain and Eureka Peak faults.

Most of the rupture was right-lateral strike-slip along north to northwest-trending faults, with maximum slip of 15 to 20 feet (4.6 to 6.1 m) on the Emerson Fault (Figure 2 and Photo 2). There was more than 3 feet (1 m) of right-lateral slip over 38 miles (61 km) of rupture. Left-lateral slip also occurred locally along northeast-

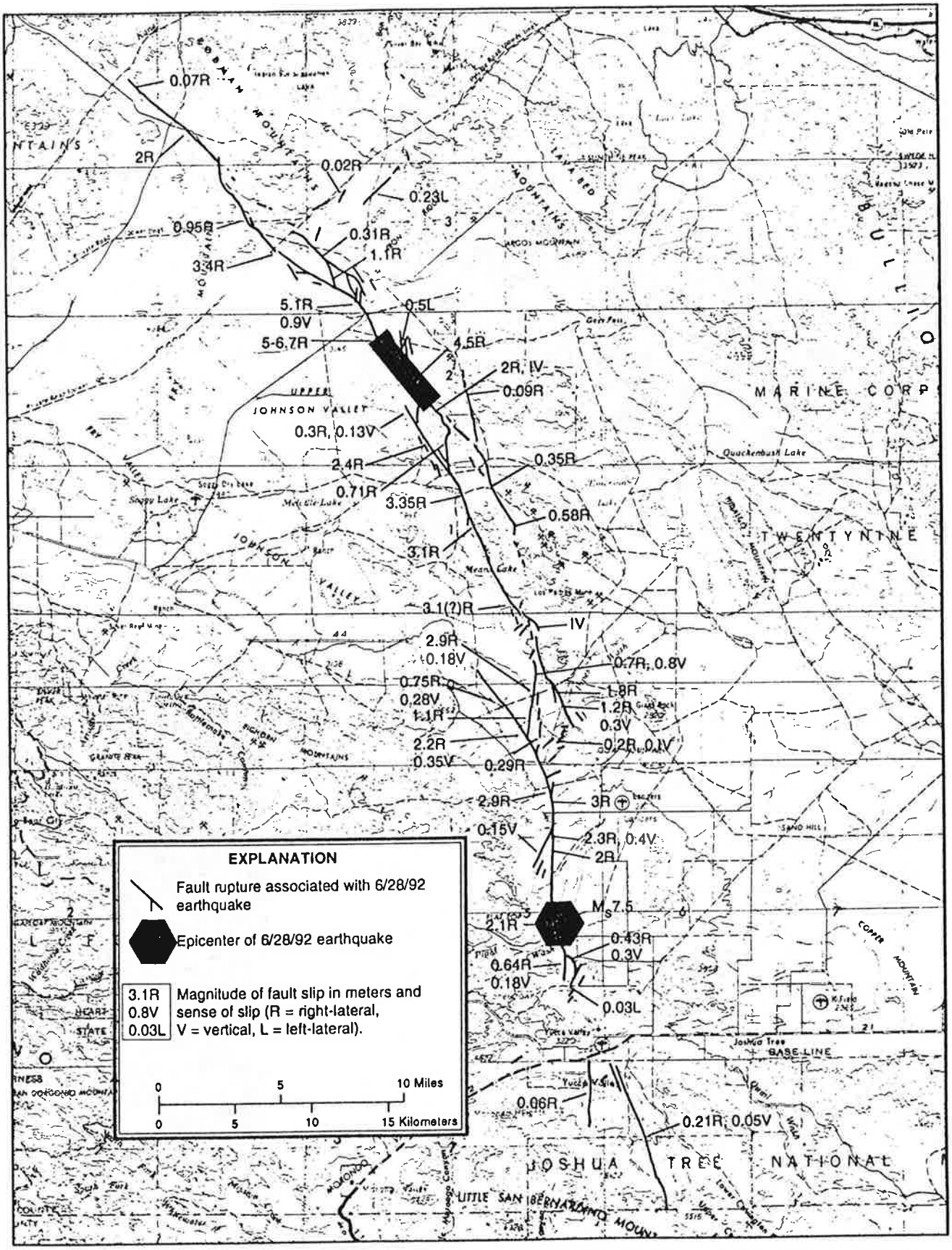

Figure 2. Surface faulting associated with the 1992 Landers earthquake. For details of shaded area, see Irvine and Hill, this issue.

Photo 2. Surface rupture along the Emerson Fault offsets road 15 to 20 feet (4.6 to 6.1 m) right-laterally, which is the near-maximum fault displacement measured for the Landers earthquake. Main rupture is a broad, fissured mole track or warp about 50 feet (15 m) wide flanked by subsidiary fissures extending 50 to 100 feet (15 to 30 m) on each side. *Photo by W.A. Bryant.*

to east-trending faults, but mostly was minor. Maximum left-lateral slip measured was about 1.5 feet (0.5 m), west of Galway Lake. A vertical component of rupture was also common and locally attained 3 feet (1 m) or more.

Zones of closely associated ruptures commonly were 33 to 66 feet (10 to 20 m) wide. In some cases there were two or three main breaks and, together with subsidiary faults, formed complex rupture zones at least 650 feet (200 m) wide. There were so many ruptures that many were obscured by reconstruction, traffic, and weather-before they could be field mapped. Fortunately, most of the ruptures were recorded on aerial photographs shortly after the earthquake. The several segments of faults that ruptured (Figure 2) are discussed below, from south to north.

Eureka Peak and Burnt Mountain Faults

These faults were not known prior to their rupture on June 28, 1992. There is no geomorphic evidence suggesting previous Holocene activity, but there is subtle evidence of the faults in older alluvium and bedrock (Treiman, 1992). An exploratory trench across the northern part of the Eureka Peak Fault revealed caliche-filled fractures in alluvium. Both faults are right-lateral faults with minor down-to-the-west vertical components. Maximum right-slip on the Eureka Peak Fault was 8.3 inches (21 cm). There was nearly 1.6 inches (4 cm) of afterslip on this fault and about half of it occurred during the first 2 weeks after the earthquake (Art Sylvester, University of California, Santa Barbara, oral communication, December 9, 1992). Little if any afterslip was recorded on other faults in the epicentral area.

Although these faults align with the Landers earthquake aftershock pattern, they do not extend continuously to the north or south as do the aftershocks. The faults also align with minor Quaternary faults to the south that are apparently related to the April 22, 1992 Joshua Tree earthquake of M_s6.3. One of these faults showed minor right-lateral and down-to-the-west vertical slip (Rymer, 1992).

Johnson Valley Fault

Rupture that caused the Landers earthquake was initiated at the southern end of the Johnson Valley Fault, at a depth of 5.6 miles (9 km). Only the southern half of the Johnson Valley Fault ruptured (Photo 3) with the minor exception of triggered (?) slip near its northwestern end (Figure 1). (Triggered slip occurs when strain stored along a fault at a shallow depth is released by shaking.) The fault was previously known and most of it was considered to be Holocene active. Maximum right-lateral displacement was about 10 feet (3 m) and most of the fault displayed more than 6 feet (2 m) of slip.

The surface ruptures splayed complexly at the south end and died-out north of Yucca Valley. The fault segment connected complexly to the north with the Homestead Valley Fault, again along a continuous aftershock zone. Near its junction with the Kickapoo Fault, the Johnson Valley Fault previously had very minor, discontinuous surface rupture associated with the Homestead Valley earthquakes of 1979 (Hill and others, 1980).

Photo 3. Exposure of Johnson Valley Fault in hillside cut, had 4.6 feet (1.4 m) of right-lateral and 1.0 foot (0.3 m) of vertical offset (scarplet at lower right). Vertical resistent feature is calcite-cemented fault breccia indicating previous faulting in Pleistocene alluvium. Note new fissures in breccia. *Photo by E.W. Hart.*

Kickapoo and Related Faults

These newly discovered faults constitute a major connection between the Johnson Valley and Homestead Valley faults. The main element is the Kickapoo Fault, which had a maximum of 9.5 feet (2.9 m) of right-lateral slip. The north end of the fault has a large vertical component forming an east-facing scarp about 3 feet (1 m) high (Photo 4). Only subtle and discontinuous evidence for this fault can be seen on air photos and in older (?) alluvium in the field. This stepover area is the approximate location of the 1979 M5.3 Homestead Valley earthquake (Hill and others, 1980).

Homestead Valley Fault

Virtually this entire 18-mile- (29 km-) long fault ruptured in 1992, developing maximum right-lateral displacement of 11 feet (3.35 m). It has multiple strands forming a wide zone, and connects complexly with the Emerson Fault. The southernmost segment, which had minor rupture in 1979, is separated from the central part of the fault by a complexly faulted hill. The eastern side of that hill (west-southwest of the Los Padres Mine) is bounded by a west-dipping thrust fault with a 3-foot- (1-m-) high scarp (Figure 2). The Homestead Valley Fault ruptures diminish to the southeast and zones of discontinuous ruptures connect it with the Johnson Valley Fault.

Emerson and Galway Lake Faults

Maximum rupture associated with the Landers earthquake occurred along the Emerson Fault near Bessemer Mine Road. There was 16.7 feet (5.1 m) of right-lateral slip just north of that road. Measurements of right-lateral displacement of a road just south of the Bessemer Mine Road range from 15 to 20 feet (4.6 to 6.1 m) (Photo 2). Only the northwestern half of the Emerson Fault ruptured in this event, although the southeastern half is considered active (Figure 1). To the northwest the fault connects complexly with the Camp Rock Fault, paralleling it for 8 miles (13 km). The Galway Lake Fault, at the southeast end of the Emerson ruptures, also ruptured with nearly 3.5 inches (9 cm) of right-lateral slip (this may have been triggered slip). The same segment had minor rupture in 1975 (Hill and Beeby, 1977). Except for some short segments, the Emerson Fault was previously recognized as a recently active fault.

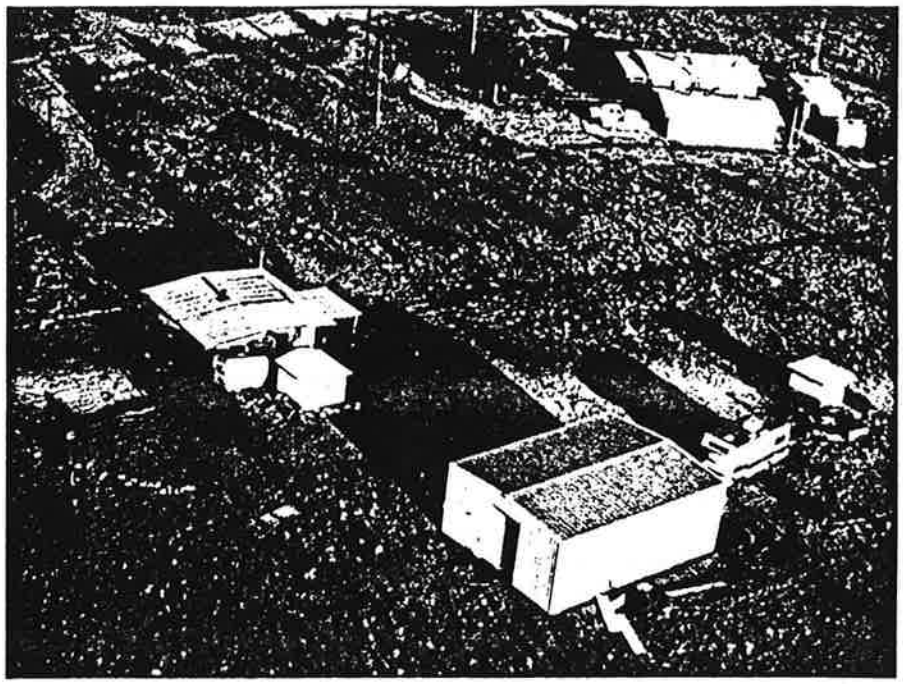

Photo 4. Newly discovered Kickapoo Fault near Charles Road shows relatively narrow zone of rupture along scarp up to 3 feet (1 m) high with nearly 3 feet (1 m) of right-lateral offset. Fault seemingly passes between house and outbuilding (see Photo 5). *Photo by W.A. Bryant.*

Camp Rock Fault

Most of the central and southeastern parts of this fault ruptured with maximum right-lateral displacement of about 6 feet (2 m). The rupture, however, was discontinuous where the Camp Rock Fault parallels the Emerson Fault, and the northwestern part of the fault did not rupture (Figures 1 and 2). The magnitude of surface fault rupture diminished substantially to the northwest. Some ruptures splayed northeast (with as much as 9 inches [23 cm] of left-lateral slip) around the southeast side of the Rodman Mountains. This suggests that a new fault zone is developing between the Camp Rock-Emerson and the Calico-West Calico fault zones, which also had minor right-slip ruptures at three localities (Figure 1). Ruptures on the Galway Lake Fault may be part of this complex stepover.

Triggered Slip on Other Faults

The Landers earthquake apparently triggered minor slip on several faults well beyond the primary fault-rupture zone. Although not well understood, this phenomenon is common with large earthquakes. Some triggered slip is coseismic and some occurs as creep or afterslip. Within the south-central Mojave Desert, rupture was triggered on the following faults (Figure 1):

Pisgah Fault—0.8 to 1.6 inches (2 to 4 cm) right lateral-slip in two zones near the Hector Mine.

Calico-West Calico Fault—maximum 0.8-inch (2-cm) right-lateral slip in three short northwest-trending segments. A broad 6-mile- (10-km-) long zone of north to northeast-trending cracks with as much as 4 inches (10 cm) of vertical offset developed east of the fault, 4 miles (6 km) northeast of Newberry Springs (Janet Sowers, William Lettis and Associates, oral communication, January 1993).

Johnson Valley Fault (northwest segment)—minor zone of left-stepping cracks; 0.08 to 0.16 inch (2 to 4 mm) right-lateral slip.

Upper Johnson Valley Fault—Post-earthquake photo interpretations suggest that fault rupture occurred along several miles of the newly named Upper Johnson Valley Fault. A field check in

November verified cracks in at least three places in zones at least 32 feet (10 m) wide (Ken Lajoie, USGS, oral communication, January 1993).

Lenwood Fault—0.6- to 1.2-mile- (1-2-km-) long zone of left-stepping cracks south of Soggy Lake.

Old Woman Fault—questionable minor extensional cracking; northwest trend.

Pinto Mountain Fault—local minor cracking with up to 0.8 inch (2 cm) of extension; right-stepping cracks suggest left-lateral displacement.

Other triggered slip was reported in Imperial Valley on the Superstition Hills Fault, the East Branch of the Elmore Ranch Fault, and the Coyote Creek Fault (Sharp, 1992) and in Coachella Valley along the Indio Hills, Mecca Hills, and Durmid Hills segments of the San Andreas Fault (Mike Rymer, USGS, oral communication, 1992). Maximum right-lateral slip on the San Andreas Fault was 0.83 inch (2 cm).

EFFECTIVENESS OF ALQUIST-PRIOLO SPECIAL STUDIES ZONES

On March 1, 1988, DMG issued Official Maps of Special Studies Zones (SSZs) for faults in the central Mojave Desert (DMG, 1988). These maps were issued in accordance with the Alquist-Priolo (A-P) SSZ Act of 1972 to assist cities and counties in regulating development to mitigate surface faulting hazards to structures for human occupancy. The 1988 maps were the result of a 1986-1987 study of the faults in the Mojave Desert, the eighth region to be evaluated under a 10-region plan (Hart, 1992; Hart and others, 1988). Under this plan, those faults with evidence of Holocene activity and reasonably well defined as surface features were zoned under the APSSZ Act. Mapping by DMG geologists was largely based on the interpretation of air photos with only limited field checking. The work of other geologists was also used. Faults zoned in the south-central Mojave Desert region are identified in Figure 1.

The Landers earthquake provides an excellent opportunity to determine the effectiveness of the SSZs established in 1988. Based on preliminary data, approximately 55 percent of the fault rupture associated with the Landers earthquake occurred within the established SSZs. About 31 percent of the rupture was outside the SSZs along previously unrecognized faults, including branch and subsidiary faults and interconnecting faults. The remaining 14 percent of the rupture outside the SSZs occurred on previously mapped faults that did not appear to meet zoning criteria. An estimated one-third of the rupture outside the SSZs was relatively minor, with fewer than 4 inches (10 cm) of displacement. By way of contrast, only 38 percent of the fault rupture from the November 1987 Superstition Hills and Elmore Ranch earthquakes was within established SSZs. Again, part of that rupture occurred on previously unmapped faults and much of it was relatively minor.

Another method of measuring the effectiveness of zoning is to evaluate the percentage of zone length within which rupture occurred. For the Landers earthquake, between the south end of the Johnson Valley Fault and the north end of the Camp Rock Fault ruptures, 92 percent of the SSZs contained fault ruptures. The great majority of the rupture within the SSZs occurred within 200 feet (60 m) of the traces shown on the SSZ maps.

U.S. Bureau of Land Management photos (scale 1:30,000) were used for interpreting most of the region. Although the SSZs established for the Johnson Valley, Homestead Valley, Emerson, and Camp Rock faults appear to be effective (92 percent ruptured), additional active faults probably could have been identified on larger-scale air photos. Even with the best possible aerial photos, many of the faults that ruptured would not have been identified as active because they were largely obscured by alluvial processes and by mining, roads, and construction. It should be recognized that not all active faults can be identified in advance. Therefore, using these techniques, investigations for possible active faults or other types of potential ground failure prior to construction of critical and sensitive structures may be warranted.

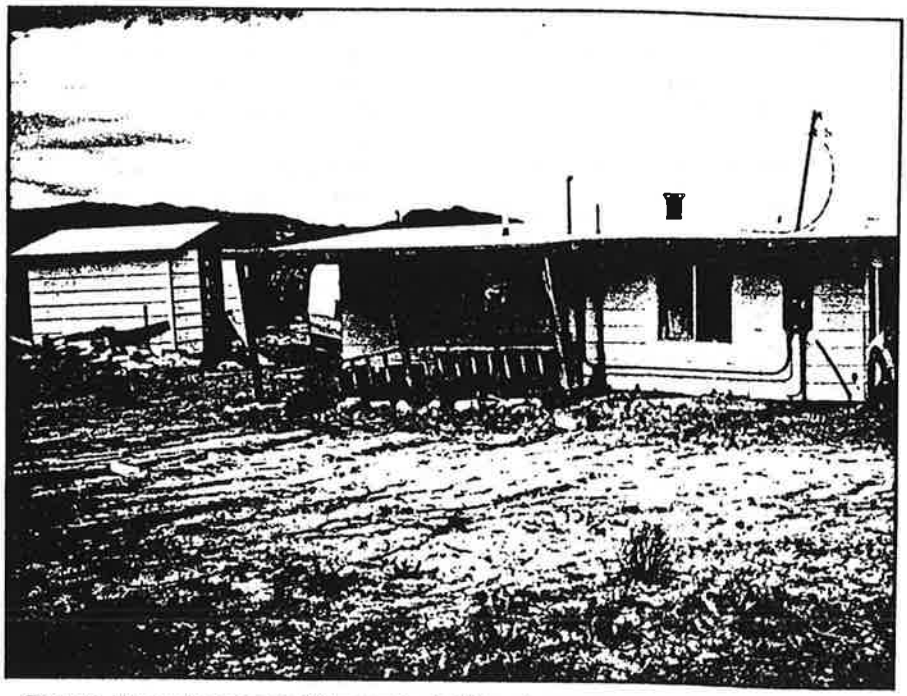

Photo 5. House damaged by Kickapoo Fault. Although main scarp and rupture passes between house and outbuilding, numerous other fissures are distributed over a zone at least 50 feet (15 m) wide. Much of the subsidiary rupture was diverted around the slab foundation of the house, offsetting the patio slab right-laterally more than 2 feet (less than 1 m) (see Photo 4). *Photo by E.W. Hart.*

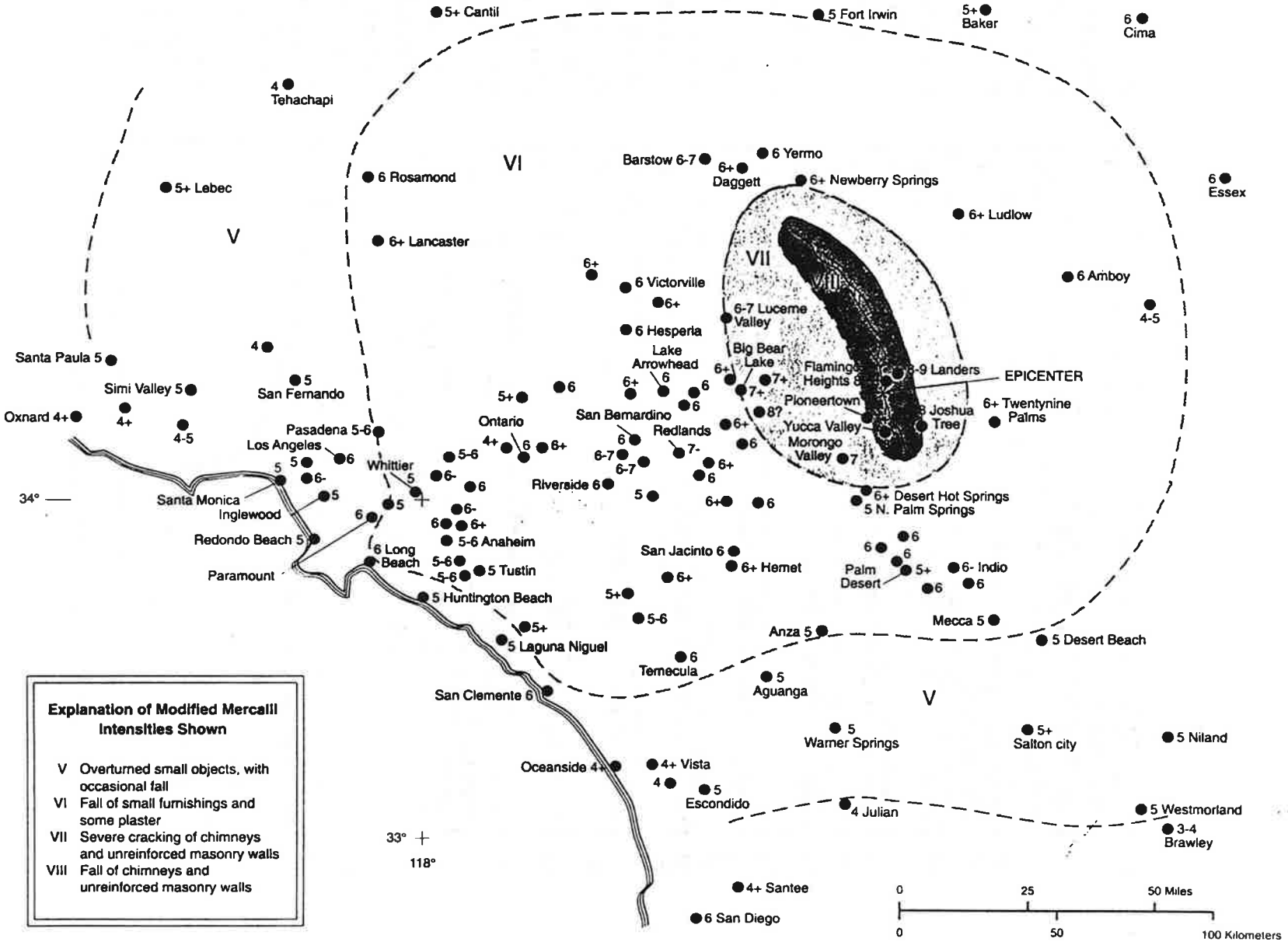

Figure 4. Preliminary Modified Mercalli Intensity map of the Landers earthquake, based largely on information from NEIC-USGS.

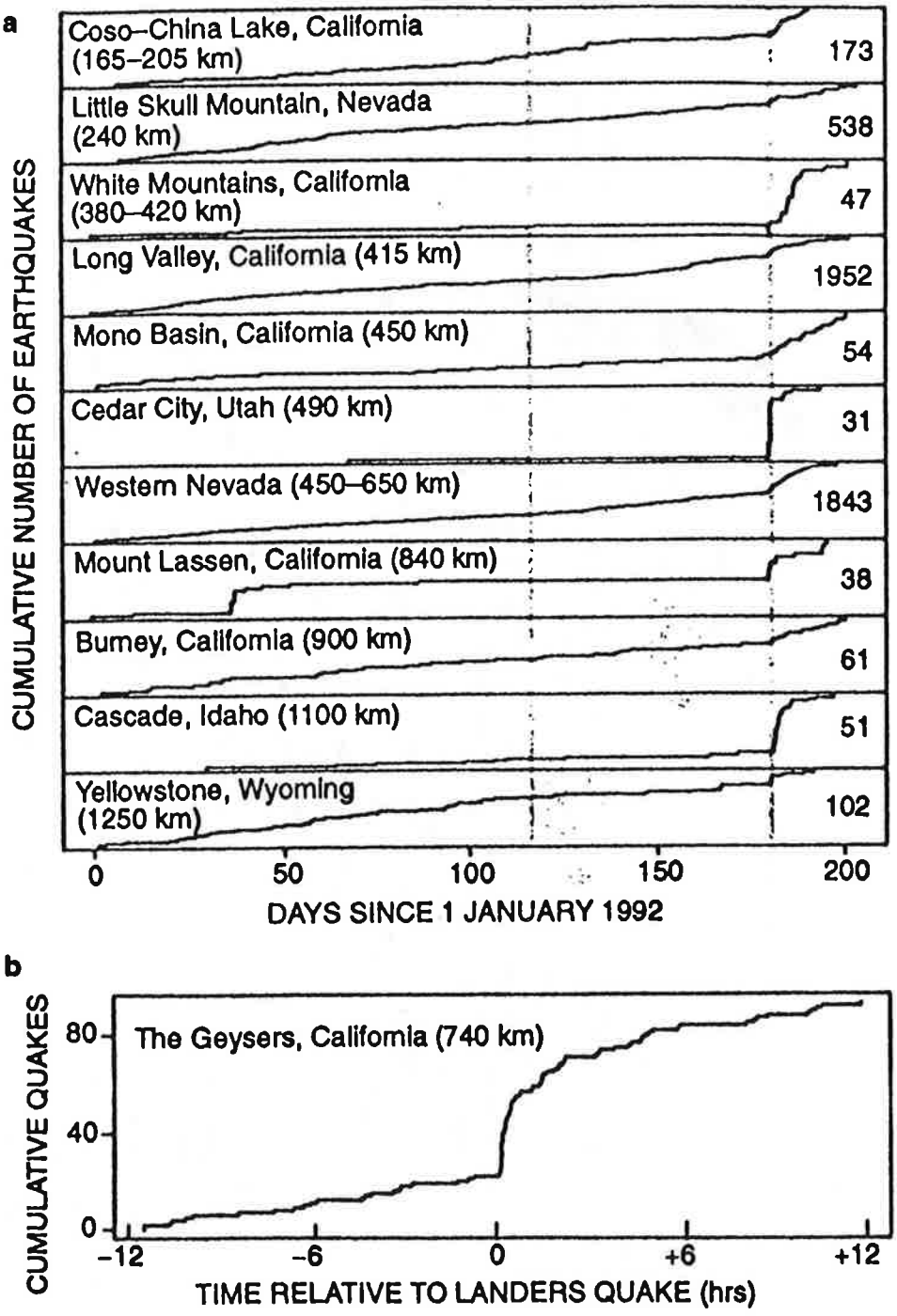

Evidence of remote triggering is seen in these plots of the cumulative number of earthquakes vs time at 12 sites in the western US. Distances from the Landers quake are shown in parentheses. In **a**, colored lines indicate the 25 April, 1992 Mendocino earthquake, which had no obvious effect, and the comparably strong Landers earthquake of 28 June, which triggered the abrupt onset of increased activity at all these sites. The numbers at right are the total number of quakes to the top of each plot. The accumulation of earthquakes at the Geysers, a geothermal field north of San Francisco, is shown in **b** for 12 hours before and after the Landers quake.

DECEMBER 28, 1993 – JANUARY 5, 1994

Preliminary Epicenters and Magnitudes

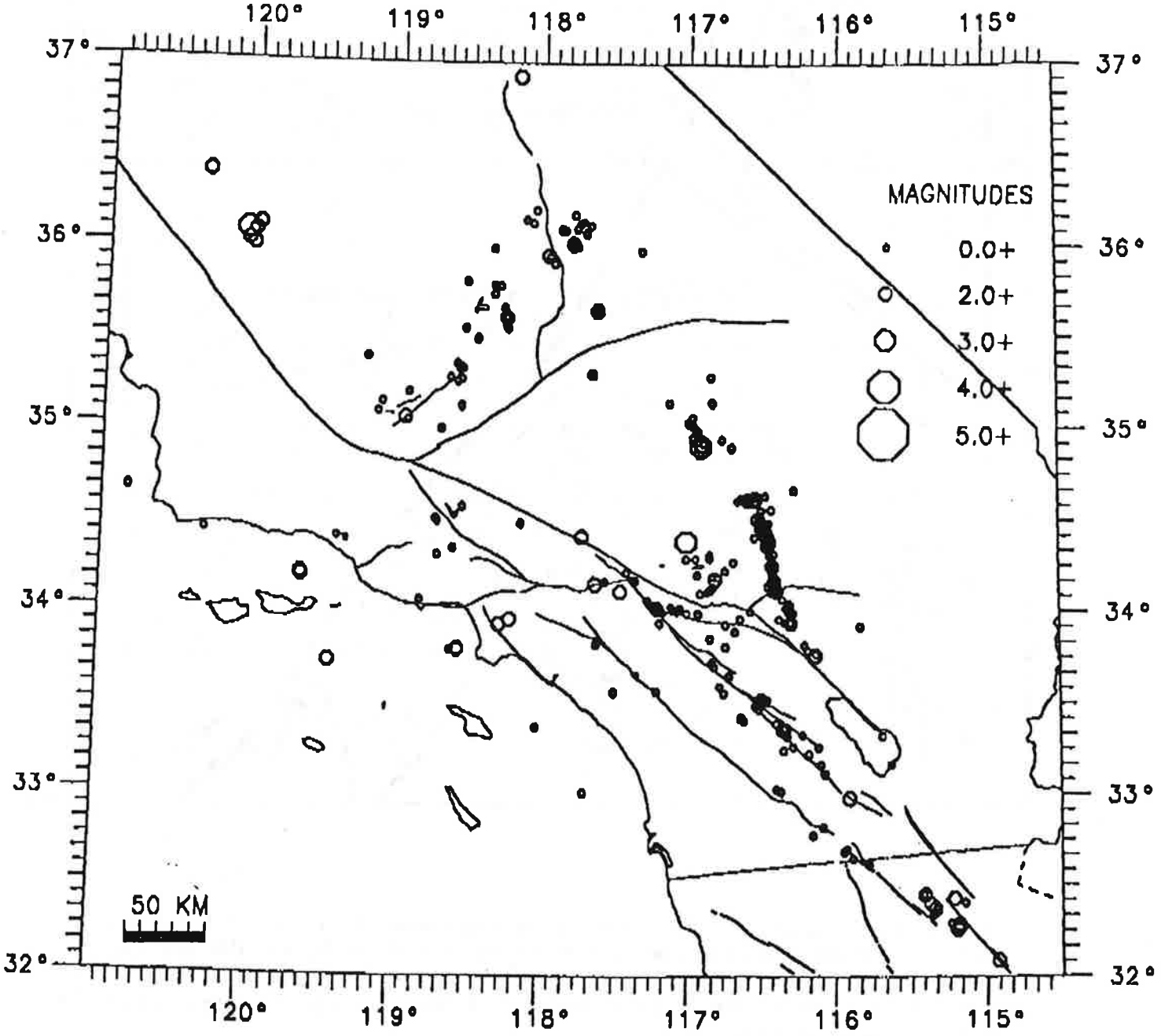

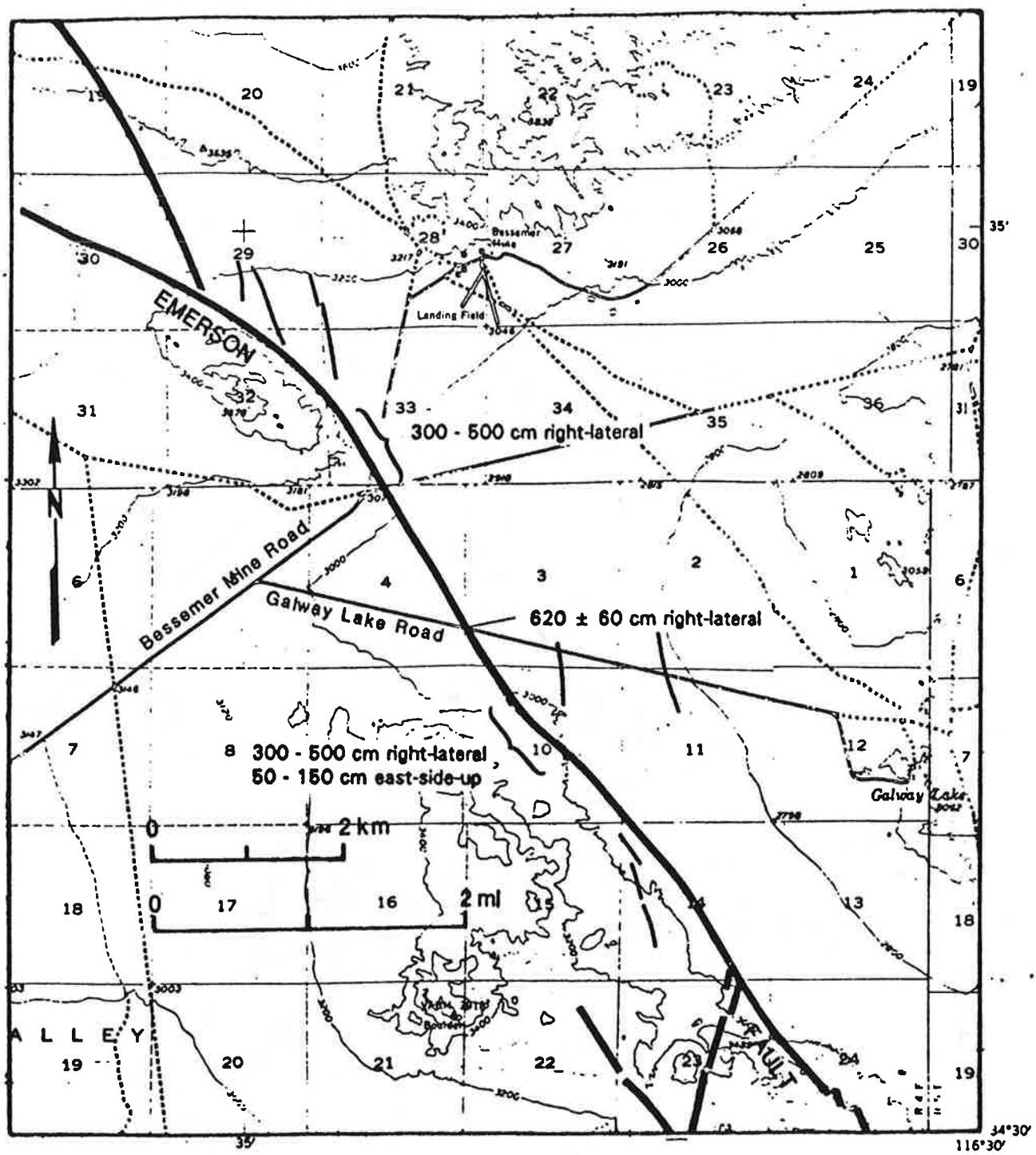

FIGURE 2. Map of the Emerson fault in the region of maximum displacement. The largest offset of 6.2 ± 0.6 meters was measured on the Galway Lake Road. Faulting shown on this map represents the largest surface breaks. Not shown are the hundreds of smaller faults and ground cracks that are pervasive across the valley between the Emerson fault and Galway Lake. (Preliminary data from Sieh et al., manuscript in preparation).

Paleogeographic evolution of the San Andreas fault in southern California: A reconstruction based on a new cross-fault correlation

Jonathan C. Matti
U.S. Geological Survey, Department of Geological Sciences, University of Arizona, Tucson, Arizona 85721
Douglas M. Morton
U.S. Geological Survey, Department of Earth Sciences, University of California, Riverside, California 92521

ABSTRACT

Distinctive porphyritic bodies of alkalic monzogranite and quartz monzonite of Triassic age that occur in the Mill Creek region of the San Bernardino Mountains and on the opposite side of the San Andreas fault at the northwest end of Liebre Mountain appear to be segments of a formerly continuous pluton that has been severed by the fault and displaced about 160 km. Reassembly of the megaporphyritic bodies by restoration of sequential right-lateral displacements on various strands of the San Andreas and San Gabriel fault zones leads to a palinspastic reconstruction for southern California that reassembles crystalline and sedimentary terranes differently from widely cited reconstructions.

Reassembled crystalline rocks establish three coherent patterns: (1) The reunited Liebre Mountain and Mill Creek Triassic megaporphyry bodies form western outliers of a province of Permian and Triassic alkalic granitoid rocks that occurs in the western Mojave Desert and San Bernardino Mountains. (2) Following sequential restorations of 160 km on the San Andreas fault and 44 km on the San Gabriel and Cajon Valley faults, the Table Mountain and Holcomb Ridge basement slices currently positioned along the west edge of the Mojave Desert near Wrightwood and Valyermo area reassembled with the Liebre Mountain and San Bernardino Mountains blocks. This restoration unites terranes of Mesozoic granitoid rock and Paleozoic(?) marble, metaquartzite, and pelitic gneiss that have strong lithologic and compositional similarities, and brings together within a single province quartz diorite and granodiorite that are hosts for three known bedrock occurrences of aluminous dike rocks ("polka-dot" granite) that previously have been used to assemble a different reconstruction for the San Andreas fault. (3) Crystalline rocks of the San Gorgonio Pass region, including Triassic monzogranite and granodiorite of the Lowe igneous pluton and Jurassic blastoporphyritic quartz monzonite, are juxtaposed adjacent to the southern Chocolate Mountains where similar rocks have been mapped.

The reconstructed crystalline rocks provide a paleogeographic framework for Pliocene and late Miocene sedimentary basins now scattered along the San Gabriel and San Andreas faults. Ridge Basin is juxtaposed adjacent to the southwestern San Bernardino Mountains in an orogenic setting compatible with stratigraphic relations, depositional fabrics, and clast compositions in the Ridge Basin fill. Synorogenic sediments of the upper Miocene Ridge Route and Peace Valley Formations accumulated in this setting at a time (9 to 5 Ma) when the western San Bernardino Mountains were undergoing uplift and erosion. The Pliocene Hungry Valley Formation was deposited toward the end of this orogenic pulse (5 to 4 Ma) when early movements on the San Andreas fault began to displace Ridge Basin away from the San Bernardino Mountains. Other late Miocene basins widely dispersed today are reassembled within an early Salton Trough that included, from northwest to southeast, the Punchbowl and Mill Creek basins, the Coachella Fanglomerate and Hathaway Formation, and the fanglomerate of Bear Canyon in the southern Chocolate Mountains.

The new reconstruction allows only about 205 km of displacement on the combined San Andreas and San Gabriel fault zones, which is about 110 km short of the 315 ± 10 km post–early Miocene offsets documented for the San Andreas in central California. This shortfall requires the existence of another Miocene strand of the San Andreas fault system in southern California. The Clemens Well–Fenner–San Francisquito fault system of Powell (this volume) provides this additional fault strand. Together, the Clemens Well, San Gabriel, and San Andreas faults generated about 315 ± 10 km of right slip comparable to displacements documented for the San Andreas fault in central California. The displacements in southern California have occurred in middle Miocene through Holocene time, and extend the history of late Cenozoic right-lateral faulting farther back into the Miocene than envisioned by traditional reconstructions for the San Andreas fault system in southern California.

Paleogeographic evolution, San Andreas fault

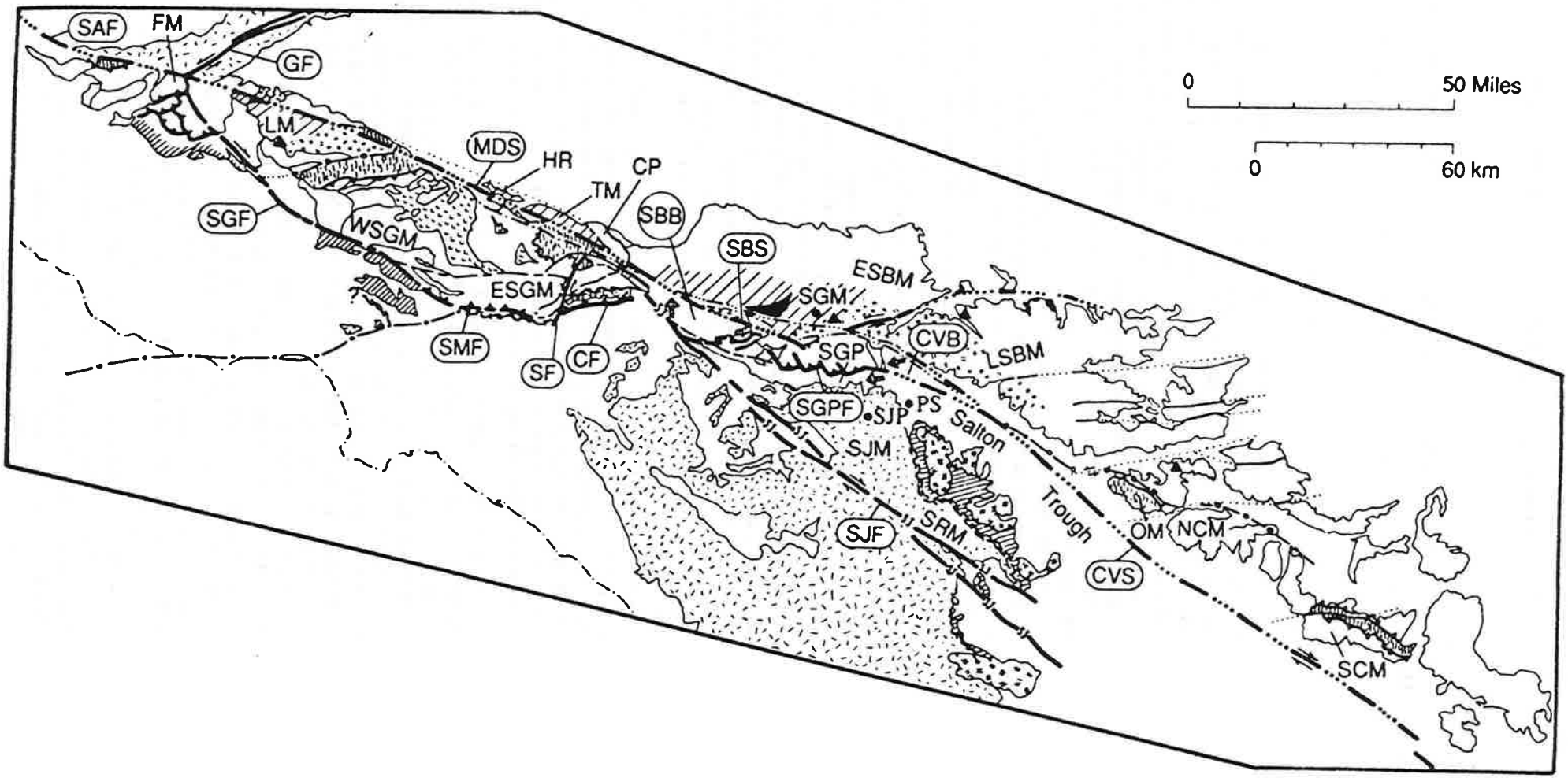

INTRODUCTION

In 1953, M. L. Hill and T. W. Dibblee proposed that stratigraphic and structural elements of the California continental margin have been rearranged by large right-lateral displacements on the San Andreas fault. In the 40 yr since this revolutionary proposal exploded conventional views of Earth history, numerous attempts have been made to document the distribution and geologic history of faults in the San Andreas family and to reconstruct the palinspastic configuration of sedimentary and crystalline terranes displaced by these faults. The search for ancient paleogeography has been particularly challenging in southern California, where structural and stratigraphic elements have been rearranged not only by displacements on the San Andreas proper, but also by displacements on a variety of right-lateral, left-lateral, compressional, and extensional fault complexes that contributed to and interacted with the San Andreas system.

Any attempt to reconstruct pre–San Andreas paleogeography in southern California must first determine how right-lateral displacements have been distributed among individual strands of the system. Total displacement on the San Andreas since its inception in the Miocene is widely accepted to be about 315 ± 10 km. In central California, this displacement has occurred mainly along the San Andreas proper (Hill and Dibblee, 1953; Crowell, 1981); however, in southern California the total displacement has been taken up by several discrete fault strands—including the San Andreas, San Jacinto, Punchbowl, San Gabriel, and Banning faults—as well as other less well-known structures (Fig. 1). The San Andreas fault alone accounts for a large fraction of the total displacement in southern California, but a comparison of palinspastic reconstructions proposed in the literature (Crowell, 1960, 1962, 1975a, 1979, 1981; Jahns, 1973; Dillon, 1975; Woodburne, 1975; Smith, 1977; Ehlig, 1981, 1982; Powell, 1981, 1986; Ross, 1984; Matti and others, 1985) shows that significant disagreement exists regarding the timing and amount of displacement on the San Andreas proper and on associated right-lateral faults. This disparity of interpretation has led to conflicting palinspastic reconstructions for dismembered terranes that now are distributed across southern California between the Chocolate Mountains and the Frazier Mountain region (Plate IIIA).

In this chapter, we add to this disparity by proposing a new model for the paleogeographic evolution of the San Andreas fault in southern California. This model is based on the hypothesis that crystalline rocks of the Liebre Mountain region have been displaced by the San Andreas fault from their original position adjacent to the southwestern San Bernardino Mountains (Plate IIIA; Matti and others, 1986; Frizzell and others, 1986). From this starting point, we use new information about the movement history of various strands of the San Andreas fault system to reconstruct how crystalline and sedimentary terranes in southern California might originally have been assembled before they were dismembered and rearranged by right-slip displacements within the system. This palinspastic reconstruction requires that the San Andreas fault proper in southern California has no more than 160 km of displacement since its inception 4 to 5 m.y. ago, and that the full history of right slip within the San Andreas transform system in southern California must be extended farther back into

Basement rocks

The diverse basement terranes of southwestern California can be grouped into rocks of Peninsular Ranges type, San Gabriel Mountains type, and San Bernardino Mountains type (Fig. 2, Plate IIIA).

Basement rocks of *San Gabriel Mountains type* (Fig. 2A) consist of two crustal layers separated by a low-angle tectonic contact—the Vincent thrust (Ehlig, 1982). The upper thrust plate consists of Mesozoic plutons of various compositions, ages, and deformational styles that have intruded prebatholithic crystalline rocks. One distinctive Mesozoic granitoid unit is the Lowe igneous pluton of Triassic age (Joseph and others, 1982a). The prebatholithic rocks largely are Proterozoic, and include orthogneisses and the anorthosite-syenite complex that is so well known from the western San Gabriel Mountains (Silver, 1971; Ehlig, 1981; Carter, 1982). The lower plate of the Vincent thrust consists of Pelona Schist—late Mesozoic quartzofeldspathic sandstone and siltstone, limestone, quartzite, chert, and mafic volcanic rocks that have been metamorphosed to greenschist and lower amphibolite facies, presumably during late Mesozoic to early Tertiary emplacement of the upper plate (Ehlig, 1968b, 1981, 1982). From the Frazier Mountain region southeast to the Salton Trough, Pelona Schist occurs as windows and fault-bounded blocks (Ehlig, 1968b), including (Plate IIIA): (1) the Sierra Pelona window in the western San Gabriel Mountains; (2) the Lytle Creek window in the eastern San Gabriel Mountains; (3) the Blue Ridge slice between the Punchbowl and San Andreas faults; (4) a large window that mostly has been buried beneath sedimentary fill of the San Bernardino Valley; and (5) the Orocopia Mountains and Chocolate Mountains windows of Pelona-type schist that are referred to as Orocopia Schist and that are separated from rocks of San Gabriel Mountains type by the Orocopia–Chocolate Mountain thrust. Both lower and upper plates are intruded by high-level Miocene granitoid plutons and dikes that were emplaced after initial juxtaposition of the two plates (Miller and Morton, 1977; Crowe and others, 1979).

Basement rocks of *Peninsular Ranges type* (Fig. 2B) consist of Jurassic and Cretaceous granitoid rocks (granodiorite, quartz diorite, tonalite, gabbro) that have intruded prebatholithic metasedimentary rocks (pelitic schist, metaquartzite, marble, quartzofeldspathic gneiss, and schist). Along its north and northeast edge, the Peninsular Ranges block is bordered by a mylonitic belt of ductile deformation that separates lower plate plutonic and metasedimentary rocks of typical Peninsular Ranges type from broadly similar upper plate rocks that appear to be parautochthonous equivalents of the more typical Peninsular Ranges suite; the autochthonous and parautochthonous suites have been telescoped along the mylonite zone (Sharp, 1979; Erskine, 1985). The ductile zone is referred to by different names locally, but Sharp (1979) recognized its regional significance and named it the Eastern Peninsular Ranges mylonite zone. The ductile zone probably continues westward into the southeastern San Gabriel Mountains, where mylonitic rocks have been mapped a few kilometers north of the Mountain front (Alf, 1948; Hsu, 1955; Morton and Matti, 1987); if so, then the San Gabriel mylonitic belt may separate lower and upper plate rocks of Peninsular Ranges type—a speculative proposal we adopt here (Plate IIIA).

Juxtaposition of Peninsular Ranges–type and San Gabriel Mountains–type rocks in the southeastern San Gabriel Mountains represents either (1) original intrusive relations between the two suites, (2) their tectonic juxtaposition by Neogene strike-slip displacements, (3) their tectonic juxtaposition by Paleogene or latest Cretaceous thrust faulting (May and Walker, 1989), or (4) a combination of some or all of these mechanisms.

Basement rocks of *San Bernardino Mountains type* (Fig. 2C) are similar to those in the Mojave Desert, and consist of Triassic through Cretaceous granitoid rocks of various compositions that have intruded prebatholithic orthogneiss (Proterozoic) and metasedimentary rocks (Late Proterozoic and Paleozoic metaquartzite, marble, pelitic schist, and gneiss). The metasedimentary rocks are comparable with rocks of the Cordilleran miogeocline (Stewart and Poole, 1975). The Mesozoic plutonic rocks include both deformed and undeformed suites that extend southeastward into the Little San Bernardino Mountains, where they intrude rocks of San Gabriel Mountains type. Strongly deformed Mesozoic granodiorite, tonalite, and quartz diorite form a discrete belt in the southeastern San Bernardino Mountains and along the western margin of the Little San Bernardino Mountains (Plate III). Like rocks of San Gabriel Mountains type, rocks of San Bernardino Mountains type may be a layered terrane with batholithic and prebatholithic rocks in an upper plate separated from Pelona Schist in a lower plate by a low-angle fault comparable to the Vincent thrust.

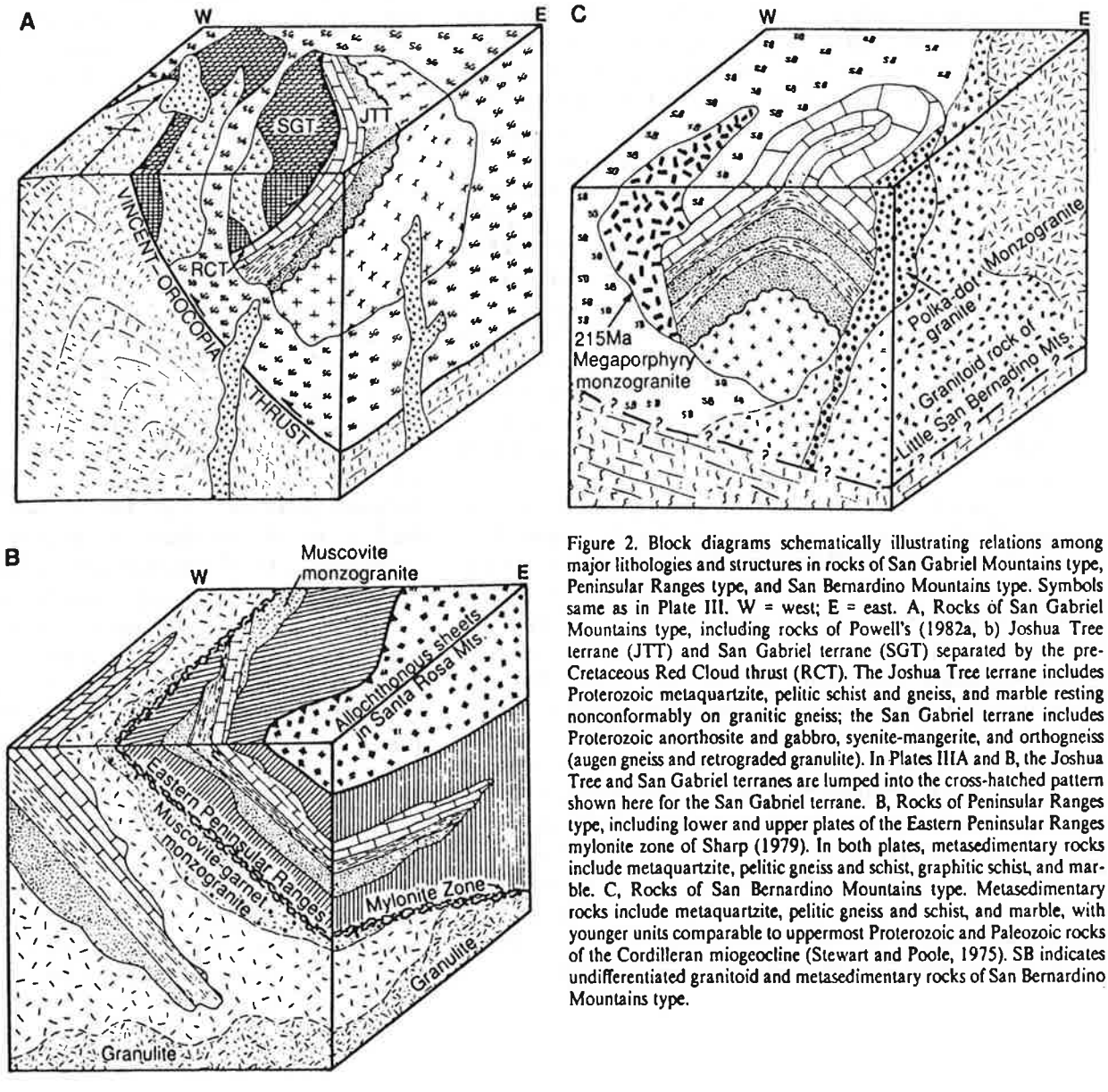

Figure 2. Block diagrams schematically illustrating relations among major lithologies and structures in rocks of San Gabriel Mountains type, Peninsular Ranges type, and San Bernardino Mountains type. Symbols same as in Plate III. W = west; E = east. A, Rocks of San Gabriel Mountains type, including rocks of Powell's (1982a, b) Joshua Tree terrane (JTT) and San Gabriel terrane (SGT) separated by the pre-Cretaceous Red Cloud thrust (RCT). The Joshua Tree terrane includes Proterozoic metaquartzite, pelitic schist and gneiss, and marble resting nonconformably on granitic gneiss; the San Gabriel terrane includes Proterozoic anorthosite and gabbro, syenite-mangerite, and orthogneiss (augen gneiss and retrograded granulite). In Plates IIIA and B, the Joshua Tree and San Gabriel terranes are lumped into the cross-hatched pattern shown here for the San Gabriel terrane. B, Rocks of Peninsular Ranges type, including lower and upper plates of the Eastern Peninsular Ranges mylonite zone of Sharp (1979). In both plates, metasedimentary rocks include metaquartzite, pelitic gneiss and schist, graphitic schist, and marble. C, Rocks of San Bernardino Mountains type. Metasedimentary rocks include metaquartzite, pelitic gneiss and schist, and marble, with younger units comparable to uppermost Proterozoic and Paleozoic rocks of the Cordilleran miogeocline (Stewart and Poole, 1975). SB indicates undifferentiated granitoid and metasedimentary rocks of San Bernardino Mountains type.

Southern extension of the Independence dike swarm of eastern California

Eric William James* Department of Geological Sciences, University of California
Santa Barbara, California, 91206

ABSTRACT

New geochronologic data show that Jurassic dikes in the western Mojave Desert and Eastern Transverse Ranges are part of the Independence dike swarm of eastern California. These occurrences extend the length of the dike swarm to more than 500 km. U/Pb zircon concordia intercept ages for dikes near Stoddard Well in the western Mojave Desert and Big Wash in the Eagle Mountains are identical within analytical uncertainties to 148 Ma zircon ages for Independence dikes north of the Garlock fault. Recognition of this widespread magmatic and tectonic event with a restricted age has important ramifications. (1) Crosscutting relations between the dikes and pre-Upper Jurassic and Cretaceous rocks help establish relative ages. (2) Persistence of dikes across several inferred terrane boundaries constrains terrane accretion ages. (3) The dike rocks represent magmatic processes in a wide range of wall-rock settings. (4) The dikes are structural markers that record translations and rotations of crustal flakes. (5) Regional persistence and dilational emplacement of the Independence dike swarm suggest that it is the last extension in a series of alternating extensional and compressional events during the Jurassic. The tectonic regime responsible for the Independence dikes may be related to arc-normal extension, changes in plate motions, or oblique subduction with left-lateral shear.

INTRODUCTION

This article presents U/Pb geochronologic data to confirm that dikes in the western Mojave are part of the Independence dike swarm and reveal an extension of the swarm >100 km southeast into the Eagle Mountains of the Eastern Transverse Ranges. These additions increase the known length of the Independence dike swarm to more than 500 km, making it the longest dike swarm in the Cordillera.

Late Jurassic Independence dikes of eastern California compose a north- to northwest-trending regional swarm (Fig. 1) extending southeastward from the central Sierra Nevada (Moore and Hopson, 1961) to the Spangler Hills north of the Garlock fault. The swarm is offset 65 km in a left-lateral sense by the Garlock fault to the Granite Mountains and continues southeast to the Soda Mountains, and possibly as far as the Providence Mountains (Smith, 1962). Southwest, in the western Mojave, dikes mapped by Dibblee (1960a, 1960b, 1960c, 1964a, 1964b) compose a probable correlative swarm (Miller and Sutter, 1982; Karish et al., 1987). These dikes are voluminous in the Ord, Fry, and Rodman mountains and westward toward Victorville. Isolated dikes crop out in the northeastern San Bernardino Mountains.

To the southeast, toward the Eastern Transverse Ranges, dikes exhibit trends, compositions, and crosscutting relations (Dibblee, 1967a, 1967b, 1967c, 1976; Hope, 1966; Powell, 1981) that make them candidates for a further extension of the Independence dike swarm (James, 1987). Dikes may be present west of the San Andreas fault in the San Gabriel Mountains, where post-Triassic dikes are cut by Cretaceous plutons (Ehlig, 1981). Dikes may extend as far south as Sonora, Mexico (Silver and Anderson, 1983).

AGE, ORIENTATION, AND COMPOSITION OF THE INDEPENDENCE DIKES

The Independence dike swarm cuts the wall rocks and older plutonic rocks of the Sierra Nevada batholith but is cut by Cretaceous plutons. Chen and Moore (1979) established a 148 Ma age for Independence dikes north of the Garlock fault by using U/Pb isotopic methods on zircon. This Late Jurassic emplacement age is unusual, occupying a relative lull between voluminous Jurassic and Cretaceous plutonism and closely postdating the Nevadan orogeny (Chen and Moore, 1979).

The dike swarm trends north to northwest, although locally trends are variable. Right-stepping en echelon dikes are common (Smith, 1962). Most dikes dip more steeply than 70°. Continuity of the swarm is interrupted in several places; it is offset by the Garlock fault, steps to the right into the western Mojave Desert, and is obscured locally by post-Jurassic plutons and cover.

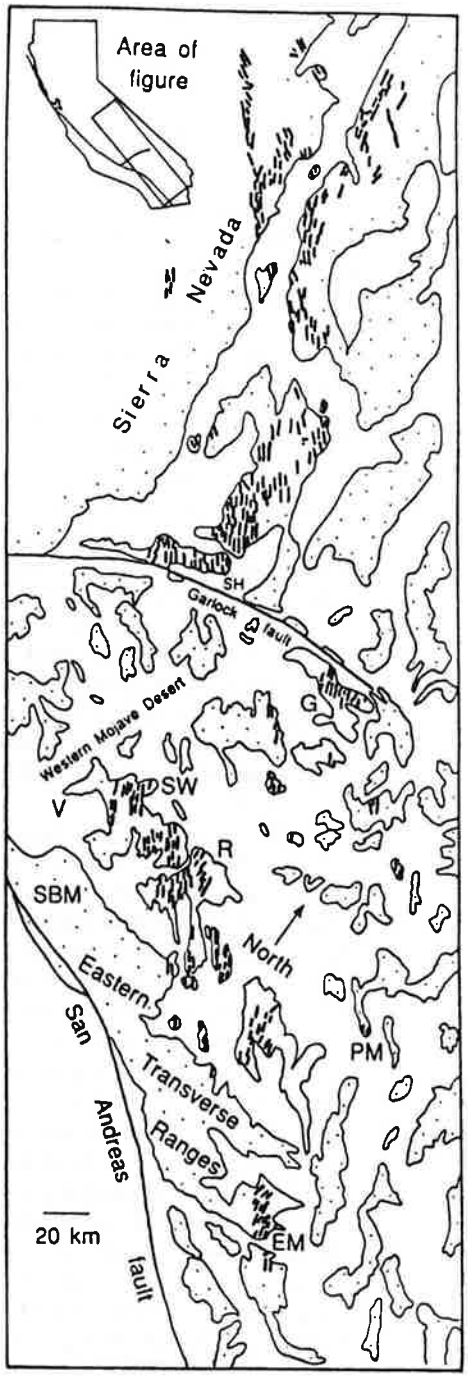

Figure 1. Distribution of Independence dikes (lines) and pre-Tertiary igneous and metamorphic rocks (stipple) in eastern California. EM = Eagle Mountains; G = Granite Mountains; PM = Providence Mountains; R = Rodman Mountains; SBM = San Bernardino Mountains; SH = Spangler Hills; SW = Stoddard Mountain; V = Victorville. Compiled and modified from Dibblee (1960a, 1960b, 1960c, 1964a, 1964b, 1967a, 1967b, 1967c, 1976), Moore and Hopson (1961), Smith (1962), Hope (1966), Chen and Moore (1979), Miller and Sutter (1982), Powell (1981), James (1987), and Karish et al. (1987).

terranes predates 148 Ma and shows the minimum westward extent of North America in the Late Jurassic.

The diversity of terranes cut by the dikes suggests that their magmas may have been derived from sources with different ages or compositions. The wall rocks also represent different possible contaminants. The range of compositions from basaltic to rhyolitic and the presence of calc-alkaline and alkaline series rocks attests to their varied geneses. Variations in apparent ages of inherited zircon from over 2 Ga (Chen and Moore, 1979) to 1.2 Ga suggest contributions from very different sources. Differences in initial $^{208}Pb/^{204}Pb$ vs. $^{206}Pb/^{204}Pb$ ratios (Fig. 3) have the same implication. High $^{208}Pb/^{204}Pb$ ratios in the Stoddard and Eagle mountains dikes are similar to leads from the Eastern Mojave (Wooden et al., 1988) but different from those north of the Garlock fault (Chen and Moore, 1979).

The dike swarm is also a widespread structural marker. Disruptions in continuity and orientation of the dikes indicate translations and rotations of crustal blocks. Two belts of dikes in the eastern and western Mojave Desert with similar patterns of Paleozoic and Mesozoic wall rocks suggest repetition by faulting (James, 1987). Northwest-trending late Tertiary to Holocene right-lateral faults in the Mojave have inappropriate orientations to account for much of this displacement. However, regional low-angle faults of several ages may be responsible. Silver (1982, 1983) suggested that the Late Cretaceous–early Tertiary Rand and Vincent–Chocolate mountains "thrust" systems and later Tertiary low-angle faults transported stacks of crustal flakes westward in the Mojave Desert. Glazner et al. (1989) have presented evidence for about 40 km of offset of the dike swarm by Tertiary detachment faults. The position of the Independence dike swarm south of the Garlock fault is the result of several displacements, the most striking of which appears to offset the dike swarm and its wall rocks from the eastern into the western Mojave Desert.

The strike of the dike swarm also records rotational history. Aside from local variations, dike trends are to the north-northwest. Dikes show little differential rotation between ranges except immediately south of the Garlock fault where they are rotated clockwise up to 45° (Smith, 1962). The scarcity of obviously rotated parts of the dike swarm suggests either that rotations are rare or that they are regional and nearly uniform. This suggestion contrasts with the results of paleomagnetic studies on Tertiary rocks in the Mojave. These investigations (Burke et al., 1982; Hillhouse and Wells, 1986; Carter et al., 1987; MacFadden et al., 1987; Golombek and Brown, 1988) suggest that parts of the Mojave Desert have rotated clockwise, other areas have rotated counterclockwise, and some parts remain unrotated. In part, differences between paleomagnetic results reflect different ages and domains of rotation. Comparing paleomagnetic data to the local trend of Independence dikes may clarify the apparently complicated rotational history.

The extent of the Independence dike swarm indicates that it is a plate margin–scale phenomenon and an important event in the Jurassic magmatic, deformational, and tectonic history of the Cordillera. Moore and Hopson (1961) noted that the dikes postdate the Nevadan orogeny and that some dikes show evidence of sinistral shear. Dunne et al. (1978) documented intrusion of left-slip faults by Independence dikes east of the Sierra Nevada. Left-lateral faults and shearing may be related to activity of the left-lateral Mojave-Sonora megashears, which Silver and Anderson (1983) suggested closely predates Independence dike emplacement. Most dikes are undeformed and represent dilational emplacement, indicating an extensional regime. The orientation of the dikes indicates that the direction of maximum extension at 148 Ma was N65°E, perhaps reflecting rebound after the Nevadan orogeny (Chen and Moore, 1979).

These observations contribute to a view of the Independence dike swarm as the last phase in

Tectonic causes for extensional magmatism alternating with compressive orogenesis are not entirely clear. However, extensional episodes like the Independence dike swarm may be rationalized in several ways. First, the dikes may represent extension at a high angle to the trench, reflecting the prevalent state of stress in a convergent margin. Despite the intuitive notion of convergence, arcs are generally extensional or neutral environments (see review and references in Hamilton, 1988). Geologic evidence for compressive orogenesis—folds, faults, and fabrics—is often dramatic and well preserved but may represent only short-lived events. The dike swarm may reflect the prevalent conditions in the Jurassic arc which were punctuated by several compressive orogenies. Alternatively, the dikes may be the consequence of a change in plate organization and relative motion. Many Cordilleran tectonic events are coincident with changes in the North American apparent polar wander path (Wright and Miller, 1988). Convergence of the Farallon and North American plates decreases radically from about 8 cm/yr to 1 cm/yr at about 148 Ma (Page and Engebretson, 1984). The lack of spread in Independence dike ages supports a discrete, rather than continuous, tectonic trigger. A third possibility is that the dikes are a consequence of transtension in an obliquely convergent margin. The substantial and variable component of left-lateral Farallon–North American motion (Page and Engebretson, 1984) could have effected transtension (and transpression) in the Jurassic plate margin. However, given the uncertainties in plate motions and ages of geologic events, specific correlations are speculative. Further work must address timing, duration, magnitude, diachroneity, and cyclicity of Jurassic extensional and compressional events and critically compare this geologic history with plate models.

APPENDIX 1. LOCATION AND PETROGRAPHY OF SAMPLES

Stoddard Well dike, lat 34°42′34.5″N, long 117°05′35.4″W. Hillside south of Stoddard Well. Tan to rusty weathering porphyritic rhyolite dike containing 64.5% groundmass of 0.02–0.03 mm alkali feldspar crystals (~30%), quartz (~50%), plagioclase (~20%), and traces of sericite; 11.2% 3–6 mm alkali feldspar phenocrysts; 11.2% 0.75–2.5 mm slightly resorbed quartz phenocrysts; 10.3% 1–2 mm plagioclase phenocrysts; and 2% chloritized biotite and traces of epidote, allanite, titanite, and apatite.

Eagle Mountains dike, lat 33°46′40.0″N, long 115°33′20.8″W. North side of Big Wash. Rusty weathering porphyritic rhyolite dike containing 73.9% recrystallized groundmass of 0.06 mm alkali feldspar

Strontium Isotopic Correlation of the La Panza Range Granitic Rocks with Similar Rocks in the Central and Eastern Transverse Ranges

GEOLOGY AND MINERAL WEALTH OF THE CALIFORNIA TRANSVERSE RANGES

Stephen E. Joseph, Terry E. Davis and Perry L. Ehlig, California State University, Los Angeles, California 90032
Stephen E. Joseph presently with California Division of Mines and Geology, 107 S. Broadway, Room 1065, Los Angeles, California 90012

ABSTRACT

Smith (1977a) correlated quartz monzonite of the La Panza Range in the southern Salinian block with that of the Thermal Canyon area, north of the Salton Sea, and with that occurring as clasts within the Vasquez Formation of Charlie Canyon in the Central Transverse Ranges. He also reported the occurrence of distinctive "polka dot granite" dikes within the eastern La Panza Range.

Joseph and Ehlig, 1977 showed that the Charlie Canyon clasts are essentially identical to the quartz monzonite of the Thermal Canyon in bulk chemistry, Rb-Sr mineral ages (74.1 ± 0.9 m.y. and 74.0 ± 0.9 m.y.) and initial $^{87}Sr/^{86}Sr$ ratios (0.7092 ± .0001 and 0.7091 ± .0002). Quartz monzonite in the western La Panza Range yielded slightly different results (79.9 ± 0.6 m.y. and 0.7083 ± .0002) leaving its correlation in doubt. Subsequent geochemical and isotopic analyses of "polka dot granite" from dikes in American Canyon in the eastern La Panza Range and dikes in the basement terrane at Warm Springs Mountain to the north of Charlie Canyon have yielded similar Rb-Sr mineral isochrons (72.0 ± 0.6 m.y. and 72.4 ± 1.1 m.y.) and similar initial $^{87}Sr/^{86}Sr$ ratios (0.7128 ± .0004 and 0.7136 ± .0003). "Polka dot granite" from dikes in the northern Orocopia Mountains to the southeast of Thermal Canyon give moderately different results (82.9 ± 2.3 m.y. and 0.724 ± .001).

These data suggest that the La Panza, Warm Spring Mountain-Charlie Canyon and Thermal Canyon terranes developed in close proximity to each other and have subsequently been displaced to their present positions by strike-slip faulting. The occurrence of "polka dot granite" in all three areas is by itself supportive of the correlation. However, there is one other similar occurrence of "polka dot granite" in the southern Sierra Nevada near the mouth of the Kern Canyon, but it yields an older Rb-Sr mineral age (100.7 ± 1.1 m.y.) and an initial $^{87}Sr/^{86}Sr$ ratio indicative of a non-continental origin (0.7042 ± .0003).

Removal of 300 km of post Middle Miocene right slip along the San Andreas fault, including 60 km along the San Gabriel fault, would place the La Panza Range about 120 km northwest of its probably initial position at the north end of the present Salton trough. The additional displacement may have occurred along the San Juan-Chimeneas-Morales-Blue Rock-San Francisquito-Fenner-Clemens Well (San Juan-Clemens Well) fault as proposed by Smith (1977a), but that has not yet been substantiated.

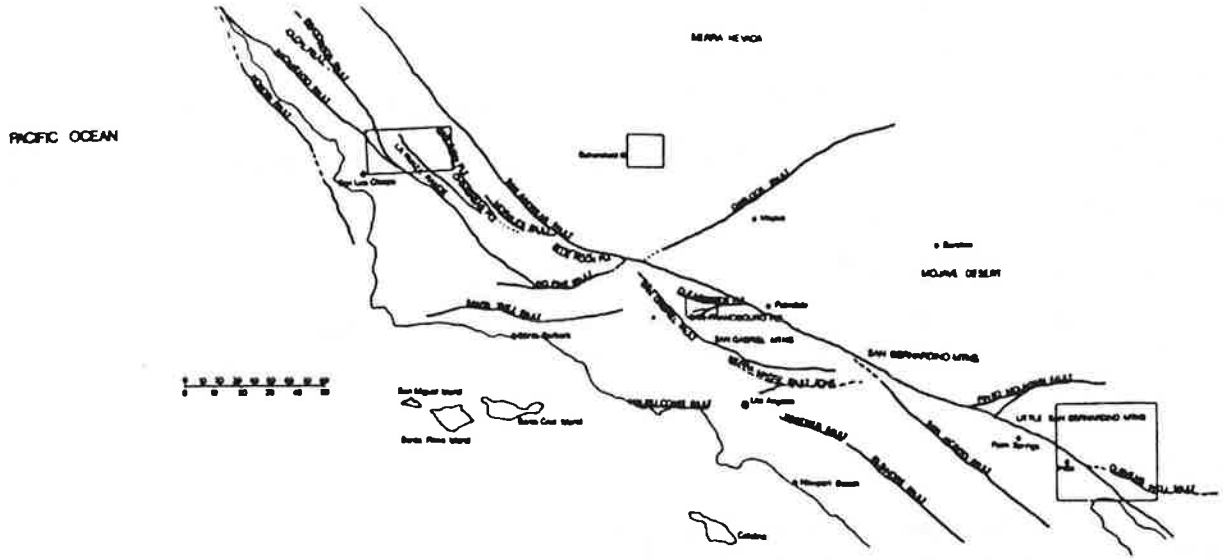

Figure 1. Generalized map of western California showing major faults and sampling localities.

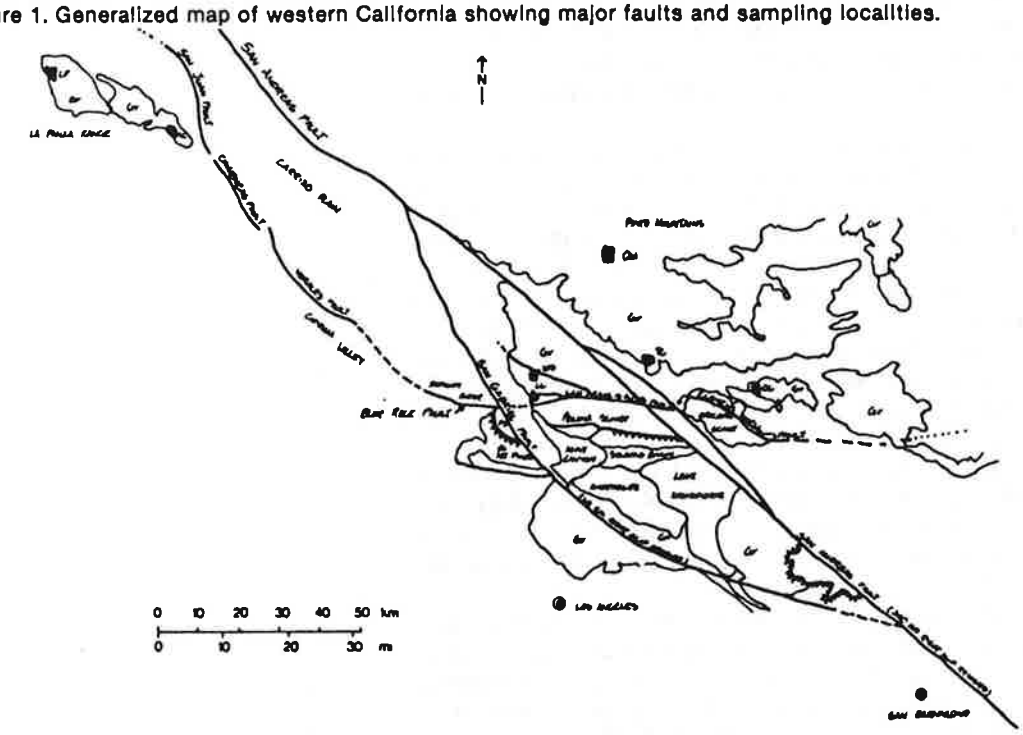

Figure 6. Geologic map showing the Central Transverse Range basement restored to its Middle Miocene position in southeastern California by removal of 240 km. of right slip on the San Andreas fault and 60 km. of right slip on the San Gabriel fault. (After Ehlig,

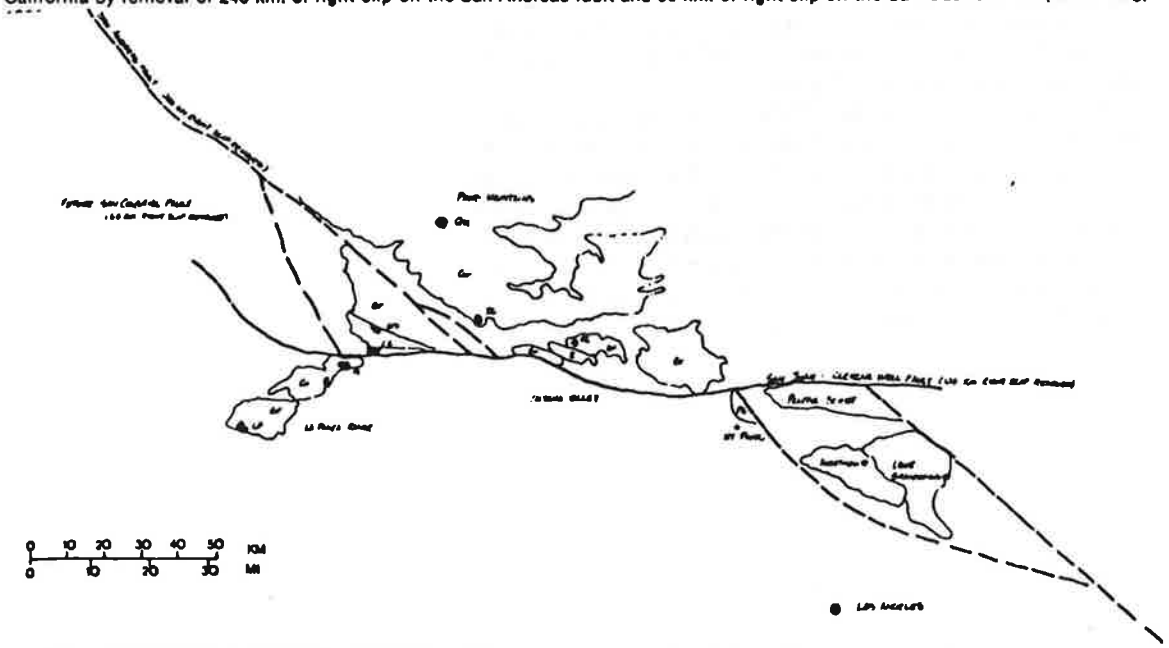

Figure 7. Geologic map showing southeastern California basement restored to its Early Oligocene position by removal of 120 km. of right slip on the San Juan - Clemens Well fault.

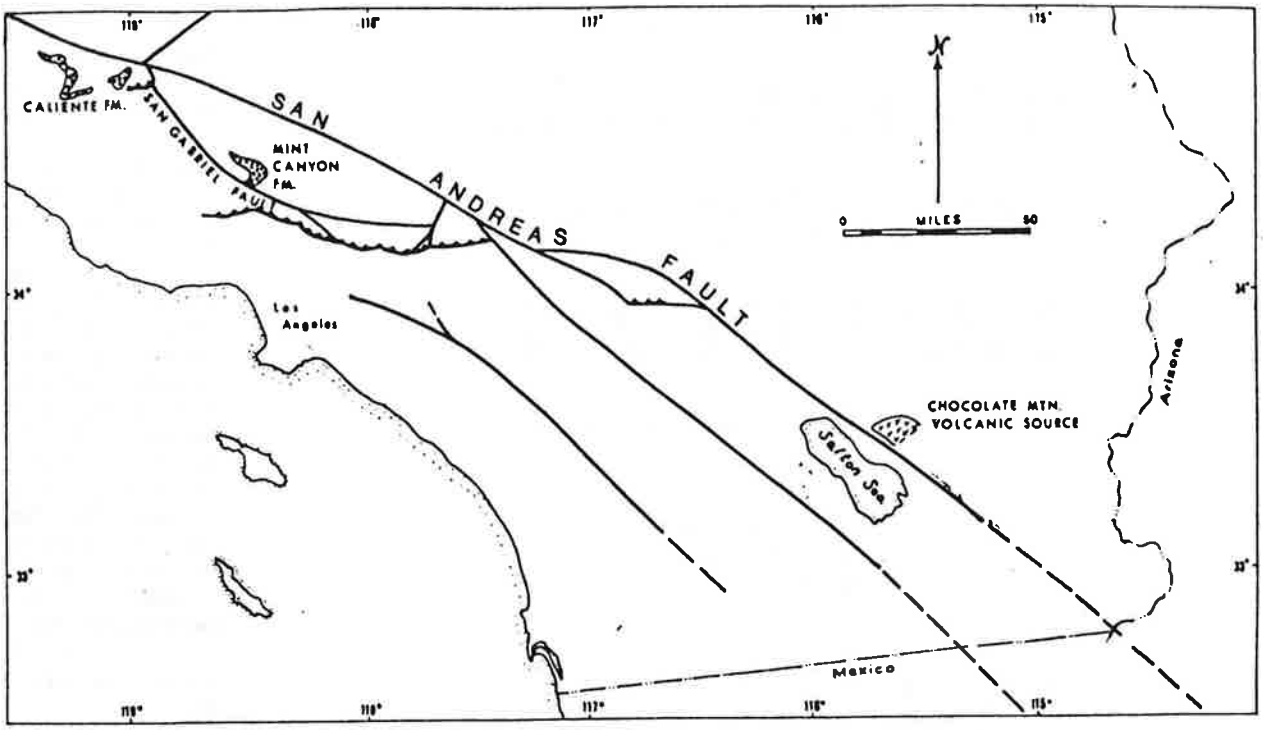

Figure 1.
Index map showing location of Mint Canyon Formation, Caliente Formation and Chocolate Mountain source terrane.

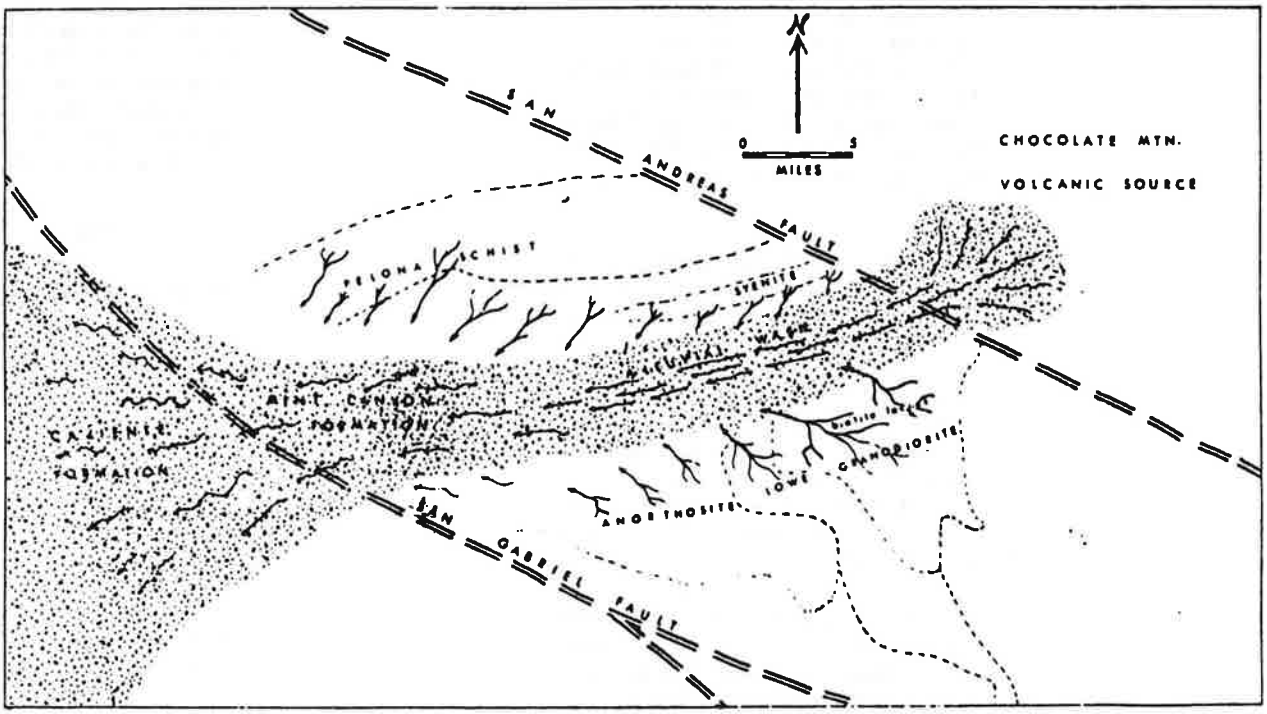

Figure 3.
Postulated drainage pattern during deposition of lower part of Mint Canyon and Caliente Formation before movement began along San Andreas and San Gabriel faults.

THE JOSHUA TREE NATIONAL MONUMENT

Riverside and San Bernardino Counties

By

D.D. TRENT, Geologist
Citrus College
Azusa, California

> Go my sons, buy stout shoes, climb the mountains, search the valleys, the deserts, the sea shores, and the deep recesses of the earth...for in this way and in no other will you arrive at a knowledge of the nature and properties of things.
>
> *P. Severinus (Circa 1778)*

Location and Physiography

Joshua Tree National Monument is on the eastern end of the broad mountainous belt called the Transverse Ranges (Figure 1). The Tranverse Ranges stretch from Point Arguello, 50 miles west of Santa Barbara, eastward for nearly 300 miles to the Eagle Mountains in the Mojave Desert.

The Monument region is made up of several distinct mountain ranges, the Little San Bernardino Mountains in the southwestern part, the Cottonwood, Hexie, and Pinto Mountains in the center, and the Eagle and Coxcomb Mountains in the eastern part. Both the southern and northern margins of the Monument are marked by steep escarpments that rise abruptly from the lower desert areas. Much of the Monument lies at elevations above 4,000 feet.

Valleys lying between these mountain ranges are of two types, those that have been formed by downdropping along faults (*grabens* or *structural basins*), and those that have been carved by erosion. Pleasant Valley, between the Little San Bernardino and Hexie Mountains, is an example of the structural type; Queen Valley, in the central part of the Monument, is an example of the eroded type.

Climate

The climate of the high desert of the Joshua Tree region is that of a mid-latitude desert with relatively moderate temperatures. For example, the average temperature at Twentynine Palms, elevation 2000 feet, is only 67.3°F (19.6°C), and at Hidden Valley Campground the average temperature is about 62°F (17°C). There are two factors causing eastern California to be a desert: 1) the "rain shadow" effect produced by the high mountains on the west, and 2) the existence during summer months of a semi-permanent high-pressure air mass, the Hawaiian High, which builds up over the northeastern Pacific Ocean and blocks the passage of frontal storm systems over California. Occasionally during the summer and fall the Hawaiian High weakens and moist air slips into the region across Arizona from the Gulf of Mexico bringing thunderstorms. For this reason August has the highest rainfall (Table 1) which, curiously enough, is usually the driest month for the more humid portions of the state.

In the winter months the Hawaiian High usually dissipates and southern California receives an average of four or five frontal storms that originate in the northern Pacific. At this time the second rainy season in the desert occurs in December and January (see Table 1). The average rainfall at Twentynine Palms is only a little over four inches but at higher elevation the average rainfall increases. The Joshua trees serve as a rain gauge in those areas of the desert where no records are kept because they require 10 inches or more of annual rainfall in order to survive.

ROCK TYPES

Metamorphic Rocks

The oldest rocks of the Joshua Tree region are those of the Precambrian *Pinto Gneiss* which range in composition from quartz monzonite to quartz diorite. Much of the rock is dark-gray and prominently foliated, but some is much lighter, sometimes nearly white and only faintly foliated. The gneiss is composed primarily of quartz, feldspar, and biotite. Where there is a significant amount of biotite the Pinto Gneiss is very dark and this distinguishes it from the other rocks in the area (Photo 1).

The Pinto Gneiss, which is exposed in much of the high desert of Joshua Tree National Monument, formed from the metamorphism of pre-existing sedimentary and igneous rocks. Radiometric dates give two ages of metamorphism, 1650 million years and 1400 million years (Powell, 1982, p. 120-121).

The Pinto Gneiss served as the host rock into which the younger plutonic rocks intruded. Examples of the intrusive contact can be seen along the trail to Fortynine Palms Oasis and northeast of Sheep Pass (Photo 2).

Igneous Rocks

At least four different major plutons have intruded the Pinto Gneiss (Figure 2). The oldest are Jurassic, and the youngest are Cretaceous. The exact dates of these Mesozoic intrusions, however, are poorly known. Isotopic ages of Jurassic plutons in California fall generally between 186 and 155 million years, and the ages of the Cretaceous plutons are mainly between 155 and 125 million years (Bateman, 1981). The Mesozoic plutons in Joshua Tree National Monument, in common with the granitic plutons of the Sierra Nevada, the Peninsular Ranges, the Klamath Mountains, and the White-Inyo Mountains, are generally believed to have originated in an Andean-type tectonic environment (Ernst, 1981).

The oldest pluton is the Twentynine Palms porphyritic quartz monzonite (Brand and Anderson, 1982). It consists of a matrix of small mineral grains which enclose large spectacular phenocrysts of potassium feldspar crystals that attain lengths of up to two inches. This pluton belongs to the important Jurassic plutonic belt of the western United States (Powell, 1982), which is significant because it may signal the onset of Andean-type tectonics on the continental margin (Miller, 1977). The rock crops out at the beginning of the trail to Fortynine Palms Oasis and is exposed along the arroyo on the east side of the Indian Cove campground.

The earliest of the Cretaceous plutons is the Queen Mountain monzogranite, which is exposed over a large area around Queen Mountain (Figure 2). It is coarse-grained, and consists of plagioclase, potassium feldspar, quartz, and either biotite or biotite and hornblende (Brand and Anderson, 1982).

The light-colored, Cretaceous White Tank monzogranite predominates in the more accessible parts of the Monument. The rock was originally recognized as a monzonite by Miller (1938), later as a quartz monzonite by Rogers (1954, 1961) and Dibblee (1968), but is now named a monzogranite (Brand and Anderson, 1982; Powell, 1982) in accordance with the modified version of Streckeisen's classification (1973) of igneous rocks. It resembles the Queen Mountain monzogranite but differs by being finer-grained, and by containing very small amounts of biotite and/or muscovite but no hornblende (Brand, personal communication). Areas underlain by the White Tank monzogranite include Indian Cove, the Wonderland of Rocks, Jumbo Rocks, White Tank, and Lost Horse Valley (Photo 3).

The youngest of the Cretaceous plutons, the Oasis monzogranite, is a distinctive garnet-muscovite-bearing pluton that is exposed in the area of Fortynine Palms Oasis (Brand and Anderson, 1982). The garnets are blood red and small, but large enough, nevertheless, to be visible without magnification. The muscovite grains impart a glittery appearance to the rock on sunny days, even in shadows.

In addition to large monzogranite and quartz monzonite plutons, there are masses of a similar granitic rock called *granodiorite*, and small dark plutons called the Gold Park diorite (Rogers, 1954, 1961; Brand and Anderson, 1982). Cutting across all of these rock masses, and thus being younger in age, are dikes of *felsite, aplite, pegmatite, andesite,* and *diorite* (Photo 4).

Even younger than these dikes are veins of milky quartz which over the years have been prospected for gold. The quartz is sometimes stained reddish brown from the weathering of pyrite, or fools gold. Pyrite is a common mineral in quartz veins and is sometimes associated with gold or other valuable minerals. Chemical alteration of the pyrite produces reddish iron oxides that stain the rock and serve the prospector as a clue that gold, silver, copper, and other metals may be present.

The pegmatite dikes are mainly quartz and potassium feldspar and have a composition close to that of granite. What makes them distinctive is the very large size attained by the mineral grains, often three or four inches long. Pegmatites may have large books of biotite and muscovite mica (isinglass).

Basalt occurs at three places in the Monument: (1) near Pinto Basin, where the basalt probably originated as *extrusive flows*, (2) at Malapai Hill on the Geology Tour Road (Photos 5 and 6), and (3) in the Lost Horse Mountains (Photos 7 and 8). In addition to basalt, another rock named *lherzolite* occurs as inclusions within the basalt at Malapai Hill and in the Lost Horse Mountains. Lherzolite is about 75 percent olivine with the remain-

der being mostly *bronzite* and *diopside*. It is considered to be derived from the mantle; thus the basalt has risen some 35 to 50 miles to carry the lherzolite inclusions to the surface.

STRUCTURAL GEOLOGY

Faults

Uplifting and downdropping, and horizontal slipping of crustal blocks in the Joshua Tree region has occurred along fractures (faults) in the earth's crust. The *Pinto Mountain fault* is one of the most prominent. The topographic break marking the fault zone is closely followed by the Twentynine Palms Highway (State Highway 62) between Morongo Valley and Twentynine Palms. The fault trends nearly east-west along the north side of the Pinto Mountains.

On the south side of the Monument the *Blue Cut fault* extends east-west through the Little San Bernardino Mountains, about one-half mile south of Keys View, under Pleasant Valley and into the Pinto Basin. The Blue Cut fault branches from the *Dillon fault* which is even further south and trends southeastward through the Little San Bernardino Mountains. The Blue Cut and Pinto Mountain faults are both left-lateral faults. They may belong to a conjugate fault set that includes the north-northwest trending right-lateral faults of the Mojave Desert (Powell, 1982, p. 109). Pleasant Valley is a graben formed by the Blue Cut fault and one of its branches (Photo 9).

South of the Dillon and Blue Cut faults is the *San Andreas fault zone*. The trace of the San Andreas fault is clearly visible from Keys View (Photo 10). The San Andreas fault south of the Monument is divided into two main branches, the *Banning* and *Mission Creek faults*. The trace of these faults is marked by the Indio Hills, a small uplifted block that is wedged between the faults, and by a number of springs and palm oases along the faults.

In addition to the major faults are many hundreds of minor faults throughout the region. Fault zones are important factors in localizing springs. Movement by faults causes impervious zones of shattered rock fragments to form an underground dam, which forces ground water to rise. The oasis at Cottonwood Springs, for example, appears to be due to a fault zone which has provided the fissures along which ground water reaches the surface. The oasis at the Visitor Center at Twentynine Palms marks the Pinto Mountain fault.

Rock Jointing

Joints are simply small fissures cutting rocks. They may occur in *sets* of parallel joints and *systems* of two or more intersecting sets. The White Tank monzogranite has a system of joints that is primarily responsible for the spectacular landforms in the Monument. The joint system in the White Tank monzogranite consists of three dominant joint sets. One set oriented horizontally has been caused by the release of pressure due to the removal of overlying rocks by erosion. These joints, sometimes called *lift joints*, cause *rock sheeting* and are caused by expansion and the release of stress in rocks, somewhat analogous to a seat cushion resuming its shape after the person sitting on it arises. Lift joints form dome-like outcroppings where vertical joints are widely spaced (Photo 3).

Another set of joints is oriented vertically, and roughly parallels the contact of the White Tank monzogranite with its surrounding rocks. The third set is also vertical, but it is approximately perpendicular to the other vertical set. The resulting system of joints forms rectangular blocks. Especially good examples of the joint system are at Jumbo Rocks, Wonderland of Rocks, and Split Rock (Photos 4 and 11).

Joints are often closely spaced along fault zones, where either there may be no apparent order to their pattern, or the major joint set may closely parallel the orientation of the fault.

Photo 4. Aplite dike cutting White Tank monzogranite on the Barker Dam trail. The horizontal shelf-like development of the cliff is from thick slabs of monzogranite blocked out by rock sheeting.

SCULPTURING THE LANDSCAPE

Weathering

One of the most impressive aspects of the landforms in the Joshua Tree region is the strange and picturesque shapes assumed by the bold granitic rock masses at the Wonderland of Rocks, Ryan Campground, Split Rock, and elsewhere in the area (Photos 11, 12). The sculpturing of these rock masses results from the combined action of rock jointing and *chemical* and *mechanical weathering*. The combination of these processes is called *spheroidal weathering*, the spalling-off of thin concentric shells of rock to form spherical rock masses. Spheroidal weathering results from slight pressures that have been built up in the outer portions of the rock from chemical decomposition along joint surfaces. It is the chemical decomposition of the aluminum silicate minerals that is primarily responsible for these pressures. For example, when potassium feldspar comes into contact with hydrogen ions and water, the following chemical reaction takes place:

potassium feldspar + hydrogen ions + water → kaolinite + potassium ions + silica

$$2KAlSi_3O_8 + 2H^+ + H_2O \rightarrow Al_2Si_2O_5(OH)_4 + 2K^+ + 4SiO_2$$

The potassium ions and silica are dissolved in water and eventually carried away by surface runoff or by ground water, leaving behind the clay. The clay mineral that has been formed is called *kaolinite*, and it occupies a greater volume than the original feldspar. This increase in volume is responsible for the pressure that causes the outer part of the cuboidal blocks of rock to expand. The expansion is especially great at the edges and corners so that gradually the blocks of rock lose their sharp edges and eventually assume a rounded or spheroidal shape.

The stresses, in addition to the popping off of thin shells of rock, cause the mineral grains of the rock to disintegrate mechanically and form a loose mineral soil called *grus*.

Frost and *root wedging* contribute to the breakdown of rocks by mechanical action. When water seeping into cracks and joints in the winter months freezes, it expands by 10 percent and breaks the rocks. Plant roots, anchored in a hairline crack or a joint, will slowly expand and enlarge the crack as the plant grows.

The concave hollows and pits that are common on joint surfaces in crystalline rocks form by a process called *cavernous weathering*. This process begins with local irregularities or perhaps temporary accumulations of mineral fragments that hold water on the rock surface. The additional moisture locally promotes kaolinization of feldspars and other aluminum silicate minerals on the surface. Once a concavity begins to develop it perpetuates itself by ponding water from rainfall, melting snow, or even dew. Furthermore, the shade provided by the concavity assists chemical decay by reducing water loss from evaporation and also provides a suitable habitat for lichen. Lichen produces organic acids which furthers the process of chemical decomposition. Loose mineral grains so produced are removed by rainwash or wind.

The undercutting of vertical surfaces, common on the shady sides of rock outcroppings throughout the Monument, have formed in a similar manner to cavernous weathering by the action of moisture trapped in the soil at the base of the vertical surface. Such undercutting probably accounts for many of the steep cliff faces as the processes of wearing back and rounding off higher up on the cliff cannot keep up with the undercutting at the base.

Good examples of cavernous weathering and undercutting exist at many places in the Monument. Skull Rock is an example of undercutting and cavernous weathering (Photo 13).

Photo 13. Skull Rock at Jumbo Rocks illustrates cavernous weathering and undercutting by subsoil notching.

Erosion

Erosion is the dynamic process that lifts up, carries away, and deposits surficial rock material. Running water, even in arid environments, is by far the most important erosional agent. Wind action is important in the desert, but the long range effects of the wind are small when compared to the action of running water.

However, weathering and erosional processes presently operating in the arid conditions of the Joshua Tree region apparently are not entirely responsible for the spectacular sculpturing of the rocks of the region. The present Joshua Tree landscape, and that of much of the Mojave Desert, is essentially a collection of relict features inherited from earlier times of higher rainfall and lower temperatures. Thus, the desert landscape is dominantly a "fossil" landscape. For example, Forty-nine Palms Canyon could not have formed in the present rainfall regime. Such deep canyons are attributed to former pluvial conditions (Bradshaw and others, 1978, p. 305) during an epoch when the area of the southwestern United States received approximately eighty percent greater precipitation than at present, the evaporation was about thirty percent less, and the mean annual temperature was 5°-8°C cooler (Flint, 1971, p. 442-451).

LANDFORMS OF THE DESERT

There are major differences between the landforms in arid and in humid regions. This is because:

1. The internal basins in the desert provide base levels of erosion that may lie well above, or even below, sea level. In humid regions, however, the ocean surface provides the base level of erosion.

2. Base levels of erosion in the Mojave Desert are constantly rising as the products of erosion accumulate in the internal basins, whereas for humid regions, the ocean provides a relatively constant base level.

3. Products from erosion in humid regions are carried great distances, eventually to the ocean. But erosion products in the desert are carried only short distances resulting in the conspicuous accumulation of loose debris in the form of sand dunes, talus, alluvial fans, and bajadas.

Typical arid landforms encountered in the high desert are:
(1) *arroyos* or dry washes, stream courses that contain water only a few hours or perhaps a few days per year;
(2) *playas*, lakes that may contain water a few weeks a year during the rainy season;
(3) *alluvial fans*, fan-shaped deposits of sediment formed at the base of mountains in arid regions;
(4) *bajadas*, the broad sloping aprons of sediment that result from the coalescing of many alluvial fans;
(5) *pediments*, erosional features on gently sloping bedrock surfaces that have been carved along the base of desert mountains.

Pediments are a curious desert landform, typical of the southwestern United States and many other desert areas of the world. Superficially, pediments look like bajadas (depositional features) rather than products of erosion of bedrock. The slopes of pediments are slight, from ½° to about 6°, and they are usually carved on homogeneous crystalline rock such as granite. Pediments may be covered with a thin mantle of gravel, but if more than ten feet of gravel cover a pediment the resulting landform is considered depositional and is called a bajada. In order to determine whether the sloping surface is a pediment or a bajada the thickness of the gravel veneer in the drainage channels must be observed.

Apparently pediments are formed by the retreat of the mountain front leaving an extensive bedrock surface that marks the path of the retreating foot of the slope. Rill wash, sheetfloods, winds, and lateral planation by streams sweep the pediment clean of debris except for local accumulations of gravel.

A pediment can be seen at Malapai Hill (Stop 6 on the "Geology Tour Road" through the Monument*). Large expanses of bare granite pavement and bold dikes weathered out of the granite are exposed on the surface of the pediment (Photo 14 and 15).

* See road guide available at the Monument headquarters.

Photo 15. Remnants of an aplite dike exposed in monzogranite on the pediment near Malapai Hill.

Some investigators regard pediments as the only true desert landforms which can be attributed solely to arid conditions operative at present (Bradshaw and others, 1978, p. 307-308). Others regard pediments as features that have evolved in a sequential manner over a period of perhaps several million years (Ollier, 1975; Oberlander, 1972). At issue are the relative roles of past and present processes in explaining the development of these arid region landforms.

The origin of pediments may be closely linked to the origin of *inselbergs*, prominent steep-sided residual hills and mountains rising abruptly from erosional plains. Inselbergs studied in Uganda are thought to be residuals of deep chemical weathering during the more humid environments of the late Tertiary and Quaternary Epochs (Figure 3A) (Ollier 1975, p. 206-207). Subsurface weathering is more intense in areas of closely spaced jointing but less so in areas of wider joint spacing. Pediments are developed by removal of these deeply weathered rock materials leaving the sparsely jointed rock residuals as inselbergs.

The origin of inselbergs in Uganda is not totally applicable to the deserts of southwestern United States where, unlike Uganda, tectonism has been active for millions of years up to the present. Tectonism has created fault block mountain ranges and downdropped basins. The internal drainage of the basins causes the basins to fill gradually with sediments derived from the adjacent uplands. As a result the local base level of erosion slowly rises. Possibly stream erosion with rising local base levels is important in forming pediments in the Mojave Desert (Figure 3) (Garner, 1974; Bradshaw and others, 1978).

Climatic conditions during the late Tertiary and the Pleistocene must have been significant in the development of pediments and inselbergs. The present climate of this region is relatively new, having been established during the Pleistocene Epoch which began only about 2.5 to 3 million years ago. Botanical evidence indicates that progressive deterioration of vegetative cover took place throughout the Mojave Desert during the Miocene and Pliocene (from about 25 million to about 3 million years ago) (Axelrod, 1950; 1958).

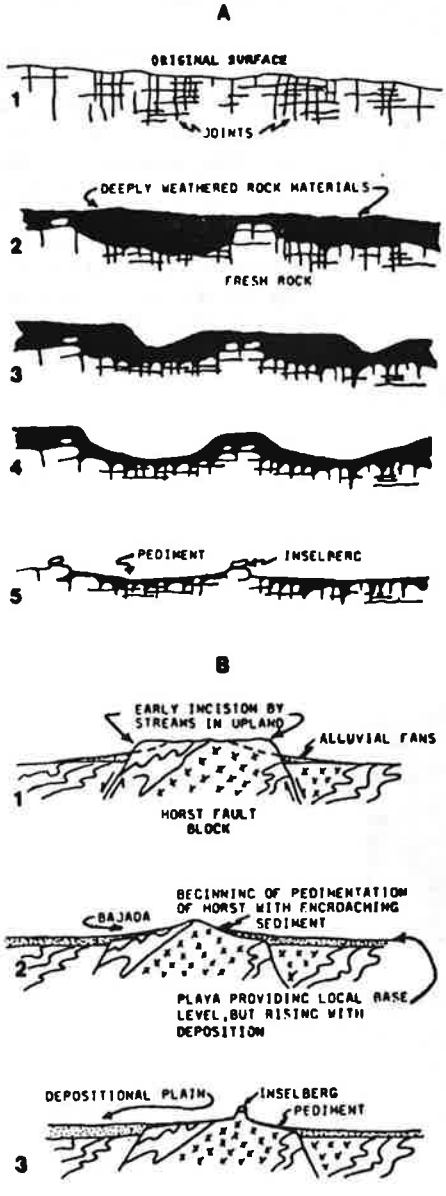

Figure 3. Two theories of pediment and inselberg development.

A. Pediment and inselberg development in Uganda: (*after Ollier, 1975*)
(1) Subsurface jointing in the original substrate.
(2-4) Deep and complete weathering of the rock with closely spaced joints, but unconsumed cuboidal blocks in regions of widely spaced joints.
(5) Removal of weathered rock leaves pediments and inselberg remnants.

B. Pediment and inselberg development in the southwestern United States from a combination of deep weathering of a horst upland, stream erosion, and rising base level in the adjacent down-faulted basins (*after Garner, 1974, and Bradshaw and others, 1978*).

The change in climate and the cor sponding change in plant cover left creasing areas of surface unprotected vegetation which promoted accelera denudation of the soil. Furthermore, renewal of soil during the Pleistoc Epoch was slowed by decreased rain causing the rate of soil erosion to exc the rate of soil formation.

Eight million years ago the landscape the Mojave Desert was one of rolling hi covered with a soil mantle that had dev oped in a hot, semi-arid to humid clima At that time the rates of soil formatic and soil erosion were closely balance The climate and the amount of vegetati cover then were similar to that existi today along U.S. Highway 395 betwe Temecula and Escondido (Oberland 1972).

Increased erosion removed the residu soils from the steeper hillsides leaving b hind the subangular and spheroidal bou ders that formerly had been th subsurface corestones which had been iso lated by chemical decomposition alon joint planes (Figure 4). These coreston features, called *boulder mantled slope* (Oberlander, 1972), can be seen along th road between the northwest entrance t Joshua Tree National Monument an Hidden Valley Campground (Photo 16)

The boulder mantles gradually crumbl away in the present arid climate leavin inselbergs, the cores of relatively un weathered, sparsely jointed granite tha form the spectacular prominences at Hid den Valley, Cap Rock, Jumbo Rocks, and along the Geology Tour Road (Photos 9 and 10). The presence of these masses o undecomposed rock is evidence that the renewal of boulder mantles by present-day weathering processes is not taking place. Thus, the granitic landscape in Joshua Tree National Monument, and elsewhere in the Mojave Desert, is a fossil landscape which has evolved over a time span of several million years (Figure 4).

Evidence for this interpretation comes from sites in the Mojave Desert such as at Old Woman Springs where reddish iron oxide and calcite-rich soils and corestones in a grus matrix have been preserved beneath remnants of lava flows. The lava flow at Old Woman Spring has a radiometric age of eight million years. Similar soils form today in warm regions under the cover of heavy brush where the average rainfall exceeds 10 inches annually.

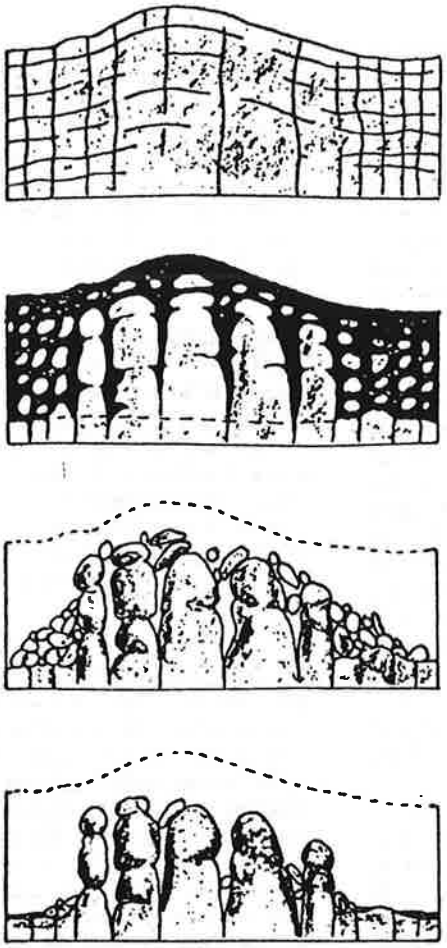

Figure 4. Schematic diagram illustrating the formation of inselbergs at Joshua Tree National Monument.

A. Vertical section through granitic rocks with a varied spacing of joints some 20 million years ago.

B. During the Pliocene after a period of sub-humid climate and decomposition of the rock by ground water that percolated downward along joints to the water table. Rotted and decomposed rock is shown in black.

C. Boulder-mantled slopes developed in the past few tens of thousands of years of the Pleistocene Epoch by the removal of the decomposed rock under arid conditions. Present day examples: along the Fortynine Palms Oasis trail and along the highway between the town of Joshua Tree and Hidden Valley Campground.

D. The present. In higher elevations with longer exposure to conditions of arid weathering, the boulder mantle has been largely decomposed leaving steep-sided bold outcrops rising abruptly above the surrounding surface. A thin veneer of grus covers the horizontal surface. Examples are at Hidden Valley, Caprock, Ryan Campground, and Jumbo Rocks.

Continuity between these relict soils, corestones, and grus beneath the basalt remnants and the present boulder-mantled slopes clearly establishes the boulder mantle as a feature inherited from a time of deep weathering in the late Tertiary Period (Figure 5).

THE FINAL POLISH

Nearly all rock surfaces in the high desert show some degree of *desert varnish*, a usually thin patina of insoluble clay, iron, and manganese oxides. In some cases the surface impregnation of varnish is so deep into the partially decomposed rock that it binds the material together and produces a dark-brown, metallic-looking rind called *case hardening*. The Pinto Gneiss and the monzogranite which crops out at Indian Cove and along the Fortynine Palms Oasis trail have good examples of desert varnish (Photo 17).

Varnish is not unique to the desert, but is best revealed there. Two current hypotheses for the origin of desert varnish are: (1) a microbial origin in which bacteria concentrate manganese oxides (Oberlander and Dorn, 1981), and (2) an inorganic origin in which clay and iron and manganese oxides that are derived from air borne dust and other sources form thin layers on the rock surfaces (Potter and Rossman, 1977; Allen, 1978).

Photo 16. Boulder mantled slopes along the road between Joshua Tree City and Hidden Valley.

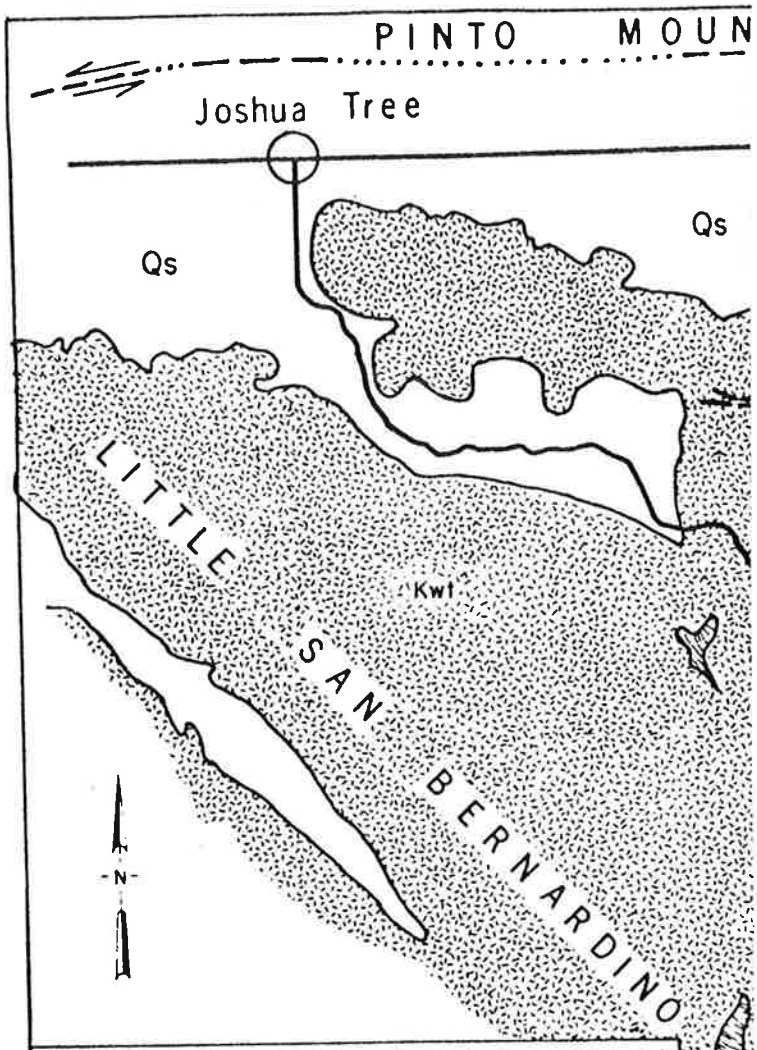

EXPLANATION

CENOZOIC	Quaternary	Qs	Surficial sediments; alluvium, windblown sand, clay; omitted where thin or insignificant
		b	Basalt
MESOZOIC	Cretaceous	Kom	Oasis monzogranite
		Kwt	White Tank monzogranite Includes small bodies of Queen Mountain monzogranite, Gold Park diorite, and granodiorite
		Kgp	Gold Park diorite, includes biotite and hornblende diorite, and quartz diorite
		Kqm	Queen Mountain monzogranite
	Jurassic	Jtp	Twentynine Palms porphyritic quartz monzonite
PRECAMBRIAN		gn	Pinto Gneiss

Contact; dashed where gradational or approximately located.

Fault; dashed where indefinite; dotted where inferred or concealed; queried where doubtful. D on downthrown side; U on upthrown side Arrows indicate directions of lateral movement.

Geology after Dibblee, 1967 and 1968; Rogers, 1961; Brand, J.H., thesis in preparation, USC; San Bernardino Sheet, T.H Rogers, CDMG, 1967.

0 1 2 3 4 MILES

Between these mountains and the mountains on the Mojave nothing is known of the country. I had never heard of a white man who had penetrated it. I am inclined to the belief that it is a barren, mountainous desert, composed of a system of basins and mountain ranges. It would be an exceedingly difficult country to explore, on account of the absence of water, and there is no rainy season of any consequence.

-Lt. R.S. Williamson
Pacific Railroad Report, 1853

Chapter 2

THE IN-BETWEEN DESERT

Lieutenant Williamson was standing at the southern edge of present-day Joshua Tree National Monument when he pondered the mysterious land beyond. Today the desert that aroused the Lieutenant's speculations is easily and safely explored by thousands of people every year. Yet this land of wide open spaces bounded by colorful but gaunt mountains still maintains, especially in the Monument where the hand of man has rested most lightly, a sense of the unknown that naturally draws out the exploring nature in people. Joshua Tree National Monument is ideally suited to satisfy that urge. Its 870 square miles encompass all types of desert terrain - from sand dunes to deeply eroded canyons to pinyon-covered mountains. Futhermore, its location between two major deserts, the Mojave and the Sonoran, gives this "in-between desert" some of the characteristics of each, including the richest desert flora to be found in the state. In Joshua Tree National Monument native palms rub shoulders with mountain-dwelling junipers, and cacti mix with Joshua tree forests, presenting an opportunity to explore and discover a unique environment.

THE MOJAVE DESERT

To the north of the Monument and penetrating into its western and central highlands is the Mojave Desert, a vast domain, yet the smallest and least complex of the four great deserts of North America. (The other three are the Chihuahuan, Great Basin, and Sonoran, of which the Sonoran is categorized into several subdivisions, the largest of which consists of the Colorado Desert.) The Mojave can be classified as "high desert", most of it lying between 3,000 and 5,000 feet above sea level. Winters can be severe, often accompanied by snowfall (usually at least once each season as far south as Joshua Tree National Monument).

Creosote (*Larrea*) is the most common shrub of the Mojave, sometimes growing in pure stands many acres in extent but more often intermixed with a variety of other plant species. As omnipresent as the creosote may be, it surrenders the role as the true hallmark of the Mojave to another plant, the spindly Joshua tree. One way by which the boundaries of the Mojave Desert have been defined is by the distribution of this strange plant. In an otherwise treeless desert, the Joshua tree has become a dominant and essential ecological element of the landscape. Only the Mojave yucca (*Yucca schidigera*) and the nolina (*Nolina bigelovii*) approach the Joshua tree in size and distribution, but they never attain the same towering stature.

Mountain ranges dot the Mojave Desert like misplaced ocean archipelagos, and constitute an important aspect of Joshua Tree National Monument. The island analogy is a good one, for being at higher elevations than the surrounding desert these far flung ranges receive more moisture and support a different plant community than the surrounding ocean of arid plains and valleys. The mountain plant community is dominated by pinyon pines and junipers, an open woodland that occurs throughout the higher parts of the Monument (above 4,000 feet) often in conjunction with the Joshua tree forests.

THE COLORADO DESERT

Approaching from the south and blending into the Mojave Desert in Joshua Tree National Monument is the Colorado Desert. This largest subdivision of the greater Sonoran Desert is characteristically low-lying in elevation (less than 3,000 feet) and considerably hotter and drier on the average than the Mojave Desert. One would expect it to be bleaker, too, yet the Colorado Desert, like the Sonoran as a whole, is botanically rich, much more so than the Mojave. Whereas few cacti have adapted to withstand the rigors of Mojavean winters, an impressive array of these succulent plants thrive in the Colorado Desert where freezes are exceptionally rare. Unlike the Mojave Desert with its single species of tree, the Colorado Desert, homeland of the mesquite, smoke tree, palo verde, ironwood, and that "Prince of Vegetables", the native palm, presents a comparatively tree-rich environment.

Two conspicuous plant species that serve as indicators of the Colorado Desert are the ocotillo (*Fouquieria splendens*) and the viciously-armed Bigelow or Teddy-bear cholla (*Opuntia bigelovii*). Prominent stands of these plants are located along the road in Pinto Basin. (The Ocotillo Patch and the Cholla Garden are described in more detail in Chapter 19.) Probably no other cactus on the desert has a more well-deserved fearsome reputation for its spines than "Bigelow's Accursed Cholla".

THE IN-BETWEEN DESERT OF JOSHUA TREE NATIONAL MONUMENT

Strategically located between two different desert domains, with its great variety of terrain and elevation, Joshua Tree offers the visitor a unique laboratory for observing a host of fascinating desert plants.

The most striking example of the strange patterns of plant distribution arising from the in-between location of the Monument occurs in the Eagle Mountains near Cottonwood Spring. Here in the rugged upper reaches of Munsen Canyon at a lofty elevation of 4,500 feet, native palm trees, a species normally associated with the low-lying Colorado Desert, are found growing beside high-country junipers, plants more at home on the mountaintops of the Mojave Desert.

Elsewhere in the Monument, where soil and climatic conditions are exactly right a particular plant species may attain local dominance. The aforementioned Ocotillo Patch and Cholla Garden are not the only examples. Myriads of hedgehog cactus (*Echinocereus engelmannii*) crowd around the eastern base of Malapai Hill, while the nearby south-facing slopes of the Hexie Mountains bordering Pleasant Valley support an extravagant display of barrel cactus (*Ferocactus acanthodes*). In another area within Pleasant Valley, diamond cholla (*Opuntia ramosissima*) predominate and assume gigantic proportions. (See Chapter 15 regarding the Pleasant Valley/Malapai Hill region.)

The more one explores Joshua Tree, the more variety one discovers. The Monument's unique location between the Mojave and Colorado deserts accounts for the great abundance of plant species. Thanks to the efforts of a few far-sighted individuals, this great laboratory has been preserved for all of us to explore, enjoy, and appreciate.

I once asked an old Colorado Desert prospector how many varieties of cactus he was familiar with. "By gosh," said he, "you city fellers have no idea how many kinds we got. I know every one of 'em. There's the 'full of stickers,' 'all stickers,' 'never-fail stickers,' 'stick everybody,' 'the stick and stay in,' 'the sharp stickers,' 'the extra sharp stickers,' 'big stickers,' 'little stickers,' 'big and little stickers,' 'stick while you sleep,' 'stick while you wait,' 'stick 'em alive,' 'stick 'em dead,' 'stick unexpectedly,' 'stick anyhow,' 'stick through leather,' 'stick through anything,' 'the stick in and never come out,' 'the stick and fester cactus,' 'the cat's claws cactus,' 'the barbed fish-hook cactus,' 'the rattlesnake's fang cactus,' 'the stick seven ways at once cactus,' 'the impartial sticker,' 'the democratic sticker,' 'the deep sticker,' and a few others."

-George Wharton James
Wonders of the Colorado Desert, 1906

We were struck by the appearance of yucca trees, which gave a strange and southern character to the country and suited well with the dry and desert region we were approaching. Associated with the idea of barren sands, their stiff and ungraceful forms makes them to the traveller the most repulsive tree in the vegetable kingdom.

-John C. Fremont, 1844

Chapter 4

ORANGES ON JOSHUA TREES

Captain Fremont was not alone in his opinion of the arborescent tree yucca we call the Joshua tree. Some 80 years later, mild-mannered J. Smeaton Chase, a desert lover if ever there was one, recorded an even more extreme reaction in his book *California Desert Trails* (1919):

> It is a weird, menacing object, more like some conception of Poe's or Dore's than any work of wholesome Mother Nature. One can scarcely find a term of ugliness that is not apt for this plant. A misshapen pirate with belt, boots, hands, and teeth stuck full of daggers is as near as I can come to a human analogy. The wood is a harsh, rasping fibre; knife-blades, long, hard, and keen, fill the place of leaves; the flower is greenish white and ill-smelling; and the fruit a cluster of nubbly pods, bitter and useless. A landscape filled with Joshua trees has a nightmare effect even in broad daylight; at the witching hour it can be almost infernal.

But the "misshapen pirate" has had friends, as well. William Manly, struggling out of Death Valley to seek help for a marooned party of 1849'ers, called the Joshua "a brave little tree to live in such barren country".

It is the Mormons, if legends be true, who derived great inspiration from this awkward plant, and in doing so gave us its common name. There are many versions to the story, but Dennis H. Stovall, writing in the September 1938 issue of *Desert Magazine*, claims to have discovered the specific incident leading to the naming of the Joshua tree. According to Stovall, a band of Mormon colonists under the leadership of Elisha Hunt, in the year 1851, was crossing the Mojave Desert enroute from Utah to San Bernardino, California. A hot sun, foretelling the approach of summer, shimmered overhead, draining the energy of humans and animals alike. As if by a miracle a cloud rolled in front of the sun, just as the party approached a Joshua tree forest. The leader exclaimed, "Look brethren! The sky is no longer like brazen brass. God has sent the clouds. It is as if the sun stood still - as Joshua commanded. These green trees are lifting their arms to heaven in supplication. We shall call them Joshua trees!"

(Note: the Spanish and Mexican explorers who first penetrated the great deserts of the Southwest referred to Joshua trees as 'cabbage palms'. The first American description of the tree yucca consists of a journal entry made by Jedediah Smith on his epic pioneer march across the Mojave Desert in 1827. He named it the 'dirk Pear tree' because in size and shape it resembles the pear tree but with leaves like the 'blade of a dirk'.)

GROWTH PATTERNS

Even in an exotic jungle setting the Joshua tree would stand out as an oddity, if only because of its unusual shape. Branches thrust out in every conceivable direction. Many of these desert trees seem to deliberately adopt the most awkward pose possible. Dangling, dead limbs often add a final grotesque touch. A few individuals display perfect crowns of many-branched limbs each terminated by a cluster of dark green, daggerlike leaves. The effect can be startlingly beautiful, as with the largest Joshua tree in the Monument, towering supremely over a court of giants in Upper Covington Flat. Other magnificent specimens raise their shaggy heads beside the Monument highway in Queen Valley (refer to Chapter 15).

It is the short, stiff, sharply pointed leaves that give the Joshua tree its botanical name *Yucca brevifolia* - the short-leaved yucca. The leaves develop at the ends of the limbs in the terminal bud where all new growth takes place. As the limb continues growing, the older leaves die and cling to the branch, forming a shag that eventually drops off to expose the rough bark beneath.

The prime characteristic of the Joshua tree is its ma branchings. Every young plant begins growing in a straigl.., upright column. These good soldiers soon rebel and begin branching, not on their own initiative, but in response to either of two events that may occur to the terminal bud; a flower t develops, or the terminal bud suffers physical damage fr insects or the elements. Either way, new leaf formation halted. To continue growing, the column forks just below the old bud into two or more limbs, each complete with a new, healthy terminal bud. The process may be repeated many times in the li of the plant, and since blooming or insect damage does not occ in each branch simultaneously, some limbs develop longer segmer than others, thus accounting for the Joshua tree's unpredictable form.

An entertaining game to pursue while passing through the Josh tree forests (on foot is best, but it can be played from a c window as well) is to look for especially large or strange shaped individuals - one often recognizes a tall, lanky relative or acquaintance. One oddity discovered by Dr. Edmund Jaeger was a Joshua tree that had shot straight up for 22 feet before div ding into four short branches. A pair of enterprising red-tail hawks had constructed a nest in this natural cradle atop t tree.

Perhaps Captain Fremont's disdain for the Joshua tree originated when he stopped to sniff one of the curious blossor The creamy white flowers occur in a cluster, or panicle, at t ends of branches, looking like an odd cross between a cauliflow and an artichoke. They possess a musty, slightly malodorous odor, but one must literally bury one's nose in a blossom to experience it. The flowering season usually commences in Marc and by May the branch tips may be heavily laden with the li green seed pods resembling giant pecans in the shell.

In addition to reproducing by seeds, the Joshua tree sends out long, bamboo-like runners. Most of the smaller Joshuas near a larger specimen will have originated by this technique. Except for the runners, most of the tree's roots are no larger diameter than a pencil. They form a large clump around the ba of the trunk, making a very effective anchor against strong desert winds.

AGE AND DISTRIBUTION

How old are Joshua trees? No sure method of age determinatio has been developed. A large tree's grizzled exterior gives an appearance of great age; in a dense forest one feels thrust back to a primordial era. Early references claim Joshua trees li over a thousand years. One problem with the Joshua tree is th although arborescent or treelike in form, it is not really a "tree" in the usual sense of the word. It is closely related to the lilies and agaves, or century plants, and while its pithy core does produce growth rings, there is controversy over wheth they represent annual rings in the manner of common oaks, pin and elms. Core sampling, a method for obtaining annual gro ring data for ordinary trees, is difficult and often impossible to perform on Joshua trees. Not only is the wood quite soft, but the centers of larger Joshuas often decay, leaving air-fill voids.

Probably the best method for estimating age is based on t assumption of an average growth rate. Over a period of years the growth of several trees in the Monument was monitored and a resultant average growth rate of 1.5 centimeters per year determined. Thus a thousand-year-old tree would presumal measure approximately 15 meters (over 45 feet) in height. such giants are found in the Monument, but a number of trees surely are in the 700 to 800 year age bracket.

Because it has appeared as scenic backdrops in so ma Hollywood films, the Joshua tree has become an emblem of t American desert. It actually inhabits only the Mojave Dese reaching its southernmost limit in Joshua Tree National Monument. In fact *Yucca brevifolia* is so closely associated with the Mojave that scientists often use its distribution to delineate th boundaries of that desert.

It is hard to imagine that the tough, fibrous, dagger-point

leaves of the Joshua tree could be a tasty morsel for any beast, yet there was one large animal that grazed on the Joshua tree forests, and in so doing presented us with information about the past history of the Mojave Desert. In the late 1940s, caves were discovered in eastern Nevada containing the preserved dung of *Nothrotherium*, an extinct ground sloth that roamed the Southwest as late as 15,000 years ago. Analysis revealed that a major constituent of the ground sloth's diet was the Joshua tree. The caves are located far to the east of the present limit of Joshua tree growth, so apparently the Joshua tree, and by inference the Mojave Desert, occupied a larger area in the past.

In Joshua Tree National Monument the Joshua trees are found at higher elevations, usually above 3500 feet, where precipitation is greater than adjacent low-lying parts of the Colorado Desert. At these elevations winter freezes often occur and there is usually at least one good snow storm per season. The hardy Joshua tree seems to thrive only where it can experience this extreme climate. Nor is it particularly attracted to water, preferring the well-drained alluvium surrounding decomposing mountains. Where conditions are right, great forests of Joshua trees proliferate, such as in Lost Horse and Queen valleys. A grove of spectacular giant Joshua trees is located in Upper Covington Flat in the northwest corner of the Monument (see Chapter 8).

A TREE OF LIFE

In the vast shrub-land of the Mojave Desert, the Joshua tree has assumed a dominant ecological role. This is most clearly demonstrated by the number and diversity of animals that have come to depend on or in some way make use of the Joshua tree.

At least 25 species of birds are known to use the tree yucca as a nesting site. Woodpeckers bore into the limbs, creating dens that are often used by other birds. Considerable engineering ability is demonstrated by Scott's oriole, whose cleverly designed domiciles are woven from dead yucca leaves and suspended like hammocks between the bristling Joshua branches.

Birds of prey use the Joshua trees for observation posts as well as nesting sites. A drive through a Joshua tree forest, especially in the early morning hours, will inevitably reveal a hawk perched on the topmost branch of a roadside Joshua tree, apparently oblivious to the automobile traffic until someone stops to take a closer look.

The loggerhead shrike, a carnivorous bird resembling the common mockingbird in both size and coloration, puts the daggerlike leaves of *Yucca brevifolia* to good use. Swooping from tree top to tree top on its hunting rounds, the shrike occasionally touches the ground and carries away a wriggling lizard. The loggerhead's more common appellation - butcherbird - is explained by its habit of skewering the remains of its prey on one of the sharp yucca leaves, hanging its meat like a butcher, perhaps to return to it later in the day.

A mammal making extensive use of the Joshua tree is the woodrat (*Neotoma*). The unmistakable signs of a woodrat at work are Joshua tree limbs from which the leaves have been neatly and uniformly trimmed close to the trunk. Nearby, perhaps around the base of another Joshua tree, will be found the pile of rubble - sticks, brush, cactus joints, and, of course, the missing Joshua tree leaves - that comprise the nest of this solitary and industrious little creature.

Insects play an important role in the life of the Joshua tree. Foremost in causing damage to the Joshua tree's terminal bud, and thus contributing to the tree's many branchings, is the yucca boring weevil (*Scyphophorus yuccae*). The larvae, issuing from eggs laid in the terminal bud, devour the surrounding plant tissue and build tough frass cases from which they emerge as adult beetles. In response to this damage, the tree exudes silica from the adjacent tissue, creating the so-called "petrified" Joshua tree wood that remains after a dead tree has completely decayed. Joshua tree limbs that have a "coolie hat" appearance at their tips formed by dead, turned-back leaves are most likely infested by this insect.

Who was here? Woodrat at left, yucca boring weevil at right.

A butterfly known as the Navajo yucca borer (*Megathymus yuccae navaho*) propagates itself by laying its eggs on juvenile Joshua trees; but not just any young plant will do. Those tree yuccas that have grown from seeds will not provide an adequate food supply for the rapacious larvae. Only by penetrating into the large runners sent out by a parent tree can the larvae mature and pupate. In some mysterious way the female yucca borer is able to differentiate between the sprouts that have germinated from seeds and those that have grown from runners, and lays her eggs only on the latter. The resulting infestation and severing of the resource-draining offshoots probably benefits the parent plant.

A marvelous example of the evolutionary development of interdependent living forms presents itself in the strange and beauti-

ful relationship between the Joshua tree and the yucca moth, *Pronuba synthetica*. The story begins many thousands of years ago when the ancestral yucca plant evolved the characteristic of having sticky pollen, as opposed to cone-bearing trees which have a dry, dusty pollen that is freely blown from tree to tree. As this occurred, the Pronuba species of moth stumbled upon a method by which it could ensure its survival, and in pursuing that method both moths and yuccas turned onto an evolutionary pathway that eventually made them dependent upon each other. What the ancestral Pronuba moth "learned" was to gather yucca pollen with which to deliberately fertilize the yucca flower and then lay its eggs in the soon-to-develop yucca ovary. The growing seeds thus serve as a guaranteed food source for the young larvae. The moth never lays so many eggs that all the yucca seeds will be devoured; some always survive to ensure propagation of new yuccas which in turn serve future generations of yucca moths.

As a result of the yucca moth's activities, those yuccas with flowers most attractive to the moth, i.e., with sticky pollen that was easier for the moth to manipulate, stood greater chances of being visited and of producing seeds. Thus the yuccas slowly lost the ability to be pollinated by any other method than that offered by the moth. The whole process probably took many thousands of years, and as different species of yuccas evolved, so did different species of Pronuba.

Another remarkable insect enters into the Pronuba-Joshua tree relationship. A small, dark-brown ichneumon wasp, if noticed at all while it buzzes around the clusters of yucca seed pods, seems most unnoteworthy. But if watched closely, it will be observed to be conducting a careful search. At last it alights, inserts its ovipositor through the tough green skin of the yucca fruit and deposits a solitary egg. Examination reveals that the wasp has invariably located one of the larvae of the Pronuba moth, which it has paralyzed to serve as food for the wasp larva that will soon hatch from the deposited egg. How the little wasp detects the deeply buried Pronuba moth larva is another desert mystery.

Even in death the Joshua tree is a source of life. Termites inhabit downed limbs and dead stumps, returning basic nutrients to the soil. Along with other insects, they fall prey to another resident of dead Joshua trees, the yucca night lizard, *Xantusia vigilis*. Insects, lizards, packrats: these in turn provide sustenance for birds and bats, snakes and other carnivores. When we learn of the full implication of the Joshua tree and its complex ecology, we cannot help but develop a great appreciation for this strange and wonderful symbol of the Mojave Desert.

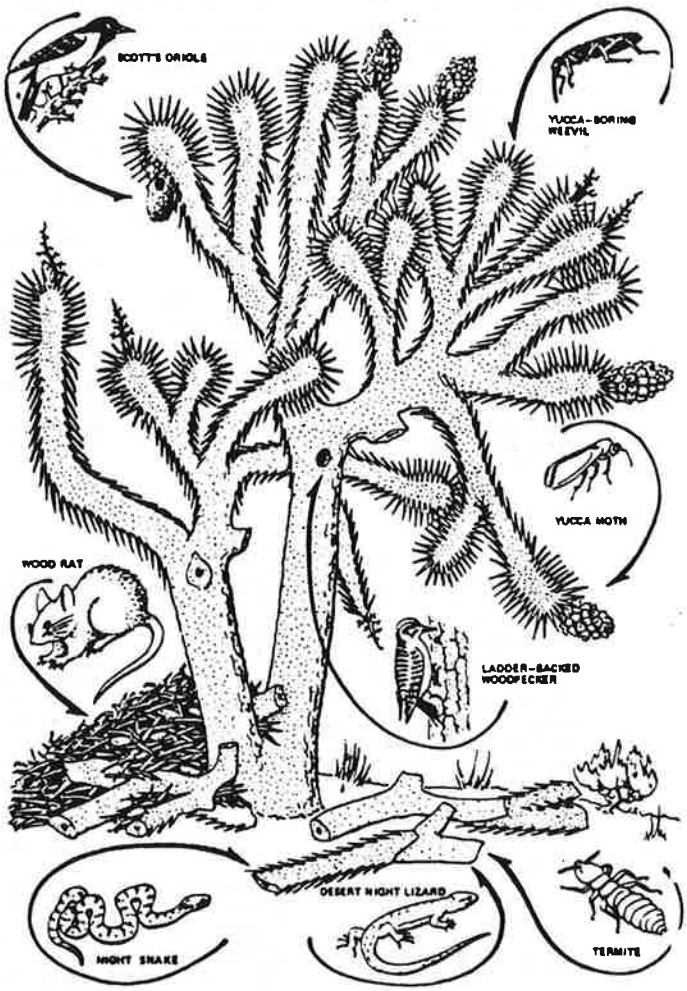

*Drawing from *An Island Called California*, by Elna Bakk ; University of California Press, 1971.

DAY TWO
JOSHUA TREE TO PENINSULAR RANGES

Leg 1 Joshua Tree to Orocopia Mountains
Stop 1 Geologic overview (roadside armwave)
Leg 2 Orocopia Mountains to Painted Canyon
Stop 2 San Andreas fault zone
Leg 3 Painted Canyon to Palm Springs
Stop 3 Palm Canyon or Palm Springs Tram
Leg 4 Palms to Pines Highway; Santa Rosa mylonite zone

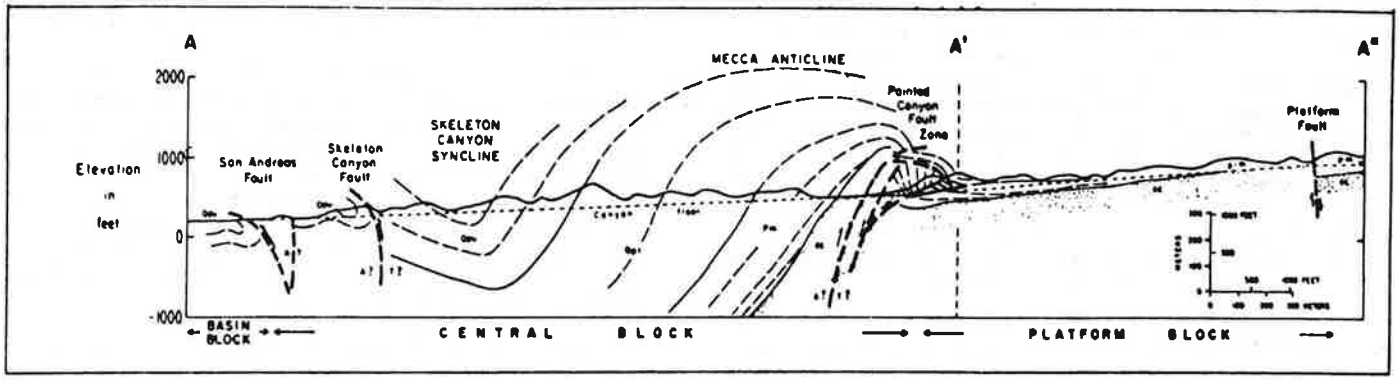

Figure 3. Geologic strip map and structural cross section parallel to Painted Canyon in the Mecca Hills.

CRYSTALLINE BASEMENT TERRANES IN THE SOUTHERN EASTERN TRANSVERSE RANGES, CALIFORNIA

Robert E. Powell
U.S. Geological Survey
345 Middlefield Road
Menlo Park, CA 94025

ABSTRACT

Within the crystalline complex of the Chuckwalla, Orocopia, Eagle, Cottonwood, Hexie, Little San Bernardino, and Pinto Mountains, pre-mid-Jurassic country rocks of Mesozoic batholiths comprise two lithologically distinct terranes, the Joshua Tree and San Gabriel terranes of Powell (1981, Dissert. Abs. Internat., v. 2, p. 538B), that are superposed along a regional, prebatholithic low-angle fault system consisting of the early and late Red Cloud thrusts. The structurally lower Joshua Tree terrane consists of Precambrian granite capped by a paleoweathered zone and overlain nonconformably by orthoquartzite that interfingers westward with pelitic and feldspathic granofels. In proximity to the early Red Cloud thrust, this stratigraphic package has been pervasively deformed to granite gneiss, stretched-pebble conglomerate, lineated quartzite, and schist. Northeast-trending, regional metamorphic isograds have been superimposed on the supracrustal quartzite and granofels. Comparison of the pelitic assemblages with experimental studies suggests peak conditions of P_{total} = 3.5 to 4 kb, T = 525 to 625°C. Early prograde metamorphism predated the thrusting event; a later retrograde stage may have overlapped in time with movement along the early Red Cloud thrust.

Lithologic units of the Precambrian San Gabriel terrane occur as three layers in an allochthon lifted from deep in the crust. The highest layer consists of sillimanite-garnet-biotite-potassium feldspar bearing pelitic gneiss intruded by porphyritic granodiorite (later deformed to augen gneiss). These rocks are intruded by foliated granitic to tonalitic rocks that form an intermediate layer characterized by metamorphic minerals and textures indicating granulite facies retrograded to amphibolite facies. Rocks of the intermediate layer in turn are intruded by syenite-mangerite-jotunite at the lowest level.

The Red Cloud thrust system is inferred to have developed in sequential structural events: (1) early thrusting that probably moved the allochthon parallel to the east-northeast/west-southwest mineral lineations recorded in both plates; (2) regional folding of the initial thrust surface along north-northeast trending axes; (3) later thrusting that broke with some component of westward movement across the folds in the older thrust surface to produce a stacking of crystalline thrust plates of the two terranes; (4) continued or renewed folding of both thrust faults with eventual overturning toward the southwest. These structural events are linked tentatively into a single tectonic episode that resulted in emplacement of the San Gabriel terrane westward over the Joshua Tree terrane between 1195 m.y. and 165 m.y. ago.

The prebatholithic terranes and the westward vergent Red Cloud thrust appear to be exotic with respect to prebatholithic rocks and structures exposed to the north and east. The discontinuity that marks the northeast boundary of the exotic terranes has been obliterated by the Mesozoic batholiths; it may represent a segment of an intracontinental transcurrent fault.

Mesozoic plutonic rocks comprise two batholithic suites aligned in northwest-trending belts. The alkalic(?) older suite, which lies northeast of the younger suite, includes biotite- and alkali feldspar-bearing gabbro and diorite intruded by monzodiorite and low-quartz porphyritic monzogranite. The calc-alkaline (?) younger suite includes hornblende-biotite-sphene granodiorite intruded by porphyritic monzogranite, then by nonporphyritic monzogranite.

Along the escarpment of the Little San Bernardino Mountains, the crystalline rocks have been pervasively foliated by a brittle cataclastic event that at least partially postdates intrusion of the younger suite of plutonic rocks. The foliation is folded in an antiform along the length of the range. The cataclasis is attributed to the Vincent-Orocopia thrust that is inferred to superpose the diverse prebatholithic and batholithic rocks of the Eastern Transverse Ranges above Pelona-type schist.

The Eastern Transverse Ranges are defined by east-west Cenozoic sinistral faults that have a cumulative westward displacement from south to north of about 50 kilometers. The left-lateral faults may form a conjugate fault set with north-northwest trending right-lateral faults in the Mojave Desert.

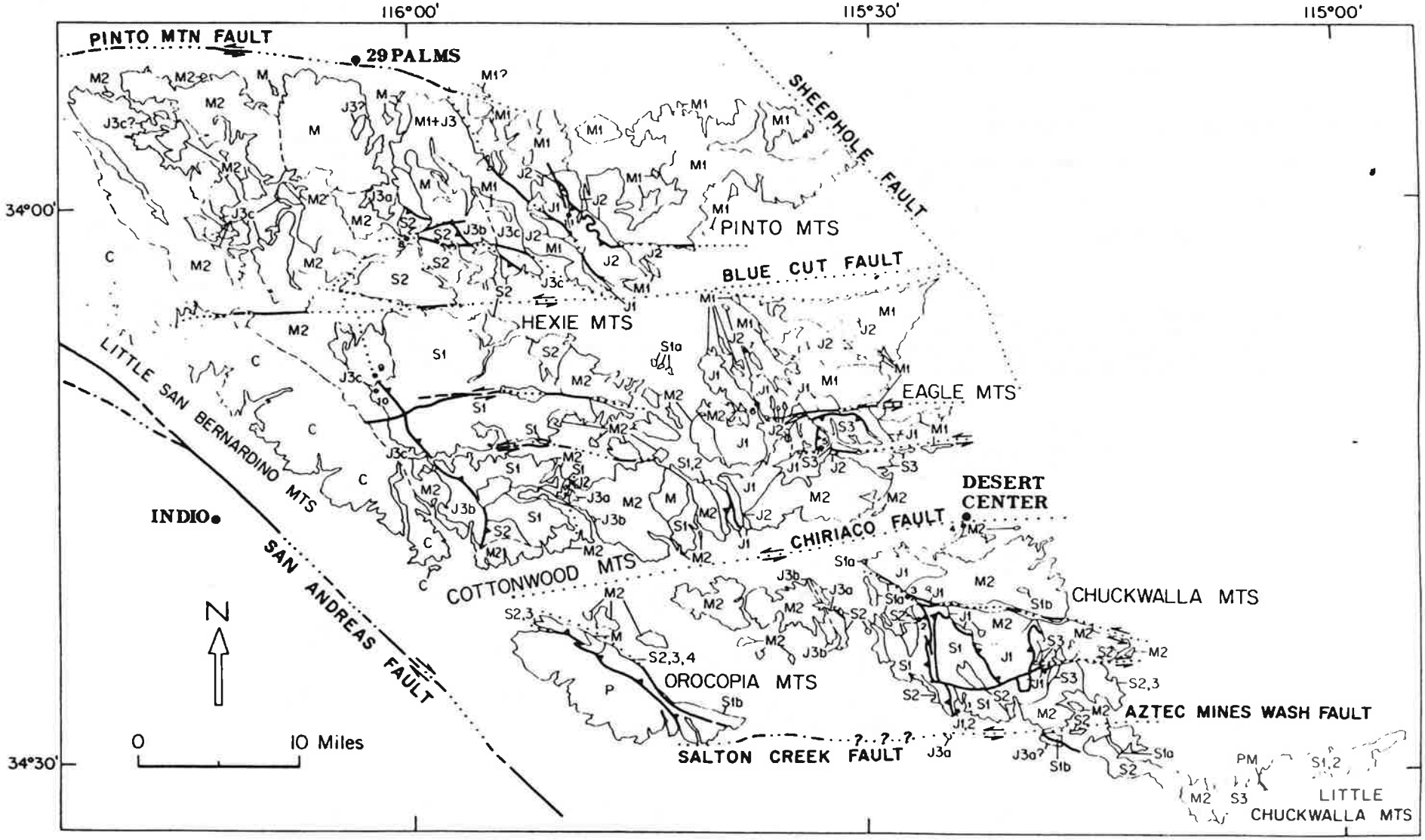

Figure 2A. Geologic map of the crystalline complex of the southern Eastern Transverse Ranges (after Powell, 1981a). Compiled from thesis maps of Powell (1981a) and the Salton Sea (Jennings, 1967), Santa Ana (Rogers, 1966), San Bernardino (Rogers, 1969), and Needles (Bishop, 1964) sheets of the Geologic Map of California (scale 1:250,000). Contacts are dashed where approximate, dotted where obscure. Faults are indicated with heavy lines; thrust faults are shown with barbs on the upper plate. Unmarked areas represent undifferentiated Quaternary and Cenozoic sedimentary and volcanic units. Geologic unit symbols are keyed in the caption to Figure 2B. • Field trip stop.

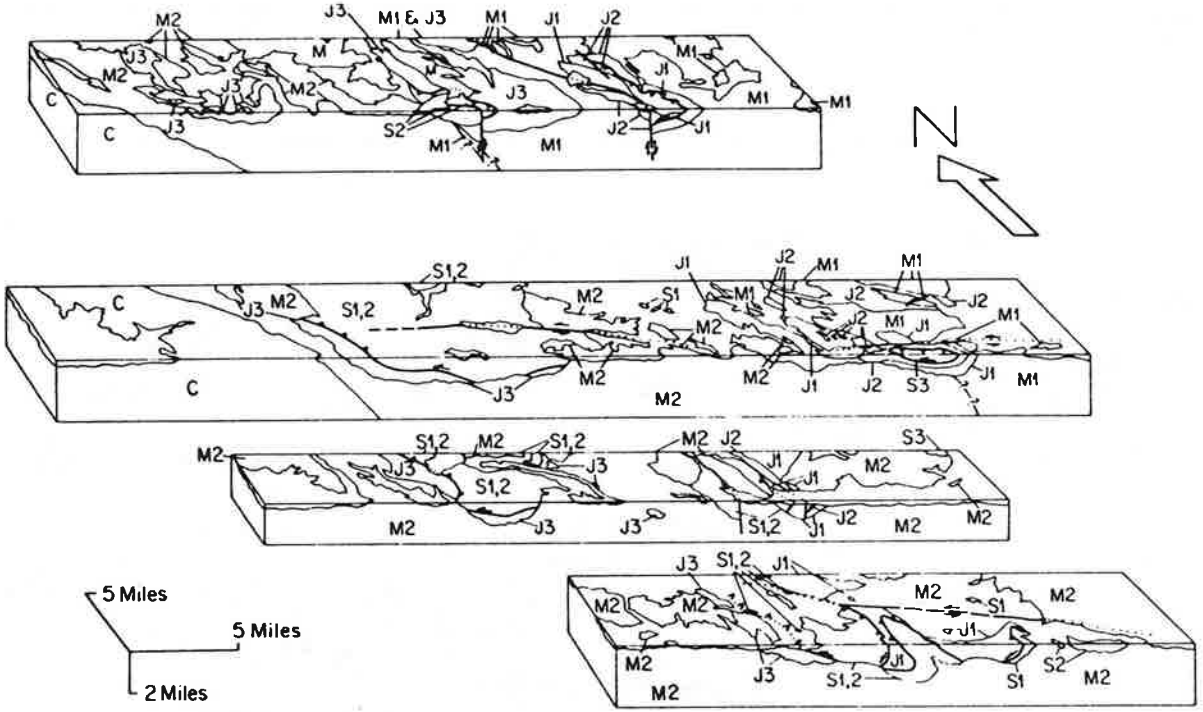

Figure 2B. Block-diagram cross-sections constructed along east-west lines of section through the Orocopia-Chuckwalla Mountains, the Cottonwood-Eagle Mountains, the Hexie-Eagle Mountains, and the Pinto Mountains, respectively, from south to north (after Powell, 1981a). The block diagrams are constructed from the geologic map (Fig. 2A) using a single-point perspective (see, e.g., Raisz, 1962) from the southeast; the cross-sectional face of each block diagram is true scale. In the legend, geologic unit symbols are listed with suggested color scheme in parentheses (darken the suggested colors on the cross-sectional faces to visually enhance them). Legend:

SAN GABRIEL TERRANE
- S1 Metasedimentary and augen gneiss (dark green)
  - S1a Metasedimentary gneiss (dark green)
  - S1b Granodioritic to monzogranitic augen gneiss (heliotrope)
- S2 Retrograded granulitic gneiss (olive green)
- S3 Syenite-mangerite-jotunite (aquamarine)
- S4 Anorthosite and norite (aquamarine)

JOSHUA TREE TERRANE
- J1 Granite/granite gneiss (orange)
- J2 Supracrustal quartzite with interbedded pelitic schist and granofels containing andalusite/sillimanite and red-brown biotite (yellow)
- J3 Supracrustal granofels, schist, and gneiss (brown)
  - J3a Quartz-biotite-cordierite granofels
  - J3b Quartz-plagioclase-biotite gneiss
  - J3c Pelitic granofels containing andalusite/sillimanite and greenish-brown biotite

PALEOZOIC-MESOZOIC PLUTONIC ROCK
- PM Permian or Triassic syenodiorite to granodiorite

MESOZOIC PLUTONIC ROCKS
- M Probable Mesozoic plutonic rocks not yet assigned to M1 or M2 (pink)
- M1 Older batholithic suite (dark pink)
- M2 Younger batholithic suite (light pink)
  - M2a Biotite-hornblende-sphene granodiorite (differentiated in Fig. 7F)
  - M2b Fine- and coarse-grained porphyritic monzogranite and non-porphyritic "polka-dot" granitoid (see text) (differentiated in Fig. 7F)
  - M2c Coarse- to very coarse-grained nonporphyritic monzogranite (differentiated in Fig. 7F)

CATACLASTIC ROCKS
- C Cataclastically foliated rocks that are derived from Mesozoic plutonic rocks and older metamorphic rocks and are characterized by fractured and fragmented mineral grains (northwest-trending dash-pattern)

PELONA-TYPE SCHIST
- P Orocopia Schist of Miller (1944) (gray)

MESOZOIC BATHOLITHIC INTRUSION
FOLLOWED BY
EMPLACEMENT OF CRYSTALLINE COMPLEX
OVER PELONA/OROCOPIA SCHIST

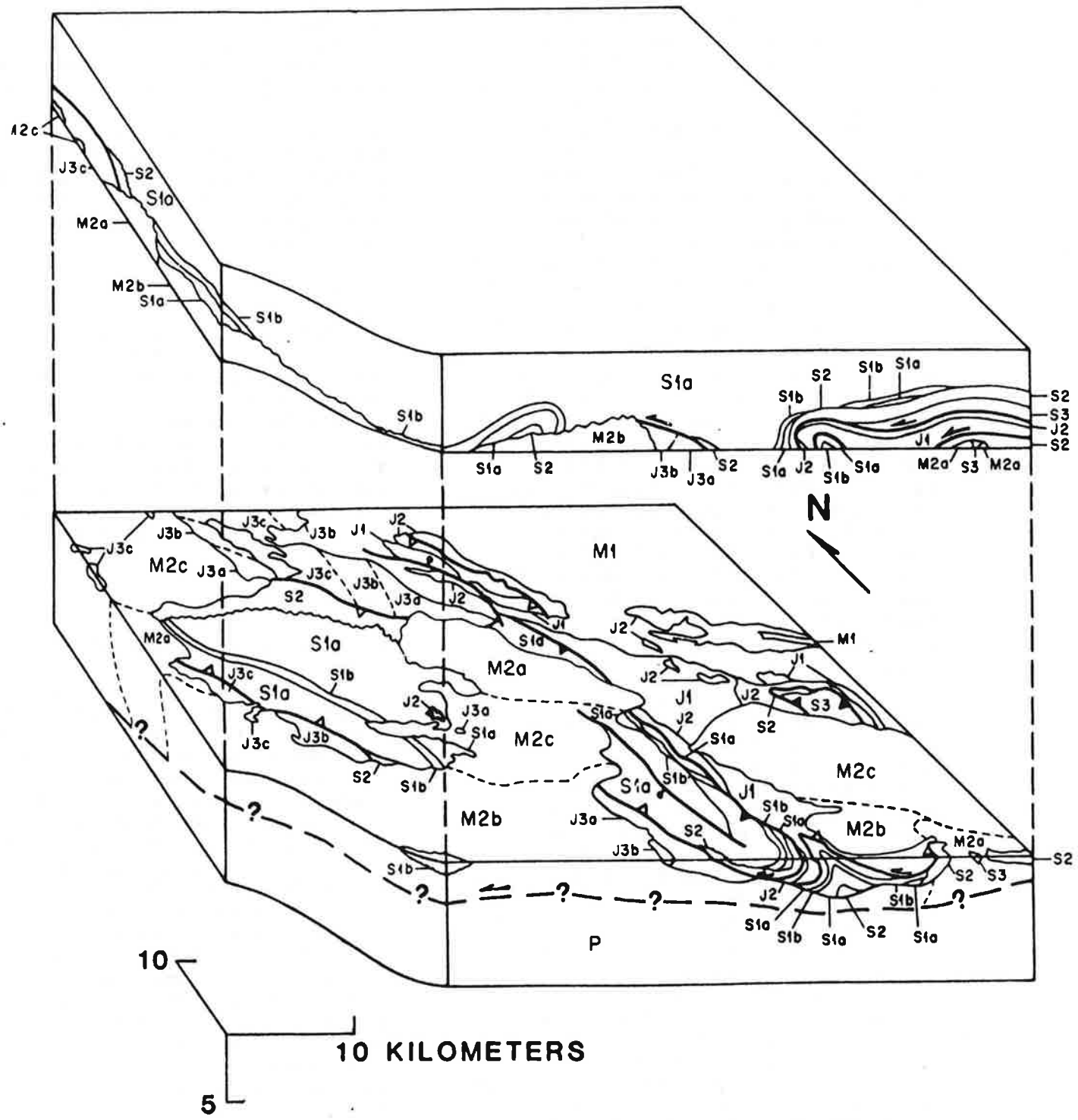

Figure 7F. Intrusion of the Mesozoic batholiths has left isolated pendants of prebatholithic terranes, from which the preceding diagrams were inferred. Mesozoic rocks include an older (Jurassic) belt (M1) and a younger belt (M2). At some time following the intrusion of the Mesozoic batholiths, the crystalline complex of the Eastern Transverse Ranges is inferred to have been thrust over Pelona-type schist (P).

GEOLOGIC SKETCH OF THE OROCOPIA MOUNTAINS, SOUTHEASTERN CALIFORNIA

By John C. Crowell
Geological Sciences Department
University of California
Santa Barbara, California 93106

ABSTRACT

The Orocopia Mountains lie adjacent to the San Andreas fault to the northeast of the Salton Sea. Basement rocks within them include Precambrian augen gneiss, migmatite, gneiss, anorthosite-syenite complex and Mesozoic granodiorite, granite, and quartz monzonite. The core of the range consists of an antiform of greenschist-facies Orocopia Schist (Mesozoic ?) that structurally underlies the folded Orocopia thrust. On the northeast, about 1460 m (4800 ft) of marine lower and middle Eocene beds, comprising the Maniobra Formation, lie south of a rugged Eocene shoreline. These beds are overlain unconformably by about 1500 m (5000 ft) of non-marine Diligencia Formation, mainly of early Miocene age. In the Mecca Hills to the west about 1500 m (5000 ft) of nonmarine sandstone, siltstone, and conglomerate constitute the Mecca and Palm Spring formations of Plio-Pleistocene age. The youngest sedimentary rocks include the Pleistocene Ocotillo Formation, a fanglomerate that extends basinward toward the southwest. Volcanic rocks, primarily of middle and late Tertiary age, are of several petrographic types and ages.

The structural evolution of the Orocopia Mountains region began with metamorphic and intrusive events involving Precambrian and Mesozoic rocks. Many of these basement rocks constitute the folded overriding plate of the Orocopia thrust, a major regional overthrust of unknown displacement and probably of late Mesozoic or earliest Cenozoic age. The unconformably overlying Cenozoic sedimentary section is irregularly deformed. Near major faults, such as the San Andreas, even Pleistocene beds are strongly faulted and folded. Major associated faults of the San Andreas system are the Painted Canyon, Eagle Canyon, Hidden Springs, and Clemens Well. On the east, folds with an eastsoutheast trend in strata of the Maniobra and Diligencia formations are associated with a system of vertical strike-slip faults; northeast striking faults have left slips and northwest striking ones, right slips.

The rocks exposed within the Orocopia Mountains range in age from Precambrian to Recent, and are here described under three headings: 1) Basement rocks, including several types of gneiss, plutonic rocks of several sorts and ages, and schist, 2) Tertiary sedimentary rocks, including marine Eocene strata, Oligocene-Miocene nonmarine beds with associated volcanic rocks, and younger sandstone and conglomerate, mainly of Plio-Pleistocene and Recent ages, and 3) other volcanic rocks.

The strucural history of the Orocopia Mountains is complex, involving deformation during the Precambrian and at several times during the Mesozoic. Major overthrusting, on the Orocopia thrust, took place in the late Mesozoic (?) and brought older metamorphic and granitic rocks above schist.. Faulting and folding has occurred at intervals in the Cenozoic, and deformation is taking place today along strands of the San Andreas fault system.

BASEMENT ROCKS

Augen Gneiss and Migmatite

The oldest rocks so far recognized within the Orocopia Mountains are augen gneisses and migmatites exposed in the southeast near Salton Creek Wash, and north of the Clemens Well fault (Fig. 1), and are part of the Chuckwalla Complex (Miller, 1944). Characteristics of the unit are large, up to 8 cm, ovoid "eyes" of pink microcline within coarse-grained microfolded gneiss. The migmatite constitutes about 20 per cent of the augen-gneiss terrain and consists of intermixtures between impure feldspathic and quartz-rich gneiss, gneissic granite, and biotite schist The augen geneiss has yielded a zircon age of 1670 ± 15 m.y. (Silver, 1971).

Figure 1. Geologic sketch map of the Orocopia Mountains, southeastern California. Subscript numbers serve to differentiate different rock units of similar types; see text of this paper and that of Crowell (1962). With reference to insert rectangle at lower left, the data are modified and simplified from unpublished mapping by Hays (WH) (1957), Ware (GS) (1958), and Crowell (JC). A-A' = Line of cross section of Figure 2. Precambrian rocks: gn = blue-quartz gneiss, ag = augen gneiss and migmatite, a = anorthosite, di = diorite, gb = gabbro, sy = syenite. Other pre-Tertiary basement rocks: gr = granitic rocks (several types), s = Orocopia Schist. Cenozoic rocks: v = volcanic rocks (several types), E = Eocene Maniobra Formation, ØMd = Oligocene - Lower Miocene Diligencia Formation, PQ = Plio-Pleistocene formations, Qt = Quaternary terrace and fanglomerate deposits, Qal = Quaternary alluvium and lake-bed deposits.

Blue-Quartz Gneiss and Gray Gneiss

Patches of gneiss crop out south and west of the Clemens Well fault, confined to the overriding plate of the Orocopia thrust, and also within hills flanking Maniobra Valley (Fig. 1). Banded gneiss, with an amphibolite-facies mineralogy, is intruded by rocks of the anorthosite-syenite group, and is characterized by quartz grains with a distinctive blue or violet color, and textures suggesting an earlier granulite-facies metamorphism. This gneiss has been dated at about 1425 m.y. by Silver (1971). Other areas of amphibolite-facies gneiss with gray quartz may or may not be of the same age. At places such gneiss occurs as isolated bodies or septa within Mesozoic (?) granitic plutons, and may therefore be younger than the definitely Precambrian gneiss. Blue-quartz gneiss is best exposed on the north flank of the Orocopia Mountains, and gray gneiss in deep gorges tributary to Painted Canyon, in the Hayfield Mountains, and in hills southwest of Maniobra Valley (Fig. 1).

Anorthosite-Syenite Complex

Irregular masses of rock belonging to an anorthosite group and closely associated with those belonging to a syenite group crop out in the overriding plate of the Orocopia thrust (Fig. 1) (Crowell and Walker, 1962). These complicated, deformed, and shattered rocks are especially well exposed north of Salton Creek Wash and along ridges just north of the crest of the Orocopia Mountains. A few small outcrops of anorthosite and related rocks crop out in Painted Canyon, and are the most easily visited exposures of these types in the region (Sylvester and Smith, this volume). The anorthosite group consists of gabbro, diorite, transition rock between gabbro and diorite or transitional between gabbro and anorthosite, white anorthosite, mafic bodies, and basic dikes (Crowell and Walker, 1962). The plagioclase of the anorthosite is oligoclase-andesine (An_{28-45}). The closely associated syenite group consists of syenite, quartz-bearing syenite, alkali granite, granophyre, and pegmatite. Blue or violet quartz, microperthite, and replacement textures of biotite after original mafic minerals are characteristic. Because the anorthosite and syenite groups are intimately associated, they are probaby related in origin. Their isotopic age is about 1220 m.y. (Silver, 1971) in origin.

Lowe (?) Granodiorite

Porphyritic granodiorite occurs in a few small outcrops just south of the mapped area near A of the

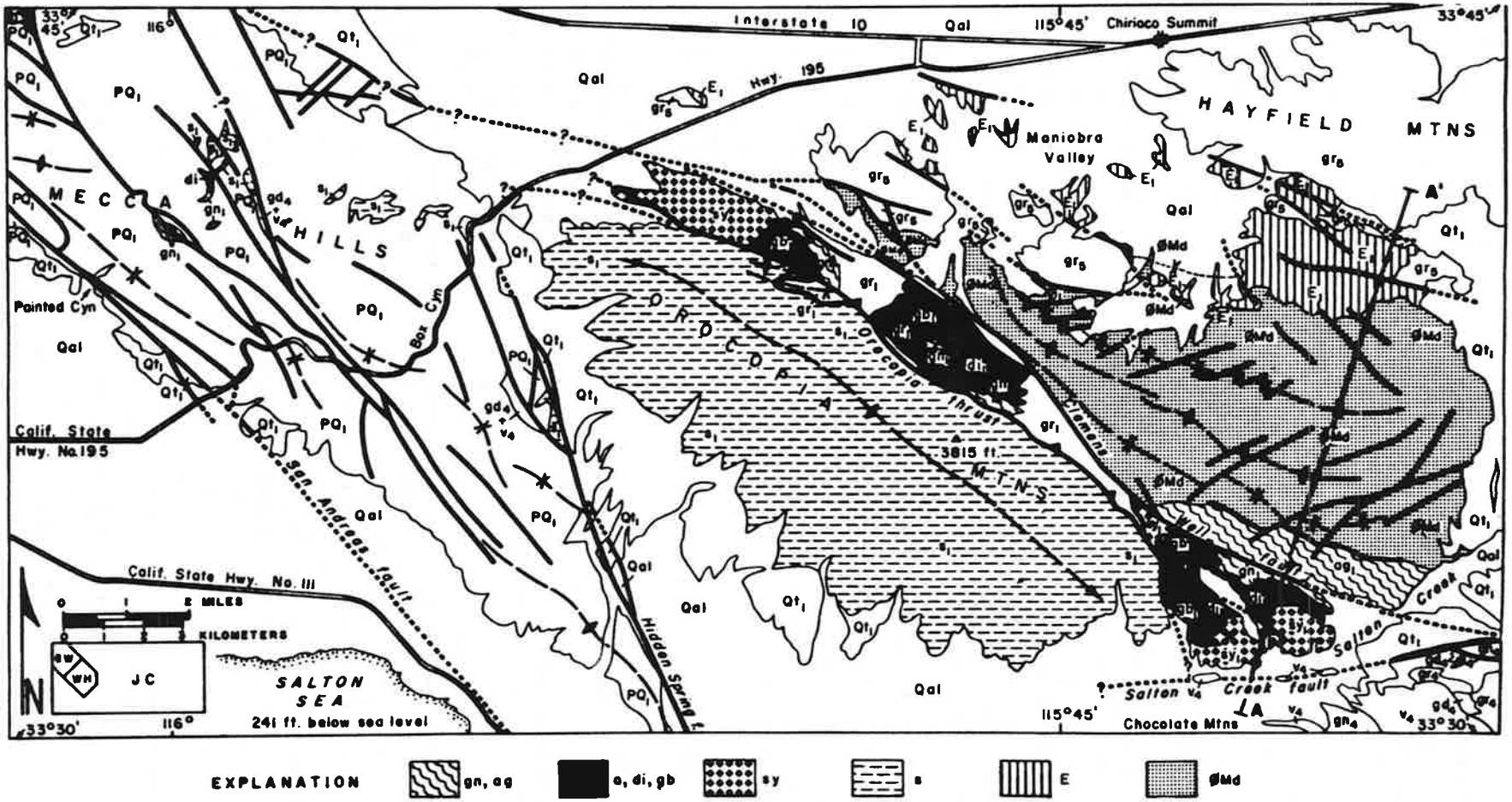
Interstate 10
Chiriaco Summit
115°45'
33°45'
116°
33°30'
Hwy. 195
Maniobra Valley
HAYFIELD MTNS
MECCA HILLS
Painted Cyn
Box Cyn
Calif. State Hwy. No.195
Calif. State Hwy. No. 111
San Andreas fault
Orocopia thrust
3815 ft.
MTNS
Hidden Spring
Salton Creek fault
Salton Creek
SALTON SEA
241 ft. below sea level
Chocolate Mtns
Qal
A
A'
EXPLANATION
gn, ag
o, di, gb
sy
s
E
gMd

cross-section line (Fig. 1, A-A') within the northern Chocolate Mountains. The rock is medium-to coarse-grained and faintly foliated, with characteristic large orthoclase phenocrysts and smaller and irregularly distributed hornblende phenocrysts. Quartz constitutes less than 10 per cent. On the basis of petrographic similarity this granodiorite is tentatively correlated with the Lowe Granodiorite of the San Gabriel Mountains which has been dated at 220 ± 10 m.y. (earliest Triassic) by Silver (1971). Similar rock has recently been discovered by John Dillon in the south-central Chocolate Mountains, near Mammoth Wash (personal comun., 1974).

Granitic Rocks

Light-colored granitic rocks intrude the gneisses and rocks of the anorthosite-syenite complex in the Orocopia thrust-plate. The main granitic rock is a fine-to medium-grained leuco-quartz monzonite with complicated migmatitic borders. In fact, there are several involved tracts of "double migmatites" where older migmatitic borders of the anorthosite - syenite complex and ancient gneisses are cross-cut and migmatized by quartz monzonite. Granite and quartz monzonite also underlie the Hayfield Mountains. These rocks, as well as those of the Chuckwalla and Little Chuckwalla Mountains to the east, have yielded K-Ar ages between 71 and 88 m.y. (Armstrong and Suppe, 1973), suggesting that cooling, perhaps the result of uplift and deep erosion, took place during late Cretaceous time. Within the Orocopia Mountain region it is not yet known how many different granitic plutons are present, nor how diverse their ages. These granitic rocks on the northeast constitute the basement floor upon which the marine Eocene strata of the Maniobra Formation were deposited.

Orocopia Schist

The central part of the Orocopia Mountains is underlain by a 2000 m (6500 ft) sequence of greenschist-facies schist reconstituted metamorphically from graywacke and mudstone, with minor amounts of chert and basic volcanic rocks. The bedded schist, predominately gray in color, is mainly composed of quartz, albite, and muscovite with minor amounts of chlorite, epidote, actinolite, and graphite. Lithologic layering, derived from sedimentary bedding, is conspicuous in almost all outcrops, but scattered isoclinal-fold hinges suggest that some of the original bedding is transposed. Although the age and environment of deposition of the original sediments and volcanics now constituting the schist are unknown, it is noteworthy that none of the granitic plutons intrude the schist, and that nowhere are rocks visible beneath the schist. These relations suggest that perhaps the strata are younger than plutonism and metamorphism, or that they were deposited on oceanic-or quasi-oceanic floor so that no sialic sources for quartz monzonite plutons lay beneath them. The age of the metamorphism of the Orocopia Schist is also unknown, but is probably Mesozoic by comparison with events involving the very similar Pelona Schist in the San Gabriel Mountains (Ehlig, 1968). The foliation of the schist in the Orocopia Mountains has been broadly folded after the emplacement of the overriding Orocopia thrust; in this regard also it is similar to the Pelona Schist and its overlying Vincent thrust. In the absence of detailed studies of the Orocopia Schist, and by relying heavily on regional correlations, I tentatively consider the age of the original strata as Mesozoic (undesignated more precisely) and the age of the metamorphism as late Cretaceous. Schist probably correlative with the

the Orocopia Schist also occurs from the central Chocolate Mountains southeastward into central Yuma County, Arizona.

CENOZOIC STRATA

Eocene Maniobra Formation

The oldest unmetamorphosed sedimentary rocks in the Orocopia Mountains consist of about 1460 m (4800 ft) of Eocene beds containing marine fossils and assigned to the Maniobra Formation (Crowell and Susuki, 1959). These brown shales, sandstones, conglomerates, and sedimentary breccias lie unconformably upon granitic basement in Maniobra Valley (Fig. 1). Coarse rocks were deposited along an ancient Eocene shoreline, or steep near-shore buttress unconformity, which is preserved along the southern base of the Hayfield Mountains. Here huge polished boulders and giant blocks have apparently tumbled from shoreline cliffs and ancient sea stacks. From this near-shore area the beds thicken and become finer grained toward the south and southwest, suggesting that the open sea, or at least a broad marine embayment, lay in that direction. The fauna, consisting of Foraminifera (including Discocyclinids), gastropods, and pelecypods, indicates an early and middle Eocene age (Cole, 1958; Crowell and Susuki, 1959; Johnston, 1961). These fossils, as well as the lithology of beds containing them, show many affinities with those of the north-central Transverse Ranges, across the San Andreas fault and between 220 and 280 km (135 to 175 mi) to the northwest (Kirkpatrick, 1958; Crowell and Susuki, 1959; Howell, this volume).

Oligocene - Lower Miocene Diligen- Formation

The Diligencia Formation, consisting of about 1500 m (nearly 5000 ft) of nonmarine conglomerate, sandstone, mudstone, and interbedded volcanic flows and sills, underlies a large region in the eastern Orocopia Mountains. The formation lies unconformably upon the Eocene Maniobra Formation on the north where it is characterized by a basal conglomerate largely composed of rounded granitic cobbles. On the south, the formation lies unconformably upon augen gneiss and migmatite one kilometer southeast of Canyon Spring (U.S.G.S. Hayfield Quadrangle).

Lithologically the formation consists of red sandstone and maroon mudstone with lesser thicknesses of well bedded calcareous yellow sandstone, dark gray limestone, thin-bedded sequences of gypsum and other evaporites, and irregular lenses of sedimentary breccia including monolithologic mosaic breccias of granitic and gneissic debris. Facies changes are pronounced within the unit, and tentative interpretations indicate that it was deposited in an intermontane valley with roughly east-west orientation. The valley was at times occupied by a lake, which occasionally dried up so that evaporites were laid down. Coarse debris entered the valley from both the north and the southwest, as shown by facies changes and paleocurrent indicators. The volcanic rocks consist of dark purplish-brown vesicular basalt flows, and pilotaxitic andesitic dikes and sil s and greenish tuff beds up to 60 cm (2 ft) thick (Crowell, 1962; Spittler and Arthur, 1973; Spittler 1974).

The formation is here named formally Diligencia, a Spanish word for stagecoach. Canyon Spring was a watering place for horses on the Butterfield Stage Route between Mecca and Ehrenberg in the late 1860's (Brown, 1923, p. 6). Until a few years ago the foundation of a

stage house still remained on the banks of Salton Creek Wash northeast from the mouth of Canyon Spring Canyon. The type section for the Diligencia Formation is here designated to include the beds along a north-south cross section from the unconformity with augen gneiss at the base, beginning at a point 850 m (2800 ft) S 75°E from Canyon Spring as shown on U.S.G.S. Hayfield Quadrangle (in the northern part of Sec. 29, T. 7 S., R. 13 E.). It is intended that the formation include not only the beds along this north-south cross section, but those to the east and west as well. Complex structure, intermixed irregular volcanic masses, and marked facies changes within the sedimentary strata preclude the establishment of a straight-forward stratigraphic column at present. No younger and distinct formations are known to overlie the Diligencia Formation in its region of outcrop except for local Quaternary fan, terrace, and alluvial deposits.

The age of the Diligencia Formation depends on its stratigraphic position, a single vertebrate-fossil find, and three K-Ar isotopic dates from interbedded volcanic rocks, one of which is unsuitable due to large analytical uncertainties. These dates are 22.4 ± 2.9 and 20.1 ± 8.9 m.y. (Crowell, 1973, Table I) and 18.6 ± 1.9 m.y. (Spittler, 1974). Recently Woodburne and Whistler (1973) have described oreodont remains from a block quite likely fallen from a sandstone bed about 365 m (1200 ft) above the base of the section, and about 0.8 km (0.5 mi) north of Canyon Spring. Woodburne and Whistler conclude from their comparison of these vertebrate remains with others in southern California "that at least the upper half of the (Diligencia Formation) is of late Arikareean, or less possibly, early Hemingfordian age." From all of this I tentatively conclude that the formation is primarily of early Miocene age but with the lower part probably extending down into the Oligocene.

SEDIMENTATION HISTORY OF THE SALTON TROUGH

by

John C. Crowell and Brian Baca

ABSTRACT

Sedimentary rocks exposed in the Salton Trough can be grouped into three sequences: (1) those strata older than either the proto-Gulf or the Gulf of California, such as the Eocene Maniobra, Oligo-Miocene Diligencia Formations, and probably the Miocene Anza Formation, (2) those laid down within the proto-Gulf, including the nonmarine Coachella Fanglomerate and Split Mountain Formations, and the marine Imperial (or Bouse) Formation, and (3) those strata deposited within the presently widening Gulf of California such as the nonmarine Palm Spring Formation with its coarse proximal facies (the Mecca and Canebrake Conglomerates) and distal fine-grained facies, the Borrego Formation. The youngest formations, of Pleistocene age, include the Ocotillo and Cabezon Fanglomerates and their fine-grained counterpart, the Brawley Formation.

Sediments as thick as 6 km apparently underlie deeper parts of the Salton Trough, and are largely Plio-Pleistocene in age. They have accumulated as the Gulf of California widened, and are undergoing metamorphism at depth in association with inferred spreading centers at the divergent plate boundary. Older strata, such as those deposited in the proto-Gulf, are envisioned as now being disrupted and occurring only around the trough margins. Older strata have also been offset by right slip along faults of the San Andreas fault system for many tens of kilometers, with the younger units displaced less than the older, in such a growing system. For example, Late Miocene fanglomerates have been offset more than 300 km from their source areas. The tectonic mobility of the region, involving both lateral and vertical movements, requires consideration in visualizing the distribution and origin of sedimentary facies. Conversely, it is the very study of facies and provenance that, in part, documents this mobility.

INTRODUCTION

Sedimentation today is actively taking place within the Salton Trough and has probably followed the same pattern back into Pliocene time as this landward apex of the Gulf of California opened and widened. Older sedimentary rocks document the history of the proto-Gulf back into Late Miocene time. Strata older than these, such as the Eocene Maniobra and Oligocene-Early Miocene Diligencia Formations of the Orocopia Mountains and the Anza Formation of the western margin of Imperial Valley were deposited under different tectonic settings before the proto-Gulf was born (Crowell and Susuki, 1959) and were not laid down within the Salton Trough itself. Here we describe briefly the nature and distribution of the sedimentary rocks of Miocene and younger age and draw inferences on what they inform us concerning the tectonic history.

Sediments accumulating within the Salton Trough today and in the immediate geologic past come from two distinctly different sources: from the Colorado River and from canyons debouching into the trough from surrounding highlands. Within the trough the Colorado River forms a low divide, about 11 m above sea level at its crest between the Imperial Valley and Salton Sea region on the northwest and the Mexicali Valley on the south. The Colorado River now enters the east side of the Salton Trough near Yuma at an elevation of about 43 m. From time to time floods carry sediments northwestward into the Salton Sea. This last happened during 1905 to 1907 when the river broke through its levees and formed the Salton Sea with a surface elevation presently about 71 m below sea level (Sykes, 1937). Prior to that event, the depression was dry, although earlier waters from the Colorado River fed prehistoric Lake Cahuilla. This lake occupied the Salton Trough at times between 300 and 1600 years ago as shown by radiocarbon dating of plant material (Hubbs and Bien, 1967). The region of the Salton Sea has therefore alternately filled and dried up as the Colorado River swung northward to flow into it, or southward into the Gulf of California. The sediments brought in by the river are dominantly very fine-grained and are characterized by high calcium carbonate content (Muffler and Doe, 1968; Van de Kamp, 1973). Reworked Cretaceous foraminifera from the Colorado Plateau are present locally (Merriam and Bandy, 1965).

Sediments derived from the walls of the Salton Trough form alluvial fans extending basinward with coarse boulder conglomerate at their heads and mud, silt, and fine sand at their distal ends. Where the stream gradients are relatively high, fanglomerate and braided-stream deposits are laid down and where the gradients on fans are low, deposition occurs in meandering channels. These facies, along with lacustrine sediments and patches of aeolian sand, have been mapped by Van de Kamp (1973). Complex interfingerings are recognizable where the sediments from the trough margins meet those from the dominating Colorado River delta. Presumably similar facies patterns exist at depth beneath the central part of the trough. Here about 6 km of strata are indicated by a few deep wells and geophysical interpretations (Keller, Chap. 6, this volume). The Standard Oil Company of California Wilson No. 1 well, drilled near Brawley, for example, penetrated about 4 km of Pleistocene and Recent fluviatile and lacustrine sediments (Muffler and Doe, 1968).

Lower Pleistocene and Neogene strata lie unconformably beneath younger beds along both the southwestern and northeastern margins of the Salton Trough (Dibblee, 1954). Facies similar to the younger sediments predominate except for marine units temporally near the Miocene-Pliocene boundary. The oldest sedimentary units so far recognized which were laid down within the Salton Trough are assigned to the Anza Formation and Coachella Fanglomerate of Middle and Late Miocene age, respectively. The main exposures of Neogene strata are in hills and mountains along the west side of Imperial Valley and the San Gorgonio Pass region, and in the Indio, Mecca and Durmid Hills. The stratigraphic relations among the various formations in Salton Trough are illustrated in Fig. 20.

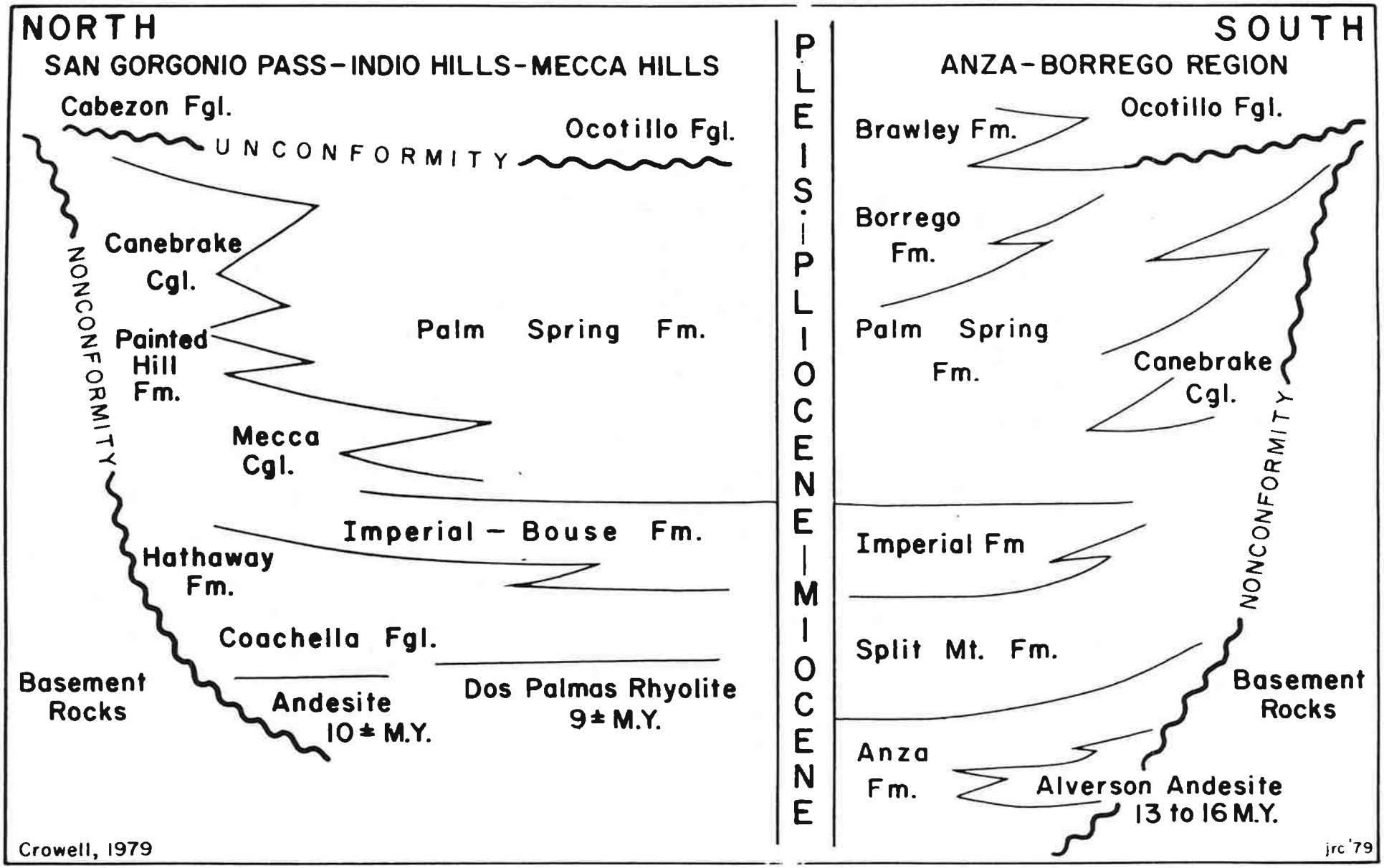

Fig. 20. Stratigraphic relations among Late Cenozoic formations in the Salton Trough region. Refer to text for explanation.

CENOZOIC STRATIGRAPHY
ALONG NORTHEAST MARGIN OF SALTON TROUGH

Miocene and younger sedimentary rocks are well exposed in four areas bordering the Salton Trough on the north and northeast: the San Gorgonio Pass region, Indio Hills, Mecca Hills, and Durmid Hills. Older sedimentary units crop out in the eastern Orocopia Mountains but were deposited in different tectonic settings, before the origin of the present Salton Trough, and the proto-Gulf of California. These older units include the Maniobra Formation (Eocene) and the Diligencia Formation (Oligocene-Early Miocene) (Crowell, 1975b). In addition, local patches of Miocene sedimentary strata are intercalated with dated volcanic rocks in the Chocolate Mountains (Crowe, 1978; Crowe, Crowell and Krummenacher, 1979).

The Coachella Fanglomerate, exposed in the eastern part of the San Gorgonio Pass region, is the oldest sedimentary unit so far recognized whose facies show that it was deposited within the Salton Trough along its northeastern margin. It consists of up to 1500 m (4500 ft) of fluviatile coarse conglomerate and debris-flow sedimentary breccia, and minor sandstone (Allen, 1957; Proctor, 1968; Peterson, 1975) lying unconformably on basement complex. Near the base of the formation is an interbedded flow of andesite breccia, dated at 10 ± 1.2 m.y. by K-Ar methods (Peterson, 1975) which places the eruption of the andesite unit in Late Miocene time. Paleocurrent indicators, thickness changes, and diminution downflow in stone size show that the fanglomerate was derived from the north, and from a source now across the northern branch of the San Andreas fault (Mission Creek fault). A possible source area containing rocks matching distinctive clasts of porphyritic quartz monzonite and magnetite has been recognized near the Cargo Muchacho Mountains, a suggested correlation that requires 215 km of right slip (Peterson, 1975). The Hathaway Formation consisting largely of conglomerate and sandstone in the San Gorgonio Pass region probably overlies the Coachella Fanglomerate and underlies the Imperial Formation (Allen, 1957; Proctor, 1968).

The marine Imperial Formation, consisting of yellow-brown and greenish mudstone, siltstone, sandstone, and a few interbeds of conglomerate, unconformably overlies the Coachella Fanglomerate in the eastern San Gorgonio Pass region (Allen, 1957; Proctor, 1968). From this region it apparently thickens southeastward to a maximum so far reported of 500 m (1660 ft) in the Texas Edom well drilled in the western Indio Hills a kilometer south of the south branch of the San Andreas fault (Banning fault). The easternmost exposure in this general region lies near the juncture between the two branches of the San Andreas fault, north of the town of Indio (Proctor, 1968). It has not been found north of the northern branch. The age of the Imperial Formation, judging from faunas, is usually given today as Early Pliocene, but some controversy still remains so that lower parts may be Late Miocene (Woodring, 1932; Durham and Allison, 1960).

Metzger (1968) named the Bouse Formation for marine beds of similar aspect to the Imperial Formation found along the Colorado River in the Parker-Blythe-Cibola region. Brackish and marine faunas, but especially a K-Ar minimum date of 3.02 ± 1.15 m.y. on an interbedded tuff (Damon, 1967, in Metzger, 1968, p. D133),

indicate that the formation is primarily Early Pliocene in age. The Bouse Formation was apparently deposited in a north-trending marine embayment extending into southern Nevada and northwestern Arizona with shorelines that have now largely been eroded away or buried beneath younger basin fill (Metzger, 1968; Blair, 1978). The formation probably correlates with the older named Imperial Formation. Pliocene and younger right slip on the San Andreas fault may have offset the Bouse from the Imperial in the Coachella Valley region. The record is too piecemeal, however, to reconstruct thickness- and facies-change lines in order to establish slip.

Within the Mecca Hills, the Mecca Formation lies nonconformably upon basement terrane, and thickens markedly toward the southwest (Sylvester and Smith, 1976). In this direction as well as upward in the stratigraphic section it intertongues with the Palm Spring Formation. The Mecca Formation consists primarily of brown conglomerate and sandstone characterized by angular, locally derived gneiss and schist detritus. The largely overlying Palm Spring Formation, however, consists of tan sandstone and drab siltstone with conglomerate beds in which granitic detritus prevails. These differences reflect source areas: as the drainage areas worked headward more and more granite terrane was tapped, especially in the Little San Bernardino-Cottonwood-Eagle Mountain chain, as the local prevailing gneiss was overlapped by large, southwest-directed coalescing alluvial fans. The Mecca Formation reaches a maximum thickness of about 180 m (600 ft) whereas the Palm Spring reaches 1500 m (4800 ft) (Dibblee, 1954). Conglomerate tongues in the middle and upper Palm Spring Formation dominated by granitic cobbles, are called Canebrake Conglomerate (Dibblee, 1954). The exposures of these nonmarine, non-fossiliferous formations lie largely within and northeast of the San Andreas fault zone. Their thickness changes and facies reflect sedimentation at the edge of a deepening trough with a platform-like margin upon which the beds overlap. The thick units of the Palm Spring Formation, however, were largely dumped into the growing trough southwest of the San Andreas fault (Sylvester and Smith, 1976). The Mecca and Palm Spring Formations are also exposed in the Indio Hills (Popenoe, 1958), and the 760 m (2500 ft) of strata within the Durmid Hills northeast of the San Andreas fault, assigned by Babcock (1974) to the Shavers Well Formation of Hays (1957), probably constitute a distal facies of the Palm Spring. The Painted Hill Formation of the eastern San Gorgonio Pass region probably correlates with the Palm Spring as well (Allen, 1957; Proctor, 1968).

The age of the Mecca-Palm Spring sequence is probably Late Pliocene and Pleistocene inasmuch as a few vertebrate remains of this age have been recovered from the upper part of the Palm Spring Formation in the central Mecca Hills (Hays, 1957). The units are younger than the Dos Palmas Rhyolite, with a K-Ar date of about 9 m.y. (Sylvester and Smith, 1976) which lies as flows nonconformably upon basement rocks and beneath coarse conglomerate correlated with the Mecca-Palm Spring in the eastern Mecca Hills. Unfortunately from the viewpoint of dating, the Imperial Formation is not exposed in the Mecca Hills, but strata assigned to the Palm Spring overlie the Imperial within the Indio Hills. Interpretations of the depositional environment and inferred age make it unlikely that the Mecca Formation correlates with either the Anza or Split Mountain Formations of the western Imperial Valley area; the Mecca Formation is considered here as considerably younger.

SALTON SEA

The Salton Sea is 35 miles long and up to 15 miles wide with an average depth of 20 feet. It was formed by accident between 1905 and 1907 when a cut was made in the banks of the Colorado River to irrigate the Imperial Valley. Flood waters broke through the cut, causing the river to flow north into the Salton Sink, an ancient sea bed. The lake's surface is 228 feet below sea level with no outlet.

Over the years three rivers—the New, the Alamo and the Whitewater—plus innumerable washes and canals have flushed saline agricultural runoff into this inland lake. Evaporation has caused a further concentration of salts. The lake is now slightly more salty than the ocean; seawater has 35,000 parts salt per million and the Salton Sea contains approximately 40,000 parts per million, with salinity increasing yearly.

Winter temperatures at the sea stay in the 70- to 80-degree range during the day, with the mercury falling into the 40s at night. Spring and fall are warmer and provide good weather for all types of water activities. Summer temperatures exceed 100 degrees daily, and the high humidity, caused by increased farming over the last 40 years, adds to the discomfort. Annual rainfall averages only 2 ½ inches.

Structure section in Painted Canyon, Mecca Hills, southern California

Arthur G. Sylvester, Department of Geological Sciences, University of California, Santa Barbara, California 93106
Robert R. Smith, Shell Oil Company, Houston, Texas 77001

LOCATION

The Mecca Hills lie on the northeast margin of the Salton Sea astride the San Andreas fault zone near its southern terminus (Fig. 1). Painted Canyon bisects the Mecca Hills and is reached by driving 5 mi (8 km) eastward from Mecca on State Highway 195, and 0.2 mi (500 m) across and beyond the Coachella Canal, to a graded dirt road which follows a powerline northwestward 2 mi (3 km) to the mouth of the canyon (Fig. 1).

A few logistical remarks are worth emphasizing. Visitors should be aware of the hazards associated with flash floods, washed out roads, soft sand, off-road vehicles, and shooters. Temperatures soar to more than 104° (40° C) in late spring, summer, and early fall. Two plants, the smoke tree and desert holly, are protected by law and should not be disturbed. Rattlesnakes and scorpions are among the endemic fauna. Nearly all aspects of the general geology can be seen adequately from the canyon floor or can be reached by short treks up side canyons. Due caution should be exercised when climbing the friable rocks of the canyon walls. In the courses of many little canyons are abrupt, vertical dry falls, around most of which are no detours.

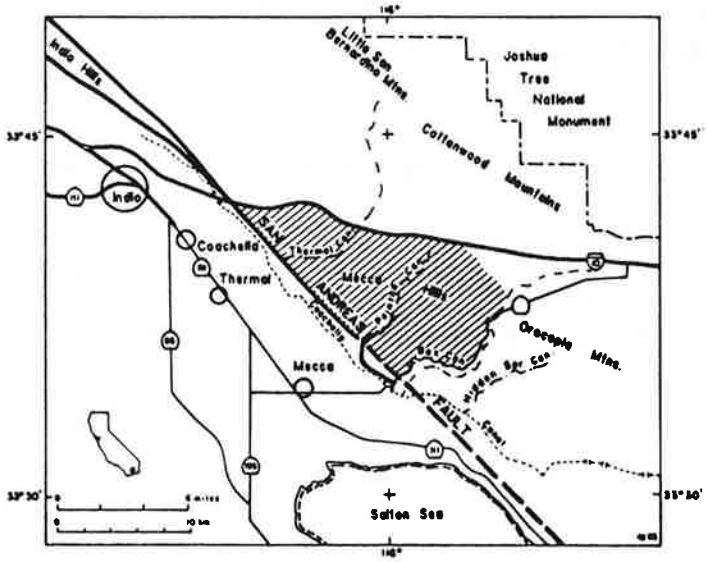

Figure 1. Index map showing the location of the Mecca Hills (ruled pattern) and Painted Canyon relative to local highways and towns.

SIGNIFICANCE

The Mecca Hills are the surficial expression of a "palm tree structure" (Sylvester and Smith, 1976), or "flower structure" in the terminology of Wilcox and others (1973). This refers to an arrangement of faults, folds and, in the case of the Mecca Hills, basement blocks, which forms as a result of convergent strike-slip faulting (Fig. 2). It is well exposed and quite accessible because basement rocks are exposed in their structural relations with the overlying sedimentary rocks, and because there is little vegetation and alluvial cover.

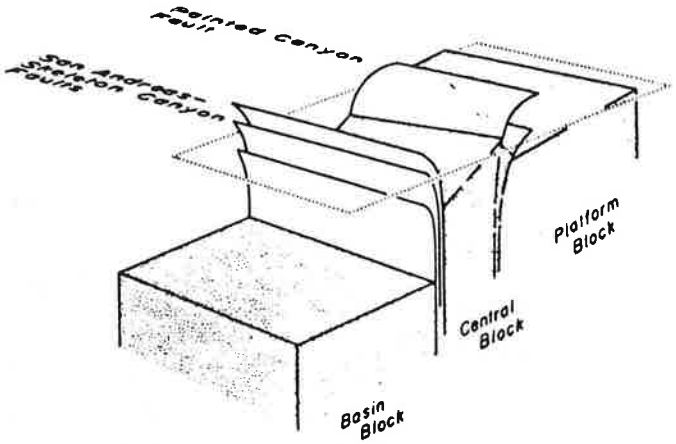

Figure 2. Idealized block diagram of the basement and principal faults in the Painted Canyon part of the Mecca Hills. Dotted parallelogram represents the surface. By permission of American Association of Petroleum Geologists.

STRUCTURAL AND LITHOLOGIC OVERVIEW

Within the part of the Mecca Hills crossed by Painted Canyon, three structural domains or blocks are distinguished by the style and degree of deformation as well as by the type and thickness of late Cenozoic sedimentary rocks; the three are informally designated the platform block, the central block, and the basin block (Fig. 2; Table 1). They are separated from one another by the Painted Canyon and San Andreas-Skeleton Canyon faults which flatten upward, carrying rocks of the central block outward upon the adjacent blocks (Fig. 3). It is this geometrical arrangement of faults relative to the three blocks which led us to designate this a "palm tree structure" (Sylvester and Smith, 1976). The structural and lithologic contrasts among the three domains are summarized in Table 1.

Basement Rocks

The basement comprises two main rock units: (1) the Chuckawalla Complex (Miller, 1944) which is chiefly Precam-

TABLE 1. LITHOLOGIC AND STRUCTURAL CONTRASTS AMONG THE THREE STRUCTURAL BLOCKS OF THE MECCA HILLS

Basin Block	Central Block	Platform Block
	Pre-Cenozoic Basement Rocks	
Not exposed	Highly sheared gneiss and granite of the Chuckawalla Complex.	Moderately sheared to unsheared gneissic and and plutonic rocks of Chuckawalla Complex; Orocopia Schist.
	Basement-sediment surface steeply tilted to the southwest.	Basement-sediment surface gently inclined to to southwest.
	Cenozoic Sedimentary Rocks	
Alluvium	Arkose and conglomeratic arkose.	Conglomeratic arkose and conglomerate.
Thickness: 12,000-15,000 ft (3,000-5,000 m)	Thicker stratigraphic sequence than in eastern block--approximately 5,000 ft (1750 m).	Relatively thin stratigraphic sequence (<2,000 ft or <750 m).
Structure of sediments beneath allivial cover is not known.	Broad, open folds, locally appressed and overturned, with axes oblique to traces of major faults.	Virtually unfolded except for minor drag folds with axes slightly oblique to fault trends.
	Steep, west-trending, normal cross-faults.	Steep-to-gently inclined, northwest-trending normal faults.

brian gneiss, migmatite, and anorthosite and related rocks intruded by Mesozoic plutonic granitic rocks, and (2) the Orocopia Schist which is thought to have been regionally metamorphosed during late Mesozoic time (Ehlig, 1981). The Chuckawalla Complex is thrust upon the Orocopia Schist in the Orocopia Mountains (Crowell, 1975), but in the Mecca Hills the two rock units are separated by the high-angle Platform fault (Figs. 2, 3).

Cenozoic Stratigraphy

Late Tertiary and Quaternary nonmarine sedimentary rocks (Table 2), including intercalated alluvial fan, braided stream, and lacustrine deposits, rest unconformably upon the Precambrian basement. Stratigraphic thicknesses, age relations and correlation of various rock units across faults are not well-known in the area because of numerous depositional discontinuities, abrupt lateral and vertical facies changes, and lack of fossils and distinctive marker beds. The overall nature of the stratified sequence, however, records a period of nonmarine deposition near a tectonically active basin margin. Clast lithology and sedimentary structures show that the sedimentary detritus was derived from the Cottonwood, Little San Bernardino, and Orocopia Mountains to the northeast and east, just as it is today.

The Mecca Formation (Table 2) is the oldest unit of the Tertiary sedimentary sequence. Composed chiefly of angular, dark red-weathering detritus derived locally from the Chuckawalla Complex and Orocopia Schist, it forms a nonconformable blanket 6–15 ft (2–5 m) thick upon the basement pediment northeast of the Painted Canyon fault. It is much thicker and coarser southwest of that fault where the contact with the basement in Painted Canyon is a buttress unconformity.

The Palm Spring Formation (Table 2) marks an abrupt change in provenance in that it was derived almost entirely from a granitic terrane. Its deposition in the Mecca Hills area marks the spreading of alluvial fans from the Cottonwood and Little San Bernardino Mountains across the pediment of the platform block. Like the Mecca Formation, the Palm Spring Formation thickens abruptly across the Painted Canyon fault and is progressively finer-grained basinward. Numerous diastems within the formation southwest of Painted Canyon indicate depositional interruptions reflecting Plio-Pleistocene episodes of folding and faulting at the margin of Salton Trough. Today, in Painted Canyon, the thicker sedimentary sequence of the central block is uplifted relative to that on the platform block. Thus, apparent tectonic inversion implied by this reversal may be resolved by vertical *separation* associated with strike-slip.

STRUCTURAL PROFILE

Basin Block

Geophysical studies by Biehler, Kovach, and Allen (1964) indicate that the depth to basement ranges from 6,000 ft (2,000 m) to as much as 15,000 ft (5,000 m) beneath Coachella Valley. A steep gravity gradient across the San Andreas fault along the southwest edge of the Mecca Hills probably indicates a near-vertical step of the basement of at least 12,000 ft (4,000 m). Thus, the San Andreas fault is the principal structural boundary between the Salton Trough and the high-standing terrane to the northeast in the Mecca Hills.

A thin strip of sedimentary rocks is upturned along the northeast edge of the basin block. Comprising distal fanglomerate

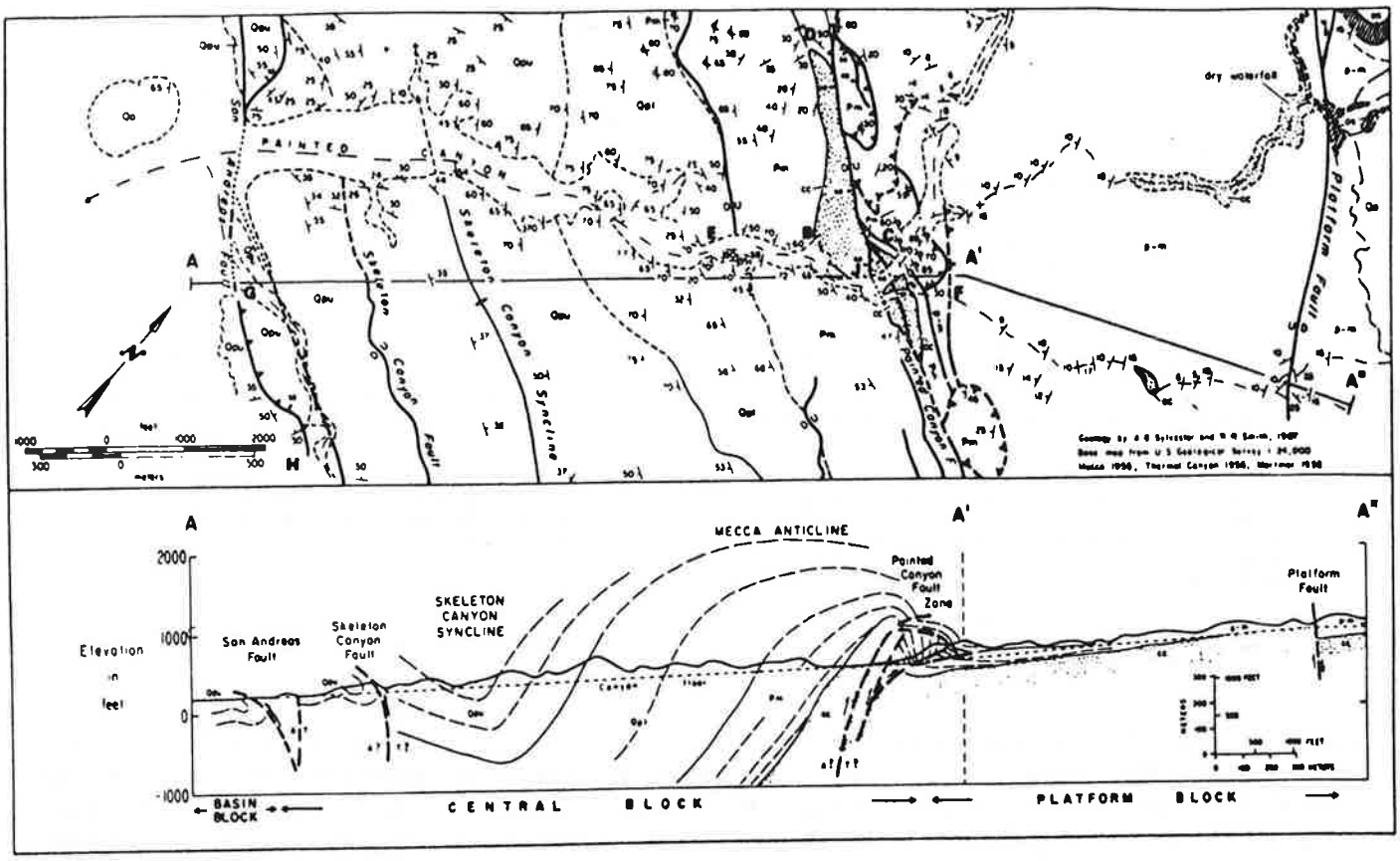

Figure 3. Geologic strip map and structural cross section parallel to Painted Canyon in the Mecca Hills. Letters B–J are localities referred to in the text. Stippled pattern is Chuckawalla Complex basement; ruled pattern is Orocopia Schist.

and lacustrine equivalents of the Palm Spring and younger Ocotillo Formations, the strata are strongly folded, especially southeast of the mouth of Painted Canyon. Here, fold axes trend west-northwest, oblique to the strike of the San Andreas fault, and locally plunge up to 70° in the same direction (locality H in Fig. 3).

Nearly monolithologic beds of Orocopia Schist clasts in the base of the Ocotillo Conglomerate (Pleistocene) show that these strata have been displaced right-laterally at least 15 mi (22 km) from their source in the Orocopia Mountains (Ware, 1958).

San Andreas–Skeleton Canyon Fault Zone

The southwest side of the central block is bounded by a complex zone of faults and folded sedimentary rocks. At the mouth of Painted Canyon, the relatively low structural and topographic relief precludes good exposures of these structures, but they may be studied in Skeleton Canyon, a major tributary marked by low hills of brick-red, phacoid-bearing fault gouge of the San Andreas fault on the southeast side of Painted Canyon (locality G in Fig. 3). The faults are steep in the bottoms of

TABLE 2. THICKNESSES, AGES AND LITHOLOGY OF CENOZOIC FORMATIONS IN THE MECCA HILLS (after Dibblee, 1954)

Formation	Lithology
Canebrake-Ocotillo Conglomerate (Pleistocene) 0-5,000 ft (0-750 m).	Gray conglomerate of granitic debris in central Mecca Hills, reddish conglomerate of schist in eastern Mecca Hills.
Palm Spring Formation (Pliocene[?] and Pleistocene) 0-4,800 ft (0-1,200 m).	Upper member: thin-bedded buff arkosic sandstone, grading basinward into light-greenish sandy siltstone. Lower member: thick-bedded buff arkosic conglomerate and arkose with thin interbeds of grey-green siltstone.
Mecca Formation (Pliocene) 0-800 ft (0-225 m).	Reddish arkose, conglomerate, claystone; chiefly metamorphic debris in basal strata.

canyons, and they flatten upward on the sides of the canyon walls. Locally, tight and nearly vertical folds are beneath low-angle segments of the gouge zones, such as at locality H.

The most recently active trace of the San Andreas fault is marked northwest of Painted Canyon by aligned gulches and ridge notches, deflected stream courses, fault gouge, nearly vertical shear surfaces with horizontal slickensides, and en echelon fractures and fault scarps in alluvium (Clark, 1984). Interpretations of several of these features are complementary and consistent, indicating right-slip movement with local vertical uplift.

Central Block

The central block is a 1 mi (1.5 km)-wide, northwest-trending zone of broad, open folds and relatively minor, high-angle faults, bounded by the Painted Canyon and San Andreas faults (Figs. 2, 3). Northwest of Painted Canyon, the axial traces of most folds trend about N70°W and define a step-right en echelon pattern. However, the folds are appressed—overturned in some instances—and trend parallel to, or are truncated by the Painted Canyon and San Andreas faults. The largest and most prominent of these folds is the Mecca anticline which forms the topographically highest part of the hills northwest of Painted Canyon. The slivers of basement exposed along the Painted Canyon fault represent the core, and are structurally the deepest exposures of the anticline.

The lower part of Painted Canyon, in the central block, is a structural depression exposing a thick, nearly flat-lying sequence of sandy siltstone and silty sandstone (upper member of Palm Spring Formation) in the trough of the shallow Skeleton Canyon syncline (Fig. 3). As one proceeds up the canyon, the stratigraphic progression is downsection into increasingly steeper tan sandstone and pebbly sandstone strata with thin, gray beds of micaceous siltstone (lower member of Palm Spring Formation) on the south flank of Mecca anticline.

A small anticline and syncline are prominently exposed in the northwest wall of Painted Canyon at locality E (Fig. 3). They are relatively minor structures and are not shown on the map because they are so small and die out laterally and vertically in very short distances: they do not project across the canyon to the southeast wall and are only gentle flexures in the next canyon to the northwest. These folds and others similar in style and position along the flank of the anticline formed in response to layer-parallel shortening in the fold limb shared by Mecca anticline and Skeleton Canyon syncline.

Painted Canyon probably received its name from the varicolored exposures of basement rocks and overlying Mecca Formation in the central part of the canyon around localities B, J, and C in Figure 3. There, dark migmatitic gneiss, intricately intruded by small, irregularly-shaped bodies of white granitic rocks of Mesozoic age, and light orange and yellow felsite dikes (K-Ar age of about 24 m.y.), is overlain by a very coarse, bouldery facies of dark red-brown-weathering Mecca Formation. The contact is a low-angle buttress unconformity that is best observed on the west wall of the canyon at locality B, where it dips 60° to the southwest. The contact and overlying beds form the core of the northwest-plunging Mecca anticline at locality D. There the northeast limb of the anticline is truncated by the Painted Canyon fault; elsewhere, however, structurally higher parts of the northeast limb are overturned and thrust short distances upon the platform block (locality C, Fig. 3).

In contrast to the relatively unsheared basement in the platform block, the basement in the anticline at locality D and adjacent to the Painted Canyon fault, such as at locality J, is pervasively fractured and sheared into a granulated mass of rock fragments ranging typically from 0.5 cm to 5 cm in diameter. The degree of fracturing is highest next to the fault. The overlying sedimentary rocks, however, are strongly fractured only within a meter or so of the fault surface; the basement-sedimentary rock contact is not a surface of slip. These field observations show that in response to contractile strain, the basement adjusted cataclastically by slip on old fractures and shear surfaces that we assume formed during a long history of pre-Mecca Formation deformation in the San Andreas fault zone; the sedimentary cover responded to deformation at the basement level by folding passively, partly by intergranular slip and partly by flexural slip concentrated in thin mudstone and siltstone beds. This mechanism is analogous to passive warping of a pliable material over a deformed mass of buckshot.

Painted Canyon Fault

The Painted Canyon fault is a major structural discontinuity at least 15 mi (24 km) long and is defined by a zone of crushed rock and fault gouge from a few centimeters to several meters wide. The fault surface dips as steeply as 70° in canyon bottoms, and it flattens upward to nearly horizontal attitudes beneath slabs of the central block that have been carried up to 330 ft (100 m) out, over the southwest edge of the platform block (locality C, Fig. 3). Beneath the low-angle segments, footwall strata of the platform block are dragged abruptly to vertical and overturned attitudes. Right horizontal separation on the Painted Canyon fault is about 2 mi (3 km), whereas the vertical separation of the basement-Mecca Formation contact locally exceeds 490 ft (150 m).

The geometry of Painted Canyon fault and of its associated structures is displayed best in the walls of central Painted Canyon as shown diagrammatically in Figure 4. In general, the structure is a faulted anticline in the hanging wall and an overturned syncline in the footwall, but it is a structure in which the two fault blocks are juxtaposed by a fault having about 2 mi (3 km) of right separation. The contact between the Mecca Formation and the crushed migmatite basement in the footwall is also a buttress unconformity, but it is tilted northeastward almost 90° from its initial gentle southwest dip (Fig. 4, see esp. section A-A'). A sequence of beds in the overturned syncline is buckled between older and younger strata in the way that the pages of a flat-lying book might be shoved and folded between their covers. The

buckled beds are bounded by a triangular arrangement of high- and low-angle faults that are best observed in Little Painted Canyon at locality F (Fig. 3). The thrust faults and associated folds are additional manifestations of contraction and uplift of parts of the central block with respect to the platform and basin blocks in transpressional deformation.

Platform Block

The upper part of Painted Canyon is incised into the northeastern structural domain: the platform block. Nearest the Painted Canyon fault, the basement rocks are overlain nonconformably by strata of the Mecca and Palm Spring Formations that are much thinner, and typically composed of coarser and more angular detritus, in this block than in the central block. The contact is a nearly planar, pre-Mecca Formation erosion surface into which channels up to 16 ft (5 m) deep were incised and filled with locally-derived, very coarse and angular Mecca Formation detritus. The erosion surface and overlying strata dip gently southwestward when mapped from canyon to canyon. Except for faulting and minor drag folds adjacent to the faults, however, strata on the platform block are undeformed.

The dry waterfall prevents further access up the canyon by motor vehicle. Near it (Fig. 3) is the best place to observe the relatively undeformed character of the basement and overlying sedimentary rocks, the details of the nonconformable contact, and the geometry of subsidiary faults and associated minor drag folds. The dry waterfall is cut into migmatite of the Chuckawalla Complex that is massive and relatively unfractured in contrast to that in the central block. Smooth and contorted flow folds in the migmatite are products of high temperature and pressure-ductile deformation in Precambrian time. About 660 ft (200 m) up the canyon from the dry waterfall are exposures of anorthosite and related rocks that Crowell and Walker (1962) described and correlated with similar rocks on the west side of the San Andreas fault in the Transverse Ranges. Farther up the canyon, these and other rocks of the Chuckawalla Complex are juxtaposed against the Orocopia Schist by the high-angle Platform fault (Fig. 3). Nearly horizontal slickensides show that the latest movement on that fault was horizontal, but drag folds with nearly horizontal axes indicate that a significant component of vertical displacement has occurred as well.

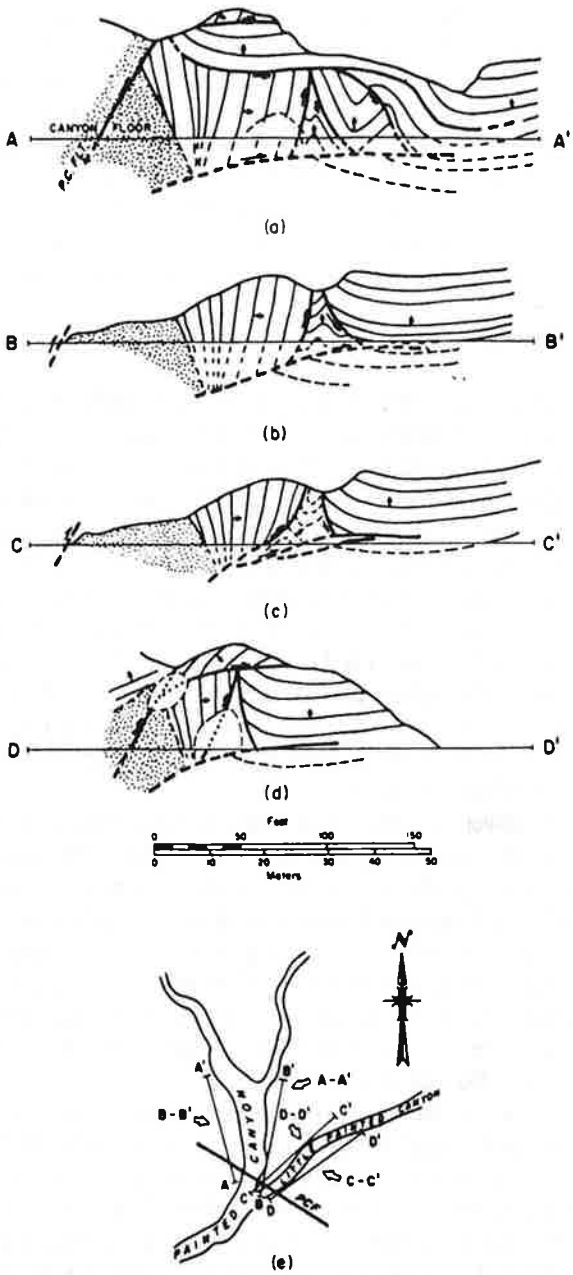

Figure 4. Generalized cross-sections of buckled strata and low- to high-angle faults in the footwall of the Painted Canyon fault. (a) Northwest wall, Painted Canyon; (b) southeast wall, Painted Canyon; (c) northwest wall, Little Painted Canyon; (d) southeast wall, Little Painted Canyon; (e) index map showing locations of cross sections. In (a), (b), (c) and (d) arrows indicate tops of beds. In (e) open arrows indicate locations of view points and view directions for each cross section.

Palm Springs Aerial Tramway (K/4) — World's most spectacular aerial ride. Mountain station, at 8,516 feet, features an Alpine buffet restaurant, cocktail lounge, gift and apparel shop, picnic area and movie theater. Mount San Jacinto State Park and Wilderness offers 54 miles of hiking trails. In summer, the Wilderness Trail Ride in Long Valley is available from 10 a.m. to dusk when Tram is open. Ride 'n' Dine features Hickory Pit Barbecue June-Labor Day and Prime Rib Oct.-Memorial Day. Cross country ski equipment rental at Nordic Ski Center. Overnight camping in Mount San Jacinto State Park and Wilderness with permit at the site. Special events. Valley Station offers snack bar/cocktail lounge, meeting room and gift shop. Admission $15.95 for adults; $9.95 children 3-12; Ride 'n' Dine $19.95 adults; $12.95 children. Annual ride tickets and group rates available. Ample parking. Tramway Dr.-Chino Canyon off Hwy. 111 (north). Open 10 a.m. weekdays, 8 a.m. weekends and holidays. Cars depart at least every half hour. Last car up 8 p.m., last car down 9:45 p.m. May-Labor Day, last car up 9 p.m., last car down at 10:45 p.m. Closed for maintenance one week in Aug. Recorded info: 325-1391. Temperature: 325-4227.

Indian Canyons (N/10) — Majestic vistas, towering cliffs and the serene beauty of Andreas, Murray and Palm canyons. Trading post, picnic grounds, hiking and horse trails. Open daily Sept. 4-July 3. S. Palm Canyon Dr., five miles from center of Palm Springs. Admission $3.50 adults, $1 children, $2 seniors, $2.50 students and military, $3.50 equestrian. 25 cents of the adult admission will be used for the Agua Caliente Cultural Museum. 325-5673.

GEOLOGY OF THE NORTHEAST BORDER OF THE SAN JACINTO PLUTON, PALM SPRINGS, CALIFORNIA

by

Robert Sydnor
Engineering Geologist
V.T.N. Corp.
Box 6-19529
Irvine, CA 92713

ABSTRACT

Intrusive relations along the northeast border of the San Jacinto pluton are well exposed in the 3-km high declevity adjacent to the Palm Springs Tramway. Here predominating granodiorite of the pluton is intermixed with tonalite, diorite, gabbro, and lesser amounts of other rocks. These mixed rocks constitute a felsic-mafic complex and several types of dikes and bodies are recognizable. Mafic magma, containing much heat, appears to have invaded a granodiorite mush so that both syn-granitic and post-granitic dikes formed.

INTRODUCTION AND REGIONAL SETTING

The San Jacinto pluton, exposed over 650 km^2, is roughly bounded by the San Jacinto fault on the west and southwest, San Gorgonio Pass on the north, and the Santa Rosa mylonite belt on the east (Fig.13). It is located in the northeastern part of the southern California batholith within the Peninsular Ranges and is believed to be Late Cretaceous in age.

The total relief is over three vertical kilometers in the study area, rising from near sea level at Palm Springs to the summit of Mt. San Jacinto at an elevation of 3,292 m.

Batholithic Rocks

Granodiorite is the most widespread rock unit of the San Jacinto pluton. Tonalite, diorite, and a small amount of gabbro are exposed in the outer parts of the pluton. One small stock of olivine norite is partially exposed near the second tramway tower. Hornblende diorite is the most common mafic rock in the Chino Canyon area and is definitely older than the hybrid (?) tonalite as shown by numerous xenoliths of diorite in the tonalite; however, the diorite and the granodiorite have inter-penetrating dikes with enigmatic age relationships.

Metamorphic Rocks

Metamorphic country rocks are exposed in the lower and middle parts of Chino Canyon, visible from the tramway road. They consist of recrystallized limestone, calc-silicate schist, quartz-mica schist, and flaser gneiss. These older metamorphic country rocks are strongly foliated, folded in places, and were evidently subjected to several periods of forcible granitic intrusion and regional tectonism. The schematic geologic cross section (Fig.14) through the axis of Chino Canyon indicates the structural relationship of the metamorphic rocks with the batholithic rocks and the location of the felsic-mafic dike complex.

Age of the Pluton

Radiometric age dates are not available for the Palm Springs/ Chino Canyon area, but K/Ar dates determined by Armstrong and Suppe (1973) for the SW part of the pluton yield an isotopic age of 84 m.y. Recent oxygen isotope studies by Taylor and Silver (1978) give a preliminary indication that the San Jacinto-Santa Rosa block is geochemically different from other plutons in the southern California batholith. It is lower in the ^{18}O and higher in $^{37}Sr/^{86}Sr$ than tonalite and granodiorite from plutons across the San Jacinto fault to the south and west.

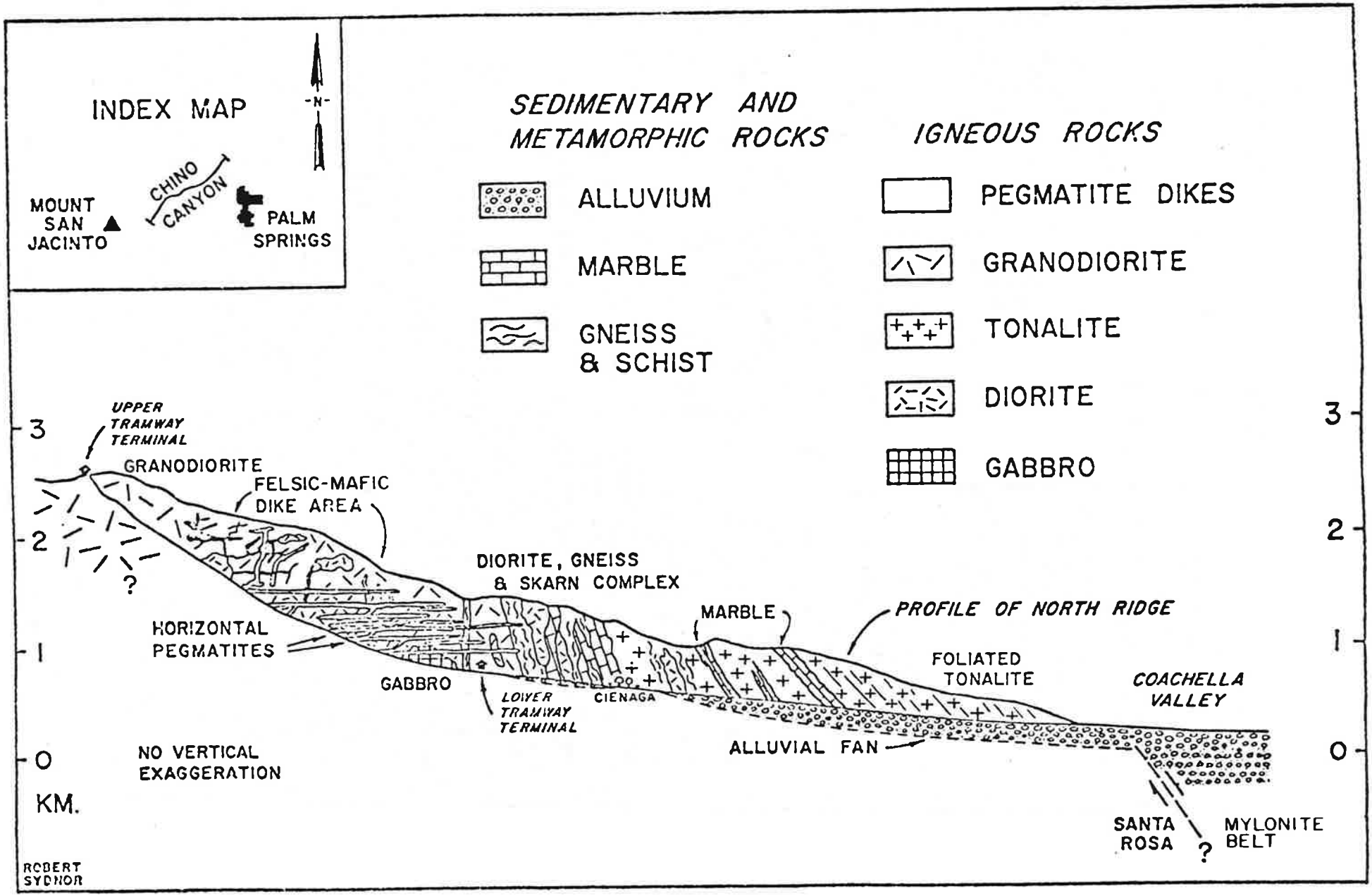

Fig. 14. Schematic cross section of Chino Canyon.

Figure 5. Geology of the lower Palm Canyon area.

GEOLOGY OF THE SAN JACINTO MOUNTAINS AND ADJACENT AREAS

Thomas W. Dibblee, Jr.
316 East Mission Street
Santa Barbara, California 93101

INTRODUCTION

The San Jacinto Mountains are among the most impressive of southern California because of their great height and proximity to the Salton trough. They are eroded from a greatly elevated mass of pre-Cenozoic plutonic and metamorphic rocks formed deep in the earth's crust but are adjacent to the deeply subsided Salton trough filled with sedimentary deposits to great depths. These contrasting terrains are within the San Andreas fault system along which irresistable lateral movements over millions of years have elevated and depressed segments of the earth's crust to create and juxtapose contrasting terrains such as those present here.

Geomorphology

The geomorphology of the San Jacinto block indicates that this basement terrain was elevated in at least three stages. The remnant of an old, subdued erosion surface is evident on the highest part of the San Jacinto Mountains between San Jacinto Peak and Tahquitz Peak, 4 miles (6 km) south at altitudes of more than 7000 ft (± 2200 m), to form a high plateau. Elsewhere this elevated old surface has been destroyed by erosion, but small remnants may occur on the high summit of the Santa Rosa Mountains, and on the summits of some lower mountains on their northeast flank. This old erosion surface was developed during an interval of erosion following the first stage of elevation.

A more extensive, elevated, subdued erosion surface is developed at lower altitudes, mostly below 5500 ft (± 1800 m) on the broad lower southwest flank of the San Jacinto Mountains. It forms somewhat of a bench that terminates northeastward against the moderately steep southwest flank of the high crest of the San Jacinto Mountains, as noted by Fraser (1931, p. 503). This elevated surface of low relief includes the summits of the lower western San Jacinto Mountains and San Timoteo Badlands, summits of dissected high alluvial fan segments around Garner Valley, and summits of the Thomas Mountain uplift. On the northeast flank of the San Jacinto Mountains, this lower erosion surface, if ever developed there, has been destroyed by erosion.

Other extensive remnants of this elevated lower erosion surface are developed on the lower northeast flank of the Santa Rosa Mountains, where it forms broad expanses of low relief cut on basement terrain. This surface slopes toward Coachella Valley around small rugged or flat-topped mountains that protrude above it. This surface of low relief is readily visible along the Palms to Pines highway (State Highway 74) along Pinyon Flat and on both sides of Deep Canyon which cuts a deep gorge through this elevated surface. South of Pinyon Flat part of this surface is covered by thin older alluvium, which is now dissected.

This extensive lower surface of subdued relief was formed during a long interval of erosion that followed the second stage of uplift of the San Jacinto block. This erosion interval was followed by the third stage of uplift during which this terrain was elevated to its present height. As a result, this elevated lower erosion surface is now being deeply dissected and largely destroyed by canyons that are being graded to the present base levels of the lowlands on each side. Because the base level of Coachella Valley is much lower than that of the Perris block, the canyons on the northeast flank are deeply incised. This is evident on the northeast flank of the Santa Rosa Mountains on which the elevated lower east-sloping erosion surface is deeply dissected by Deep Canyon, Palm Canyon, and their tributaries. The Cenozoic sedimentary deposits on the San Jacinto block have been severely eroded to badlands as a result of this latest uplift; for example, in the vicinity of Hemet and in the San Timoteo Badlands.

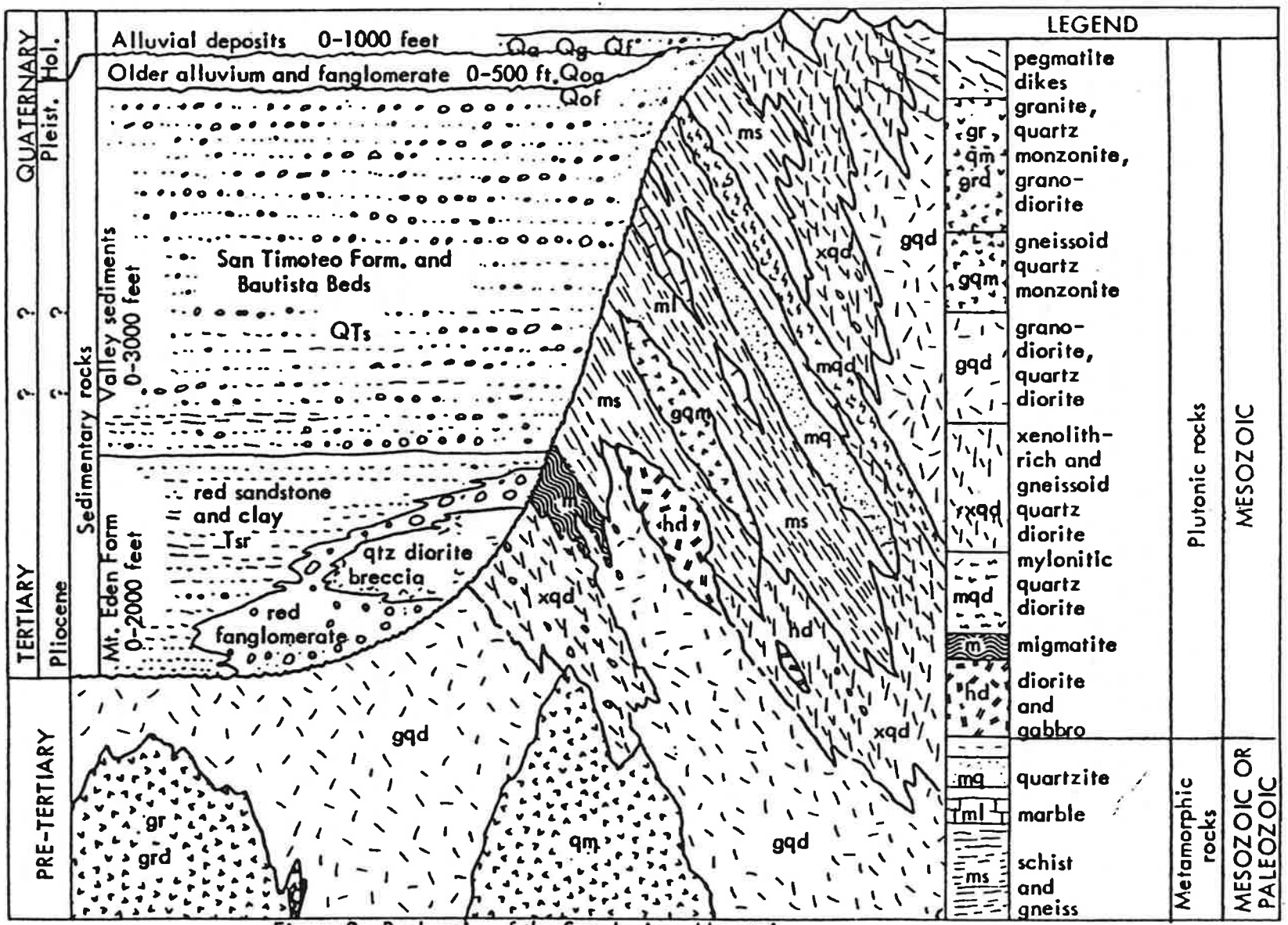

Figure 8. Rock units of the San Jacinto Mountains.

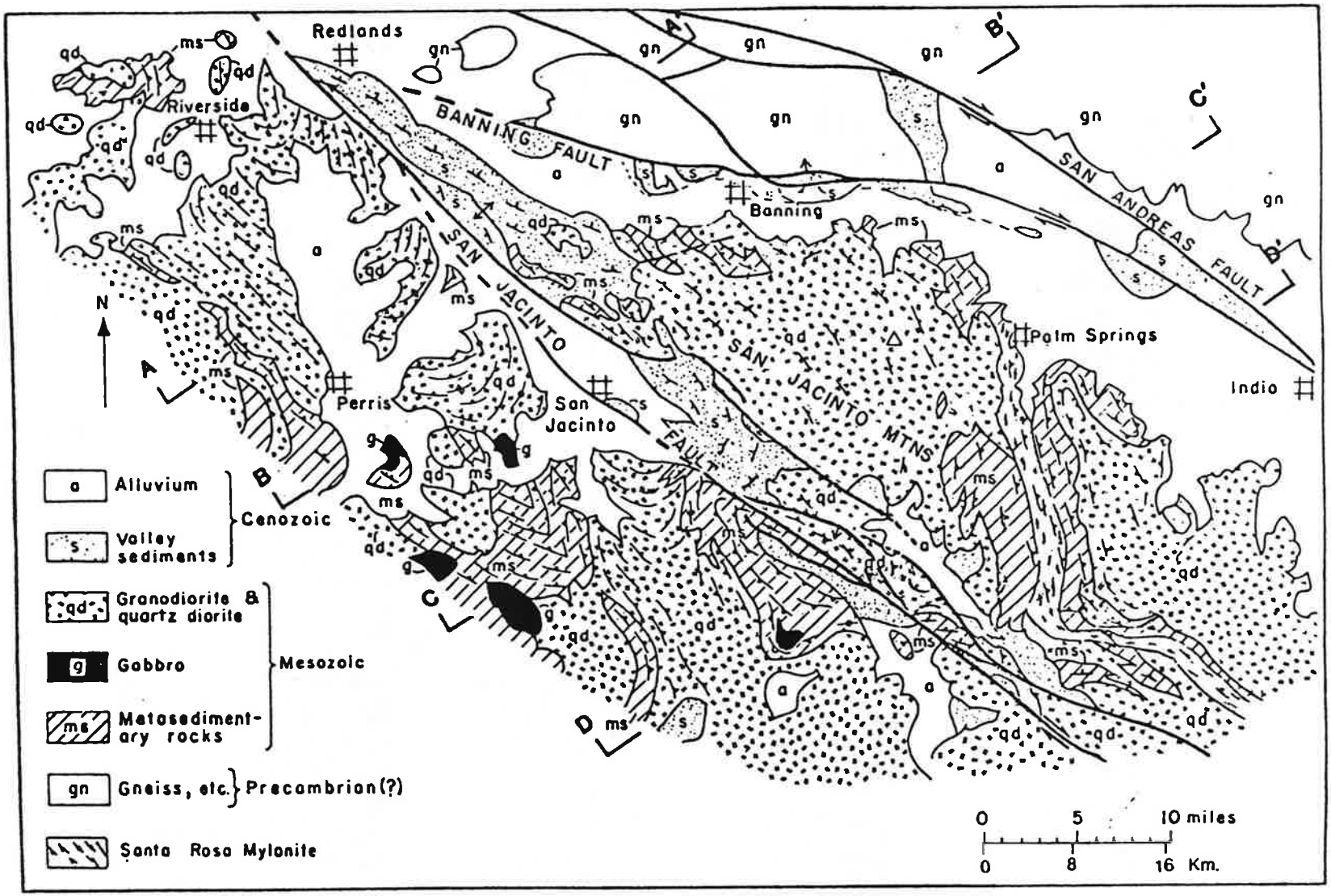

Figure 3. San Jacinto fault zone in the San Jacinto Mountains and vicinity. Modified from Dibblee, 1968.

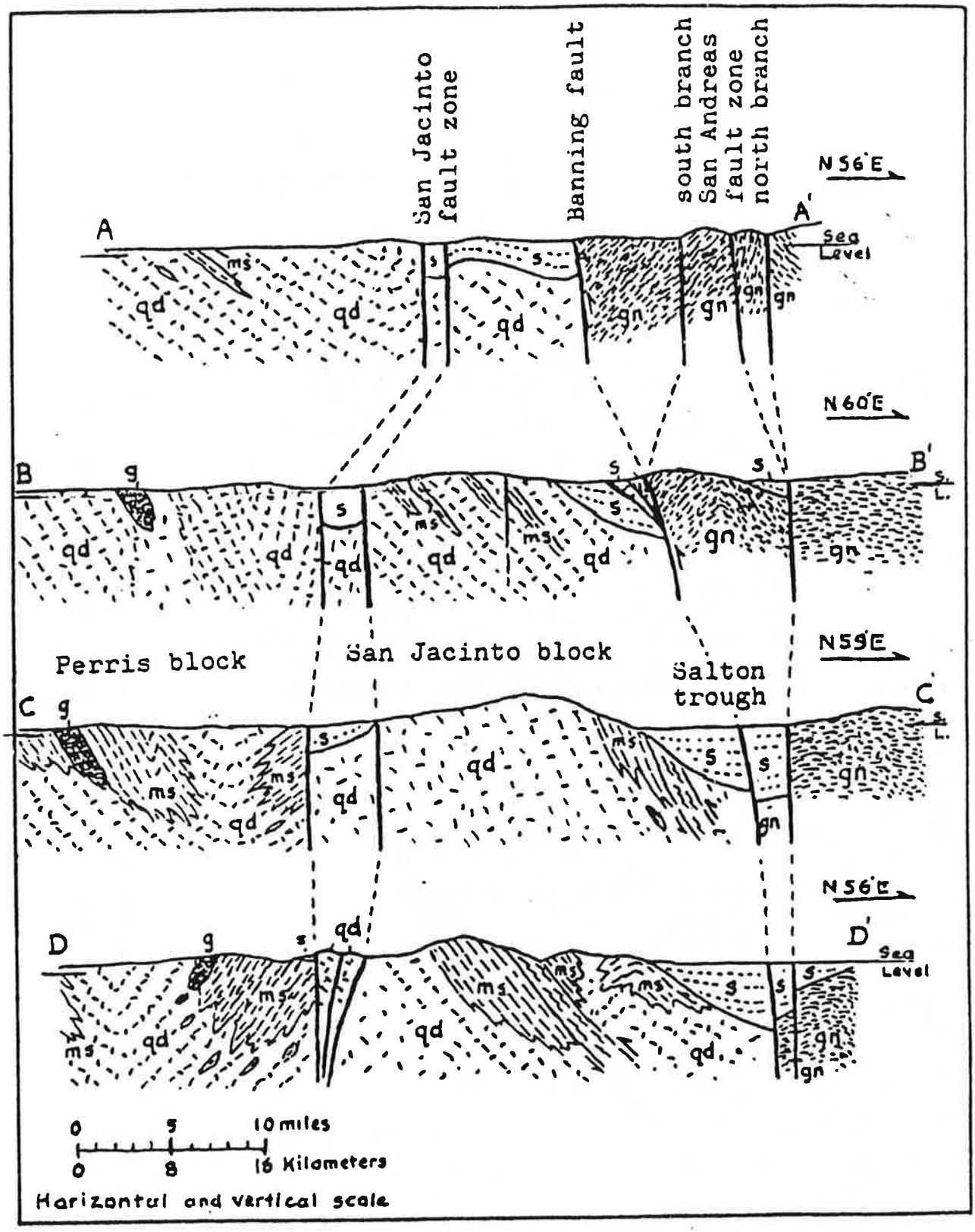

Figure 4. Geologic cross-sections of the San Jacinto Mountains and vicinity. For locations and symbols see figure 3.

HISTORY OF GOLD MINING IN THE SOUTH SAN JACINTO MOUNTAINS

Mark E. Unruh and Robert W. Ruff

In the early 1890's the gold mines of Garner Valley were developed through a huge fraud (Tapper and Lolmaugh, 1979). The person or persons responsible for this swindle apparently had enough gold to "salt" several claims. This started gold fever in the area. Salting mines was accomplished by loading a shotgun with gold dust and firing it into the rock. Hundreds of people poured into Garner Valley to "strike it rich". An Englishman by the name of Harold Kenworthy invested enough money in this gold mining venture that a town was named after him. The town flourished, and around 1892, a two-story hotel and a school were built (Leadabrand, 1971).

At one time as many as 89 mining claims were established in the area, but relatively few were located in the gold bearing part. When the swindle was discovered around 1895, most of the miners deserted the area. Serious mining did not begin until 1900 when the Hemet Belle was developed by Emile Chilson. This mine, which is the only one actively worked today, changed hands so many times in the early stages of its development that it became known locally as the "Grubstake Mine". The Hemet Belle was worked sporadically for several years until 1917.

In the following years, few prospectors took interest in the area. However, three groups of claims were kept up. Dexter Mayne of Hemet, bought and reclaimed the Hemet Belle in 1951 and during the next 29 years built a road to the mine, developed the mine and assessed its potential. In 1980, he sold the mine to Dr. W.R. Howell of Los Angeles.

During his 29 years of prospecting in the area, Mayne claimed or reclaimed and developed three other mines: the Cadmium, the Bismuth and the Golden Crown. The Cadmium, an adjoining claim to the Hemet Belle, was sold along with it. Mayne kept the Bismuth claim. He reclaimed this claim in 1970 and has been working it slowly, but steadily, since that time. The Golden Crown was sold to Greg Sims in 1977. Originally this claim had a five-stamp mill to work gold ore from one quartz vein varying two to twelve inches wide. Development consisted of surface mining and a 100-foot-deep shaft. The shaft was later abandoned due to infiltrating water. the current owner and one employee are developing the mine further. Operations were planned to start during the summer of 1981. Mercury amalgamation and heap leaching are to be used to extract the gold.

Another prospector who took an interest in the area was Charles Munz of Garden Grove. Munz is the current owner of the Gold Shot mine. This mine was first discovered around 1927 by Mr. and Mrs. Penrod who lived in the canyon (now known as Penrod Canyon). Mrs. Penrod panned enough gold out of Penrod Creek (also known as Gold Shot Creek) to support herself and her sick husband, and in 1929 sold the claim to Gold Shot Mines, Inc. Operations lasted only a few years at the Gold Shot and an adjoining claim, the Golden Libra, before the corporation dissolved, leaving Charles Munz and a Mr. Sam Gibson as owners of the two claims. Mr. Gibson died in 1948, leaving Mr. Munz as the sole owner.

While working in the area, Munz also developed two other claims in the vicinity of, and adjacent to, the Gold Shot. They are the Big Jim and the Triangle (also known as Gold Shot II).

Big Jim was mined only near the surface for a short time prior to its abandonment. However, Munz has kept up his other three claims by working there from time to time. Because of the low tenor of the ore, his claims have not shown a substantial profit, but the recent rise in gold values has sparked increased activity in the area though losses are heavy due to vandalism and theft. "God must have been looking over them when they shot off the hinges to the door of my powder room" (Charles Munz, personal communication, 1981).

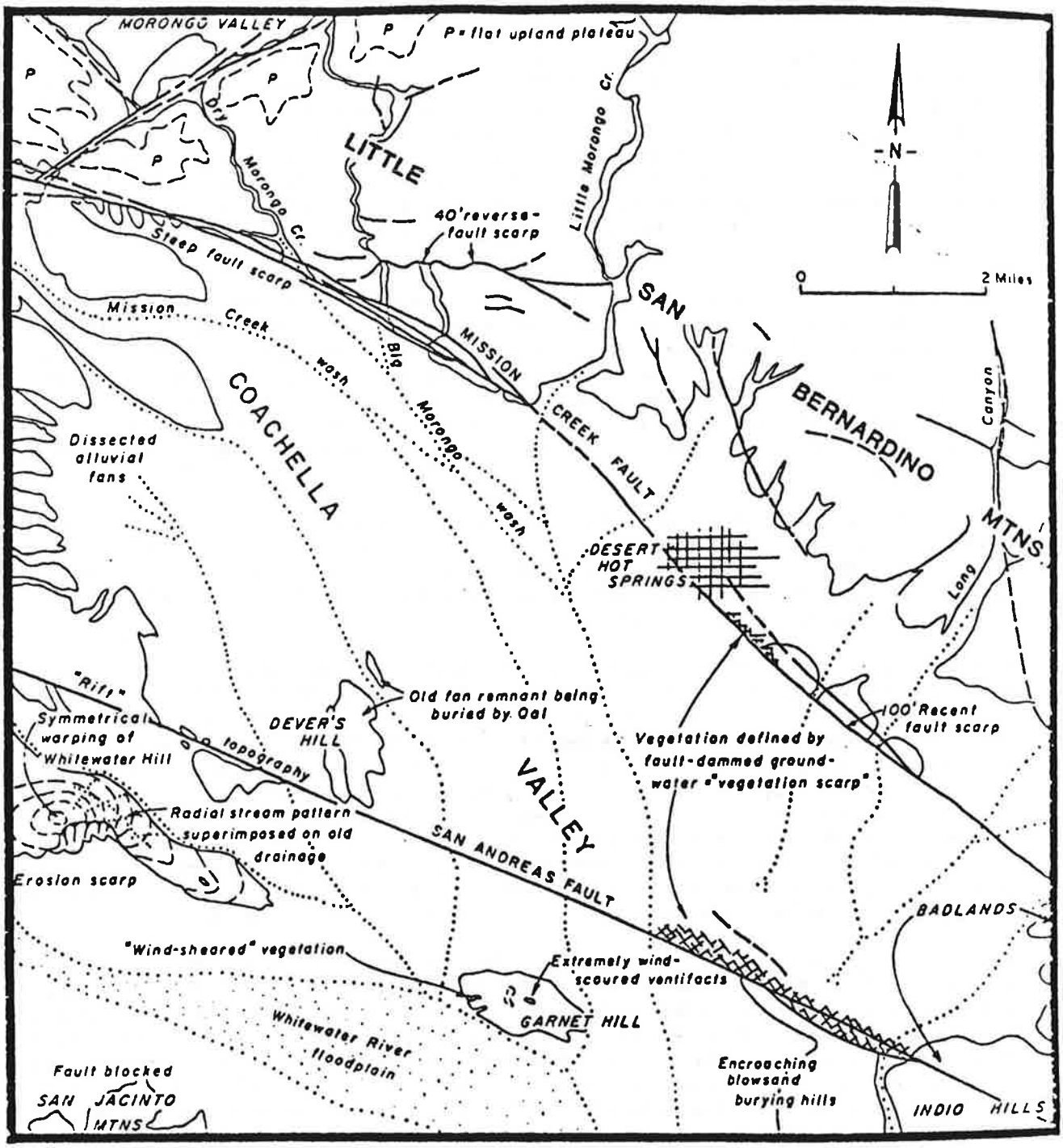

Figure 13. Geomorphic map of the Desert Hot Springs area (from Proctor, 1968).

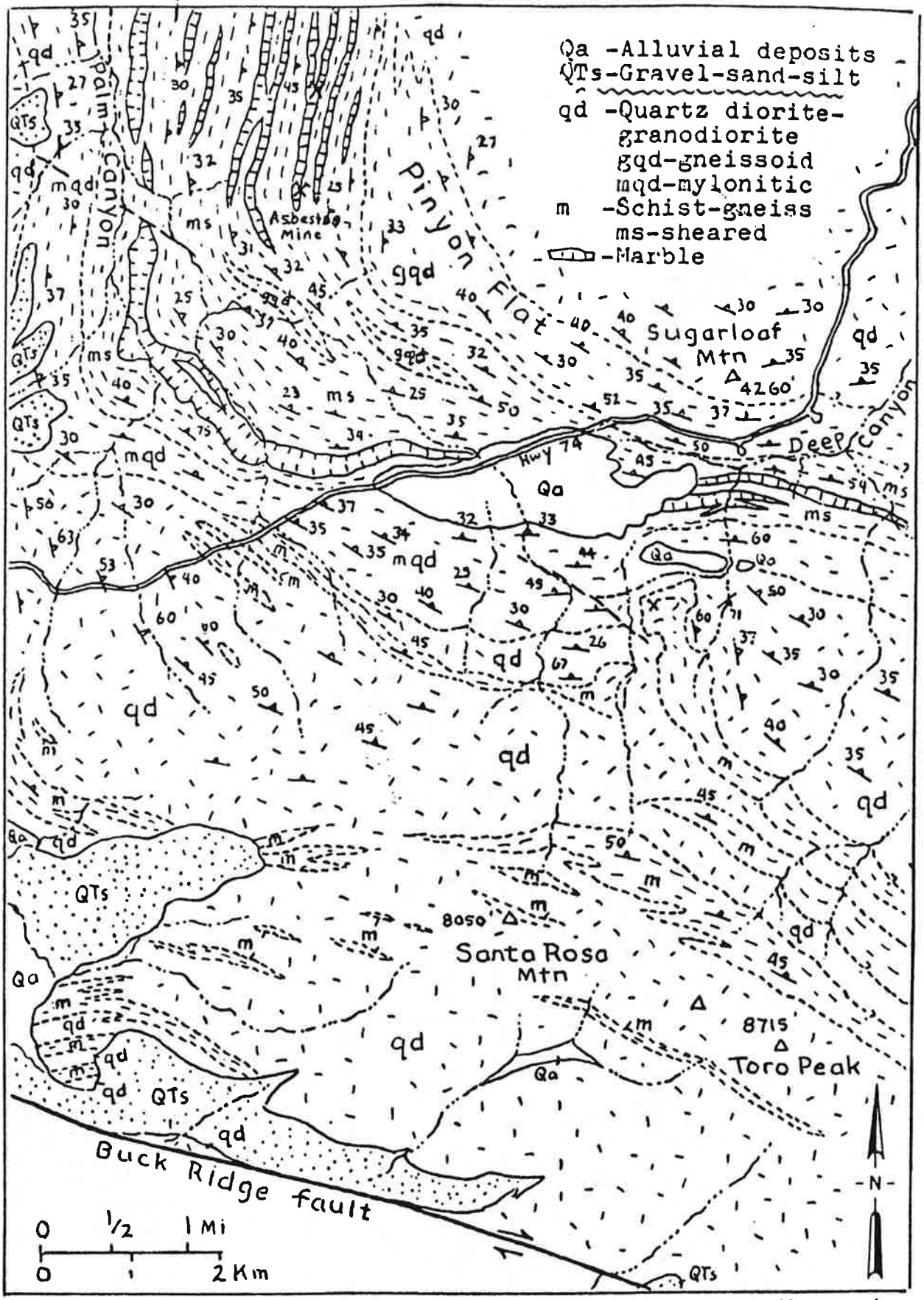

Figure 9. Reconnaissance geology of the Santa Rosa Mountain-Pinyon Flats area. Modified from Wright (1946), Sharp (1967), and Parcel (1972).

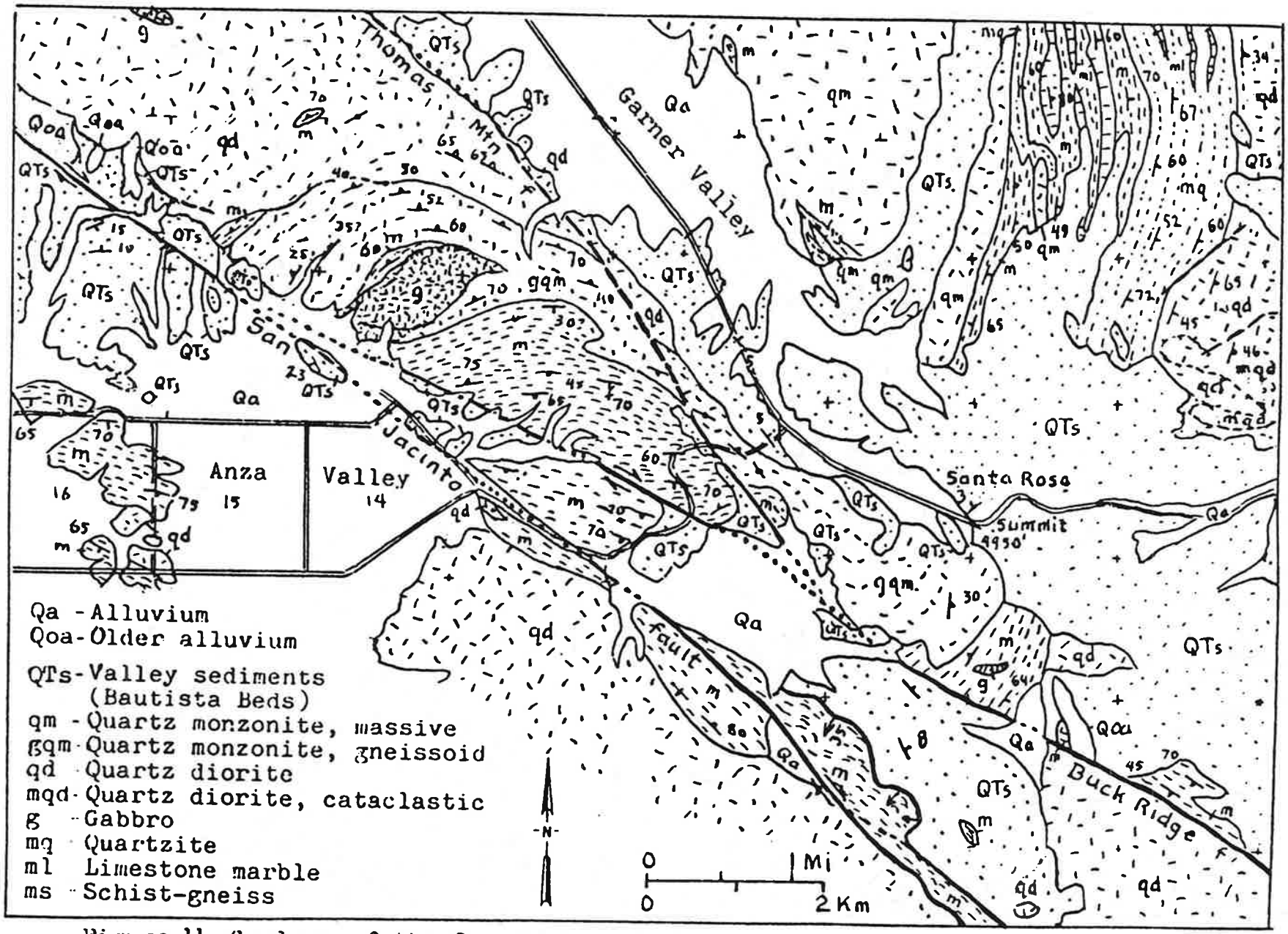

Figure 11. Geology of the San Jacinto fault zone in the Santa Rosa Summit area. Compiled from Sharp (1967) and Brown (1980).

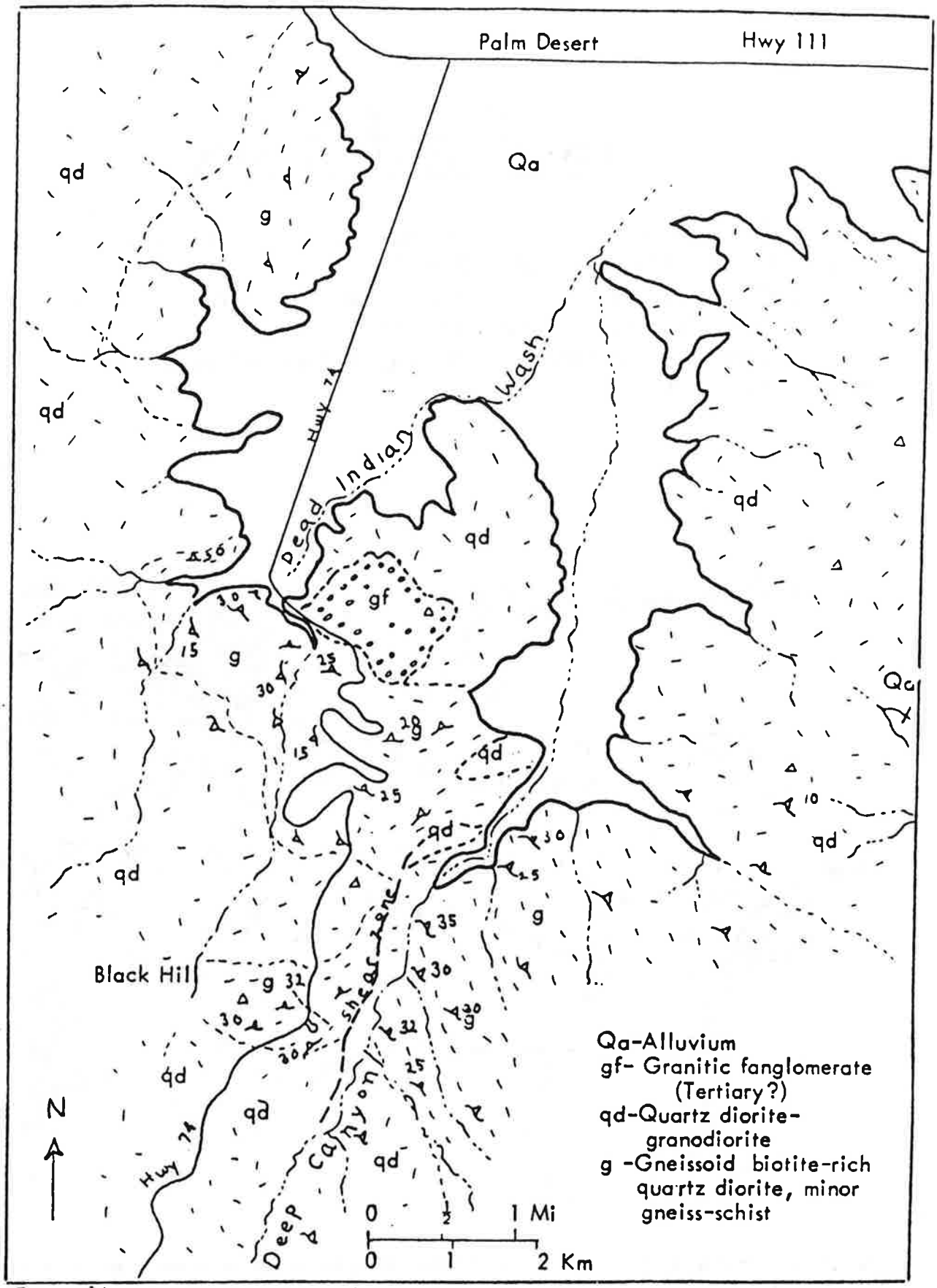

Figure 16. Reconnaissance geology of lower Deep Canyon area south of Palm Desert.

DAY THREE
PINYON FLAT TO CSUN

Stop 1 Santa Rosa mylonite zone and giant sphene crystals
Leg 1 Pinyon Flat to Burnt Valley Area
Stop 2 Pre-batholithic country rock, and San Jacinto fault zone
Leg 2 Burnt Valley to Cucamonga fault zone
Stop 3 Cretaceous mylonite zone and Holocene thrust zone
Leg 3 to CSUN

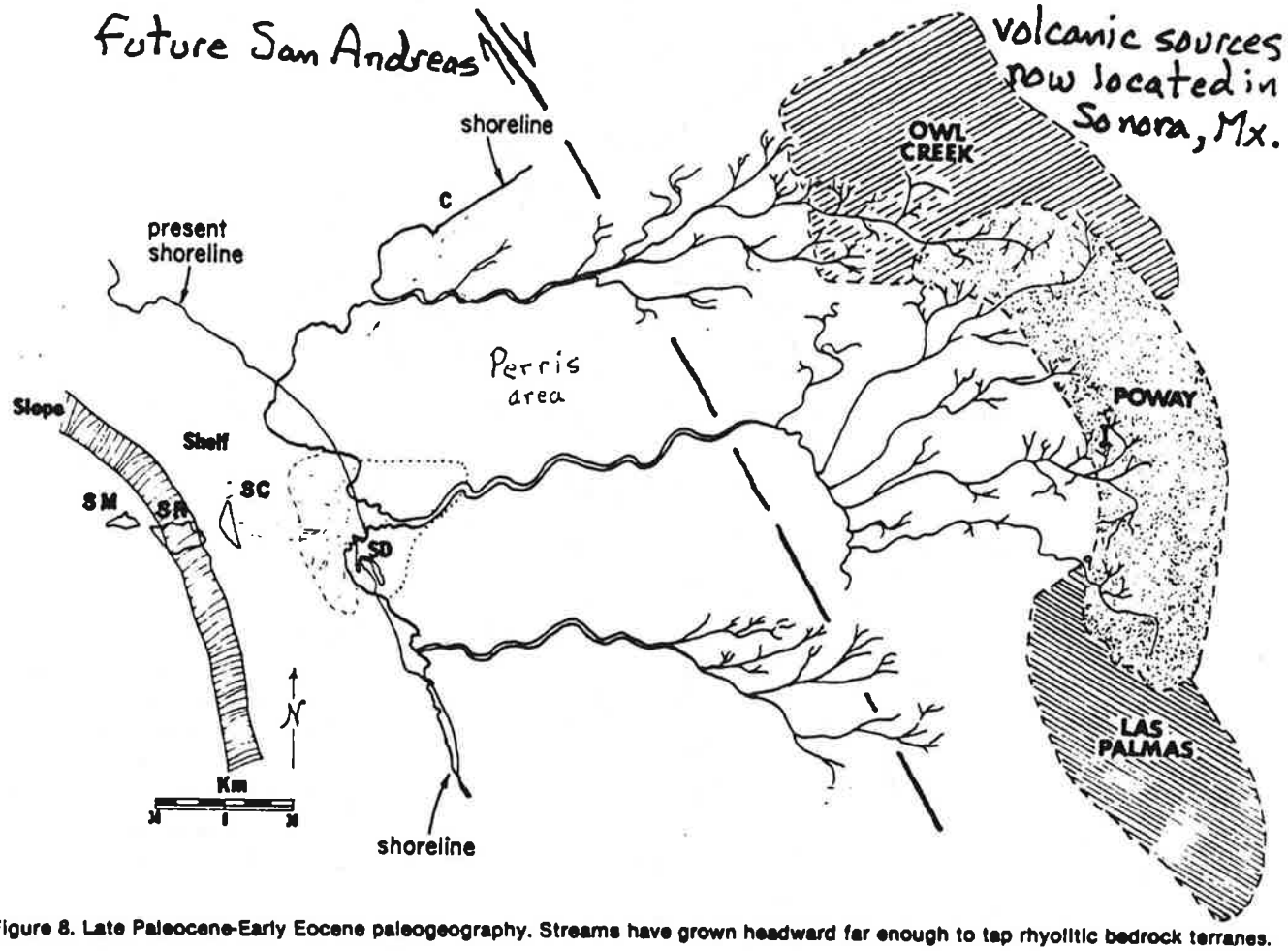

Figure 8. Late Paleocene-Early Eocene paleogeography. Streams have grown headward far enough to tap rhyolitic bedrock terranes.

Pre-San Andreas evolution of the Peninsular Ranges terrain: Paleozoic/Mesozoic 'basement', the Cretaceous batholith, and the great shear zones

INTRODUCTION

The Peninsular Ranges batholith of southern California, United States, and the Baja California peninsula, Mexico (Fig. 32-1) is one part of the chain of great Mesozoic Circum-Pacific batholiths. The development of plate tectonic theory over the past two decades has provided a framework in which the origin of the circum-Pacific batholiths and associated supracrustal rocks can be understood. In particular, the formation of batholiths along continental margins by the subduction of oceanic lithosphere and arc magmatism is recognized as a major factor in the growth of continents (Hamilton, 1981). More recently, geologic, geophysical, and paleontologic studies indicate that some crustal blocks (tectonostratigraphic terranes) have been displaced from their sites of origin in the Pacific basin to collide with, and become accreted to, western North America (Coney *et al.*, 1980; G. A. Davis *et al.*, 1978; D. L. Jones *et al.*, 1983). Paleomagnetic studies suggest that the northward translation and clockwise rotation of allochthonous terranes relative to the North American craton have been major elements in shaping the western Cordillera (Beck, 1980; Beck *et al.*, 1981). In particular, paleomagnetic studies of rocks of the Peninsular Ranges of southern California and Baja California indicate that these rocks originated more than 1000 km south of their present location (Hagstrum *et al.*, 1985, 1986).

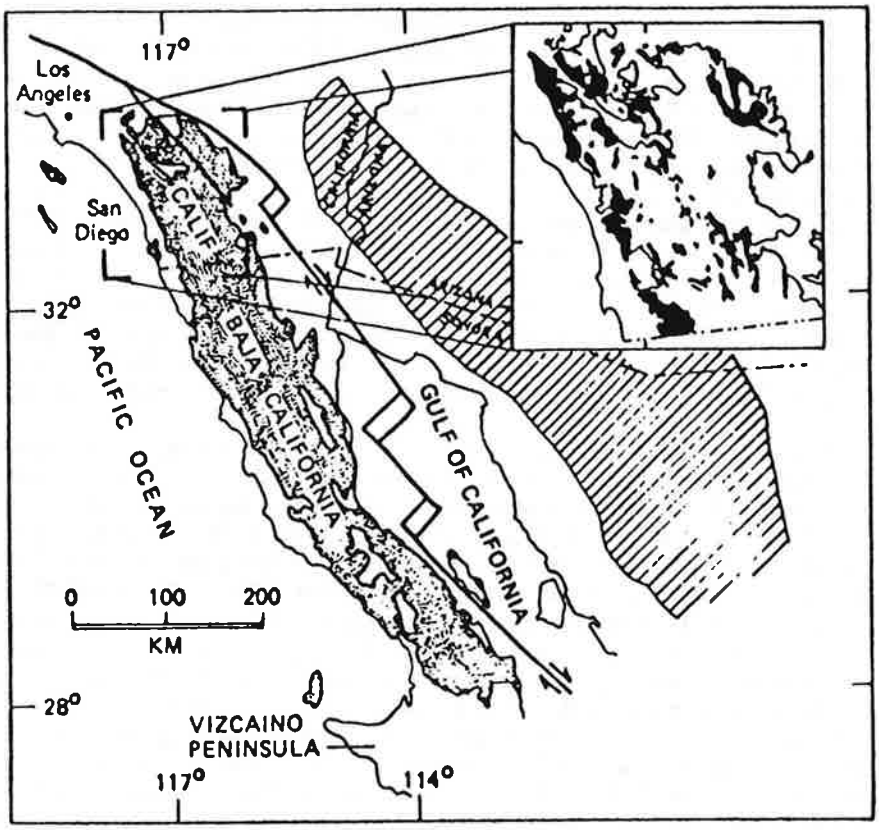

FIG. 32-1. Index map showing location of the Peninsular Ranges batholith and the study area. Stipple pattern indicates batholith and associated prebatholithic rocks (from Jahns, 1954). Line pattern indicates Jurassic-Cretaceous volcanic-plutonic ensialic arc; ensialic arc and Gulf of California-San Andreas rift-transform system from Hagstrum *et al.* (1985). Inset map shows study area, solid areas are prebatholithic screens, modified from Rogers (1965) and Strand (1962).

Fossils have been found in prebatholithic rocks at several localities, but the correlation of rocks between screens is based chiefly on lithologic similarities. In the Baja California peninsula, detailed studies of prebatholithic rocks over the past decade have revealed a wide range of depositional environments, from miogeoclinal to eugeoclinal, and a variety of ages, from early Paleozoic to mid-Cretaceous (Gastil and Miller, 1984). Many screens in the batholith either have not been studied in detail or do not contain materials that are suitable for paleontologic or radiometric dating, and therefore their ages and relations to one another are poorly understood. Nevertheless, volcanic and epiclastic rocks of Mesozoic age generally occur on the wide side of the batholith, and epiclastic rocks of Paleozoic age occur on the east side (Gastil *et al.*, 1975; Hill and Silver, 1983; Larsen, 1948).

The volcanic and volcaniclastic rocks on the west side of the batholith are deposits of an island arc that was active in latest Jurassic time and continued into the Early Cretaceous (Gastil *et al.*, 1975; Silver *et al.*, 1963, 1979). The island arc may have been paired with an eastern ensialic magmatic arc of similar age located in what is now southern Arizona and west-central Sonora (Fig. 32-1; Gastil *et al.*, 1978, 1981). An alternative hypothesis suggests that the western magmatic arc was originally the southwestern part of a single Mesozoic arc built on continental crust in the north and oceanic crust in the south (Gastil *et al.*, 1972; Gastil and Miller, 1983). In this case, the southern part of the arc was tectonically displaced to its present position by right-lateral transform faulting possibly associated with oblique subduction of the Farallon plate beneath western North America between the Late Cretaceous and late Miocene (Beck and Plumley, 1979; Erskine and Marshall, 1980; Hagstrum *et al.*, 1985; Teissere and Beck, 1973). Whether or not the island arc was paired with an eastern ensialic arc, the exposure of blueschist-facies rocks throughout the continental borderland and at several onshore localities in the Peninsular Ranges is compelling evidence for the existence of a late Mesozoic subduction zone off the southwest Cordilleran margin (Ernst, 1984).

Prebatholithic rocks in southern California underwent regional dynamothermal metamorphism of low pressure-high temperature (Abukuma) type (Miyashiro, 1961) probably beginning in the Late Jurassic and continuing throughout the Early Cretaceous, synchronous with intrusion in the western part of the batholith (Gastil *et al.*, 1975; Schwarcz, 1969; Silver *et al.*, 1969; Todd and Shaw, 1979). Structures formed during metamorphism and intrusion include northwest-striking, east-dipping isoclinal folds and foliation, and mineral lineations that generally plunge down the dip of foliation. Metamorphic grade varies from greenschist facies in the western part of the batholith to upper amphibolite facies in the eastern part. The metamorphic gradient from greenschist to upper amphibolite facies is locally abrupt in the northern part of the batholith (Schwarcz, 1969), but it is more gradual in the batholith east of San Diego (Todd and Shaw, 1979). Contact metamorphism due to the emplacement of the batholith is generally absent, although its effects are recognized locally in areas of lowest-grade regional metamorphism (Gastil *et al.*, 1975) and can be profound where batholithic rocks intruded carbonates under amphibolite facies conditions (Burnham, 1959). In general, the metamorphic grade increases to the east as shown by progressive development of partial melt leucosomes, metamorphic layering, transposition of bedding, and loss of recognizable primary structures.

The Peninsular Ranges batholith was emplaced between 140 and 80 m.y.b.p. Silver, *quoted in* Hill, 1984; Silver *et al.*, 1979). In the area east of San Diego and in northern Baja California, U-Pb zircon ages of plutons on the west side of the batholith range from 120 to 105 m.y. with no systematic geographic distribution, while those of plutons on the east side range from 105 to 89 m.y. and decrease progressively eastward. This distribution of plutonic ages suggested to Silver *et al.* (1979) that a magmatic arc was fixed, or stationary, on the west side of the batholith for much of Early Cretaceous time and began to migrate eastward at about 105 m.y.b.p. However, this hypothesis may be too simplistic because preliminary data suggest the existence of plutons that are older than 105 m.y. in the eastern part of the batholith (R. G. Gastil, written communication, 1986).

The batholith exhibits systematic west-to-east variations in lithology, geochemistry, and structural character (Baird and Miesch, 1984; DePaolo, 1981; Gastil, 1975, 1983; Larsen, 1948; Silver *et al.*, 1979; Todd and Shaw, 1979). Plutonic compositions range broadly from gabbro and tonalite in the west, to granodiorite and granite with more alkaline compositions in the east; tonalite is probably the most abundant rock type in the batholith (Gastil, 1975, 1983). Both western and eastern intrusive rocks are calcic (Silver *et al.*, 1979; Todd and Shaw, 1986).

During the period when the greatest volume of plutonic rocks was emplaced (120-90 m.y.), the region was uplifted and unroofed, and large volumes of metamorphic and plutonic detritus were shed westward into marine basins along the continental margin (Gastil *et al.*, 1978; Kennedy and Peterson, 1975; Patterson, 1979; Schoellhamer *et al.*, 1981). By Eocene time, rivers carried gravels from the continental interior westward across the deeply eroded batholith to the continental shelf (Gastil *et al.*, 1981; Kennedy and Peterson, 1975; Minch, 1972). The present-day tectonic setting of peninsular California began to take shape about 37 m.y. ago in the late Eocene and early Oligocene (Berggren *et al.*, 1985), when the Pacific-Farallon ridge first encountered the North American trench and the San Andreas transform fault system was initiated (Engebretson *et al.*, 1985).

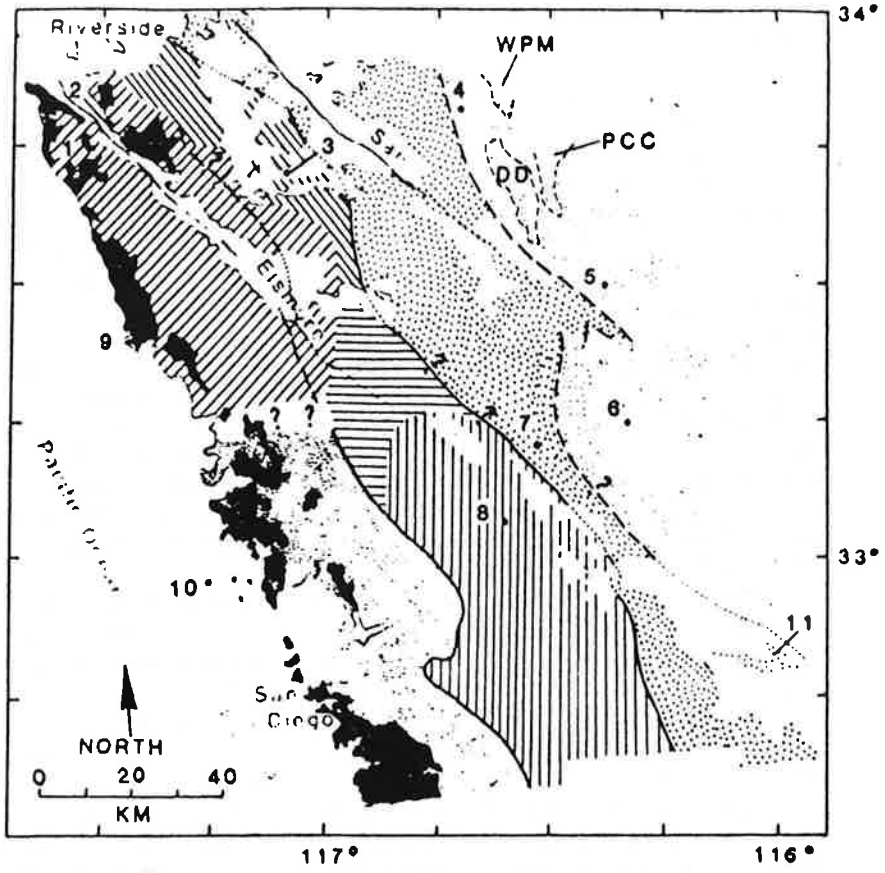

Sedimentary and volcanic deposits (Quaternary, Tertiary, and Late Cretaceous)

ZONE I Metamorphosed volcanic and volcaniclastic rocks

Santiago Peak Volcanics (latest Jurassic) and quartz latite porphyry including Temescal Wash Quartz Latite Porphyry (Larsen, 1948)

Metavolcanic rocks of unknown age with scarce metasedimentary layers

ZONE II Metamorphosed submarine fan deposits

Bedford Canyon Formation (Jurassic and Triassic) and rocks generally regarded as equivalent; west of dashed line, includes significant metavolcanic component

French Valley Formation (Triassic?)

Julian Schist (Triassic?) and rocks generally regarded as equivalent

Undivided metasedimentary rocks

ZONE III Metamorphosed miogeoclinal and transitional(?) sedimentary rocks

Metasedimentary rocks transitional between Zones II and III (Mesozoic? and Paleozoic)

Miogeoclinal metasedimentary rocks (Paleozoic? and late Precambrian?); short dashed lines outline rock units cited in text, DD=Desert Divide Group, WPM=Windy Point metamorphic rocks, PCC=Palm Canyon Complex

FIG. 32-2. Prebatholithic zones in northern Peninsular Ranges batholith generalized from distribution of rock types in screens; plutonic rocks not shown. Solid lines are approximate boundaries between zones, long dashes separate subzones that have different ages, lithologies, or depositional settings. Data from Strand (1962), Rogers (1965), and sources cited in text, modified by unpublished data of authors. Locations mentioned in text: (1) Santa Ana Mountains, (2) Temescal Wash, (3) Winchester, (4) San Jacinto Mountains, (5) Santa Rosa Mountains, (6) Borrego Valley, (7) Ranchita, (8) Julian, (9) Camp Pendleton, (10) Del Mar, (11) Coyote Mountains.

Systematic variations in composition, size, and structural characteristics of plutons across the batholith have led workers to propose a number of classifications, all of which have common features. Larsen (1948) noted the geographic asymmetry in the distribution of plutonic rock types across the northern part of the batholith, pointing out that transitions between lithologic zones are sharp and trends are parallel to the long axis of the batholith. Gastil (1975, 1983) divided the plutonic rocks of the batholith into five compositional belts, four of which are present in southern California and the Baja California peninsula. These are, from west to east, (1) the Pacific Margin belt (western Transverse Ranges, Channel Islands of southern California; Isla Cedros and Vizcaino Peninsula, Baja California peninsula), which includes allochthonous oceanic plutonic rocks of Triassic, Jurassic, and Early Cretaceous age (Moore, 1984); (2) the gabbro belt (western part of the Peninsular Ranges), consisting chiefly of gabbro, tonalite, and granodiorite; (3) the leucotonalite belt (eastern Peninsular Ranges), which includes relatively large, homogeneous leucocratic plutons that vary from "potash feldspar-free tonalite to granodiorite"; and (4) the granodiorite-granite belt (easternmost part of Baja California peninsula and western Sonora, Mexico), which includes large adamellite plutons with well-formed, large, pink K-feldspar crystals.

On the west side of the batholith, Silver *et al.* (1979, p. 105) reported diverse lithologies that range from "gabbros and quartz gabbros to abundant tonalites (relatively mafic and inclusion-rich) with fairly abundant silica-rich leucogranodiorites and rare adamellites" and noted the prominence of hornblende throughout these rocks. On the east side, they found a relatively limited range of lithologies that are dominated by "sphene-hornblende-biotite-bearing tonalites and low K_2O granodiorites." Oxygen isotopic compositions of plutonic rocks reflect the west-to-east lithologic asymmetry noted above. Plutons on the west side of the batholith have "normal" igneous $\delta^{18}O$ values (+6 to +8.5), while those on the east side have values of +9 to +11 or higher, with a sharp discontinuity, or "step," between the two regions (Taylor and Silver, 1978; Fig. 32-5). The $\delta^{18}O$ step coincides approximately with the boundary between the older, western static arc and the younger, eastern migrating arc of Silver *et al.* (1979). Rare earth element (REE) abundances also vary systematically across the batholith (Gromet, 1979; Gromet and Silver, 1979). Slightly fractionated REE patterns, commonly with negative Eu anomalies in plutons in the western region of the batholith give way to middle and heavy REE fractionated and depleted patterns with subdued Eu anomalies, if any, in the central region of the batholith, and to strongly enriched patterns of light REE in eastern plutons.

Major elements of about 334 granitoid rocks of the northern Peninsular Ranges batholith were analyzed by statistical methods in order to characterize the source materials of the batholith (Baird and Miesch, 1984). The data indicate that the granitoid rocks formed from the mixing of basaltic and quartzofeldspathic end-member magmas whose compositions reflected variations in their source materials. The boundary between the two different source regions is a north-northwest-striking discontinuity that lies near the center of the batholith and is interpreted as the western margin of major continental crustal contribution to the batholith. This discontinuity coincides approximately with the $\delta^{18}O$ and 105-m.y. U-Pb age steps discussed above.

Todd and Shaw (1979, 1985, 1986) divided intrusive rocks into a syntectonic sequence in the western part of the batholith and a late- to posttectonic sequence that occurs chiefly, but not exclusively, in the eastern part of the batholith. The syntectonic intrusive sequence includes both I-type granitoids, those with geochemical and isotopic characteristics primarily derived from partial melting of an igneous protolith, and S-type granitoids, those with characteristics primarily derived from partial melting of a crustal sedimentary, or metasedimentary, source (Chappell and White, 1974; A. J. R. White and Chappell, 1977). The western extent of S-type granitoids was considered to mark an I-S line in the batholith (Fig. 32-5).

Most workers consider the Santiago Peak Volcanics and the Alisitos Formation to represent the deposits of a fringing island arc that collided with, and was accreted to, western North America in late Mesozoic time (Gastil *et al.*, 1981). Todd and Shaw (1985) suggested that compressive structures in Early Cretaceous plutons and their metamorphosed wallrocks east of San Diego were caused by collision of the Santiago Peak island arc with the Triassic and Jurassic marginal basin. The exact location and nature of the contact between arc-related rocks and marginal-basin sediments in the northernmost part of the batholith are unclear, in large part because the distribution, ages, and affinities of metavolcanic rocks there are not fully known. In the batholith east of San Diego, the westernmost screens consist mainly of metavolcanic rocks (Fig. 32-2, close stipple). The southern part of the prebatholithic boundary between Zones I and II is considered to be the approximate midpoint of a 5- to 10-km-wide zone of interfingering metavolcanic and metasedimentary wallrocks (Todd and Shaw, 1985; Fig. 32-6). Metasedimentary rocks are rare in screens west of this interfingering zone, and, as mentioned above, minor orthoamphibolite layers are present in the Julian Schist well east of the zone. The location of the prebatholithic boundary between Zones I and II is uncertain in the area between the Santa Ana Mountains and 33°N (Fig. 32-2). The southwesternmost screens in this area contain metamorphosed felsic and mafic volcanic rocks (Todd, unpublished mapping), which suggests that the boundary strikes north-northwest, nearly parallel to the I-S line (Fig. 32-5). Further to the north, screens that lie west of the dashed line in Fig. 32-2 contain interstratified metasedimentary rocks ("Bedford Canyon Formation") and metavolcanic rocks[4] (R. Engel, 1959). This line, inferred to be the boundary between Zones I and II, marks the eastern limit of screens containing significant amounts of metavolcanic rocks. Minor amphibolite layers of possible volcanic origin occur east of this boundary in the French Valley Formation (Schwarcz, 1969). The relations above suggest that the Mesozoic marginal basin received detritus from both a western(?) volcanic arc and eastern cratonic highlands prior to collision.

Further evidence for the existence of a major prebatholithic tectonic contact, or suture, in the northern part of the batholith are the north-northwest-striking lithologic, geochemical, and geophysical discontinuities in plutons discussed in the preceding section (Fig. 32-5). Although their origins are not well understood, these discontinuities almost certainly reflect a fundamental west-to-east contrast in the composition of the prebatholithic crust that in part formed the source rocks for the plutons (Shaw *et al.*, 1986; Taylor and Silver, 1978; Todd and Shaw, 1985, 1986). The I-S line, gabbro line, and $\delta^{18}O$ step all reflect a change in source rock from primitive, oceanic crust on the west to continental crust and/or continentally derived sediments on the east. From the relative positions of the prebatholithic boundary between Zones I and II, the I-S line, and the gabbro line, Todd and Shaw (1985) suggested that the prebatholithic suture between the Santiago Peak volcanic arc and the Mesozoic marginal basin dipped to the east (Fig. 32-6). Thus, the suture was oriented subparallel to regional batholithic structures that imply northeast-southwest shortening (northwest-striking, northeast-dipping tight to isoclinal folds, axial plane foliation, and ductile shears). The eastward offset of the lithologic and geochemical discontinuities from this prebatholithic boundary (Fig. 32-6) is probably an artifact of the eastward dip of the suture. The geometry produced by the inferred east-dipping suture and by regional structures that suggest northeast-southwest compression, and a pervasive, steep northeast-plunging lineation indicate that the Santiago Peak arc was thrust beneath the western edge of North America.

The gravity-magnetic boundary shown in Fig. 32-5 is the projected surface trace of the contact, inferred from geophysical modeling, between a western region of residual gravity and magnetic highs and an eastern region of gravity lows and sparse magnetic anomalies (Jachens *et al.*, 1986). This contact apparently marks the transition from oceanic crust intruded by relatively mafic, I-type plutons on the west to continental crust and sediments intruded by relatively leucocratic late- to post-tectonic plutons on the east. The boundary lies near, but is not coincident with, the magnetite-ilmenite line, which separates rocks containing magnetite ± ilmenite on the west from those with ilmenite as the chief opaque oxide on the east (Diamond *et al.*, 1985). The geophysical modeling implies the existence at depth of a remarkably regular contact that dips about 45° to the east and extends to a depth of 15 km or more. North of the segment of the gravity-magnetic boundary shown in Fig. 32-5, the gravity and magnetic fields are complex, and the contact, if present, cannot be identified (R. C. Jachens, oral communication, 1986). South of this segment, the contact is well defined, dips about 40° to the east, and extends to a minimum depth of 10 km (A. Griscom, oral communication, 1986). The relatively simple geometry of this contact suggested to Jachens *et al.* (1986) that it is tectonic rather than intrusive and is probably the subsurface location of the prebatholithic suture. Alternatively, the gravity-magnetic contact may be a syn- or postintrusive ductile shear zone that formed during an episode of Early cretaceous ductile deformation (discussed below).

Two major zones of ductile deformation have been recognized in the northern part of the batholith, the Early Cretaceous Cuyamaca-Laguna Mountains shear zone in the south-central part of the study area, and the Late Cretaceous eastern Peninsular Ranges mylonite zone in the eastern part (Fig. 32-4). The older zone strikes north-northwest and dips steeply to the east, while the younger zone strikes predominantly from north-northwest to northwest and dips moderately to the east. Intrusion probably preceded and accompanied deformation in both zones.

Eastern Peninsular Ranges Mylonite Zone

The eastern Peninsular Ranges mylonite zone (Sharp, 1979) is a 100-km-long belt of deformation located in the eastern part of the northern Peninsular Ranges batholith. The zone strikes southward from Palm Springs to the southern Santa Rosa Mountains, where it is offset to the west by two strands of the right-lateral San Jacinto fault (Sharp, 1967; Fig. 32-7). Southeast of Borrego Springs, the zone is buried beneath alluvium. The mylonite zone is probably part of a more extensive zone of deformation that lies beneath the Coachella and Imperial Valleys and the Gulf of California. Spatially associated with the mylonite zone are a series of east-dipping low-angle faults that strike subparallel to, but generally dip more gently than, the regional east-dipping mylonitic foliation. Although ductile mylonitic deformation and brittle low-angle faulting were probably parts of a single protracted episode of deformation, the chronologic and kinematic relations between the two are uncertain. The two types of deformation are discussed separately below.

Ductile deformation Rocks in, and associated with, the eastern Peninsular Ranges mylonite zone have been divided into three units, based on lithology, rock fabrics, and contact relations. From structurally lowest to highest these are (1) strongly deformed mylonitic rocks that define the mylonite zone itself, (2) metasedimentary tectonites and anatexites of the Palm Canyon Complex, and (3) "upper-plate" granitic rocks (Fig. 32-7). All of these rocks are linked structurally by the presence of a foliation and lineation that are uniform in attitude, and the three units probably represent different parts of a broad zone of deformation that have been juxtaposed by ductile shearing and later low-angle faulting. For this reason, the Palm Canyon Complex and "upper-plate" granitic rocks are considered parautochthonous rather than allochthonous. The critical features of each unit are summarized below.

The Mylonite Zone. The rocks of the mylonite zone are autochthonous to the batholith and have not been displaced by movements along low-angle faults (Fig. 32-7). As the mylonite zone is approached from the west, rocks of the northern Peninsular Ranges batholith grade rather abruptly into mylonite gneiss, mylonite, and ultramylonite characterized by the presence of an intense foliation and a well-developed stretching lineation. The foliation is regionally consistent, striking north-northwest and dipping 35-55° eastward. The attitude of the lineation is extremely uniform in a given region, but its trend changes systematically from eastward in the southern part of the mylonite zone to about N55°E in the San Jacinto and northern Santa Rosa Mountains. Classic shear indicators such as multiple foliations and asymmetric fabrics described by Platt and Vissers (1980), S. H. White *et al.* (1980), and Lister and Snoke (1984) indicate an east-over-west sense of shear (thrust) throughout the zone (Simpson, 1984). This sense of shear is confirmed by asymmetric quartz textures in mylonitic plutonic rocks and in quartz-rich leucocratic dikes that were transposed along the foliation (Erskine, 1986a). Sharp (1979) proposed westward to southwestward thrusting in the mylonite zone based on regional geologic studies. Engel and Schultejann (1984) reached a similar conclusion based on studies of highly deformed metasedimentary rocks and gneiss in and adjacent to the eastern Peninsular Ranges mylonite zone. They described Late Cretaceous imbricate thrusts and nappes that first moved westward and later north-northwestward over the rising autochthonous core of the batholith.

The contact of the mylonite zone with underlying plutonic rocks dips less steeply (30-40°) than the mylonitic foliation, and the geometric relations between the two are consistent with the expected geometry of a postcrystalline shear zone (Ramsay, 1980). Based on examination of microstructures in the southern part of the eastern Peninsular Ranges mylonite zone, Simpson (1985) concluded that the mylonite zone represents a postintrusive shear zone. However, a number of structural relations between intrusive rocks both below and within the northern part of the mylonite zone suggest that deformation was, in part, contemporaneous with intrusion (Anderson, 1983; Erskine, 1986b). The concordance of foliation, lineation, and strained mafic inclusion fabrics in plutonic rocks below the mylonite zone with mylonitic foliation and lineation within the zone supports this view. In addition, at least one plutonic unit within the mylonite zone (leucogranite of Cactus Spring, Matti *et al.*, 1983) has the geometry and structure that would be expected of an intrusion that invaded an active deformation zone and crystallized before deformation ceased. It appears likely that rocks within the region were deformed prior to, during, and following intrusion of the eastern part of the batholith.

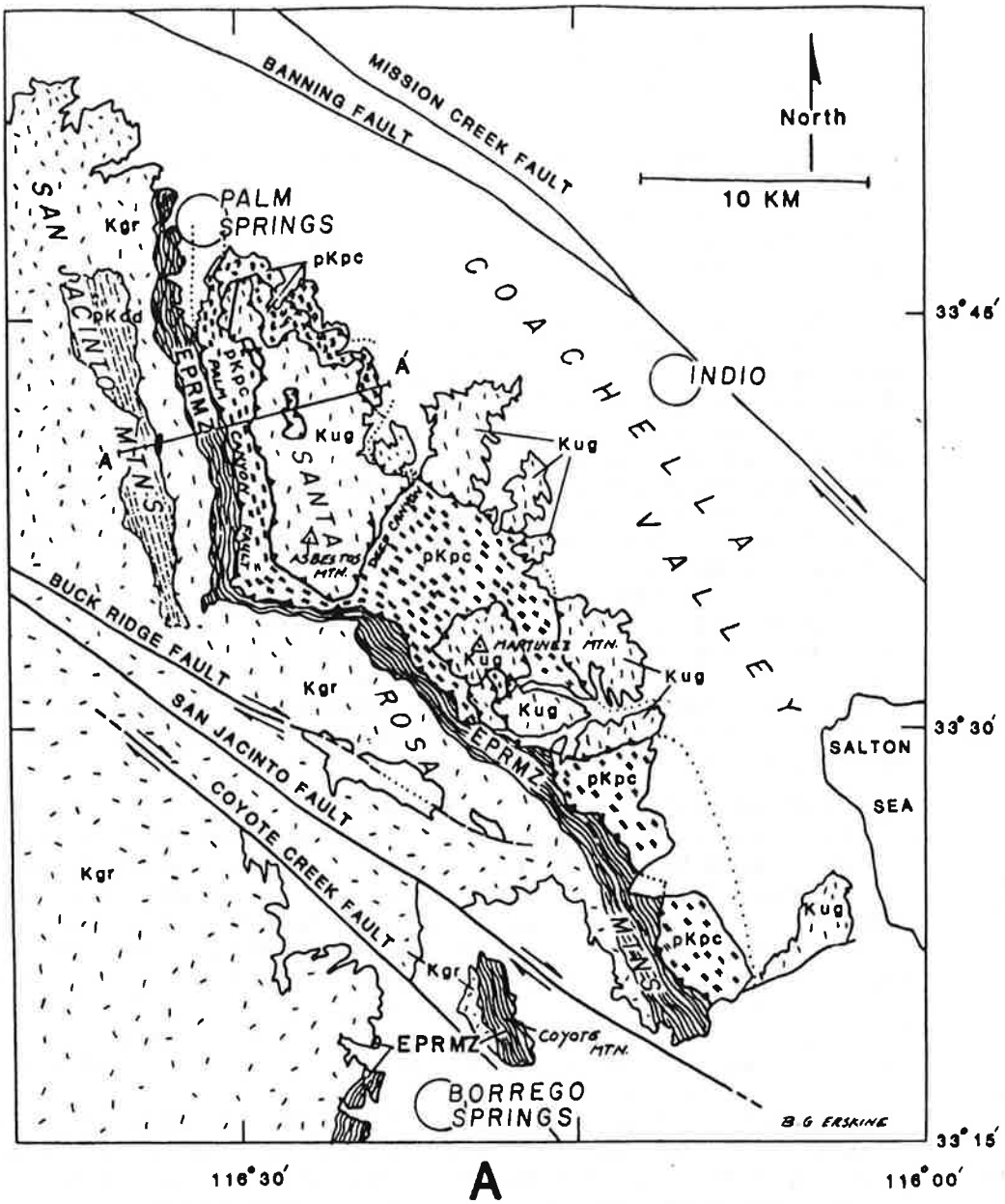

A

FIG. 32-7. Generalized geology of part of the San Jacinto and Santa Rosa Mountains, modified from Erskine (1986a) and Sharp (1979). (A) Geologic map. (B) Enlarged cross section A-A', vertical and horizontal scales equal.

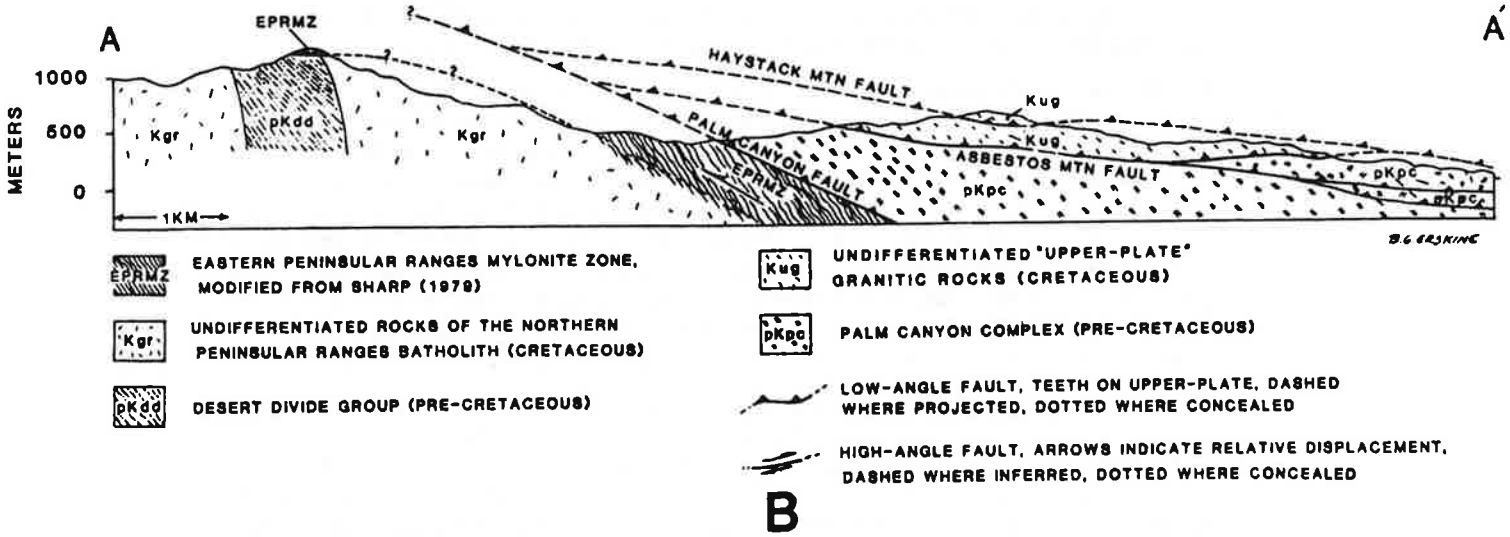

B

FIG. 32-7 Continued

Although the age of mylonitization is not well constrained, it probably began at some time between 97 and 62 m.y.b.p. U-Pb ages of zircons from tonalite plutons in the San Jacinto Mountains indicate emplacement ages of 97 m.y. (Hill, 1981, 1984), providing a lower limit for the onset of deformation. The upper limit is constrained by concordant 62-m.y. apatite-sphene-zircon fission-track ages of mylonitic rocks in the northern part of the mylonite zone (Dokka, 1984). These ages suggest rapid uplift of the region at that time.

Palm Canyon Complex. The Palm Canyon Complex is the name given to a group of mylonitic metasedimentary rocks, anatexites, and orthogneiss located above the Palm Canyon fault (Fig. 32-7). The unit is well exposed from the mouth of Palm Canyon southward for at least 30 km to the area between Deep Canyon and Martinez Mountain, where about 5–6 km of section is exposed in a structural culmination. The structural top and bottom of the complex are truncated by low-angle faults. The most characteristic feature of the Palm Canyon Complex is the presence of substantial volumes of mylonitic, garnetiferous leucogranite anatexites that are associated lit-par-lit with the metasedimentary rocks and orthogneiss. The anatexites are strongly foliated and commonly carry a well-developed downdip lineation that has the same east-northeast plunge as lineation in the mylonitic rocks below the Palm Canyon fault. Metasedimentary rocks that lack anatexite textures are generally nonmylonitic, except for the calc-silicate and marble tectonites that are found throughout the Palm Canyon Complex. A variety of minor structures are present within the nonmylonitic metasedimentary rocks, but rarely do these rocks possess the well-developed northeast down-dip lineation characteristic of the anatexites and rocks of the mylonite zone.

The foliation and lineation in the Palm Canyon Complex appear to have formed during anatexis of the pelitic schists, and these structures therefore record deformation at high grades of metamorphism. The lack of significant anatexites in similar metasedimentary rocks in the Desert Divide Group to the west suggests that the Palm Canyon Complex represents the relatively deep part of a thick section of deformed rocks that was juxtaposed against shallower rocks by westward thrusting along the mylonite zone and later along the Palm Canyon fault.

"Upper-Plate" Granitic Rocks. The term "upper-plate" granitic rocks refers to all granitic rocks that occur as parautochthonous sheets and klippen above the Palm Canyon Complex (Fig. 32-7). The most completely studied unit of these granitic rocks is the granodiorite of Asbestos Mountain, which occupies a klippe above the Asbestos Mountain fault in the northern Santa Rosa Mountains. Foliation and lineation in the "upper-plate" granitic rocks are roughly parallel to the regional mylonitic structures, except where the parautochthonous sheets are folded. However, this foliation dips less steeply than that of rocks within the underlying mylonite zone and Palm Canyon Complex. The presence of east-dipping foliations and east- to northeast-trending lineations in the parautochthonous granitic rocks suggests that these rocks were emplaced during the episode of regional deformation that produced the mylonite zone.

The granodiorite of Asbestos Mountain is lithologically and geochemically similar to autochthonous plutonic rocks of the northern Peninsular Ranges batholith[6] (Anderson, 1983; Erskine, 1986a; Hill, 1984). These similarities suggest that the Asbestos Mountain unit and, by inference, the other "upper-plate" granitic rocks are not exotic to the batholith. However, the "upper-plate" rocks are anomalous in relation to the eastern part of the batholith in that they are magnetite-series granitoids, whereas the granitic rocks beneath the mylonite zone are ilmenite series. This suggests that either the source terrane of the upper-plate rocks lay some 60 km to the west, west of the magnetite-ilmenite line (Fig. 32-5), or as seems more likely, a belt of magnetite-series granitoids may once have occupied the eastern part of the batholith and been tectonically displaced.

Conditions of Metamorphism. The pressures and temperatures that existed during mylonitic deformation are not precisely known, but they can be inferred from the *P-T* conditions of metasedimentary rocks in and adjacent to the mylonite zone. As mentioned in the section on prebatholithic zones, the pressures and temperatures at the peak of metamorphism were probably similar for rocks below and above the mylonite zone: 3.2–4.5 kb and 650–800°C (Erskine, 1986a; Hill, 1984). Theodore (1970) reported a broader range of pressures (3.4–7.0 kb) and a relatively restricted range of temperatures (580–660°C) at the peak of metamorphism during mylonitization in rocks at Coyote Mountain. Following recalibration of the metamorphic reactions used by Theodore to estimate *P-T* conditions, these ranges were revised to 600–700°C and 3–5 kb (Hill, 1984).

Brittle deformation Spatially associated with the eastern Peninsular Ranges mylonite zone are imbricate low-angle faults that bound the packets of deformed rocks described in the sections above. It is unclear at present whether the low-angle faults are west-directed thrusts, east-directed normal faults, or a combination of the two. The low-angle faults have a complex movement history that probably involves several stages of reactivation. The termination of mylonitic deformation and the commencement of low-angle faulting may be related to the 62-m.y.b.p. uplift and cooling of the region documented in the northern Santa Rosa Mountains by fission-track dates (Dokka, 1984).

The earliest event, or events, that can be recognized in the tectonic history of the northern part of the Peninsular Ranges batholith was the deposition of one or more Paleozoic marine sedimentary prisms along the southern part of the Cordilleran continental margin (no. 1, Fig. 32-8). Evidence for the timing and plate tectonic setting of the disruption of the Paleozoic continental margin is scattered throughout peninsular California and the northwest part of mainland Mexico. Scattered occurrences of carbonate-rich Paleozoic rocks in the eastern part of the batholith were once thought to lie considerably west of the North American craton (Gastil *et al.*, 1978, 1981). Studies of newly recognized Paleozoic rock sequences in peninsular California and mainland Mexico (Gastil and Miller, 1984) suggest that the craton originally extended westward into what is now peninsular California, and that the Paleozoic miogeoclinal and deeper-water, or transitional, facies extended from southern Nevada through peninsular California to western Sonora (Dickinson, 1981; A. E. J. Engel and Schultejann, 1984; Gastil and Miller, 1984; Hill, 1984).

Although earlier tectonic events cannot be ruled out, the Paleozoic continental margin probably began to break up in late Paleozoic time. Upper Paleozoic arclike volcanic and plutonic rocks, and marginal basin or trench deposits at several localities in Baja California and mainland Mexico (no. 2, Fig. 32-8) suggest the existence of a late Paleozoic convergent margin (Gastil *et al.*, 1978, 1981). During Triassic and Jurassic time, a thick wedge of clastic rocks was shed westward from cratonic highlands into one or more deep marine basins marginal to the North American continent (nos. 3, 4, Fig. 32-8). The plate-tectonic setting of these basins, whether fore-arc, back-arc, or trench, is not known.

Studies of arc-related rocks in the California continental borderland indicate that a volcanic-plutonic island arc began to accumulate in the ocean basin off the southwest coast of North America in Late Triassic time, and extended along the length of the borderland by Middle Jurassic time (Gastil *et al.*, 1978; 1981; no. 5, Fig. 32-8). Ophiolitic rocks, spatially associated with this arc, were considered to be fragments of ancient oceanic crust formed during Triassic rifting (Gastil *et al.*, 1978, 1981; Rangin, 1978). However, recent studies by Moore (1983, 1984, 1986) indicate that ophiolitic rocks in the southern part of the continental borderland formed in more than one plate tectonic setting. There, the Vizcaino terrane is composed of three smaller paleo-oceanic terranes, two of which include ophiolitic rocks that formed in one or more Late Triassic marginal basin-island arc systems, and a third that includes pre-middle Mesozoic ophiolitic rocks that may have formed at a midocean ridge. Moore concluded that these terranes were probably not associated with a continental margin before the Late Jurassic. The Vizcaino terrane was probably accreted to the Baja California peninsula by Early Cretaceous time, and is separated from Cretaceous volcanic and plutonic rocks of the peninsula (including the Alisitos Formation) by a major structural discontinuity (Rangin, 1978).

By Late Jurassic time, a fringing volcanic island arc represented by the Santiago Peak Volcanics probably extended from the continental margin in what is now southern California southward to an oceanic island in northern Baja California (the Alisitos Formation) (Silver *et al.*, 1963, 1969; nos. 6, 7, Fig. 32-8). The Santiago Peak segment of the arc was probably emergent and located just inboard of a deep ocean basin (Adams, 1979; Balch, 1981; Buesch, 1984). Scarce metavolcanic layers in flysch-type metasedimentary rocks east of the Santiago Peak segment of the arc may represent incursions of arc detritus into the Late Jurassic marginal basin, or may include older arc-related rocks. If these volcanic layers are as old as Triassic or Early Jurassic, then a fringing arc was never far from the coast of North America.

Collision of the Santiago Peak–Alisitos arc with western North America in the Early Cretaceous resulted in folding of the continental-margin deposits and eventual underthrusting of the arc beneath the continental margin (no. 8, Fig. 32-8; Gastil *et al.*, 1978, 1981; Todd and Shaw, 1985). As indicated by the end of prebatholithic marine deposition and the onset of deformation, the arc apparently arrived first in the northern part of peninsular California. In the Santa Ana Mountains, the Triassic and Jurassic Bedford Canyon Formation was probably folded, overturned, uplifted, and eroded prior to depositional and/or tectonic emplacement of the Santiago Peak Volcanics. Even if the contact between the two units were entirely tectonic, the difference in intensity of deformation between them suggests that the Bedford Canyon Formation was deformed before it came in contact with the Santiago Peak Volcanics. In the batholith east of San Diego, the uppermost Jurassic and Lower Cretaceous(?) Santiago Peak Volcanics were folded and metamorphosed in Early Cretaceous time. In the eastern part of the study area, this deformation fabric may have been superposed upon a pre-Late Jurassic fabric. In Baja California, the Alisitos Formation of Aptian and Albian age had been deformed and uplifted by late Albian time (Gastil *et al.*, 1978, 1981). The staggered arrival of the island arc suggested to Gastil *et al.* (1981) that it was offset by a series of transform faults that connected paired western and eastern magmatic arcs. However, it is possible

that the Santiago Peak and Alisitos arc segments represent fragments of an island arc that was dismembered by northward-directed transform faulting and that the older fragments traveled farther, and arrived earlier, than the younger ones. In this case the arc rocks of the continental borderland could have belonged to the same dismembered island arc.

By Early Cretaceous time, the locus of magmatic activity in the northern part of the batholith had moved eastward from the Santiago Peak volcanic arc to the vicinity of the Triassic and Jurassic marginal basin (no. 9, Fig. 32-8). The volcanic rocks that were superjacent to the Early Cretaceous plutons have been removed by erosion, but downfolded and foundered volcanic strata and/or subvolcanic pyroclastic rocks probably occur in plutonic ring complexes in the western part of the study area (Todd, 1983). Early Cretaceous plutons intruded the east-dipping suture between the accreted fringing island arc and the folded marginal basin. West-to-east variations in the compositions of these plutons reflect the composition of the prebatholithic crust above and below the suture: partial melts of oceanic arc rocks in the structurally lower, western block produced I-type granitoid magmas, and melts of predominantly flysch-type sedimentary rocks in the structurally higher, eastern block produced predominantly S-type granitoid magmas. Melting in the mantle wedge above the subducted slab produced basaltic magmas that probably provided some of the heat for melting crustal materials and rose simultaneously with I- and S-type granitoid magmas into the overlying crust.

Regional compression continued during Early Cretaceous intrusion in the batholith east of San Diego (Todd and Shaw, 1979; no. 10, Fig. 32-8). Deformation was essentially penetrative in plutons and wallrocks in the western part of the area, and early fabrics were modified by diapiric intrusion. Deformation became concentrated in the east-dipping Cuyamaca–Laguna Mountains shear zone (no. 11, Fig. 32-8; Fig. 32-4), which is slightly east of and subparallel to the inferred position of the prebatholithic suture. The fabric in this part of the batholith indicates that the direction of maximum shortening was approximately east-northeast. If the predominant north-northwest orientation of the prebatholithic zones and the magmatic arc reflect the trend of the outboard trench and subduction zone, then convergence at this time was approximately normal to the continental margin. Steeply plunging lineations in both plutonic and metamorphic rocks of the shear zone indicate that movements were predominantly dip-slip. The apparent west-to-east depth contrast in S-type granitoids and metamorphosed flysch-type sedimentary wallrocks across the zone suggests that the east side was thrust over the west side (deep-seated thrust).

Approximately 100 m.y. ago, the locus of magmatism moved eastward into what had been the Paleozoic miogeocline, and a markedly different type of magma was produced (younger, late- to post-tectonic intrusive sequence) (Clinkenbeard *et al.*, 1986; Hill, 1984; Silver *et al.*, 1979; Todd and Shaw, 1986; no. 12, Fig. 32-8). Although plutons of the younger sequence are not penetratively deformed, strong fabrics did develop locally. In the Cuyamaca–Laguna Mountains shear zone, and in a 40-km-wide zone that lies east of, and parallel to the shear zone, the older plutons of this sequence (~100 m.y.) were locally intensely deformed. The younger plutons of the sequence (98–95 m.y.) are relatively massive or are weakly foliated parallel to their walls. Intrusion of these relatively undeformed plutons across the shear zone indicates that movements in it ended about 100–98 m.y. ago.

The eastward migration of magmatism may have coincided with a change from east-northeast shortening to northwest-southeast shortening in the western part of the batholith (no. 13, Fig. 32-8). Folds and faults that suggest northwest-southeast compression developed west of the Cuyamaca–Laguna Mountains shear zone during, and/or following, the last stages of westward thrusting in that zone (V. R. Todd, unpublished data). The youngest rocks that are involved in northwest-southeast shortening are plutons of Granite Mountain and La Posta type, one of which has nearly concordant hornblende and biotite K-Ar ages of 103 and 101 m.y., respectively. The relations above suggest that sometime between 102 and 98 m.y.p.b., shortening in this region changed from a direction approximately normal to the continental margin to one that was subparallel to it.

Uplift and erosion began in the western part of the batholith while the younger group of plutons was being emplaced (Gastil *et al.*, 1981; no. 14, Fig. 32-8). In the northern Santa Ana Mountains, the oldest postbatholithic marine deposits are late Turonian (Schoellhamer *et al.*, 1981), while to the south in San Diego County, postbatholithic continental deposition preceded Campanian marine deposition (Kennedy and Peterson, 1975). In northern Baja California, marine deposition was also taking place in Late Cretaceous time, just a few m.y. after intrusion of 90-m.y.-old plutons (Silver *et al.*, 1979).

Sometime between 97 and 62 m.y., the eastern Peninsular Ranges mylonite zone

developed in the eastern part of the batholith (no. 15, Fig. 32-8). The zone cuts miogeoclinal wallrocks and plutonic rocks, the latter probably equivalent to the late-to post-tectonic intrusive sequence of the southern part of the study area. In parts of the eastern Peninsular Ranges, deformation was contemporaneous with intrusion, high-grade metamorphism, and anatexis. Although the structure of the mylonite zone is complex (Fig. 32-7), its overall geometry and fabrics are similar to those of the older Cuyamaca-Laguna Mountains shear zone with the exception that foliation in the younger shear zone dips less steeply than that in the older shear zone. Shear-sense indicators in the mylonite zone, the pervasive down-dip lineation, and the development of anatexites in the metasedimentary rocks that overlie the mylonite zone, suggest that the eastern side was thrust over the western side (A. E. J. Engel and Schultejann, 1984; Erskine, 1986a). The amount of shortening across the mylonite zone has been estimated to be on the order of 50–100 km (A. E. J. Engel and C. G. Engel, 1982; Silver, 1982, 1983). North-northwest-directed thrusting and tectonic transport are interpreted to have overlapped with, and followed, Late Cretaceous westward thrusting in parts of the eastern Peninsular Ranges mylonite zone (A. E. J. Engel and Schultejann, 1984). A problem with this interpretation is that the linear tectonic elements attributed by these authors to north-northwest tectonic transport are collinear with the east-northeast mylonitic linear fabric elements that are generally considered to have formed during westward tectonic transport (Erskine, 1986c).

In its early stages, the relatively deep-seated Peninsular Ranges mylonite zone probably graded upward into a low-angle fault system. At some time prior to 62 m.y., the mylonite zone began to be displaced by low-angle faults that juxtaposed different structural levels of the mylonitic terrane (no. 16, Fig. 32-8). This transition from ductile mylonitic deformation to brittle low-angle faulting probably accompanied uplift and unroofing of the eastern part of the batholith in the latest Cretaceous and early Tertiary (no. 17, Fig. 32-8). The oldest low-angle faults were probably west-directed thrusts (Erskine, 1986a, c). Uplift continued and by late Paleogene time the region was undergoing extension (no. 18, Fig. 32-8). Low-angle normal faults displaced rocks eastward and structurally downward against high-grade metamorphic rocks of the mylonite zone (Dickinson, 1981; A. E. J. Engel and Schultejann, 1984). These Late Cretaceous and Paleogene structures were displaced and reactivated by the Neogene Gulf of California-San Andreas rift-transform system.

ALFRED O. WOODFORD — *Pomona College, Claremont, California 91711*
JOHN S. SHELTON — *Encyclopedia Britannica Films, Inc., 6519 Fountain Ave., Hollywood, California 90028*
DONALD O. DOEHRING — *Department of Geology, University of Massachusetts, Amherst, Massachusetts 01002*
RICHARD K. MORTON — *Eastern Municipal Water District, P. O. Box 248, Hemet, California 92343*

Pliocene-Pleistocene History of the Perris Block, Southern California

ABSTRACT

The Perris Block, 30 to 90 mi southeast of Los Angeles, is an eroded mass of Cretaceous and older crystalline rock, sculptured by six erosion surfaces. Two are narrow valley systems and the other four nearly horizontal planes or remnants thereof. The oldest surface is a bowl and narrow valley system with its base at an elevation of 1,100 to 1,400 ft; it is partially filled with alluvium which has yielded a lower Pliocene (Clarendonian) mammalian fauna. It was probably warped slightly before any of the younger surfaces were cut. The nearly horizontal erosion surfaces, listed in the proposed order of their formation, are now at elevations of approximately 1,700, 2,500, 2,100, and 1,500 ft and are thought to be in quasi equilibrium with the present major drainage systems. The second narrow valley system has a base near sea level; it was probably formed just after the 1,700 ft horizontal surface.

The Perris Block lies between the Los Angeles Basin and the lofty San Jacinto Mountains. The latter are marked by an elevated, low-gradient valley system. During Pliocene and Pleistocene time the Los Angeles Basin sank many thousands of feet, the San Jacinto Mountains rose considerably, and the Perris Block oscillated vertically. The vertical tectonics must have been governed by deep horizontal flow, isostatic in nature, and related to the somewhat greater flow-couple indicated by right-lateral strike-slip faulting on the San Jacinto fault system.

INTRODUCTION

The Perris Block, a mass of moderately high land 30 to 90 mi southeast of Los Angeles, is composed chiefly of crystalline rocks of Cretaceous and earlier ages. Thin sedimentary and volcanic units mantle the crystalline rocks in a few places. Two of these units have been determined to be early Pliocene in age from paleontologic and radiometric data. The datum horizons fix in time a Pliocene-Pleistocene succession of episodes of erosion and sedimentation. We present first the observed data, then we discuss the implications of relative age inherent in the data, the relation of the block to the Los Angeles Basin, the local Pliocene-Pleistocene geologic history, and the place of the block in its late Cenozoic environment.

The Perris Block was defined by English (1926) as the mass between the San Jacinto and Elsinore-Chino fault zones, bounded on the north by the "San Gabriel" (Cucamonga) Fault (Fig. 1). The southern and southeastern boundaries of the block, which are vague, were left undefined by English. We use an approximate southern boundary against the Temecula and other small basins, determined by a rather complex group of faults that extends southeast from Murrieta (Fig. 2). We also use a doubtfully faulted eastern boundary along Wilson Creek, at about 116° 50′ W. long. The highest point in the block thus defined is Red Mountain (Fig. 2), 4,573 ft, in the southeast, and the lowest point is at 530 ft on the Santa Ana River north of Corona. The climate of the block is semi-arid with a typical annual rainfall of 13 in. The Santa Ana River, which rises in the high, relatively humid San Bernardino Mountains, flows southwest across the northwest end of the block (Fig. 1). The San Jacinto River has its headwaters in the high and relatively humid but smaller San Jacinto Moutains. It flows southwest across the central part of the block and empties into Lake Elsinore, a sink in the Elsinore fault zone. In 1862, 1884, and 1916 to 1917, this lake overflowed into Temescal Creek, which follows a structural and topographic low along the Elsinore fault zone northwest to the Santa Ana River. The southern part of the Perris Block drains into Temecula Creek (Santa Margarita River) and through the mountains to the sea.

The crystalline bedrock complex includes

metamorphosed siliceous sedimentary rocks, metavolcanic rocks, and intrusive mid-Cretaceous plutons (Dudley, 1935; Larsen, 1948). Local superjacent (and adjacent), slightly consolidated, valley-filling continental sediments are in part lower Pliocene (Fig. 3, CD; Proctor, 1961; Proctor and Downs, 1963), in part Pleistocene (Frick, 1921; Merrill, 1963). Details of superjacent and bedrock geology have been mapped by Henderson and Aultman (1934), Jenney (1968), and Morton (1969).

An important unit in the southwest is the Santa Rosa Basalt (Mann, 1955). This flat-lying lava caps the Hogbacks, on the Perris Block northeast of Murrieta, and also covers the much more extensive Mesa de Burro and other high-standing mesas southwest of the block. Locally, the lowest member of the lava sequence is an alkali basalt that is lower Pliocene by potassium-argon measurement (Hawkins, 1970).

The Perris Block is sculptured by erosion surfaces at several levels (Table 1). The most striking surface is the top of the 2,100 ft Gavilan plateau, cut across varied plutonic and metamorphic rocks, and separated from the surrounding lower areas by scarps. The few residual steep-sided peaks that surmount the plateau yield runoff that is wholly inadequate for the erosion of the broad flat surface. Other erosion surfaces on the block were even more clearly formed under circumstances different from those that now prevail. Study of the relations of all the surfaces leads, step by step, to the recognition of a series of geomorphic events and the historical order in which they occurred. One surface is older than the lower Pliocene sediments, another is later than these sediments but older than the overlying Pliocene basalt, and so on. The present coexistence of all the surfaces, now in part protected by overlying sediments or lava, but mostly exposed as a composite surface in quasi equilibrium, does not prevent the recognition of an age series.

The early geomorphic work in the region was done by Sauer (1929) and Dudley (1936) at a time when the models of W. M. Davis and Walther Penck were dominant. Dudley used a Davisian approach to the study of the Perris Block, while Sauer's work in a nearby part of the Peninsular Ranges was Penckian. Wahrhaftig (1965) studied local erosion surfaces on quartz plutonites in the Sierra Nevada of California. He hypothesized that the surfaces originate from local base levels which are established by retarded weathering-erosion rates of exposed bedrock. He also speculated that the mechanism may be applicable to the Peninsular Ranges as described by Sauer. Our methodology and results follow no single model but constitute a synthesis of concepts originating with Davis, Gilbert (1877), and Wahrhaftig (1965). We follow practically all other students of semi-arid geomorphology in recognizing the existence of steep-sided residual mountains that project above the level of an erosional-depositional plain, but we leave these features unexplained. Our conclusions are close to those of Dudley (1936), with modifications and additions based largely on the work of Bean (1955) and Proctor (1961).

Table 1. Erosion Surfaces of the Perris Block, in the Order of Their Formation, with the Oldest at the Bottom

Paloma Surface	Approx 1,500 ft elev
Gavilan-Lakeview Surface	Approx 2,100 ft elev
Magee Surface	Approx 2,500 ft elev
Deep valley Surface	Base near 500 ft elev
Perris Surface	Approx 1,700 ft elev
Bowl and narrow valley Surface	Base near 1,100–1,400 ft elev

On the central part of the Perris Block we find evidence of repeated changes of local or general base level, without intra-block faulting or general tilting. Rejuvenation no doubt at first affected chiefly the trunk streams, whose gradients were markedly increased, probably beginning at or near the downstream edges of the block. At somewhat later stages, most streams attained nearly stable compound long profiles in quasi equilibrium[1], with alternate convexities and concavities, so that extensive areas continued to develop under the conditions that prevailed before the change of base level. Some erosion surfaces on bedrock have been buried by alluvium and later exhumed. Relics of old surfaces on bedrock have long persisted, even though they are constantly reduced in area and are fated to disappear if a single base level lasts long enough. An extreme contrast exists between the short life, in years, of a constructional or erosional surface on unconsolidated alluvium (or deeply weathered bedrock) and the long life of an erosional surface on unweathered crystalline bedrock.

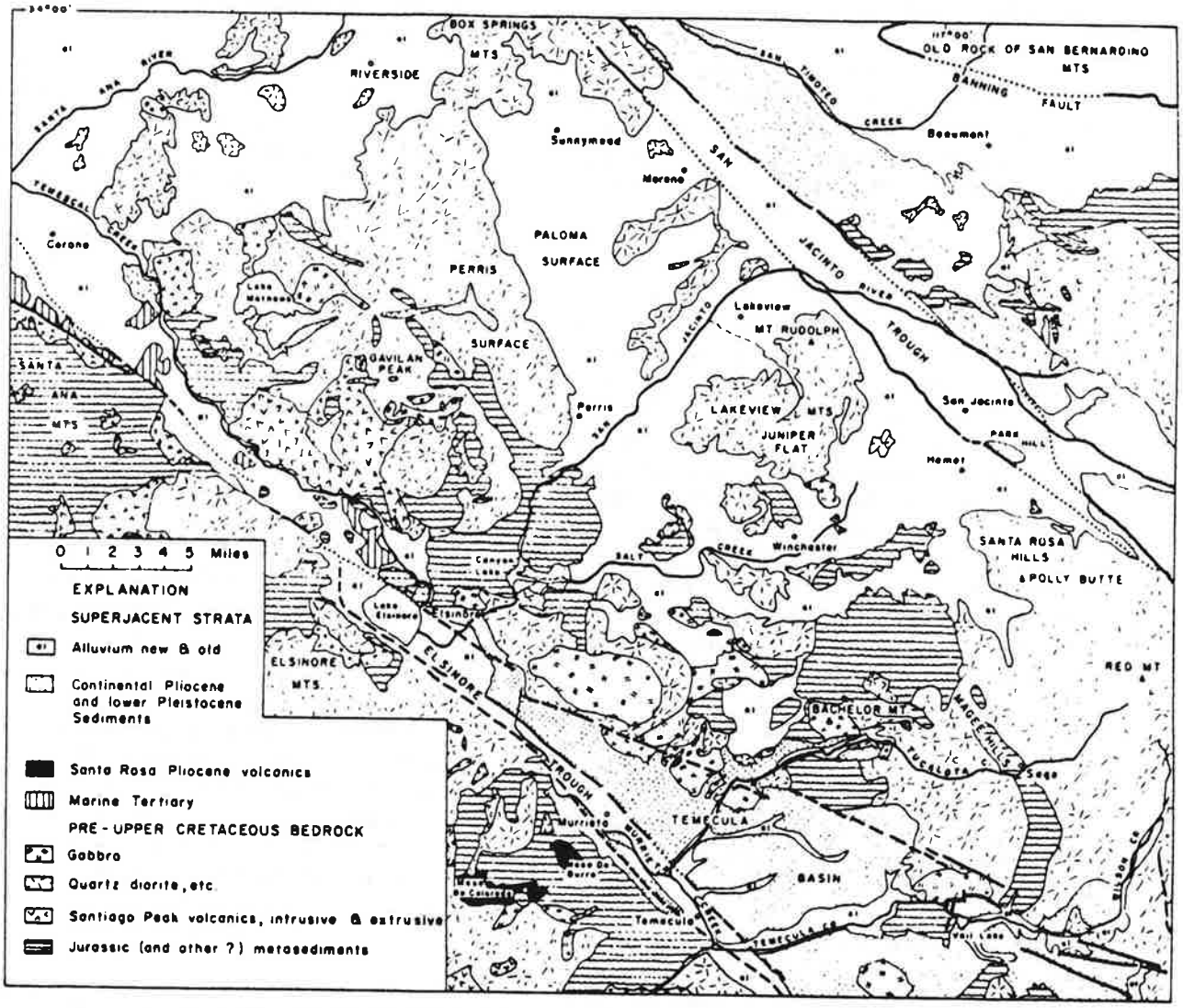

Figure 2. Geologic map central and southern parts of the Perris Block (modified *from* Rogers, 1965).

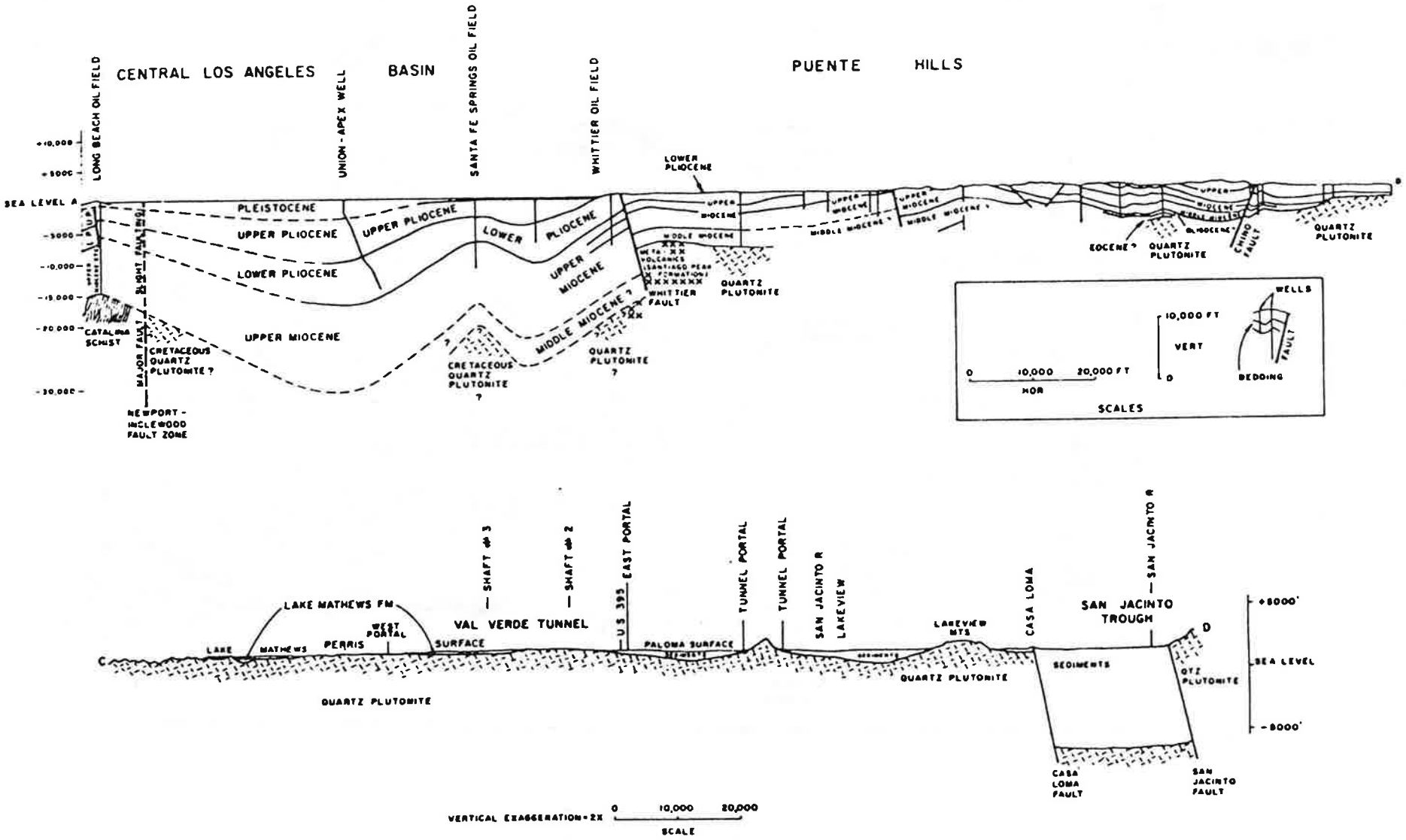

Figure 3. Structure sections. AB, Los Angeles Basin, including Puente Hills; CD, Perris Block. AB *after* Durham and Yerkes (1964), Yerkes and others (1965) and unpublished sources. For east dip of Casa Loma fault *see* Proctor (1962).

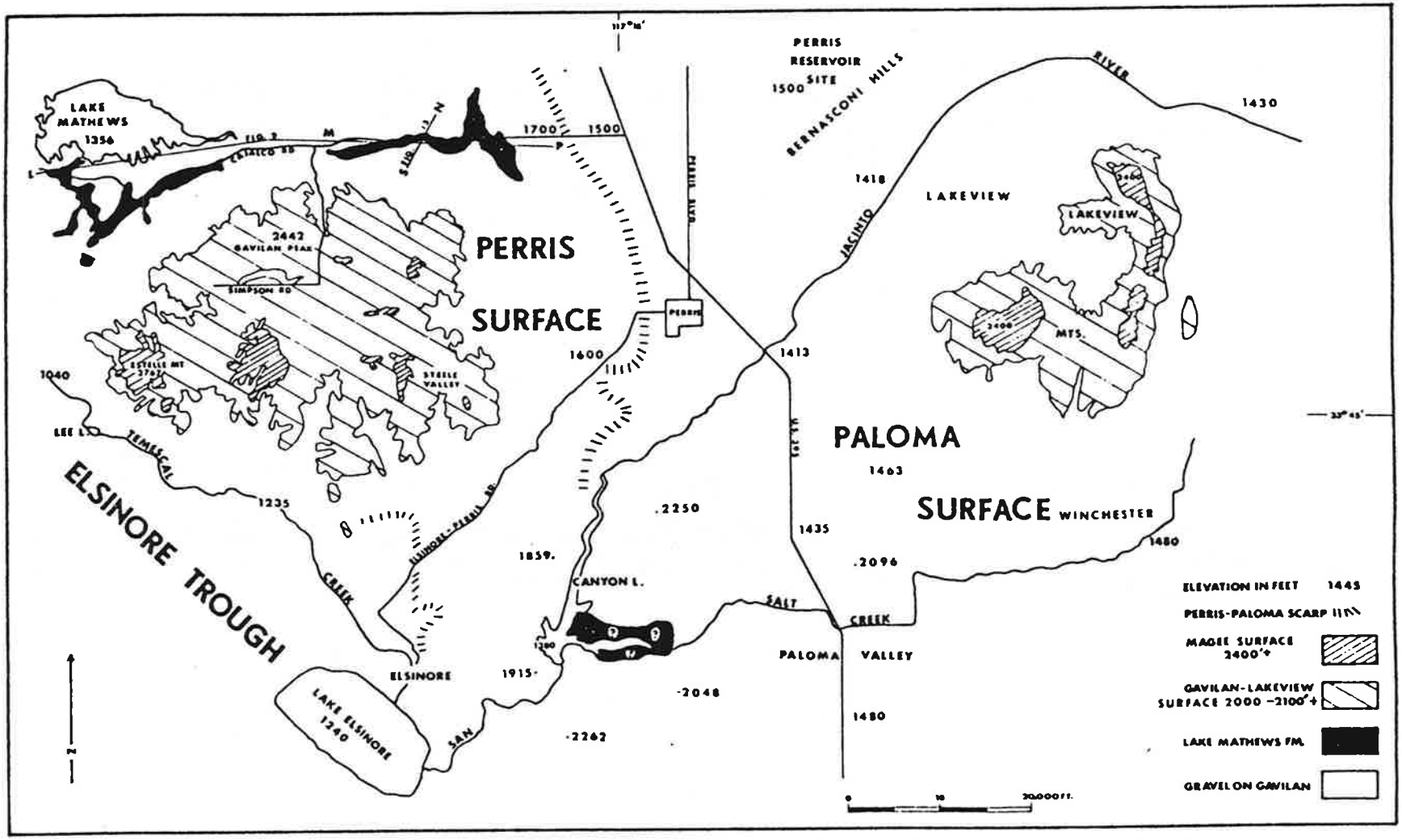

Figure 4. Map of the central part of the Perris Block, showing the distribution of the Lake Mathews Formation (lower Pliocene), Gavilan-Lakeview and Magee Surfaces, and the locations of Figures 5 (LMP) and 6 (SN). Spot elevations on the Paloma surface are between 1,400 and 1,500 ft; higher points in the Paloma area (1859, 2250, 2096, and so forth) are monadnocks and other projecting peaks.

ORIGINAL ELEVATIONS OF SURFACES

Quasi equilibrium of stream gradients, with local base levels, makes difficult the determination of the original elevations of old surfaces. The Paloma Surface, however, is forming today, mostly at elevations of 1,400 to 1,600 ft. The early Pliocene(?) bowl and valley probably had floors within 300 or 400 ft of sea level, as the valley floor gradient was flat, and the probably contemporary sea reached a point 4 or 5 mi west of Lake Mathews (Gray, 1961, p. 36). The Perris Surface, surely early Pliocene, may have formed at similar low elevations above sea level. The Gavilan-Lakeview Surface was probably originally nearly horizontal, as flat as the major part of the Paloma Surface is today. Its drainage may have discharged into an embayment of the Pleistocene sea at the Coyote Hills in the east-central Los Angeles Basin, 30 mi west of the Gavilan (compare Hoskins, 1954). A Gavilan-Lakeview trunk stream, even if it followed a route as devious as the present course of Temescal Creek and Santa Ana River, probably had a fall, from the Gavilan to the sea, of 1,000 ft or less. We do not dare to hazard guesses as to the original elevations of the Magee or deep valley surfaces.

PLIOCENE-PLEISTOCENE GEOLOGIC HISTORY

Early in the Pliocene, some 10 m.y. ago (compare Evernden and others, 1964), the Los Angeles Basin was mostly rather deep sea, probably between 2,500 and 4,000 ft deep. This sea shoaled at its eastern edge, and became very shallow marine in the Elsinore Trough, 5 mi southeast of Corona and just north of Bedford Wash (near C, west of Lake Mathews, in Fig. 1; *see* Gray, 1961). This locality was probably in an embayment, behind the slowly rising peninsula of the Santa Ana Mountains, which projected into the Los Angeles Basin from the southeast. The crest of the incipient Santa Ana Mountains may not have exposed any rocks older than early Cenozoic. East of Temescal Canyon, continental deposition was going on in the Lake Mathews bowl and in a narrow channel that extended eastward from the south side of the bowl (Figs. 4, 5, and 6).

The Perris Surface developed slightly later in the Pliocene. It was probably more widespread than its surviving representatives, and may have covered the greater part of the Perris Block, including most of the area now occupied by the Paloma Surface (Fig. 4). Relics are left 5 mi southeast of Perris and at Quail Valley between the arms of Canyon Lake (Fig. 16). Some southwest-sloping barbed tributaries of the deep valley system at and near the Perris Reservoir site are probably deepened relics of the upper courses of parts of the Perris Surface drainage.

The Perris Surface extended far to the southwest, across what is now the Elsinore Trough. The Santa Rosa basalts spread over the southern part of the surface, from the Hogbacks northeast of Murrieta southwest to Mesa de Burro, Mesa de Colorado, and other mesas. Since the age of the basal basalt is about 8.3 m.y., the more widespread overlying members are no doubt about 7 or 8 m.y. old and the underlying Perris Surface about 9 m.y. old.

The drainage on the Perris Surface may have been concentrated in two principal systems, a northern ancestral San Jacinto River and a southern Murrieta River. We can speculate about details of the San Jacinto River's history,

but at this time we are in doubt as to the history of the Murrieta River.

The ancestral San Jacinto River in early Pliocene time probably received drainage from both the ancestral San Jacinto Mountains and more northern sources. The San Jacinto Mountains were probably located, with respect to the Perris Block, 11 mi northwest of their present position (Fig. 1). H. D. English (1953) found 11-mi right-lateral offsets on the San Jacinto fault for both the lower Pliocene Mt. Eden Formation and the lower Pleistocene San Timoteo Formation. This offset is roughly consistent with the post–middle Cretaceous offset of 15 mi found much farther south on the San Jacinto fault zone by Sharp (1967) and the 18-mi reinterpretation of Sharp's data by Bartholomew (1970). Bartholomew suggested that 10 mi of offset has occurred since the late Pleistocene.

The early Pliocene drainage probably flowed onto the Perris Block from the northeast in three main branches. The northern branch may have cut the Moreno gap to the level of the Perris Surface, the central branch may have cut the gap at Lakeview, and the southern branch may have cut the Hemet-Winchester (Salt Creek) gap. The northern and central branches may have joined on the Perris Surface above the present site of Perris, and the combined stream may have followed approximately the line of the Perris-Elsinore road to a junction with the southern branch, which had passed through the gap now occupied by the east arm of Canyon Lake (Fig. 4).

The cutting of the Moreno, Lakeview, and Hemet-Winchester gaps to the level of the Perris Surface, and a combination of other events, made possible the cutting of the deep valley system of the northeastern part of the Perris Block (Fig. 8). Other significant events were the strike-slip fault movement of the San Jacinto Mountains to a more southeastern position, the faulting and fault-block depression that produced the San Jacinto Trough, and the diversion of the northern drainage. After these events, the only considerable source of water flowing over the northeastern Perris Block was from the San Jacinto Mountains, which had already reached a position that was largely southeast of the San Jacinto Trough. The water mostly entered the Trough at its southeast corner, in an ancestral San Jacinto River. In deep-valley time, subsidence of the trough must have been checked, so that the river piled upon the graben surface a narrow and rather steep cone of alluvium 12 or more mi long and 2 to 5 mi wide. The fanhead at the southeast corner of the graben must have been high, corresponding to a present elevation of at least 1,700 ft; the toe, at the northwest, was probably below 500 ft. The river, wandering on its fan, at times discharged into the beheaded Hemet-Winchester stream valley. This valley must have been blocked at Canyon Lake, perhaps by volcanic debris, now removed by erosion. This debris may have come from cinder cones related to the Santa Rosa lavas, or from the same sources as the siliceous tuffs widespread in the lower Pliocene of the Los Angeles Basin (Wissler, 1943, p. 216). The volcanic vents have not been located; they may be hidden by alluvium. Alternatively, the west-flowing drainage may have been interrupted by minor faulting west of Canyon Lake or by a north-south upwarp. In one way or another, the Hemet-Winchester stream was diverted northward east of Canyon Lake, and followed either the Lakeview or the Moreno course back to the San Jacinto Trough. In this way, the deep valleys were cut. Perhaps the return to the trough was at first through the Lakeview gap; later, when that exit had been dammed by the rising surface of the growing fan in the trough, the deep valley through Moreno was cut.

The hypothetical fan and gorge system of the ancestral San Jacinto River has rather remotely similar modern analogs in and near San Antonio fan, at the northwest corner of the Perris Block in the vicinity of Pomona and Claremont (Eckis, 1928; Eckis and Gross, 1934). San Antonio fan has a north-south length of 17 mi, a 2,100-ft elevation at its head, and a 500-ft elevation at its toe; it has a distributary, San Jose Creek, that cuts west through a rocky gorge somewhat similar to the gorges of the deep-valley system. San Jose gorge, however, is cut mostly in Miocene sediments of the Los Angeles Basin's east side, and discharges into San Gabriel River at a level below that of the San Antonio fan.

In deep-valley time, a lake may have existed at least temporarily at the north end of the San Jacinto Trough. It may possibly have been, at times, an enclosed playa, but more probably it discharged continuously northwest, either along the line of San Timoteo Creek, north of Riverside, to the Santa Ana River, or northeast around the San Jacinto Mountains into Salton Trough. Sediments of this age are not known in the San Timoteo badlands, through which the discharge must have gone; the time may be represented by a lacuna in the badland sedi-

ments, as an unconformity was found in those sediments by English (1953).

Next, probably in late Pliocene time, somewhat more than 3 m.y. ago, the deep valley system was filled, and the whole central and northern parts of the Perris Block were covered by a blanket of alluvium that rose to the Gavilan-Lakeview level and perhaps to the Magee level. The evidence for the lost alluvial fill is chiefly the superposition of the San Jacinto River, previously described.

The Magee Surface may have been cut in earliest Pleistocene time, beginning some 3 m.y. ago. The Gavilan-Lakeview Surface may have developed in mid-Pleistocene time, 2.5 to 1.5 m.y. ago. At the end of that time, just before the downcutting began that led to the superposition of the San Jacinto River, that river must have had about its present course. Farther north, the Gavilan-Lakeview Surface shows the presence of at least one other trunk stream, perhaps flowing northwest from the Gavilan and joining the Santa Ana River between Riverside and Corona (Fig. 2).

During Pleistocene time, most of the mantle of Pliocene sediments and volcanics was removed from the Perris Block by erosion. Some of the basalt debris was deposited in the Temecula Arkose of the Temecula Basin (Mann, 1955; dated as earliest Pleistocene Villafranchian by Merrill, 1963, and Seay, 1964), but much of it was probably carried out of the region by the Temecula–Santa Margarita River and more northern streams. Finally, the Paloma and other new portions of the present compound surface were formed. Erosion to the Paloma level was mostly in areas of alluvial fill, but moderate sized areas of the Perris Surface were probably destroyed at this time. One such area of Perris Surface was probably above Paloma Valley and extended south to the lava-capped Hogbacks near Murrieta.

STRUCTURAL ENVIRONMENT OF THE PERRIS BLOCK

The Perris Block is probably bounded everywhere by fault zones, but at the south and southeast the displacements on the faults are small, probably only hundreds or a few thousands of feet. That is, Perris Block belongs structurally with the mountainous Peninsular Ranges to the southeast, between the Elsinore and San Jacinto fault zones.

Right-lateral strike slip, almost everywhere accompanied by smaller dip slip, characterizes the fault zones that bound the blocks. Strike slip on the San Jacinto fault zone has been 15 to 18 mi since the mid-Cretaceous (Sharp, 1967; Bartholomew, 1970); most of this movement may be post-Pliocene, as indicated above. Post-Miocene right-lateral movement on the Elsinore-Whittier-Chino fault zone has been much less, probably not over 3 mi at most, dying out to the north. Farther west in the Los Angeles Basin, some right-lateral movement, probably totaling several thousand feet, has occurred in the Pliocene, Pleistocene, and Holocene along the Newport-Inglewood zone. Significantly greater movements cannot have taken place in the Los Angles Basin, for numerous local sedimentary units, including several tuff beds, can be correlated across the fault zone.

The Perris Block has been repeatedly uplifted, and occasionally depressed, since the beginning of Pliocene time. The net uplift has been only a thousand feet or so, much less than the many thousands of feet of uplift undergone by adjacent mountain masses, notably the San Jacinto range (Fraser, 1931, p. 538-540). Other nearby areas, notably the central part of the Los Angeles Basin, have been depressed tens of thousands of feet. All these vertical tectonic changes must have been accompanied by sub-crustal movements in more or less horizontal directions. The subcrustal adjustments must have been deep; they did not result in southwest-northeast horizontal movements sufficiently large and shallow to be detected by surface observations or by borings. The adjustments were probably chiefly isostatic. The deep isostatic flow must have been integrated with the somewhat greater post-Pliocene flow indicated by right-lateral strike slip on the San Jacinto fault system.

Sonora, Mexico, source for the Eocene Poway Conglomerate of southern California

Patrick L. Abbott
Department of Geological Sciences, San Diego State University
San Diego, California 92182
T. E. Smith
Department of Geology, University of Windsor
Windsor, Ontario N9B 3P4, Canada

ABSTRACT

Alluvial-fan conglomerates of the Eocene Poway Group are composed largely of exotic rhyolite and dacite clasts derived from far to the east of their Eocene depositional site. Remnants of the Upper Jurassic bedrock source of the Poway rhyolite clasts may yet be exposed in hills in Sonora, Mexico. For this study, pieces of bedrock were taken from hills 13 km west of El Plomo in Sonora. Clasts texturally and mineralogically similar to the Sonoran bedrock were collected from the apex of the Eocene alluvial fan in San Diego County, California. Nine couplets of bedrock and conglomerate clast samples (textural twins) were analyzed for 16 trace elements selected for their wide range of behaviors during magmatic and alteration processes.

Statistical comparisons of the trace-element data, by using the standard error-of-the-difference method, show that there are no significant differences between the two populations. These data strongly suggest that the rhyolitic bedrock hills west of El Plomo were part of the source terrane for the Eocene conglomerate in San Diego. The latitudinal separation between bedrock source and the site of deposition is only the 2° created by the opening of the Gulf of California. This implies that any boundary separating a paleomagnetically defined, Baja-Borderland terrane from the craton since Eocene time was at least 100 km east of the Gulf of California in northernmost Sonora.

INTRODUCTION

In the late 1970s, samples of rhyolitic bedrock and conglomerate were gathered in Sonora, Mexico, and rhyolitic conglomerate clasts were collected from Eocene formations in California and Baja California. The trace-element chemical compositions of these samples were determined for nine elements (Zr, Y, Cr, Sr, Rb, Zn, Ba, Mn, Ti) and were compared statistically by using the standard error-of-the-difference technique (Abbott and Smith, 1978). The data indicated two correlations. One was between source rocks collected in Sonora and conglomerate clasts from the Eocene Poway Group in San Diego, California (Fig. 1). A second and more compelling correlation emerged between these same alluvial-fan conglomerates of the Poway Group on mainland California and the coeval submarine-fan conglomerates of the Jolla Vieja Formation on Santa Cruz Island (Fig. 1).

The same statistical study of trace-element compositions showed that rhyolitic clasts from coeval conglomerates in the basal Sespe Formation of the Santa Ana Mountains and the Las Palmas Gravels of Baja California were not related to the Sonoran bedrock, to the Poway or Jolla Vieja Formations, or to each other. Thus, trace-element geochemistry served to discriminate between rhyolitic clasts in coeval conglomerates in adjoining areas and to define an east-west–oriented piercing point formed by west-directed Eocene fluvial-alluvial-fan–submarine-canyon–submarine-fan systems that have undergone two major offsets since their deposition (Abbott and Smith, 1978). The sedimentary system apparently has been separated to the northwest from its source terrane by the opening of the Gulf of California, and the submarine depositional systems seem certain have been dismembered from their terrestrial system supplier by right-lateral faulting located offshore in the southern California continental borderland.

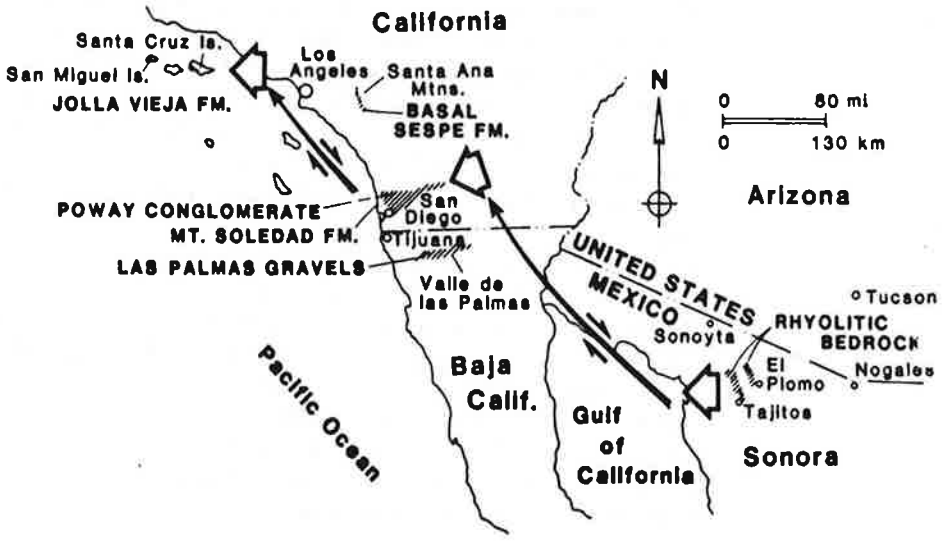

Figure 1. Location map. Three large arrows represent dismembered segments of east-west-oriented piercing point created by bedrock-fluvial-alluvial-fan-submarine-canyon-submarine-fan depositional system.

Recent paleomagnetic data have spawned new hypotheses on the latitudinal locations of source rocks and sedimentary deposits. For example, Champion et al. (1986) have used paleomagnetic data from Cretaceous and Eocene strata of the Californias to track a northward translation of Baja California in excess of 1000 km. Their data indicate that during Eocene time the Poway Conglomerate would have been deposited at about lat 17°N, while the equivalent part of cratonal North America (i.e., Sonoran source rocks) would have been at about lat 35°N.

The relation between the Baja California–southern California area and mainland North America was addressed by Hagstrum et al. (1987) in another paleomagnetism-based study. They stated that 9° of northward translation of the Californias block has occurred since Late Cretaceous and before early Miocene time. Hagstrum et al. cited the paleomagnetic data of Bobier and Robin (1983) on 102 to 45 Ma basement rocks near Mazatlan, Sinaloa, that appear to have traveled northward with Baja California, thus placing the eastern bounding faults well east of the Gulf of California and within mainland Mexico.

The large northward translation of the C lifornias indicated by paleomagnetic data may ot be congruent with our geologic correlation (Abbott and Smith, 1978). In an attempt to strengthen the geologic correlation between he Eocene Poway Conglomerate and rhyolitic ed rock in Sonora, a new suite of samples was col lected from a 7 × 1 km string of bedrock hi ir Sonora. The samples have been analyzed f a wider range of trace elements than in the origi nal study and then compared statistically.

Late Cretaceous juxtaposition of metamorphic terranes in the southeastern San Gabriel Mountains, California

DANIEL J. MAY* *Department of Geological Sciences, University of California at Santa Barbara, Santa Barbara, California 93106*
NICHOLAS W. WALKER *Department of Geological Sciences, University of Texas at Austin, Austin, Texas 78713*

ABSTRACT

New structural, petrological, and geochronological data from the southeastern San Gabriel Mountains define the amalgamation history of suspect terranes in this region. Four metamorphic terranes constitute the area—the Cucamonga, San Antonio, San Gabriel, and Baldy terranes—and were juxtaposed in two discrete episodes during the Late Cretaceous.

The Cucamonga, San Antonio, and San Gabriel terranes were juxtaposed along subparallel, east-west–trending, left-lateral mylonitic fault zones during the first episode. The Cucamonga terrane consists of Lower Cretaceous granulite-facies gneissic rocks. These rocks were intruded in the Late Cretaceous by granitic rocks as the Cucamonga terrane was faulted ductilely against the southern margin of the San Antonio terrane. Mylonitized units were subjected concurrently to retrograde amphibolite-facies metamorphism. Metasedimentary pendants in the San Antonio terrane were metamorphosed under upper-amphibolite–facies conditions as plutonic rocks were emplaced syntectonically. Along its northern boundary, the San Antonio terrane was juxtaposed concurrently against the San Gabriel terrane, a terrane consisting of Precambrian gneiss and Precambrian and Mesozoic intrusive rocks. The boundary is represented by the Middle Fork Complex, a ductile zone intermingling rocks of the two terranes.

After palinspastic restoration of local Cenozoic fault displacements, the left-lateral mylonitic fault zones separating the terranes appear as parts of a major sinistral transform system along the southern margin of the San Gabriel Mountains. Displacement for each of the mylonitic fault zones was approximately several tens of kilometers and was part of a broad left-lateral shear system. This system is modeled as a lateral ramp or tear fault to a west-directed, synplutonic, ductile thrust system underlying the San Gabriel terrane. Crosscutting syn- and post-tectonic intrusives indicate that most of the displacement occurred between ~88 and 78 m.y. ago. No lithologic, isotopic, or structural data support previous assertions that these terranes were accreted to North America during the Tertiary.

The Late Cretaceous synplutonic juxtaposition of the Cucamonga, San Antonio, and San Gabriel terranes was followed by underthrusting of oceanic rocks of the Baldy terrane (that is, Pelona Schist) along the Vincent thrust. Precise timing of this episode is as yet uncertain.

*Present address: Geology Department, Victoria University, P.O. Box 600, Wellington, New Zealand.

INTRODUCTION

The Mesozoic and Cenozoic geologic history of southern California contains the record of a convergent and transform continental plate margin. One aspect of this history has been the production of a chaotic assemblage of basement and sedimentary terranes for which the geologic relationships are poorly understood. Uncertainty in the paleogeographic setting of some of these terranes has led to their being labeled "suspect terranes" (Coney and others, 1980). The place of origin and timing and mechanism of accretion of many of these suspect terranes have not been established, but there is a growing body of geologic, geochemical, and geochronologic evidence which suggests that at least some of them are parautochthonous fragments locally displaced along the continental margin (Silver and Mattinson, 1986; Seiders and Blome, 1988). Such evidence contradicts the interpretation of paleomagnetic data from several of these terranes as indicative of formation at low latitudes and accretion to North America as exotic blocks (Champion and others, 1984, 1986; Fry and others, 1985; Hagstrum and others, 1985, 1987; Morris and others, 1986).

The San Gabriel Mountains are an excellent setting in which to examine several suspect terranes and their boundaries and investigate their origin. Preliminary terrane maps define two suspect terranes for this area—the Tujunga and Baldy terranes (Blake and others, 1982). The Tujunga terrane is a composite crystalline terrane exposed in the hanging wall of the major regional thrust system that juxtaposed it above the Baldy terrane. Together, these terranes form part of a much larger composite terrane, the Santa Lucia–Orocopia allochthon, interpreted to have been accreted to the southern California region in the latest Paleocene or Eocene (Vedder and others, 1983; Champion and others, 1984).

Dibblee (1982) described several smaller terranes within the composite Tujunga terrane in the San Gabriel Mountains (Fig. 1). Three of these are well exposed in the southeastern portion of the range: the Cucamonga, San Antonio, and San Gabriel terranes. These terranes each contain regionally metamorphosed rocks that were derived from different protoliths and/or have different geologic histories. Each also contains lithologically similar Cretaceous intrusive units. Another unit, the Middle Fork Complex, is described for the first time in this paper as a structurally complex formation with lithologic affinities to both the San Antonio and San Gabriel terranes.

Superimposed on these lithologic associations are structural domains characterized by variably developed mylonitic fabric (Fig. 2). The boundaries between terranes occur within belts of steeply dipping mylonitic rocks, including all of the strongly deformed Middle Fork Complex. Data presented herein indicate that in the Late Cretaceous, the Cucamonga, San

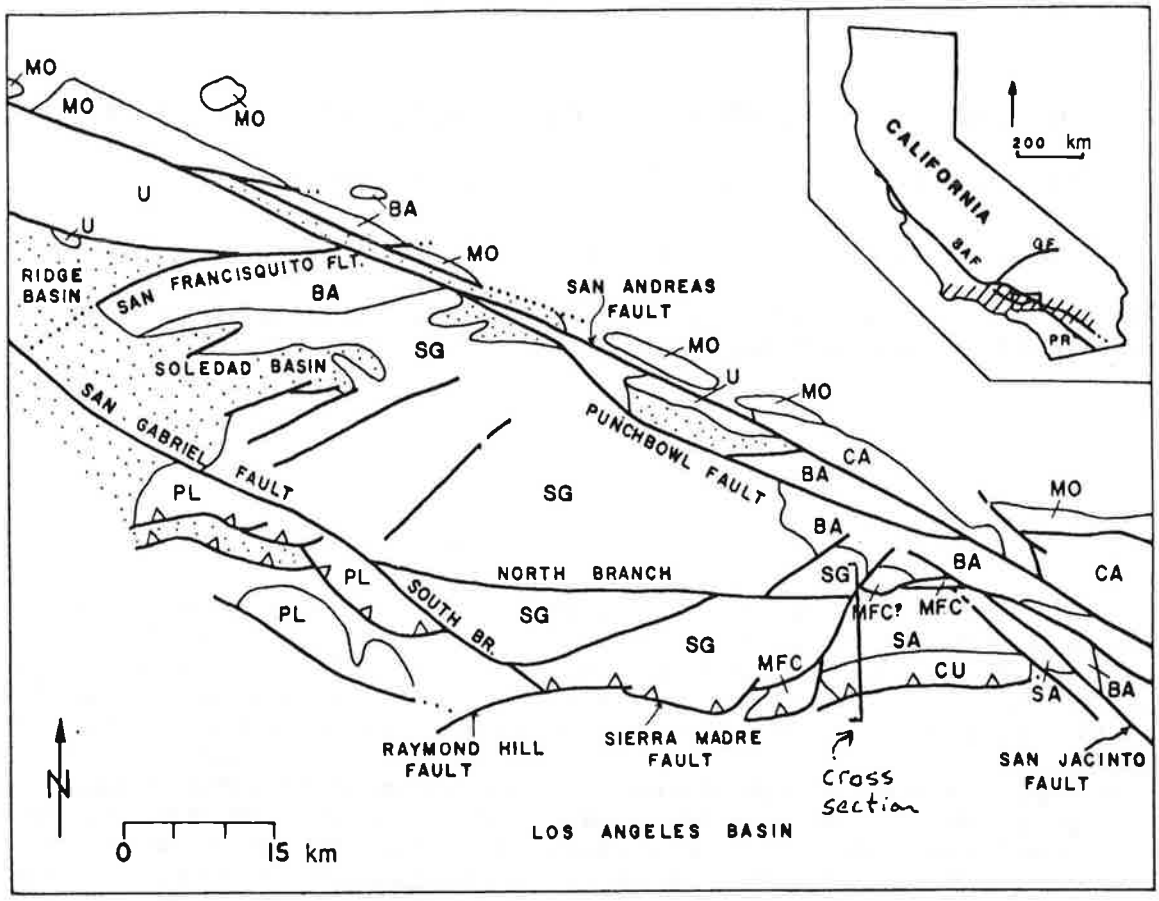

Figure 1. Basement terranes and Cenozoic faults of the San Gabriel Mountains and vicinity. Modified from Dibblee (1982). Terrane abbreviations: BA, Baldy; CA, Cajon; CU, Cucamonga; MO, Mojave; MFC, Middle Fork Complex; PL, Placerita; SA, San Antonio; SG, San Gabriel; U, undesignated. Queried where designation is uncertain. Stippled areas represent Cenozoic sedimentary rocks.

Inset map in upper right-hand corner shows location of San Gabriel Mountains in middle of Transverse Ranges province (ruled region). Abbreviations: GF, Garlock fault; PR, Peninsular Ranges; SAF, San Andreas fault.

Antonio, and San Gabriel terranes were juxtaposed along ductile faults represented by the mylonite belts (fault rock terminology after Wise and others, 1984) and simultaneously intruded by granitic plutons. Posttectonic Late Cretaceous biotite granite intrusions stitched the terranes together. The timing of this juxtaposition is summarized in the cross section and stratigraphic column of Figure 3.

This Late Cretaceous juxtaposition is the first "amalgamation" episode recognized in the San Gabriel Mountains. In the eastern Transverse Ranges, Powell (1981, 1982a) has documented a pre-Middle Jurassic thrust system that superposed the San Gabriel terrane above another crystalline terrane called the "Joshua Tree terrane"; however, no Joshua Tree terrane rocks have been identified in the San Gabriel Mountains.

Following the juxtaposition of the Cucamonga, San Antonio, and San Gabriel terranes, and posttectonic intrusion of Upper Cretaceous granite, the rocks of these terranes were superposed above the Pelona Schist of the Baldy terrane (Ehlig, 1981). The terrane boundary locally is named the "Vincent thrust" and is characterized by a thick zone of mylonitic rocks located in the hanging wall (Fig. 2). Note that all the rocks in the hanging wall of this thrust are defined as the composite Tujunga terrane. The juxtaposition of the Tujunga terrane above the Baldy terrane is the second "amalgamation" episode recognized in the San Gabriel Mountains. The Baldy and Tujunga terranes were later intruded locally by a granodiorite pluton of Miocene age.

The subsequent Neogene and Quaternary history is dominated by faulting related to the San Andreas fault system. This faulting has disrupted the original distribution of terranes and produced a cataclastic overprint on some of the mylonitic terrane boundaries (Fig. 4). Relative to the main body of the San Gabriel Mountains, the southeastern portion has been displaced northward during the late Cenozoic, between the left-slip San Antonio Canyon fault and the right-slip San Jacinto fault, from an initial position to the south of the present range front. The area currently is being uplifted by reverse faulting along the north-dipping Cucamonga fault zone at a rate greater than 3 mm/yr (Matti and others, 1985).

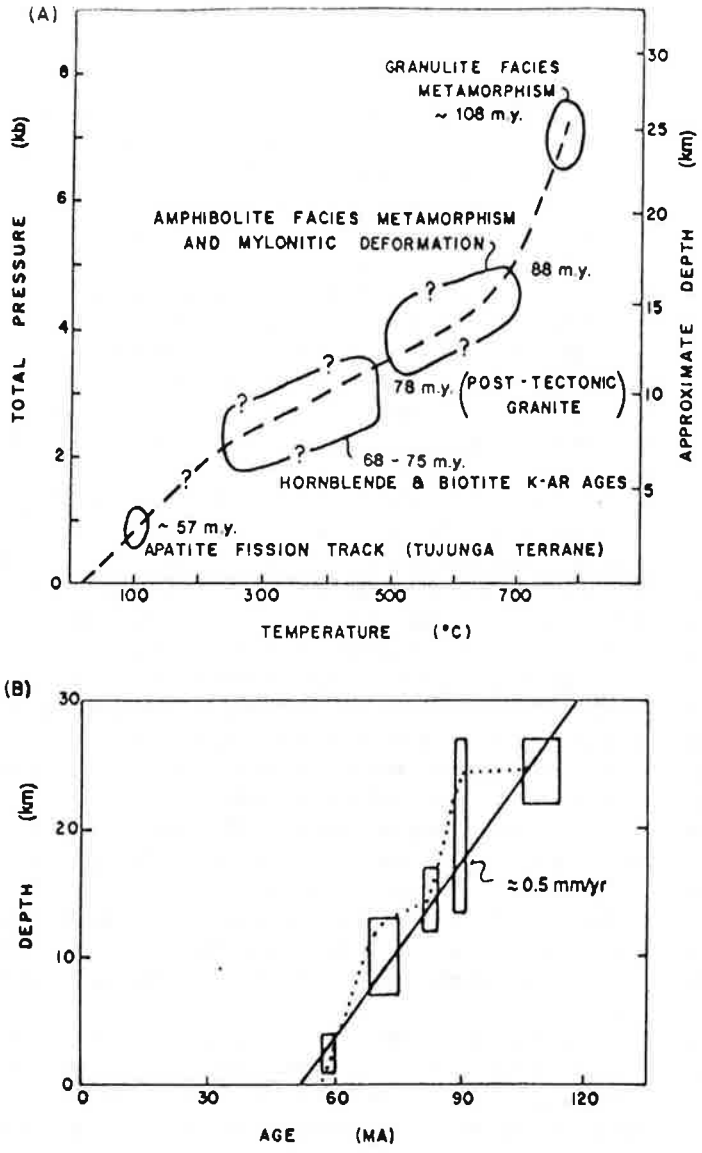

Figure 9. (A) P-T-time path for the Cucamonga terrane. Following mylonitic juxtaposition between 88 and 78 m.y., this path is shared by the San Antonio terrane. The pre-Late Cretaceous setting of the metasedimentary rocks in the San Antonio terrane is unknown. P-T fields represent uncertainty in estimated metamorphic conditions and/or blocking temperatures for K-Ar and fission-track data and assumed geothermal gradient. Age estimates based on U-Pb zircon ages discussed in text, K-Ar cooling ages (Miller and Morton, 1980), and fission-track ages (Mahaffie and Dokka, 1986).

(B) Age-depth plot for the Cucamonga terrane. Average uplift rate, assuming continuous uplift, is shown by solid line. Dotted line represents episodic model. Shaded fields indicate uncertainty in age or depth estimate. Queried field represents ~88 m.y. hypersthene tonalite orthogneiss, which may represent deep or mid-crustal levels.

Cooling Ages and Uplift History

Biotite and hornblende K-Ar ages from syntectonic intrusive units in the San Antonio terrane and a biotite K-Ar age from the posttectonic biotite granite all fall within the age range 68–75 m.y. (Miller and Morton, 1980). No age difference is apparent between mylonitic and less deformed units, and the youngest ductilely deformed rocks from the northern mylonite belt and Middle Fork Complex have biotite K-Ar ages of 70–73 m.y. Hornblende K-Ar ages from deformed tonalite in the San Gabriel terrane structurally above the Vincent thrust zone are 66 m.y. Fission-track ages from zircons, apatites, and sphenes from throughout the eastern San Gabriel Mountains are generally slightly younger than the K-Ar ages and range from 57 to 70 m.y. (Mahaffie and Dokka, 1986).

The K-Ar ages indicate a temperature drop of at least 200 °C: from hornblende argon-retention temperatures of ~500 °C to temperatures <300 °C (and possibly as low as 200 °C) as indicated by biotite ages (Krummenacher and others, 1975; Mattinson, 1978). This temperature drop implies relatively rapid latest Cretaceous cooling. This cooling continued in the early Tertiary, as the fission-track ages suggest that much of this region had cooled to temperatures below 100 °C by ~57 m.y. ago. This represents depths at most of several kilometers.

Ideally, the geochronological and petrological data might be combined in the form of retrograde pressure-temperature-time paths for the various terranes and these PTt paths used to assess tectonic models. At this point, only the PTt path for the Cucamonga terrane is established (Fig. 9A). Regional granulite-facies metamorphism occurred as late as 108 m.y. B.P. in a deep crustal setting (with P ~ 8 kbar and T ~ 750 °C). Late Cretaceous retrograde mylonitic deformation of the granulites and concurrent metamorphism of the metasedimentary rocks in the San Antonio terrane occurred under amphibolite-facies conditions (P ~ 4 kbar, T ~ 675 °C) during pluton emplacement (~88 to 78 m.y. ago). Petrographic features in mylonitic rocks from each of the transcurrent belts indicate decreasing temperature during deformation. The PTt paths of the San Antonio and San Gabriel terranes have not been established prior to this interval, but following juxtaposition of the terranes, they shared the same cooling history, as demonstrated by similar K-Ar and fission-track ages.

The inferred uplift history for the Cucamonga terrane is shown in Figure 9B. Although episodic periods of accelerated uplift may have occurred associated with specific tectonic events, the data suggest that uplift occurred throughout the Late Cretaceous and that uplift rates did not exceed 1 mm/yr for any significant interval. The average uplift rate during the latter half of the Cretaceous is ~0.5 mm/yr, a value similar to rates determined in numerous studies of Cordilleran batholithic rocks.

There is no obvious imprint in the cooling ages or derived uplift history which signifies when the Baldy terrane was underthrust. U-Pb crystallization ages fron intrusive units only bracket this episode between the Late Cretaceous and Miocene. Ehlig (1981) has proposed an age of ~60 m.y., based on Rb-Sr and K-Ar mineral and whole-rock ages from mylonitic rocks in the Vincent thrust zone and samples of Pelona Schist, but this is likely to be a minimum age, given the cooling history of the

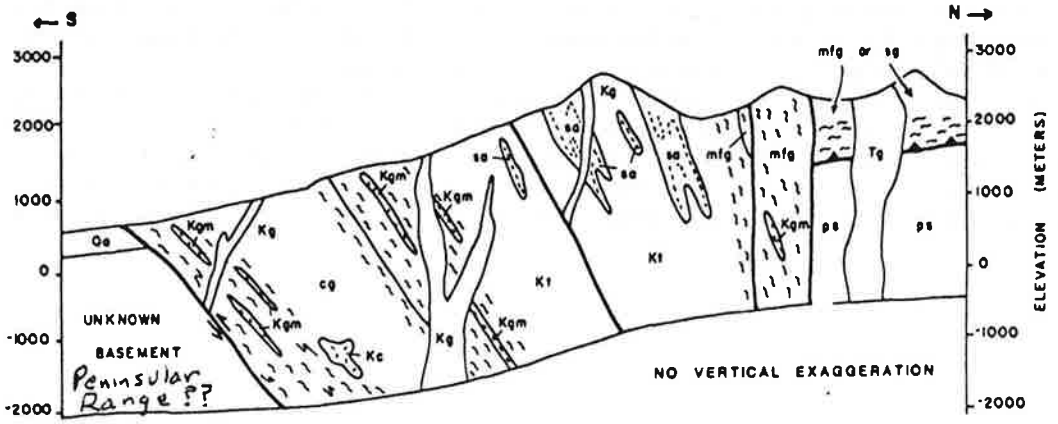

Cucamonga Terrane

The granulite-facies gneiss of the Cucamonga terrane is atypical when compared to other Cretaceous metamorphic rocks in southern California. The nearest documented Cretaceous granulite-facies rocks are at the southernmost end of the Sierra Nevada batholith, but these rocks differ in composition from those in the Cucamonga terrane and appear to represent an uplifted batholithic root (Ross, 1985; Saleeby and others, 1987).

Ehlig (1981) related the gneissic rocks of the Cucamonga terrane to the metasedimentary rocks of the San Antonio terrane, and there are some lithologic similarities between the two. Also, syn- and post-tectonic granitic units from both terranes possess a component of inherited Precambrian zircon and nearly identical common Pb isotopic ratios, implying that a similar basement underlies the pair or that their metasediments were derived from a common source. The gneissic rocks in the Cucamonga terrane, however, are clearly polymetamorphic and of notably higher grade. They also lack significant quartzite, and marble is uncommon. For Ehlig's correlation to be correct, the gneiss of the Cucamonga terrane would have to have formed from different sedimentary facies than those in the San Antonio terrane and have undergone a different metamorphic history. On a regional scale, such a polymetamorphic history is not unusual, and a multi-stage history has been proposed for some of the rocks correlated above with the San Antonio terrane. Although the goechronology of metamorphism, plutonism, and deformation differs in detail between these numerous areas, the timing of these events is largely limited to the Late Cretaceous throughout the length of this belt.

Perhaps the simplest account of the Cucamonga terrane would be to therefore consider it yet another pendant, albeit a rather unusual one, within the belt of metasedimentary pendants and intrusive rocks containing the San Antonio terrane. The Cucamonga terrane was first metamorphosed during the mid-Cretaceous, at a different position and much deeper crustal level than the San Antonio terrane. During the Late Cretaceous, the Cucamonga terrane was juxtaposed against the San Antonio terrane during renewed plutonic activity.

Exotic versus Native Origin

The preceding discussion suggests that all these terranes are kindred terranes for which the Cretaceous paleogeographic distribution has been disrupted within a major Late Cretaceous ductile fault system involving both thrust and left-lateral movements. The question of whether these rocks are exotic or native is not immediately addressed from study in the San Gabriel Mountains; however, regional arguments for a native origin for the San Gabriel terrane have already been presented. The San Antonio–Placerita and Cucamonga terranes could have been introduced to southern California relatively late in the Mesozoic, but they were underlain or in close proximity to "native" crust (that is, comparable in age to the San Gabriel terrane) prior to intrusion of the Upper Cretaceous granitoids.

The synplutonic, Late Cretaceous amalgamation of the San Antonio–Placerita and Cucamonga terranes against the San Gabriel terrane might best be interpreted as the local disruption of a continental arc in which kindred rocks representing different crustal levels have been juxtaposed. There are no data to support models suggesting that this was an accretion event. Shearing along the southern margin of the San Gabriel terrane represents local disruption of native terranes (or at least native since the mid-Cretaceous) rather than accretion of exotic terranes. Later underthrusting of the Baldy terrane may have been a related or separate event; however, identification of a subduction complex as an exotic terrane is a moot point.

The history proposed above contradicts models of major Cenozoic northward translation based on measured paleomagnetic inclinations. The geophysical data have been interpreted as evidence for the accretion of far-traveled, exotic terranes within a broad dextral plate margin during the early and middle Cenozoic. No accretionary boundaries of the proper age, however, have yet been identified in southern California.

No paleomagnetic data have been obtained directly from rocks of the San Gabriel terrane. Its identification as an exotic terrane is based on its being part of a composite Tujunga terrane and on proposed ties with the Salinia terrane. Paleomagnetic data from the latter suggest northward translation of more than 2,000 km and early Tertiary accretion (Vedder and others, 1983; Champion and others, 1984, 1986). Arguments for a native origin for the San Gabriel terrane have already been given, and the Salinia terrane correlates most closely with the San Antonio–Placerita terrane. The juxtaposition of these latter terranes against the San Gabriel terrane during the Late Cretaceous is not compatible with the timing of accretion or the expected fault movements predicted from paleomagnetic studies.

Similarly, paleomagnetic data from the Peninsular Ranges (Fry and others, 1985; Hagstrum and others, 1985, 1986; Morris and others, 1986) suggest major northward translation of the Peninsular Ranges batholith during the Paleogene. A large transform fault between the San Gabriel Mountains and Peninsular Ranges would make an ideal boundary for accretion; however, the transcurrent fault zone described here is too old and has the opposite sense of motion.

In addition, by the Late Cretaceous, a number of features link the rocks in the San Gabriel Mountains with those in the northeastern Peninsular Ranges. These include lithologic similarities between metasedimentary rocks from the San Antonio terrane with pendants in the eastern Peninsular Ranges (Powell, 1982b); lithologic, geochemical, and isotopic similarities between Upper Cretaceous granitic rocks in the two regions (Baird and others, 1979; Silver, 1982b); and coeval synplutonic deformation of similar style in both areas. A model in which the southeastern San Gabriel Mountains are displaced from the northeastern Peninsular Ranges during regional Late Cretaceous ductile thrust faulting is presented by May (1986). No lithologic, isotopic, or structural data support models for later accretion of the Peninsular Ranges against the San Gabriel Mountains. Because the San Gabriel terrane is native or was at least in place by the Cretaceous, this refutes major Paleogene translation of the Peninsular Ranges.

No one has yet satisfactorily reconciled the contradictory geologic and paleomagnetic data. Until fault zones capable of accommodating the translations proposed from the paleomagnetic inclination data are identified in southern California, it is perhaps more sensible to consider the paleomagnetic data rather than the rocks as suspect.

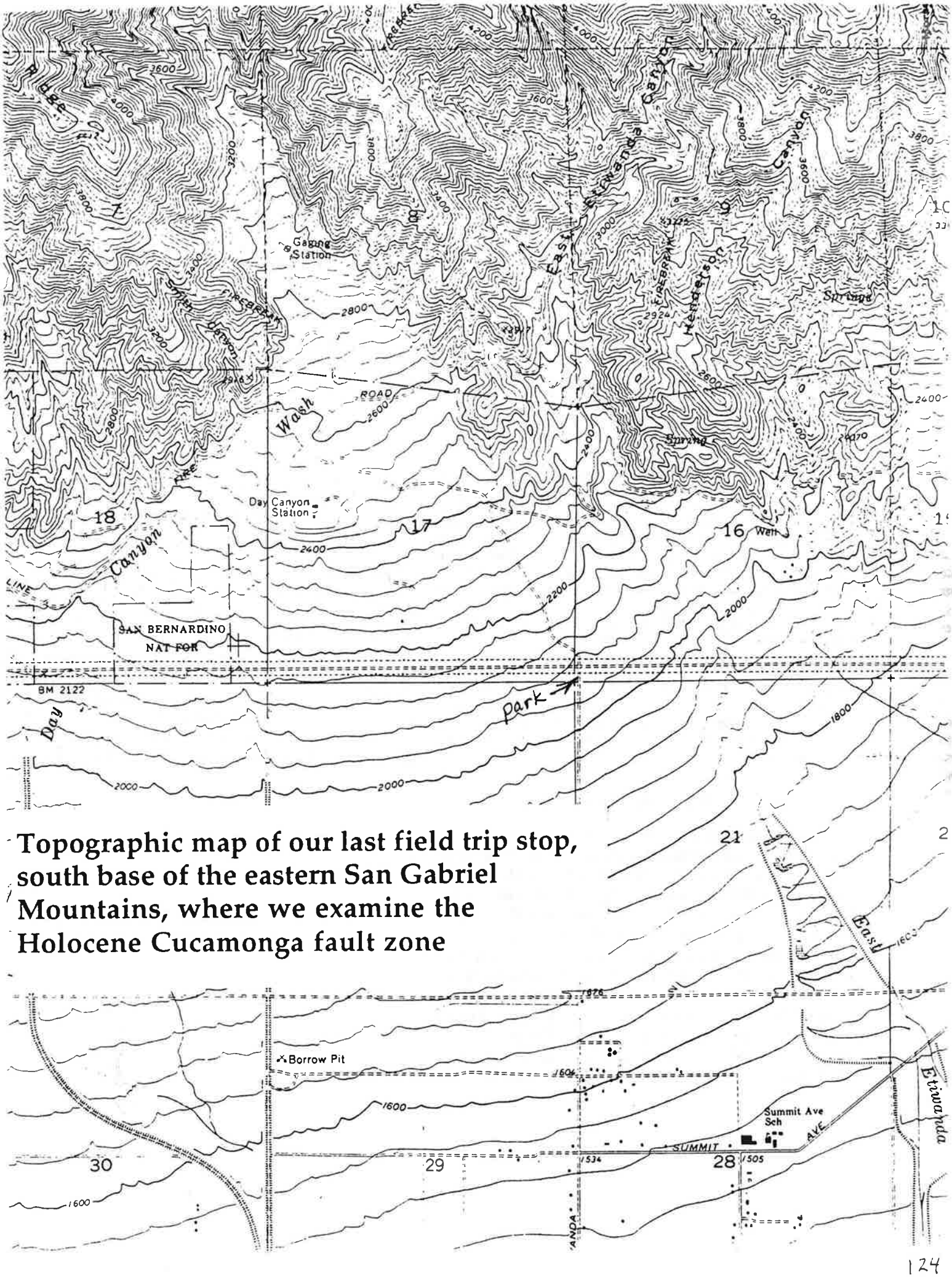

Topographic map of our last field trip stop, south base of the eastern San Gabriel Mountains, where we examine the Holocene Cucamonga fault zone

1. SEISMICITY AND TECTONICS OF THE CUCAMONGA FAULT AND THE EASTERN SAN GABRIEL MOUNTAINS, SAN BERNARDINO COUNTY

By CHRIS H. CRAMER[1] and JOHN M. HARRINGTON[2]

ABSTRACT

During the spring of 1977, the California Division of Mines and Geology conducted a microearthquake investigation of the Cucamonga fault in San Bernardino County. An array of eight portable seismographs was deployed between Lytle Creek and San Antonio Canyon in the eastern San Gabriel Mountains from mid-March to early July. Three months of usuable records were obtained, and more than 200 microearthquakes ($M = -1.0$–3.0) were located.

Microearthquake activity having focal depths of less than 10 km occurs beneath much of the easternmost San Gabriel Mountains, but microearthquake activity down to focal depths of 17 km occurs along the margins of the San Gabriel Mountains, beneath the Pomona Valley (Fontana and Chino area), and in the San Jose Hills. The San Jacinto fault is presently active, and the Cucamonga, Red Hill, San Antonio Canyon, Walnut Creek, and San Jose faults have associated seismic activity suggesting that they are active features. Activity from 1900 to 1974 has been high for this region.

Twenty-seven focal-mechanism determinations provide new information about the tectonics of the eastern San Gabriel Mountains. Strike-slip mechanisms dominate the region; thrust-type mechanisms are mainly confined to the interior of the eastern San Gabriel Mountains. Fault motions indicated by these focal-mechanism determinations show that the San Gabriel Mountains east of San Antonio Canyon have been detached from the rest of the range and are being actively forced northward and uplifted from the south by the north edge of the Peninsular Ranges province.

INTRODUCTION

Between March 16 and July 8, 1977, the California Division of Mines and Geology (CDMG) monitored the Cucamonga fault and the easternmost San Gabriel Mountains for microearthquake activity (fig. 1.1) Interest in the Cucamonga fault stems from the presence of Quaternary fault scarps along much of its length, indications obtained from the regional seismograph network of the California Institute of Technology (CIT) of earthquake activity beneath the eastern San Gabriel Mountains, and the proximity of the fault to the Pomona Valley—a region of rapid urbanization. This study is the first detailed microearthquake investigation of the Cucamonga, the Red Hill, and other faults between Lytle Creek and San Antonio Canyon. The resulting microearthquake locations and focal mechnisms indicate that many of these faults are active and also provide insight into the tectonics of the region.

TECTONIC SIGNIFICANCE

The inferred movements along the major faults in the study area based on focal mechanisms are shown in figure 1.8. Of primary interest are the tectonic forces acting on the easternmost tip of the San Gabriel Mountains, which we will refer to as the Cucamonga block. Although the complex interactions occurring in the study area are simplified in the diagram, it serves to highlight the general pattern of deformation in the area.

As discussed above and presented on figure 1.8, the triangular-shaped Cucamonga block exhibits relative

SLIP RATES AND FAULTING RECURRENCE: A PRELIMINARY STATEMENT

In the east-central part of the Cucamonga fault zone, two alluvial fans that emanate from Day and East Etiwanda Canyons form a 3-km-wide apron that is traversed by fault strands A, B, and C (fig. 12.1). This alluvial apron provides an ideal opportunity to examine the detailed history of these faults during late Pleistocene and Holocene time because the fanhead areas have not been modified extensively by agricultural or urban development and because the alluvial succession on the two fanheads is cut by spectacular fault scarps (fig. 12.5) that provide an opportunity to link the history of faulting to the history of alluvial sedimentation. We have conducted detailed stratigraphic and scarp-profiling studies on the two fanheads, and we have trenched the strand C scarp in an effort to obtain information on rates of slip, recurrence of faulting, and the amount of ground rupture during a typical earthquake (Matti and others, 1982; Morton and others, 1982; Matti and Tinsley in Clark and others, 1984; J. C. Matti, D. M. Morton, J. C. Tinsley, and L. D. McFadden, unpubl. data 1980–84). In this report we summarize data and preliminary interpretations that will be presented elsewhere.

Alluvial deposits on the Day Canyon and East Etiwanda Canyon fanheads are traversed by thrust-fault strands A, B, and C, which form conspicuous scarps that were created by recurring ground-rupturing displacements. In trenches across strand C, the fault zone is about 2 m wide, dips about 35° N., and projects near the middle of the scarp face; elongate cobbles within the fault zone have been rotated and aligned parallel to the plane of movement. Profiles across the fault scarps show that strand C has surface offsets ranging from 2 to 16 m (Matti and others, 1982, fig. 13); where strands A and B merge to form strand A/B, the scarp has offsets ranging from 8 to 40 m (Matti and others, 1982, fig. 14). The scarp heights vary systematically with the age of the alluvial units that they disrupt: The scarps are highest in the oldest units and are progressively lower in progressively younger units, indicating that strands A, B, and C generated recurring ground ruptures throughout the evolution of the latest Pleistocene and Holocene alluvial succession. Since the deposition of oldest sediment of unit yf_1, the faults have generated about 36 m of cumulative surface offset (Matti and others, 1982).

Our reconstruction of alluvial and faulting history on the Day Canyon and East Etiwanda Canyon alluvial fans leads to a fault-movement model in which a typical ground-rupturing earthquake generates a surface offset of about 2 m (Matti and others, 1982; Morton and others, 1982). This figure is suggested by fault-scarp profiles which show that surface offsets in alluvial units of different ages differ by multiples of about 2 m. We suggest that during latest Pleistocene and Holocene time, earthquakes having vertical displacements of about 2 m had an average recurrence of about 625 yr. This recurrence estimate is approximate and depends upon three factors: (1) a well-constrained measurement of 36 m of cumulative surface offset on strands A, B, and C since the accumulation of unit yf_1; (2) our inference that the 36 m of cumulative offset represents 18 2-m ground-rupture events; and (3) our interpretation that the first recognizable scarp-forming event occurred about 13,000 yr ago and the last recognizable event occurred 1,000 to 1,750 yr ago. The 13,000-year estimate is a maximum age for undated sediment of unit yf_1 based on a comparison of its soil profiles with alluvial soil profiles in the Cajon Pass region that have yielded radiometric ages of about 12,400 yr B.P. (Weldon, 1983; J .C. Tinsley and J .C. Matti, unpub. data 1984). The 1,000–1,750-yr figure is our best estimate for the age of unit yf_4 that depositionally overlaps strand C and in trench exposures appears to be unfaulted; the numerical age is based on a mean-residence-time soil-carbon date of $2,230 \pm 80$ yr from the soil profile of an older unit buried by the unfaulted deposits (Matti and others, 1982, p. 41), and on a comparison of soil profiles in the unfaulted unit with soil profiles elsewhere in the region that have yielded radiometric ages of about 1,000 to 2,000 yr. If 36 m of cumulative surface offset on strands A, B, and C represent 18 ground ruptures of about 2 m each, then the average recurrence interval for the 11,250-yr period between the first recognizable ground-rupture event 13,000 yr ago and the last recognizable event 1,750 yr ago is about 625 yr. If the next 2-m ground rupture event occurred tomorrow, then 19 events in 13,000 yr would yield an average recurrence of 684 yr—close to the 700-yr average recurrence we proposed earlier (Matti and others, 1982; Morton and others, 1982).

Measurements of fault-plane dips and determinations of surface offsets for thrust-fault scarps suggest minimum slip rates of 4.5 mm/yr for the 13,000-yr period between the first recognizable faulting event and the present, and 5.5 mm/yr for the 11,250-yr period between the first and last recognizable faulting events (J. C. Matti and J. C. Tinsley, unpub. data 1984; compare with Morton and others, 1982, and Matti and Tinsley in Clark and others, 1984). Estimates of seismic moment indicate expectable surface-wave magnitudes of 6.5 to 7.2 for fault-rupture lengths of 10 to 25 km, assuming an average stress drop of 60 bars, an average seismogenic crustal thickness of about 10 to 15 km, a maximum seismogenic crustal thickness of about 20 km, and crustal materials having average properties of elasticity and rigidity (J. C. Tinsley and J. C. Matti, unpub. data 1984).

GEOMETRY AND HISTORY OF THE CUCAMONGA FAULT ZONE

GENERAL FEATURES

The Cucamonga fault is an east-striking thrust-fault complex. Although commonly referred to as the Cucamonga fault, the mountain-front area is best considered as a fault zone. The surface expression of this fault zone in most places is about 1 km wide. At Day Canyon, this width is doubled if the Etiwanda Avenue scarp is considered as the south margin of the zone. Within the Cucamonga fault zone, we have identified many individual faults, many of which do not extend very far laterally on the geologic map (pl. 12.1) because the faults are discontinuous or poorly exposed. Temporal and structural relations between these faults and Quaternary alluvial units suggest that faulting has occurred intermittently on the various strands of the zone and may have shifted from one part of the zone to another during different episodes of the Quaternary. In this way, faulting has been distributed throughout a relatively wide fault zone rather than being confined to a single fault strand.

Individual faults occur in three different geologic settings. (1) In the mountains, faults and shear zones occur in crystalline basement rock. The number of faults and the pervasiveness of fracturing and crushing generally increase southward toward the mountain front. (2) Within a 500-m-wide zone at the mountain front itself the cataclasite progressively is more fractured and sheared by numerous discontinuous or discontinuously exposed faults; here, some of the reverse and thrust faults have placed basement rock over older Quaternary alluvial units. (3) The most conspicuous evidence for tectonism within the Cucamonga fault zone is a series of fault scarps that occur on the aprons and heads of most of the Quaternary alluvial fans which flank the eastern San Gabriel Mountains (fig. 12.5).

FAULTING WITHIN CRYSTALLINE ROCK

Within crystalline rock, the faults are exposed best in canyon walls because poor exposures obscure many faults on hillslopes. Fault-gouge layers in crystalline rock generally range in thickness from 1 cm to several tens of centimeters. The faults and shears commonly undulate and splay in a complex fashion both downdip and along strike, and the structures commonly anastomose. With few exceptions, individual faults dip north into the mountains at moderate angles. The mean of 49 measured dips is 43°, and the range is 0° to 80°. The nearly consistent downdip plunge of slickensides in gouge indicates that latest movements were dip-slip. The fact that some of these structures do not break even the oldest Quaternary alluvial units indicates early Quaternary or pre-Quaternary tectonism within the Cucamonga fault zone.

In the eastern part of the Cucamonga fault zone in Morse Canyon, 400 m north of the mountain front, la Tertiary conglomerate is faulted against crystalline bas ment rock along reverse faults. Here, the faults do not appear to break nearby older alluvial deposits. East of Sa Sevaine Canyon, in the Duncan Canyon bench area, tl same conglomerate unit is overlain by cataclasite along a thrust fault that appears to be older than strand A to the south. Here, we are not certain whether this old strand breaks older alluvial deposits.

At several localities along the mountain front, cataclasite is thrust over older alluvium (figs. 12.7 to 12.9 a relation that we observed at nine separate localitie Most of these are at the south edge of the mountains, spectacular examples occurring on the east margin of the De Canyon fanhead embayment (fig. 12.7) and at Ea Etiwanda Canyon (fig. 12.8). Two additional localities occur farther north toward the interior of the mountains. Between Deer Canyon and Day Canyon, 500 m north the mountain front, a patch of ridge-capping older grav is in thrust contact with cataclasite (fig. 12.9). At Demens Canyon a similar distance north of the mountain fror cataclasite again is thrust over older alluvium. The isolated examples indicate that Quaternary displacements within the Cucamonga fault zone occurred not only at th mountain front but also within basement rocks distances as far as 500 m north of the mountain front.

These relations within the mountain front indicate that tectonism within the Cucamonga fault zone has been pr longed and intermittent. Reverse-fault and thrust-fau activity occurred (1) after the deposition of late Tertiary sediments, (2) before the deposition of older Quaterna alluvial deposits, and (3) after the deposition of old Quaternary alluvial deposits.

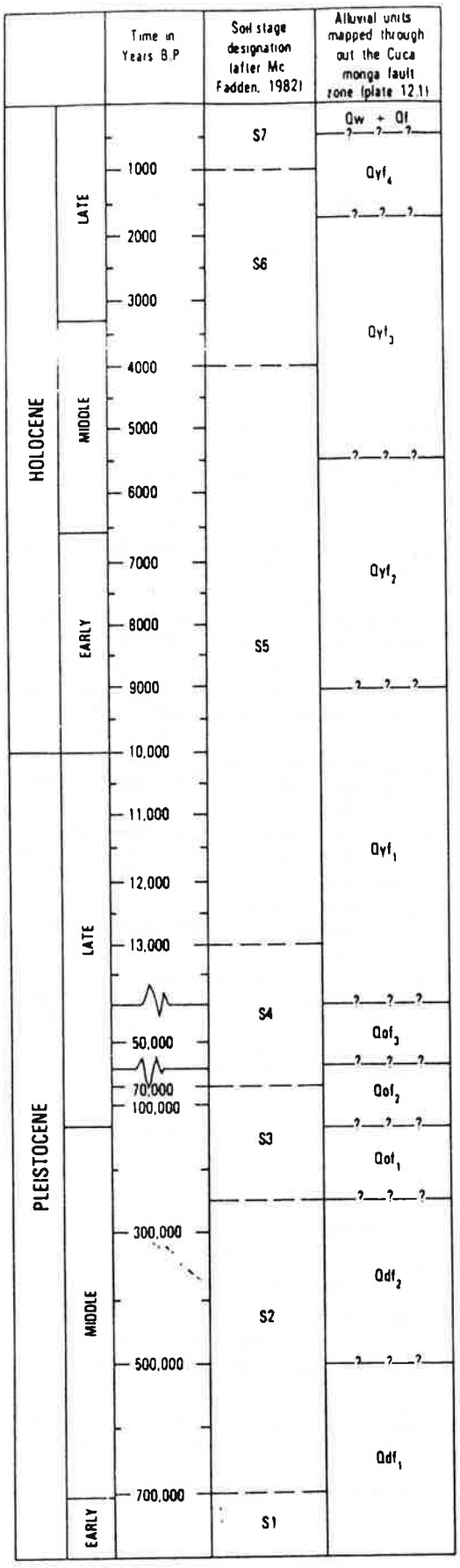

FIGURE 12.6.—Diagram illustrating approximate stratigraphic relations between Quaternary alluvial units mapped throughout the Cucamonga fault zone and pedogenic soil stages recognized by McFadden (1982). The numerical ages of the alluvial units are not known; time scale is included at left to show our best estimate of the approximate age for each unit. Subdivisions of the Holocene arbitrarily separate the epoch into three equal parts; subdivisions of the Pleistocene from G. M. Richmond, U.S. Geological Survey (written commun. to J. I. Ziony, U.S. Geological Survey, 1984).

We recognize 11 Quaternary alluvial units within the Cucamonga fault zone, and we use six criteria to identify these units: (1) topographic position within flights of stream terraces; (2) degree of erosional dissection; (3) preservation of primary depositional features such as channel-and-bar morphology; (4) structural and temporal relations to various fault strands of the Cucamonga fault zone; (5) differences in lithology and physical stratigraphy between some alluvial units; and (6) differences in soil-profile characteristics. On the basis of these criteria we recognize four major groups of alluvial units (fig. 12.6): (1) sediment in washes and on alluvial-fan surfaces that is actively transported by modern stream flows, or that presently is inactive (Qw and various categories of Qf on the geologic map); (2) latest Pleistocene and Holocene alluvial-fan deposits that are slightly to moderately dissected and that have pedogenic soil profiles lacking significant argillic horizons (various categories of Qyf on the geologic map); (3) late Pleistocene alluvial-fan deposits that are well dissected and that have pedogenic soil profiles containing moderately developed argillic horizons (various categories of Qof on the geologic map); and (4) Pleistocene alluvial-fan deposits that are extremely dissected and that have pedogenic soil profiles containing well-developed argillic horizons (various categories of Qdf on the geologic map).

Nearly every alluvial fan within the Cucamonga fault zone displays a nested series of fluvial terraces. On each fan it is relatively easy to work out relative age relations and to subdivide the alluvial-terrace succession according to the six criteria cited above. However, it is not so easy to correlate individual alluvial units from one alluvial fan to another or from the alluvial-fan surface to the remnant flights of terraces clinging to the walls of upstream bedrock canyons. This correlation problem exists because the individual alluvial units cannot be identified and correlated simply on the basis of lithology or some striking aspect of geomorphology. For example, units identified on the geologic map as Qyf_1 through Qyf_4 generally look the same in terms of their color, bedding characteristics, grain-size distribution, sand-gravel ratios, and degree of consolidation. In the absence of radiometric age determinations, the only reliable means of correlating the alluvial units is by subtle to pronounced differences in their soil-profile characteristics and by subtle differences in the weathering characteristics of bedrock cobbles and boulders on the alluvial-fan surfaces. Correlation by these techniques would require detailed soil-profile investigations from all alluvial units within the Cucamonga fault zone, and this level of study was beyond the scope of our preliminary investigation.

12. THE CUCAMONGA FAULT ZONE: GEOLOGIC SETTING AND QUATERNARY HISTORY

By Douglas M. Morton and Jonathan C. Matti

ABSTRACT

The Cucamonga fault zone is a 1-km-wide east-striking thrust-fault complex that forms the south front of the eastern San Gabriel Mountains. The fault separates crystalline rocks of the mountains from Quaternary alluvium of the upper Santa Ana River valley and thus forms an important geologic and geomorphic boundary in this part of southern California.

A wide variety of Precambrian to Mesozoic crystalline rocks is exposed in the mountain block north of the Cucamonga fault zone. A petrologically and structurally complex assemblage of metamorphic rocks occurs within and immediately north of the thrust zone. Originally metasedimentary and plutonic in origin, these rocks have undergone prograde metamorphism to granulite and (or) upper amphibolite facies followed by retrograde metamorphism to amphibolite and lower facies. The retrograde episode was accompanied by intense penetrative deformation. This brittle and ductile deformation created a wide variety of penetrative fabrics whose layering is oriented predominantly east-northeast. Lineations, consisting of parallel minor-fold axes and mineral streaking, trend east-northeast and plunge at small angles to both east and west. The intensity of cataclasis progressively increases toward the mountain front and the Cucamonga fault zone, where the layering is parallel or subparallel to strands of the fault zone. It is not known whether all or part of the cataclastic deformation is genetically related to the Cucamonga fault zone, or whether the cataclastic rocks merely provided zones of structural weakness along which subsequent fault movement occurred.

North of the granulitic and cataclastic rocks is an east-oriented foliated to cataclastically deformed body of Mesozoic quartz diorite. Cataclastic layering in the quartz diorite parallels that in rocks to the south, and deformation is most intense in the southern part of the body. North of the quartz diorite are a variety of metasedimentary and granitic rocks that also display cataclastic textures.

Within the Cucamonga fault zone we recognize two major groups of Quaternary alluvial units. Older alluvial units are Pleistocene and, from oldest to youngest, include units df_1, df_2, of_1, of_2, and of_3. Younger alluvial units are latest Pleistocene and Holocene and, from oldest to youngest, include units yf_1 through yf_4 and various units of inactive and active alluvium of channel washes and alluvial-fan surfaces.

Faulting within the Cucamonga fault zone has recurred episodically throughout most of Quaternary and, probably, latest Tertiary time. The oldest faults are in the north part of the fault zone, where some faults cut crystalline basement rock but do not break even the oldest Quaternary alluvial units. Younger faults, Cucamonga strands A, B, and C, occur farther south at the mountain front. Here, strand A breaks older Quaternary alluvial units but is concealed beneath younger Quaternary alluvial units. Strands B and C occur south of strand A and form conspicuous scarps in young Quaternary alluvial fans. These relations suggest that faulting within the Cucamonga fault zone may have migrated southward during late Pleistocene and Holocene time.

The alluvial units record the movement history of fault strands. Confirmed displacements on strand A, the oldest structure, occurred after deposition of unit df_2 and again after accumulation of the youngest deposits of unit yf_1, but not since that time. Strands B and C both evolved during the deposition of unit yf_1, and recurrent displacements on these two strands disrupted the evolving alluvial deposits of units yf_1 through yf_3. Displacements on strand B apparently ended during early stages of the deposition of unit yf_3, whereas displacements have continued on strand C. The latest movement on strand C occurred before the deposition of unit yf_4 which overlaps the fault on Day Canyon fan; this unit may be as old as 1,750 to 1,000 years.

Quaternary faulting within the Cucamonga fault zone has generated a complicated pattern of fault strands where individual strands merge and diverge locally; all strands apparently merge along a single trace in the western part of the fault zone. Thus, although strands A, B, and C form individual faults in the eastern part of the zone, to the west strands B and C merge to form strand B/C and strands A and B/C ultimately merge to form strand A/B/C. The latest episodes of faulting may have occurred mainly on strand C in the eastern 15 km of the Cucamonga fault zone, rather than throughout the entire 25-km length of the fault zone. The more complicated pattern of faulting in the eastern part of the zone may reflect interaction between the Cucamonga and San Jacinto fault zones: northwestward migration of the Perris block and the Peninsular Ranges by Quaternary right-lateral slip on the San Jacinto fault zone may have been taken up partly by reverse- and thrust-fault displacements along the Cucamonga fault zone.

INTRODUCTION

REGIONAL SETTING

The name "Cucamonga fault" generally is applied to the eastern part of the frontal-fault zone that bounds the south margin of the San Gabriel Mountains (Lamar and others, 1973; Morton and Yerkes, 1974; Ehlig, 1981). In our usage, the Cucamonga fault extends from the San Antonio Canyon area eastward to the Lytle Creek area (fig. 12.1). Along this reach, the frontal-fault zone separates the upper Santa Ana River valley to the south from the most prominent peaks of the eastern San Gabriel Mountains (figs. 12.2, 12.3).

Manuscript received for publication on September 28, 1981.

northward movement along its western and eastern boundaries, but shows relative southward movement along its southern boundary. Such movements appear contradictory considering the north-south compressive stresses throughout the region. In reality, the Cucamonga block has been detached from the rest of the San Gabriel Mountains and is being actively pushed northward and thrust up from the south.

Within the larger tectonic framework of southern California, the San Andreas fault system, particularly the San Jacinto fault, appears to be a major plate boundary. High rates of deformation and seismic-strain release, particularly on the San Jacinto to the south, support this concept. Continued northward movement of the Pacific plate forces the Peninsular Ranges province northward into the Transverse Ranges—a major resistive element to movement along the plate boundary. The northern edge of the Peninsular Ranges province is being thrust under the San Gabriel Mountains. Because the Cucamonga block forms the easternmost point of the San Gabriel Mountains and is next to the active plate boundary, it has been sheared off from the rest of the San Gabriel Mountains along the faults in San Antonio Canyon and is presently being forced northward.

Internal deformation is also occurring in the Cucamonga block because of the tectonic forces acting upon it and because it is adjacent to an active plate boundary. The eastern part of the block is actively being sheared by internal right-lateral faults, as discussed in the previous section. Internal thrusting on a fault or faults north of the

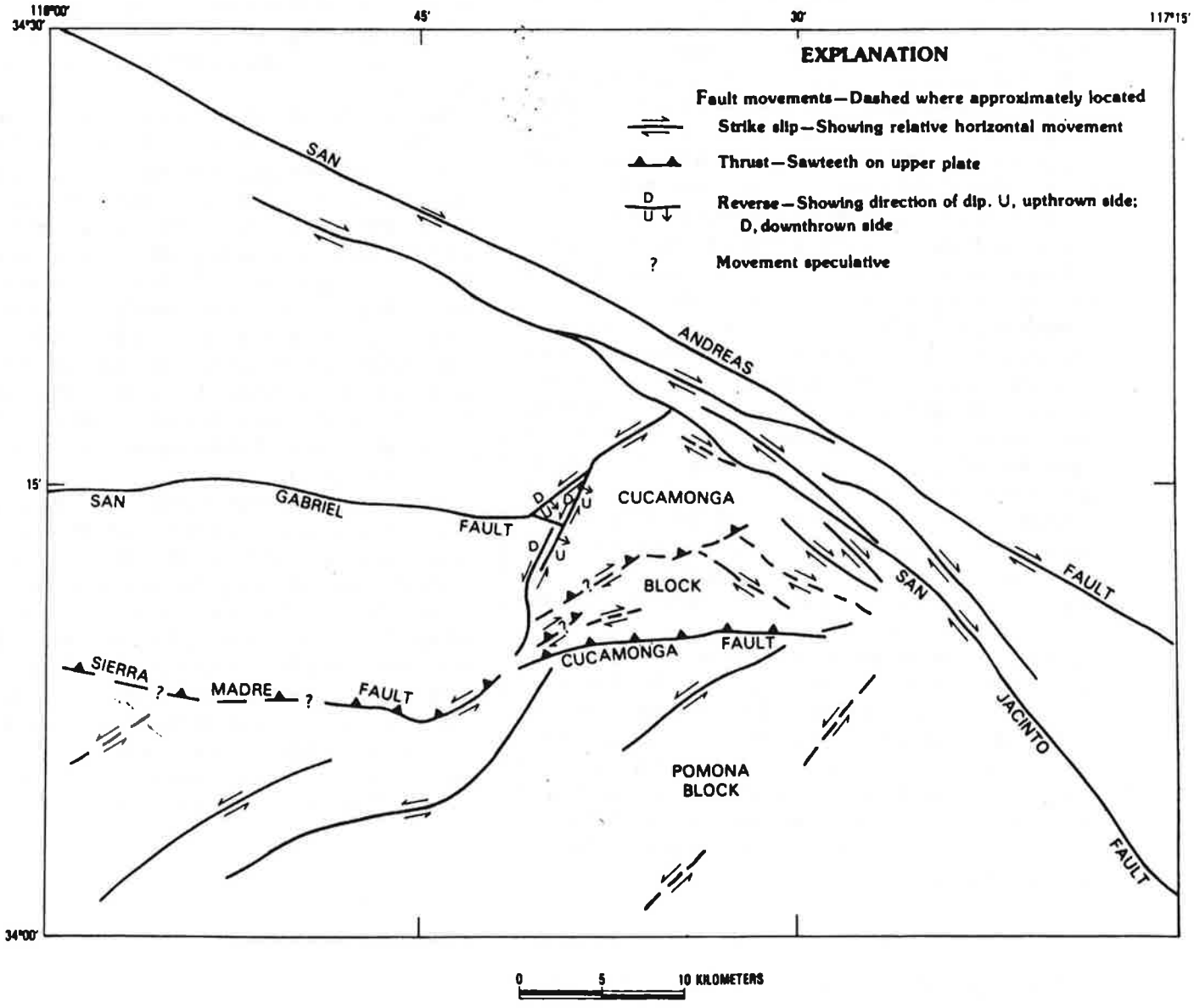

FIGURE 1.8.—Fault movements inferred from focal mechanisms in figure 1.7. See text for tectonic implications.

Cucamonga fault is suggested by composite focal mechanism k. Thus the east end of the block is accommodating the northward movment by horizontal shearing, whereas the central and western parts are meeting greater horizontal resistance to northward movement and hence are accommodating by vertical uplift. Such movements would explain why the greatest topographic relief is in the western part of the block and why the topographic relief decreases to the east within the block.

West of San Antonio Canyon the range front is farther south than along the south edge of the Cucamonga block. Also, topographic elevations and frequency of seismicity in historic times are lower here than in the Cucamonga block (figs. 1.2 and 1.3). These factors, as well as a greater distance from the major plate boundary represented by the San Jacinto fault, point to lower rates of tectonic deformation in the San Gabriel Mountains west of San Antonio Canyon than farther to the east.

The truncation of the San Gabriel fault at San Antonio Canyon is also explained by this tectonic model of the eastern San Gabriel Mountains. The recent northward movement and uplift of the Cucamonga block has cut off the older San Gabriel fault. Although several fault zones can be suggested as eastern extensions of the old San Gabriel fault within the Cucamonga block, more recent deformation and movement within the Cucamonga block has probably eliminated that older trace.

South of the San Gabriel Mountains, the dominant sense of motion is left lateral strike slip. Differential movements along these left-lateral faults are occurring in the northern Peninsular Ranges province as it forces its way northward and then adjusts to the movements of the Cucamonga block. Accordingly, the San Jose and Walnut Creek faults are major active tectonic features, movement along which corresponds with the northward yielding of the Cucamonga block. This concept is supported by both the historical and current seismicity near these faults. The high rate of seismicity near Fontana and Chino indicates a similar pattern of deformation closer to the major plate boundary where there is less resistance to the northward movement of the Peninsular Ranges block. The left-lateral sense of the Red Hill fault is thus explained. Also the alignment of the Red Hill fault with the eastern end of the Cucamonga fault may indicate that (1) movement along the Red Hill fault is controlling the orientation of the eastern end of the Cucamonga fault or (2) the left-lateral Red Hill fault truncates the Cucamonga fault at Bullock's Canyon.

CONCLUSIONS

This microearthquake survey of the eastern San Gabriel Mountains in the vicinity of the Cucamonga fault has provided new insight into the seismicity and tectonics of the region. The data show a diffuse seismicity pattern under the San Gabriel Mountains between San Antonio Canyon and Lytle Creek. Concentrations of microearthquake activity occur along San Jacinto fault system and beneath Fontana—less activity occurring near Chino and beneath the San Jose Hills. Focal mechanisms indicate dominantly strike-slip fault movements except for thrust-fault movements in the core of the eastern San Gabriel Mountains. Focal depths within the San Gabriel Mountains are less than 10 km, but on the margins and in the surrounding areas, focal depths extend below 10 km, the deepest (17 km) occurring beneath Fontana. The deeper microearthquakes generally seem to be associated with strike-slip faults.

Microearthquake activity suggests that several faults may be active besides the San Andreas and San Jacinto faults. The Cucamonga fault appears to have had thrust-type microearthquakes on it about 7 km beneath Cucamonga Peak. Three microearthquakes suggest that the Red Hill fault is an active left-lateral strike-slip fault. Microearthquakes on the faults in San Antonio Canyon show oblique-reverse (left-lateral) movement. Several microearthquakes in the San Jose Hills indicate that the Walnut Creek fault and possibly the San Jose fault are active left-lateral faults. The microearthquake activity beneath Fontana and near Chino indicate the possibility of buried left-lateral faults beneath Pomona Valley at those two locations.

The fault movements indicated by our study of focal mechanisms provides a detailed picture of the tectonics of the eastern San Gabriel Mountains. The eastermost triangular tip (Cucamonga block) has been broken off the main body of the San Gabriel Mountains and is being forced northward and thrust up by the northward tectonic movement of the Peninsular Ranges province. Such movement fits the larger tectonic framework of the province, which apparently is being forced northward into the Transverse Ranges by plate-tectonic motion with the northern edge of the province being thrust under the San Gabriel Mountains. Internal deformation is occurring

2. QUATERNARY GEOLOGY AND SEISMIC HAZARD OF THE SIERRA MADRE AND ASSOCIATED FAULTS, WESTERN SAN GABRIEL MOUNTAINS

By Richard Crook, Jr., C. R. Allen, Barclay Kamb, C. M. Payne, and R. J. Proctor[1]

ABSTRACT

This detailed study of a 40-km-long section of the Sierra Madre and associated fault zones in the central Transverse Ranges, along the south side of the San Gabriel Mountains, is aimed at providing information for evaluating the seismic hazard that these faults pose to the heavily populated area immediately to the south. Evidence on the location of fault strands and the style and timing of fault movements during the Quaternary was obtained from detailed geologic mapping, aerial-photograph interpretation, alluvial stratigraphy, structural and stratigraphic relations in some 33 trench excavations at critical localities, and subsurface data.

We present a time-stratigraphic classification for the Quaternary deposits in the study area, based on soil development, geomorphology, and contact relations among the alluvial units. We distinguish four units, with approximate ages, as follows: unit 4, about 200,000 yr to middle Quaternary; unit 3: about 11,000 to 200,000 yr; unit 2; about 1,000 to 11,000 yr; and unit 1; younger than about 1,000 yr. We use this classification to evaluate on a semiquantitative basis the evidence for fault activity in the study area and to infer the relative seismicity of different segments of the Sierra Madre fault zone during the Quaternary. Alluvial-fan development (particularly fanhead incision and the ages of alluvial-fan deposits) also gives clues as to relative seismicity.

The most active segment of the Sierra Madre fault zone within the study area is the westernmost section, adjacent to the faults that broke during the 1971 San Fernando, Calif., earthquake. The age of activity, as indicated by the occurrence of Holocene faulting, decreases toward the east. Along the Sierra Madre fault, through La Cañada, Altadena, Sierra Madre, and Duarte, is abundant evidence of late Pleistocene faulting. Total vertical displacement is more than 600 m, but there is no evidence for Holocene fault movement. These observations suggest that the presently applicable recurrence interval between major earthquakes in the central and eastern sections of the Sierra Madre fault zone is longer than about 5,000 yr. The local magnitude (M_L) of the largest credible earthquake that could occur on the Sierra Madre fault zone in the study area is estimated at 7, on the grounds that the fault zone is probably limited mechanically by subdivision into separate arcuate segments about 15 km long.

The Raymond fault, which branches southwestward from the Sierra Madre fault in the eastern part of the study area, shows well-defined evidence of a late Quaternary history of repeated fault movements. Displacements of alluvial strata observed in trench excavations across the fault give evidence of five major seismic events, whose times of occurrence can be estimated from radiometric dating at approximately 36,000, 25,000, 10,000–2,200 (two events), and 2,200–1,500 yr B.P. Further evidence suggests at least three more faulting events in the past 29,000 yr, for which specific dates cannot be determined. Because some additional events probably remain undetected, we infer that an average recurrence interval of about 3,000 yr, with an average vertical displacement of 0.4 m per event, is applicable to the Raymond fault in its present state, as indicated by its history of movement over the past 36,000 yr. This level of activity is distinctly higher than that found for the Sierra Madre fault zone in the central and eastern parts of the study area. If the entire 15-km length of the Raymond fault would rupture in a single event, as seems likely, a maximum credible earthquake of $M_L 6\frac{3}{4}$ can reasonably be assumed.

[1]All authors: California Institute of Technology, Pasadena, California.

Manuscript received for publication on October 1, 1981.

INTRODUCTION

PURPOSE AND SCOPE

The purpose of this study is to understand better the seismic hazard posed by the frontal-fault system of the San Gabriel Mountains of southern California along a 40-km-long segment from the mouth of Big Tujunga Canyon to the mouth of San Gabriel Canyon. This segment of the fault system, known locally as the Sierra Madre fault, lies adjacent to or within the foothill communities of Sunland, Tujunga, La Crescenta, Glendale, La Cañada-Flintridge, Altadena, Pasadena, San Marino, Sierra Madre, Arcadia, Monrovia, Bradbury, Duarte, Azusa, and Glendora; the total combined population of these communities is approximately 350,000. Although it has long been recognized that this area shares a relatively high seismic exposure with the rest of southern California, particular impetus was given to this study by the 1971 San Fernando earthquake because the fault zone whose displacement caused this earthquake lies immediately adjacent west of, and is approximately continuous with, the Sierra Madre fault zone (fig. 2.1). The major question is whether or not these two areas share a similar seismic hazard. Indeed, it has even been suggested that because strain has already been relieved in the San Fernando segment, faults of the same system to the east and west are the most likely candidates for future earthquakes.

The investigative technique used in this study was primarily a field investigation of faults to determine their precise locations, subsurface configurations, seismic histories, and present activity. There is abundant evidence

from worldwide experience that those faults that have had displacements most often in the recent geologic past—particularly the past 11,000 yr—are most likely to slip during significant earthquakes in the near future. Thus, in this study, we placed special emphasis on the determination of recent fault movement. To determine this movement required detailed and systematic mapping of the fault zones, mapping and interpretation of Quaternary alluvial and physiographic features, compilation of various kinds of information on subsurface fault configuration and displacements, and excavation of numerous trenches across faults suspected of being active. Most of our conclusions are based on the dating of faulted and unfaulted strata exposed in 33 trenches that were excavated as part of this study. This dating involved the use of standard radiometric techniques as well as the development of a time-stratigraphic classification for the Quaternary alluvial units exposed in the study area.

Historical seismicity is also an important clue to understanding seismic hazard; however, both the historical and instrumental records of earthquakes in southern California are so brief that extreme caution must be used in interpreting these statistically inhomogeneous data (Allen and others, 1965). The primary contribution of the present study is in looking farther back into the recent geologic history than is possible with the historical and instrumental data, so as to obtain a more meaningful statistical data base from which to extrapolate into the future. The current seismicity of the San Gabriel Mountains, particularly in terms of the focal mechanisms and tectonic implications of contemporary earthquakes, is discussed by Pechmann (this volume).

METHODS OF STUDY AND SOURCES OF INFORMATION

The basic method of study involved three principal elements: (1) delineation of fault traces by geologic mapping based on surface inspection, trenching, and inter-

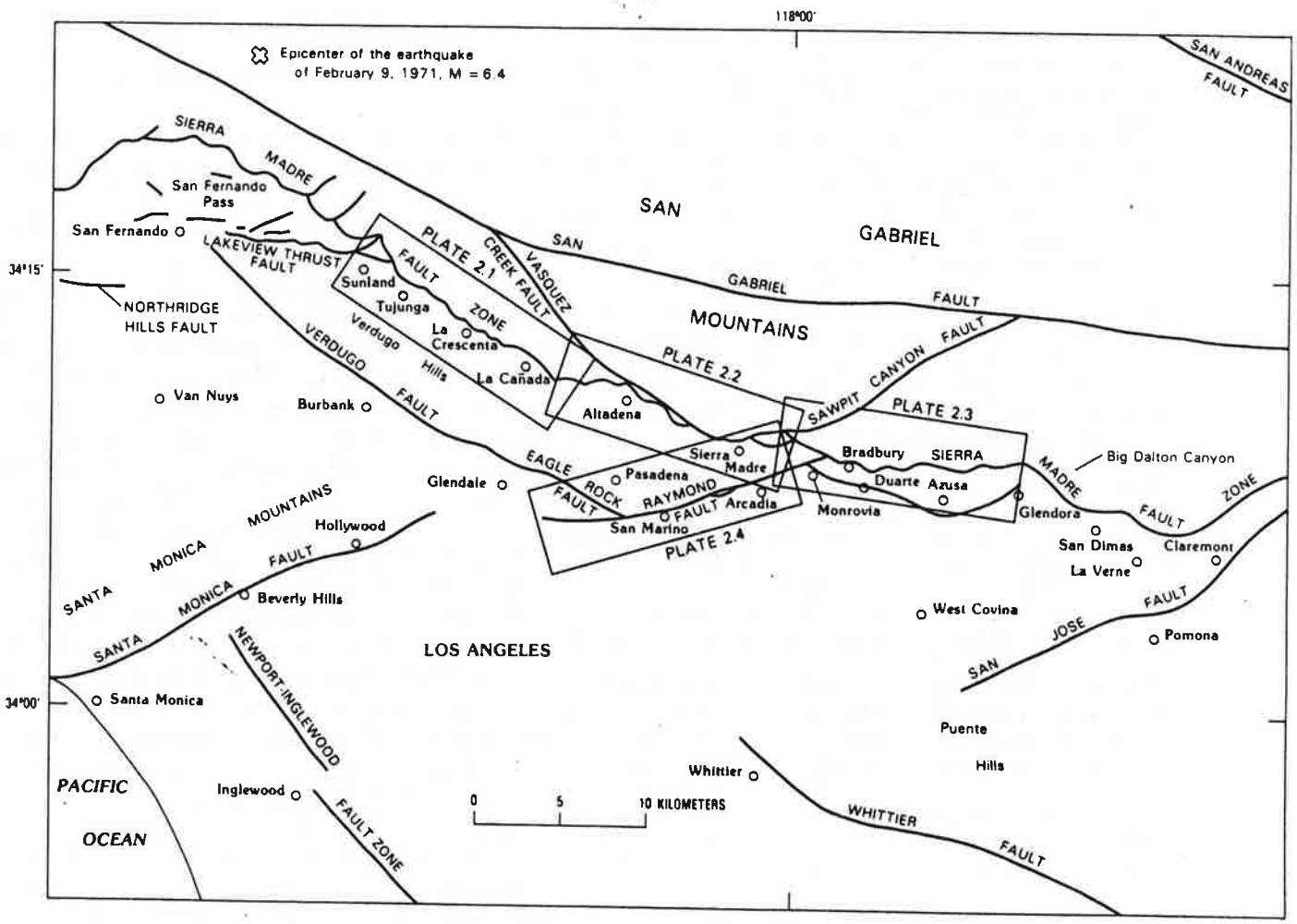

FIGURE 2.1.—Index map of study area in southern California, showing faults studied in this investigation (pls. 2.1–2.4) and their relation to other major fault systems in the Los Angeles area.

pretation of aerial photographs; (2) determination of subsurface fault locations, configurations, and displacements from exploratory-borehole and water-well logs, from water levels, and from various geophysical data; and (3) deduction of the local history of fault movement by the use of chronologic information on the Quaternary deposits associated with fault traces.

GEOLOGIC MAPPING

Geologic mapping of the fault zones was done in the field at a scale of 1:12,000 on topographic base maps prepared from U.S. Geological Survey 7½-minute quadrangle sheets. The results, edited for presentation at a scale of 1:24,000, are presented in plates 2.1 though 2.4. Plates 2.1 through 2.3 cover the Sierra Madre fault zone in three segments from Big Tujunga Canyon on the west to the San Gabriel River on the east. The Raymond fault zone is shown in plate 2.4; its limits were chosen so as to include only those sections of the Raymond fault showing evidence for, or suspected of, Quaternary faulting.

Mapping was carried out during 1976 and 1977 with the assistance of Richard Lewis, Raymond Durkan, and Thomas Anderson. Where available, mapping by other workers was field checked and either used intact or altered where our opinions differed or where new exposures exist. Use was made of maps prepared by the following authors and agencies: Eaton (1957) and Beattie (1958), at the southwest and extreme west ends of plate 2.1; the Metropolitan Water District of Southern California (unpub. data, 1964–74), on plates 2.2 and 2.3; Morton (1973), in the east half of plate 2.2 and on plate 2.3; Saul (1976), central portion of plate 2.2; California Division of Mines and Geology (1964), at the extreme east end of plate 2.3; Buwalda (1940) on plate 2.4; and Lamar (1970) at the extreme west end of plate 2.4. Stratigraphic nomenclature and age assignments of stratigraphic units may not necessarily be those adopted by the U.S. Geological Survey.

AERIAL PHOTOGRAPHS

Extensive use was made of the oldest available aerial photographs. These are the Spence oblique aerial photograph collection (1922–52) at the University of California, Los Angeles (UCLA), Geography Department, and the Fairchild aerial photograph collection (1928–60) at the Whittier College Geology Department, Whittier, Calif. More recent aerial photographs were also examined. Special photographs for this study were taken on January 8, 1976, by I. K. Curtis, who provided a set of 48 vertical photographs at a scale of 1:12,000. Ground-view photographs dating back to the 1880's were also examined at the Henry E. Huntington Library in San Marino.

TRENCHING

A total of 33 trenches were excavated and logged during this project (table 2.1). The important features observed and conclusions reached are summarized below in the supplementary section entitled "Trenching." In addition, trenching by other workers helped to define the Raymond fault at localities (64), (67), and (68) (pl. 2.4).

DRILLING

A series of 14 exploratory boreholes were drilled at the Jet Propulsion Laboratory (JPL) of the California Institute of Technology (CIT) in 1977; the drilling and logging were done by Le Roy Crandall & Associates under contract to JPL. We selected 11 of the borehole sites in an effort to delineate the number and location of the branches of the Sierra Madre fault zone beneath JPL; The results of this study are described below (see pls. 2.2 and 2.6).

RADIOCARBON DATING

All materials penetrated in trenches or exposed in outcrops and suspected of containing carbonaceous remains were sampled for radiocarbon dating. A total of 13 samples were deemed significant enough in placement and rich enough in carbon to be dated (see table 2.2).

SEISMIC-REFRACTION AND MAGNETOMETER SURVEYS

Unpublished information obtained from surveys by the Envicom Corp. and by Le Roy Crandall & Associates was utilized in the Duarte-Azusa area to help locate buried fault traces at localities [30] and [32] through [34] (pl. 2.13).

CLAST SOUND-VELOCITY MEASUREMENTS

We developed and tested a new method for ascertaining on a quantitative basis the relative ages of alluvial units. The extent of weathering of clasts of a definite, recognizable lithology was determined by measuring the seismic-wave velocity of the clasts, which decreases with increasing weathering. Seismic velocity was measured with a portable instrument used commercially for measuring the speed of sound in concrete (see appendix entitled "Measurement of Progressive Clast Weathering").

BOREHOLE-LOG AND WATER-LEVEL DATA

We searched the water-well files of the Los Angeles County Flood Control District for pertinent information contained in driller's logs and for water levels as they pertain to ground-water barriers or buried faults. Additional borehole-log information was supplied by the Metropolitan Water District of Southern California. Information gathered from this search that proved to be important is noted on the geologic maps (pls. 2.1-2.4).

is probably unit 2 alluvium. In trench 20C, the fault is overlain by 0.6 m of unfaulted bedded silty sand with a Holocene soil (fig. 2.10). This unit contained an in-place root that yielded a ^{14}C age of 2,200 ± 80 yr B.P.

The lower fault could not be traced into Pasadena Glen or Hastings Canyon, although it must have moved recently enough to have cut the Kinneloa fan surface (loc. 19, pl. 2.2), as indicated by the fact that the faulted colluvium is younger than the incision of unit 3 surfaces. The sides of the incised channel are mantled by the faulted colluvium.

The positions of the two high-angle faults in most of this reach are inferred from two series of aligned canyons and notches in ridges. The lower fault is exposed in Bailey Canyon, and further evidence is provided by the patches of unit 4 alluvium high on a ridge on the east side of the canyon.

In this area, a minimum total vertical displacement of approximately 330 m has occurred since deposition of unit 4—210 m along the high-angle fault in the basement and 120 m along the thrust faults. This conclusion is based on displacement of the unit 4 alluvium-basement depositional contact.

Both Pasadena Glen and Hastings Canyon contain mutually exclusive, distinctive rock types in outcrop—the Lowe Granodiorite in Pasadena Glen and porphyritic andesite in Hastings Canyon. This unique feature allows a distinction between alluvial deposits from each of the two adjacent drainages. Thus, left-lateral offset of these distinctive unit 4 deposits cannot be more than 1.2 km from their source drainage.

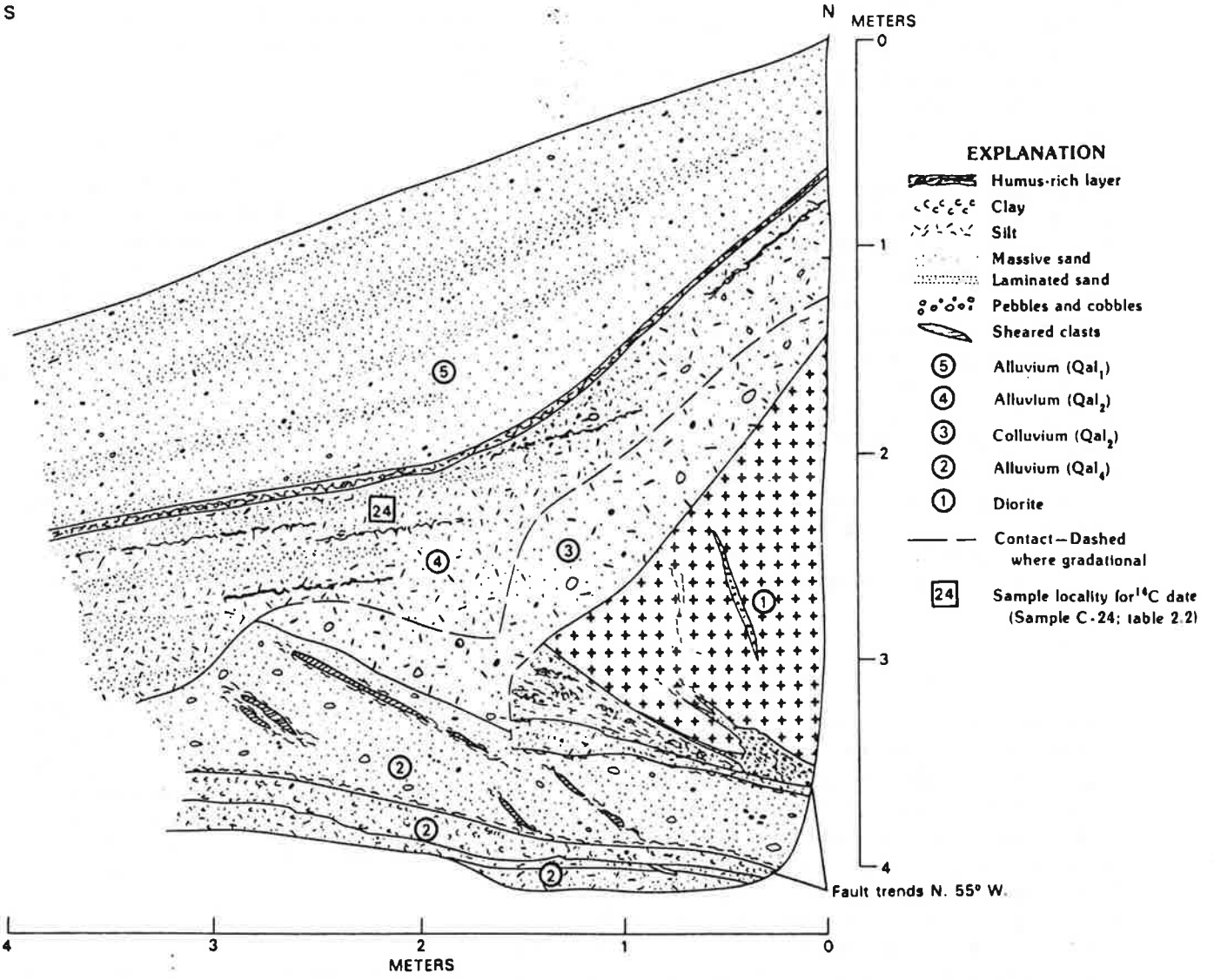

FIGURE 2.10.—Log of west wall of CIT trench 20C (bearing, N. 23° E.) in Pasadena Glen, Pasadena, showing a branch of Sierra Madre fault (see fig. 2.9 for location).

In this segment, the Sierra Madre fault zone consists of several separate traces—two low-angle thrusts involving alluvial units that lie at the base of the mountain front, and two high-angle faults to the north within the basement complex. The two low-angle thrusts are nearly parallel and less than 100 m apart (fig. 2.9). The upper fault thrusts gneiss over unit 4 alluvium and can be traced nearly continuously from the Eaton Canyon area to the Sunnyside debris basin, where it becomes much steeper and more complex. The lower trace is not nearly so well defined. It is exposed at the surface in two localities separating diorite from unit 4 alluvium and was exposed at two localities in CIT trenches 20A, 20B, and 20C, where it was seen to have disrupted colluvium overlying unit 4. The fault could not be traced into the valley fill, which

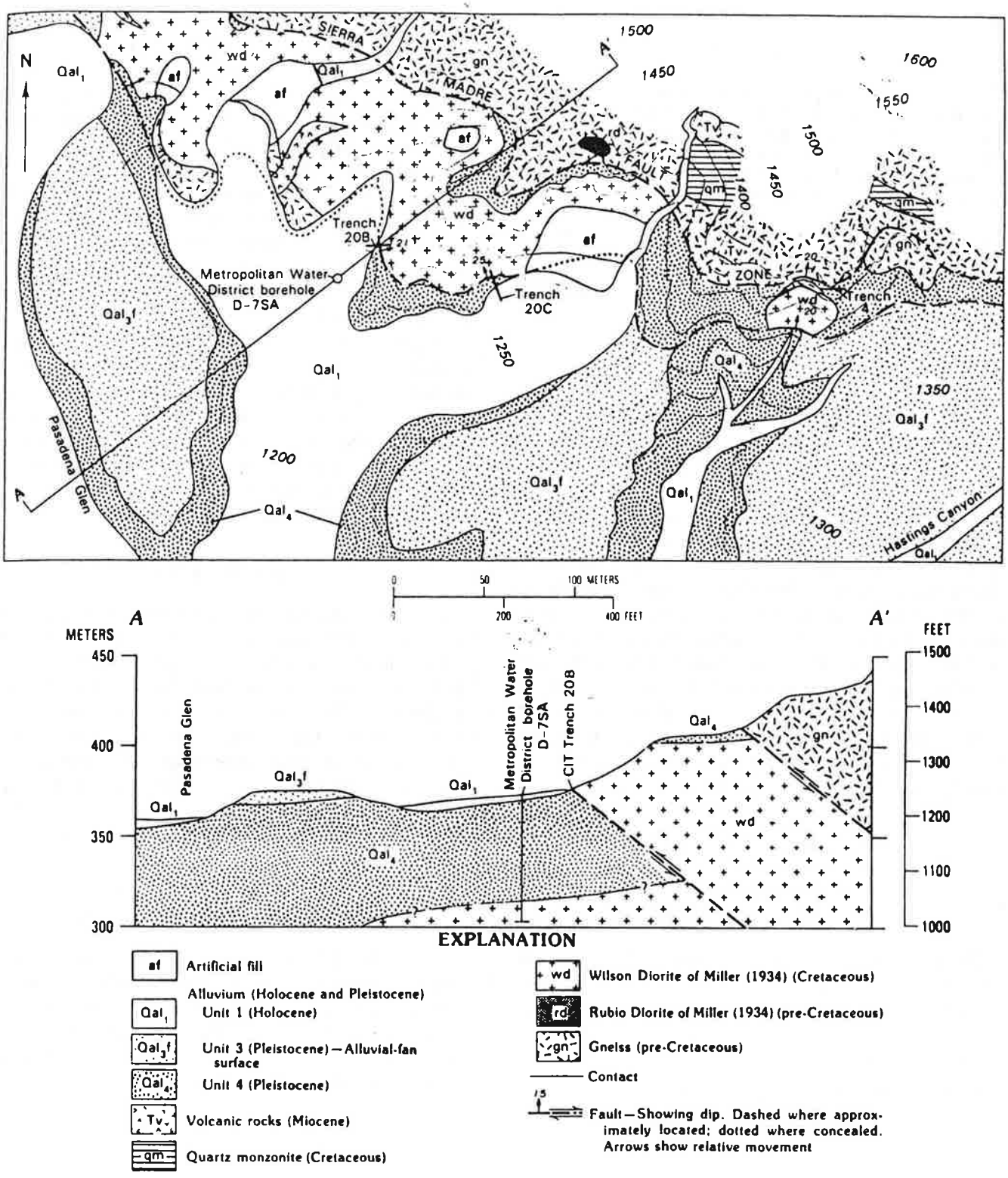

FIGURE 2.9.—Detailed geologic map and cross section of Pasadena Glen-Hastings Canyon area, showing traces of two thrust faults and locations of CIT trenches 20B and 20C (see fig. 2.10 for cross section of trench 20C and pl. 2.2 for locations).

3. EXPLORATORY TRENCHING OF THE SANTA SUSANA FAULT IN LOS ANGELES AND VENTURA COUNTIES

By Richard Lung[1] and R. J. Weick[1]

ABSTRACT

Determining the fault-rupture hazard in tectonically active urban areas, especially in many parts of California, is important in land-use regulation. Our exploratory trenching in 1977, comprising 29 excavations at two sites along the Santa Susana fault zone, demonstrated the usefulness and limitations of such fault investigations in locating faults and determining their relative or limiting age, depending upon whether material over the fault can be chronostratigraphically dated. At one site we were successful only in bracketing the fault location, but at another we were able to document the probable age of last movement as greater than 10,000 yr. Because of the complexity of the fault zone, much work remains to be done before the potential hazards associated with it can be fully evaluated.

INTRODUCTION

A subsurface exploration program was conducted in 1977 to study the recency of faulting in the Santa Susana fault zone at selected locations in western Los Angeles and southeastern Ventura Counties. The study complemented the surface and subsurface investigations of Robert S. Yeats and others from Ohio University, Athens, Ohio. Whereas their study concentrated on the late Tertiary history and subsurface structure by utilizing extensive oil-well data and mechanical-modeling techniques, our study focused on the Holocene displacement history and land-use implications associated with potentially active faulting. The two principal sites of field study were located in the Limekiln Canyon area at the northern edge of the Porter Ranch area in Los Angeles County, and in the Tapo Canyon area north of Simi Valley in Ventura County (fig. 3.1).

FIELD INVESTIGATION AND GEOLOGICAL SETTING

STUDY OBJECTIVES AND METHODS

The primary aims of the study were as follows: (1) determine the age of the latest movement and the extent of faulting within the Santa Susana zone by exploratory trenching, detailed mapping, and sampling of datable materials; (2) evaluate criteria useful in detecting and determining fault activity and recency; and (3) prepare guidelines appropriate for subsurface investigation of proposed developments in potentially active fault zones.

Initial tasks included a review of previous pertinent geologic maps and reports, particularly those by Yeats (1976), Saul (1975), Weber (1975), and various private consultants. Conflicting fault locations, as mapped by others, were noted, and attempts were made to reconcile these by detailed geologic mapping, aided by a study of aerial photographs. After this work was completed, the field investigation proceeded with a two-stage trenching program starting at Limekiln Canyon, followed by trenching at Tapo Canyon. A series of 28 backhoe trenches and pits, plus a preexisting sidehill cut (figs. 3.2 and 3.3), were excavated in the two areas to locate the fault traces, and particularly to locate places where the fault might be covered by relatively recent deposits containing carbonaceous or other age-datable materials.

REGIONAL SETTING

The two localities are approximately 16 km apart, in the east-central and west-central parts of the Santa Susana fault zone. This zone merges with the Oak Ridge fault on the west, and with the San Fernando fault zone on the east. The fault zone consists of a series of convex-upward, moderately steep to low-angle thrusts with the Modelo Formation of Miocene age overriding deposits of Pliocene to Quaternary age on the south. The strip map and cross sections on figure 3.1 are from Yeats (1976) and show the general structural and stratigraphic relations along the fault zone.

LIMEKILN CANYON EXPLORATION

In the intitial trenching east of Limekiln Canyon, we attempted to pinpoint the location of the southern trace of the fault zone, which at that time was considered by others to be the more recently active trace (fig. 3.2). Materials found in four trenches, however, indicated that the fault must be farther south than previously thought,

[1]Leighton and Associates, 1151 Duryea Avenue, Irvine, CA 92714.

Manuscript received for publication on February 5, 1981.

and within an existing tract development. We attempted to expose the fault in a series of 13 pits along the base of the foothills west of Limekiln Canyon. Because of the extensive overburden, however, the exploration was only successful in restricting the fault location to a zone approximately 53 m wide, slightly north of the location

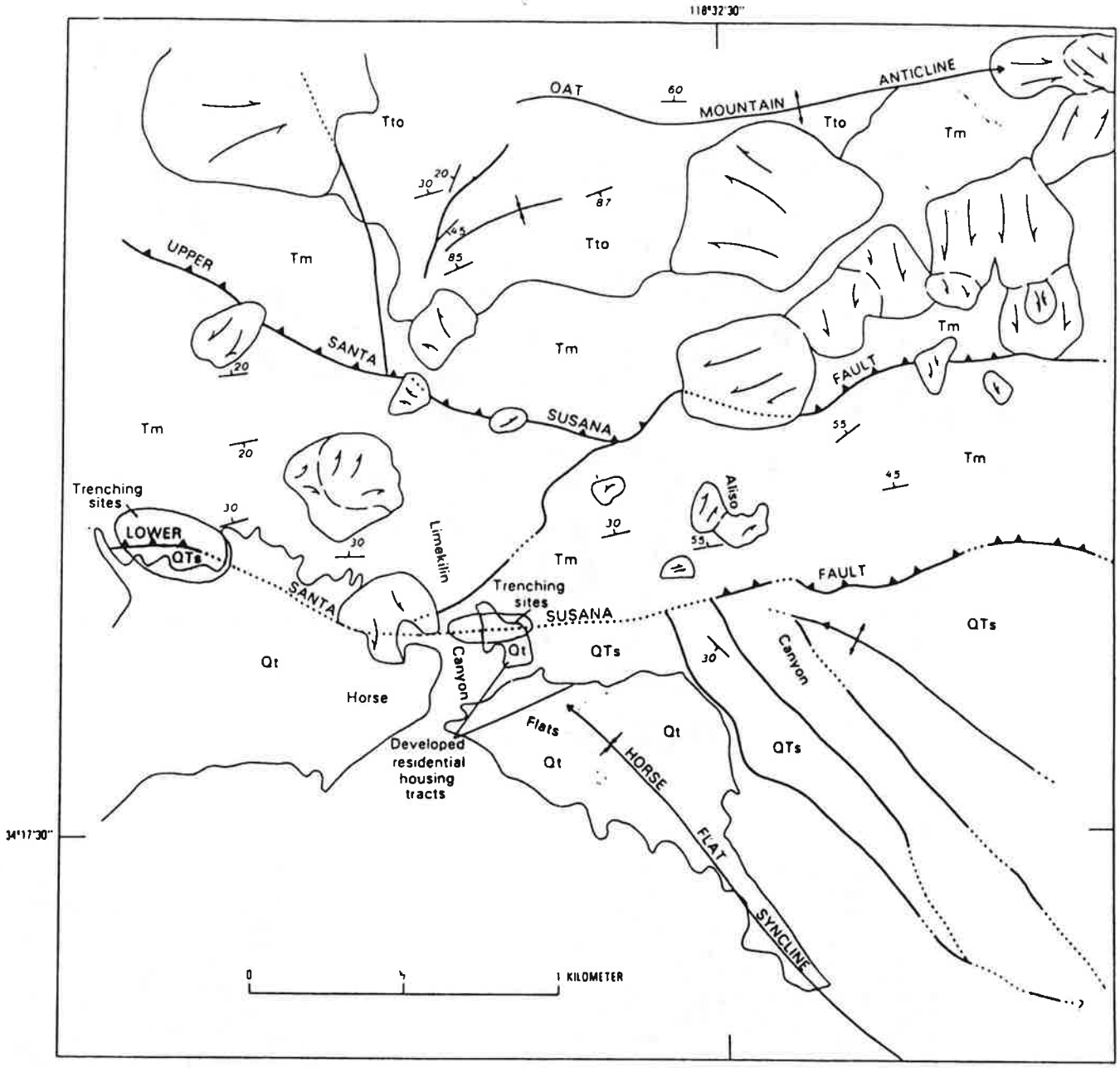

EXPLANATION

- Qt — Terrace deposits (Pleistocene)
- QTs — Saugus Formation, undifferentiated (Pleistocene and Pliocene)
- Tm — Modelo Formation (Miocene)
- Tto — Topanga Formation (Miocene)
- Landslides—Arrows indicate direction of movement
- Contact—Approximately located
- Fault—Approximately located; dotted where inferred
- Thrust fault—Approximately located; dotted where inferred; sawteeth on upper plate
- Anticline—Showing direction of plunge
- Syncline—Showing direction of plunge
- 25 — Strike and dip of inclined beds

FIGURE 3.2.—Generalized regional geologic map of the Porter Ranch area. Modified after Saul (1975).

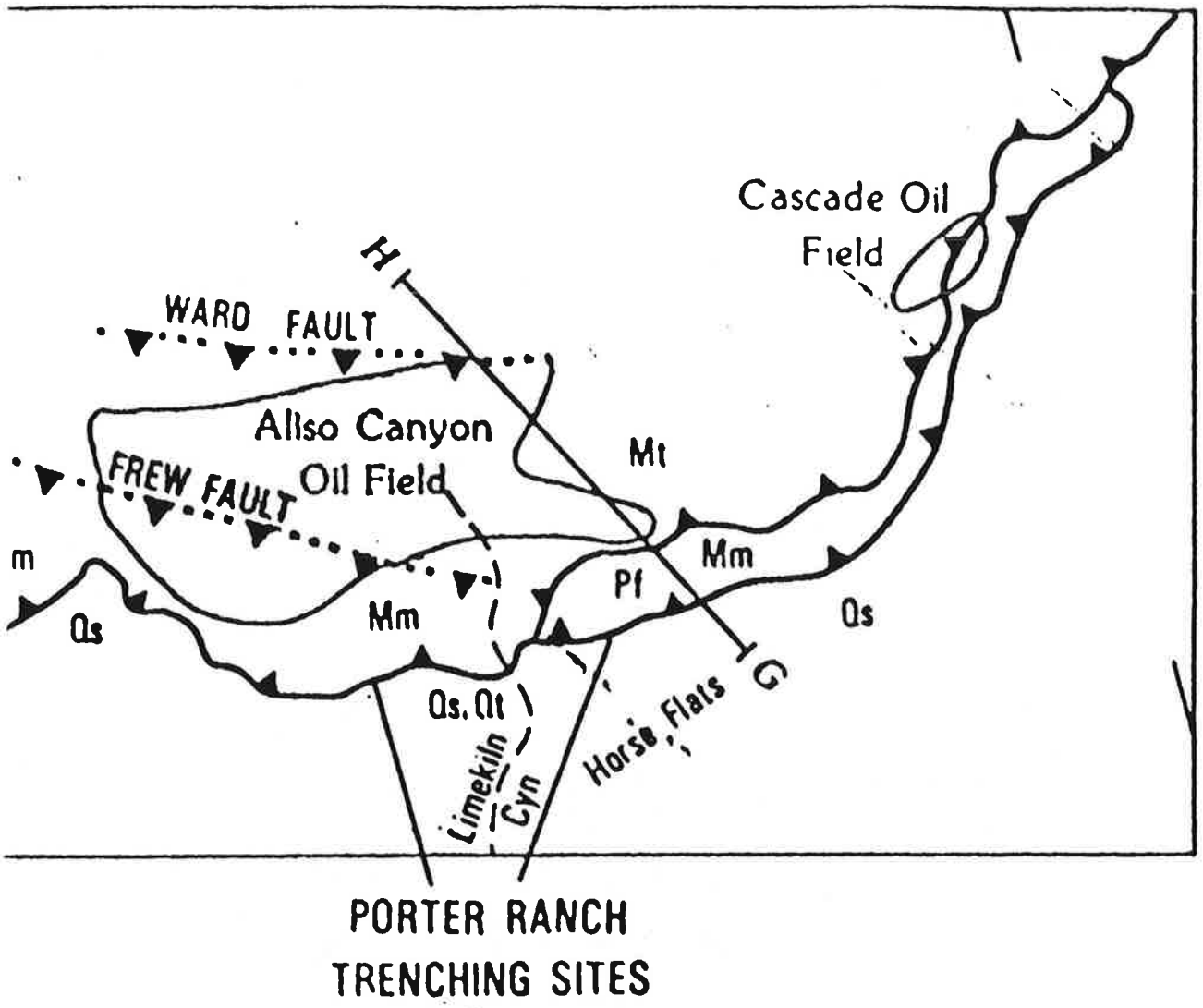
119°30'W
Cascade Oil Field
H
WARD FAULT
Aliso Canyon Oil Field
FREW FAULT
Mt
m
Mm
Pf
Mm
Qs
Qs
Qs, Qt
Limekiln Cyn
Horse Flats
G
PORTER RANCH
TRENCHING SITES

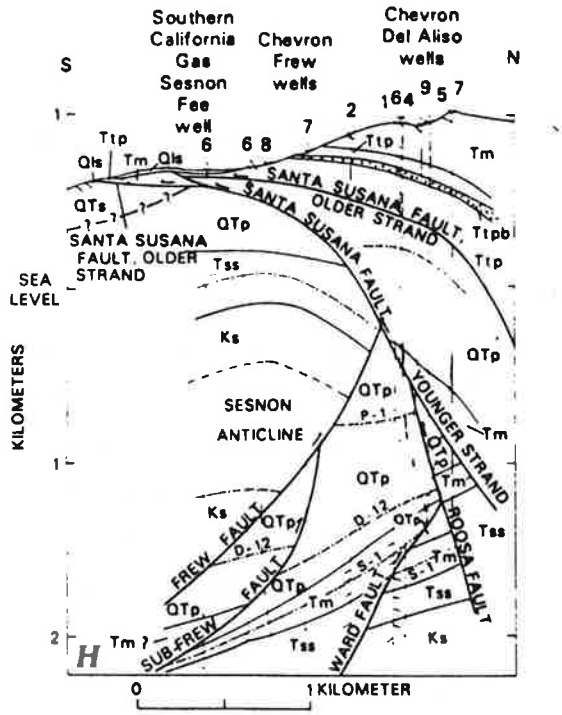
Southern California Gas Sesnon Fee well
Chevron Frew wells
Chevron Del Aliso wells
S
N
SEA LEVEL
KILOMETERS
SANTA SUSANA FAULT, OLDER STRAND
SANTA SUSANA FAULT, OLDER STRAND
SANTA SUSANA FAULT
SESNON ANTICLINE
YOUNGER STRAND
FREW FAULT
SUB-FREW FAULT
WARD FAULT
ROOSA FAULT
H
0
1 KILOMETER

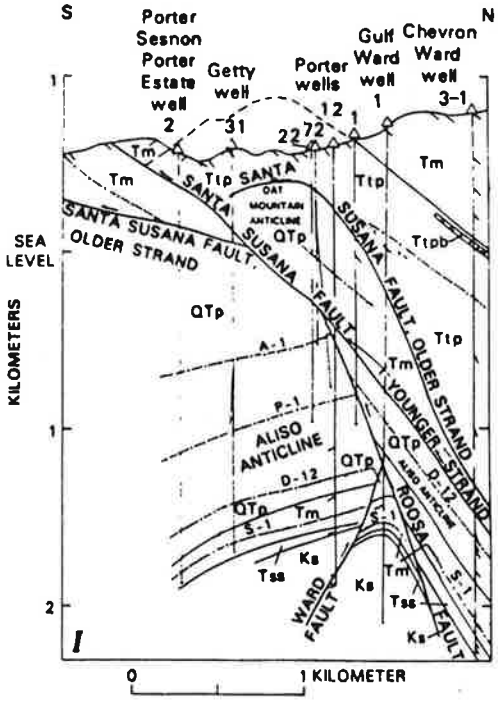
Porter Sesnon Porter Estate well 2
Getty well 31
Porter wells 12
Gulf Ward well 1
Chevron Ward well 3-1
S
N
SEA LEVEL
KILOMETERS
SANTA SUSANA FAULT, OLDER STRAND
SANTA SUSANA FAULT
SUSANA FAULT, OLDER STRAND
YOUNGER STRAND
ALISO ANTICLINE
WARD FAULT
ROOSA FAULT
I
0
1 KILOMETER